

MONOAMINE OXIDASE IN NEURONAL CELL DEATH

JULIA FITZGERALD

A thesis submitted in partial fulfilment of the requirements
of Nottingham Trent University for the degree of Doctor of
Philosophy

January 2008

THIS WORK IS THE INTELLECTUAL PROPERTY OF THE AUTHOR, AND MAY ALSO BE OWNED BY THE RESEARCH SPONSOR(S) AND/ OR NOTTINGHAM TRENT UNIVERSITY. YOU MAY COPY UP TO 5 % OF THIS WORK FOR PRIVATE STUDY, OR PERSONAL, NON-COMMERCIAL RESEARCH. ANY RE-USE OF THE INFORMATION CONTAINED WITHIN THIS DOCUMENT SHOULD BE FULLY REFERENCED, QUOTING THE AUTHOR, TITLE, UNIVERSITY DEGREE LEVEL AND PAGINATION. QUERIES OR REQUESTS FOR ANY OTHER USE, OR IF A MORE SUBSTANTIAL COPY IS REQUIRED, SHOULD BE DIRECTED IN THE FIRST INSTANCE TO THE AUTHOR.

ACKNOWLEDGEMENTS

Firstly I thank Professor Ellen Billett for giving me the opportunity to do this research, for being very supportive during my PhD, the motivation, guidance, time and most of all for inspiring me in this subject. I can't thank you enough.

I am extremely grateful to Dr Christoph Ufer for teaching me so perfectly about molecular biology and his great friendship.

Thank you Dr Luigi DeGirolamo (Gino) for teaching me and all your help, support and laughs over the years.

I would like to thank Professor Hartmut Kuhn at Charité, Humbolt University, Berlin for his generosity in the collaboration and for inviting me to work in his laboratory.

Thank you to the Biomedical Science department at Nottingham Trent University and Lab 106 for all their help, advice and friendship; Dr Cheryl Wells, Aslihan Ugun-Klusek, Dr Richard Howden, Dr Begoña Caneda Ferron, Dr Katy Beck, Florence Burte, Heidi Hanes, Bomber Harris, David Munoz and Lindsey Durose. It has been a pleasure.

Dr Alan Hargreaves has been very helpful in discussions and so has Dr Renée Germack. Dr Juncal Caubilla-Baron and Dr Olivier Sonntag have been a godsend with regards to the formatting of the thesis and Dr Sonntag drew the chemical structures. The late Dr Richard Jones passed on his confocal expertise and was my friend.

I would like to thank my friends and family for being supportive, especially Pat and Ron Allcock, Peter Jackson, Mike and Herma Fitzgerald, Judith, Jude and Lizzie.

Most of all, this thesis is for my parents, Hazel Fitzgerald and Andrew Fitzgerald and my brother, Dr Daniel Fitzgerald.

Finally, I gratefully acknowledge the financial support for this work, Nottingham Trent University, but also funding from The British Council, Berlin Charité, Deutscher Akademischer Austauschdienst, The Leverhulme Trust and The Biochemical Society.

CONTRIBUTIONS

The MAO-A and MAO-B immunohistochemistry on human liver sections, shown as a positive control for MAO-A and MAO-B specific antibodies in Figure 3.3 were done by Dr Siva Sivasubramaniam at Nottingham Trent University.

ABSTRACT

Monoamine oxidase (MAO) is an oxidative enzyme that deaminates a variety of amine substrates, including the neurotransmitter dopamine. The enzymatic reaction requires molecular oxygen and produces hydrogen peroxide as a by-product. MAO is localised in the outer mitochondrial membrane and exists as two isoforms, MAO-A and MAO-B, which are differentially expressed in the body and differ in their substrate and inhibitor specificities. Previous studies have suggested that MAO-generated reactive oxygen species (ROS) contribute to oxidative stress in the cell and can directly inhibit electron transport, cause damage to mitochondrial DNA and enhance cell death signalling. In this study the role of MAO in cell death was investigated in dopaminergic neuroblastoma (SH-SY5Y) cells, in three diverse models of mitochondrially-mediated apoptosis. The relevance of MAO in cell death signalling was confirmed with the use of two unrelated MAO inhibitors and the creation of stable SH-SY5Y cell lines that either over express MAO-A or have reduced levels of MAO-A. The study is the first to over express MAO-A using recombinant technology and to use miRNA to stably knock-down MAO-A expression in human neuronal cells.

Results confirm that MAO-A is involved in modulating cell death but the mechanism and extent of the involvement depends on the apoptotic inducer. In classical apoptosis induced by staurosporine (STS), cells undergo rapid morphological and biochemical changes indicative of mitochondrially-mediated apoptosis, which is partly dependent on ROS production by MAO-A and induction of mitogen-activated protein kinase (MAPK) signalling cascades. MAO-A protein and catalytic activity are increased in this model, however the mechanism by which this occurs is unknown and is not a result of increased gene transcription. In death induced by growth factor withdrawal, the MAO-A gene is up regulated via p38 and JNK MAPK pathways, which occurs downstream of caspase activation. In both the STS and growth factor withdrawal models, MAO inhibition reduced apoptosis. Most significantly reduced levels of MAO-A expression in 'knock down' cells protected against cell death induced by the complex I inhibitor rotenone, suggesting that MAO has an important role in mitochondrial function. Over expression of MAO-A resulted in stress and apoptosis, followed by a period of cellular senescence and eventually death by necrosis. These data compliment the effects of chronic exposure to oxidative stress in ageing and neurodegeneration.

For the first time this work has shown that the MAO-A isoform is an important regulator of STS-induced apoptosis, that MAO-A gene expression is regulated by JNK signalling, and that MAO-A is significantly involved in mitochondrial dysfunction induced by complex I inhibition. These data raise important questions regarding predisposition to the development of neurodegenerative diseases such as Parkinson's disease and to approaches used for their treatment.

ABBREVIATIONS

5-HT	Serotonin	dsDNA	double stranded DNA
AAF	Agonistic anti-Fas antibody	ECL	Enhanced chemiluminescence
Ab	Antibody	ER	Endoplasmic reticulum
AD	Alzheimer's disease	ERK	Extra signal regulated kinase
ADP	Adenosine diphosphate	ETC	Electron transport chain
AIF	Apoptosis inducing factor	FAD	Flavin adenine dinucleotide
ALS	Amyotrophic Lateral Sclerosis	FADD	Fas Associated protein with Death Domain
AMC	Amido methyl coumarin	FADH	Reduced flavin adenine dinucleotide
ANT	Adenine nucleotide transporter	FBS	Foetal bovine serum
APP	Amyloid precursor protein	FU	Fluorescence unit
ATP	Adenosine triphosphate	GM	Growth media
BA	Benzylamine	GPx	Glutathione peroxidase
BCA	Binchoninic	GSH	Glutathione
bp	Base pair	GSSG	Reduced glutathione
C3	Caspase-3	H₂O₂	Hydrogen peroxide
C8	Caspase-8	HBSS	Hank's buffered salt solution
C9	Caspase-9 C-terminal apoptosis recruitment domain	HD	Huntington's disease
CARD		hMAO	Human MAO
cDNA	complementary DNA	IAP	Inhibitor of apoptosis
Cep	Cephalon	IMM	Inner mitochondrial membrane
Clor	Clorgyline	JNK	c-jun N-terminal kinase
CNS	Central nervous system	MAO	Monoamine oxidase
COMT	Catechol-O-methyl transferase	MAPK	Mitogen activated protein kinase
CpG	C-phosphodiester bond-G	miRNA	Micro RNA
Cyt-c	Cytochrome-c	Mito	Mitochondria
DA	Dopamine	MM	Mitochondrial membranes
DCDHF	2,7-Dichlorodihydrofluorescein diacetate	Mock	Mock transfected
DED	Death effector domain	MOM	Mitochondrial outer membrane
DISC	Death inducing signalling complex	MOMP	Mitochondrial outer membrane potential
DMEM	Dulbecco's modified eagles medium	mRNA	messenger RNA
DOPAC	2-(3,4-dihydroxyphenyl)acetic acid	mtDNA	Mitochondrial DNA
DOPAL	3,4-dihydroxyphenylacetaldehyde	MPTP	1-methyl 4-phenyl 1,2,3,6-tetrahydropyridine
DOPEGAL	3,4-dihydroxyphenylglycolaldehyde	MPP⁺	1-methyl-4-phenylpyridinium ion
DNA	Deoxyribonucleic acid	NA	Noradrenaline

NAC	N-acetyl cysteine	qRT-PCR	Quantitative reverse transcription polymerase chain reaction
ND	Neurodegeneration	RNA	Ribonucleic acid
Neg	Negative	ROS	Reactive oxygen species
NGF	Nerve growth factor	RT	Reverse transcription
NO	Nitric oxide	RT-PCR	Reverse transcription polymerase chain reaction
O₂^{•-}	Superoxide radical	SD	Standard deviation
OH[•]	Hydroxyl radical	SEM	Standard error
Oligo	Oligonucleotide	SFM	Serum free media
OMM	Outer mitochondrial membrane	sh	Short hairpin
PARP	Poly (ADP) ribose polymerase	SNpc	Substantia nigra pars compacta
PBS	Phosphate buffered saline	SOD	Superoxide dismutase
PCR	Polymerase chain reaction	ssDNA	Single stranded DNA
PD	Parkinson's Disease	STS	Staurosporine
PEA	Phenylethylamine	SW	Serum withdrawal
PIDD	p53 induced protein with a death domain	TBS	Tris buffered saline
PINK1	PTEN induced putative kinase 1	TCP	Tranylcypromine
PIP₃	Phosphatidylinositol (3,4,5)-triphosphate	TNF	Tumour necrosis factor
PKB/Akt	Protein kinase B	TPA	12-O-tetradecanoylphorbol-13-acetate
PKC	Protein kinase C	UPP	Ubiquitin proteasome pathway
PMSF	phenylmethanesulphonylfluoride	VDAC	Voltage dependent anion channel
PTP	Permeability transition pore	WT	Wild type

TABLE OF CONTENTS

ACKNOWLEDGEMENTS	III
ABSTRACT	IV
ABBREVIATIONS	V
TABLE OF CONTENTS	VII
LIST OF FIGURES	XII
LIST OF TABLES	XVI

GENERAL INTRODUCTION	2
1.1. Monoamine oxidase	2
1.1.1 A brief history	2
1.1.2 Structure and catalytic mechanism	3
1.1.3 Isoenzyme classification	5
1.1.4 MAO inhibitors	6
1.1.5 Distribution and physiological significance of MAO.....	8
1.1.6 MAO Genetics.....	9
1.2. Neurodegeneration	10
1.2.1 Common pathobiology.....	10
1.2.2 Parkinson's Disease	11
1.2.3 Alzheimer's and other neurodegenerative diseases.....	14
1.2.4 Huntington's disease and Pick's disease.....	14
1.3. Free radicals and oxidative stress.....	15
1.3.1 Hydrogen peroxide	15
1.3.2 Mitochondrial ROS.....	16
1.3.3 Antioxidant defences	18
1.3.4 Free radical production by MAO in neurons	19
1.4. Cell signalling	20
1.4.1 Protein kinase signalling	20
1.4.2 Mitogen activated protein kinase (MAPK) signalling.....	21
1.4.3 Regulation of MAO expression by protein kinase signalling	24
1.4.4 H ₂ O ₂ as a signalling molecule	25
1.5. Cell death	26
1.5.1 Apoptosis	26
1.5.2 Mitochondria-mediated apoptosis	28

1.5.3	Death receptor-mediated apoptosis	30
1.5.4	Calcium and apoptosis	30
1.5.5	Apoptosis and neurodegeneration	31
1.6.	Overall aims of thesis	32
MATERIALS AND METHODS		34
2.1.	Materials	34
2.1.1	Cell culture	34
2.1.2	General laboratory reagents	34
2.1.3	Specialised laboratory reagents	34
2.1.4	MAO inhibitors	35
2.1.5	Kinase inhibitors.....	35
2.1.6	Antibodies	35
2.1.7	Molecular biology.....	36
2.1.8	Specialised equipment	37
2.2.	Tissue culture methods	38
2.2.1	Cell culture	38
2.3.	Biochemical methods	40
2.3.1	Assessment of cell viability	40
2.3.2	Treatment of SH-SY5Y cells	42
2.3.3	Cell extraction	43
2.3.4	Estimation of total protein in cell extracts	43
2.3.5	Biochemical Assays.....	44
2.3.6	Immunohistochemistry	45
2.3.7	Immunocytochemistry	45
2.3.8	Immunofluorescence.....	46
2.3.9	Detection of ROS.....	46
2.3.10	Mitotracker.....	47
2.3.11	Gel electrophoresis and Western blotting	47
2.3.12	Dot blotting	47
2.4.	Molecular biology methods	48
2.4.1	Preparation of RNA and reverse transcription	48
2.4.2	Real-Time-PCR (qRT-PCR)	49
2.4.3	Conventional PCR	51
2.4.4	Restriction endonuclease digestion reactions.....	51
2.4.5	Overexpression of MAO-A in SH-SY5Y cells	52

2.4.6	MAO-A knockdown in SH-SY5Y cells	56
-------	--	----

THE ROLE OF MAO IN MITOCHONDRIA-MEDIATED NEURONAL APOPTOSIS59

3.1.	Introduction.....	60
3.1.1	Previous work.....	60
3.1.2	An InVitro Model of Neuronal Apoptosis	60
3.1.3	Antioxidants	65
3.1.4	Aims of Chapter	66
3.2.	Results	68
3.2.1	Characterisation of apoptotic model.....	68
3.2.2	Changes in MAO in STS-induced apoptosis	74
3.2.3	Relevance of MAO in STS induced apoptosis.....	76
3.2.4	MAO enhanced apoptosis: mechanism of action.....	80
3.3.	Discussion.....	84
3.3.1	Development of an in vitro model of neuronal apoptosis.....	84
3.3.2	The role of MAO in STS-induced neuronal apoptosis	85
3.3.3	Effects of STS on MAO expression	87
3.3.4	Regulation of apoptosis by MAO.....	89
3.3.5	Conclusion.....	90

THE ROLE OF MAO-A IN SELECTED MODELS OF NEURONAL APOPTOSIS92

4.1.	Introduction.....	93
4.1.1	Receptor-mediated apoptosis	93
4.1.2	Complex I inhibitors	95
4.1.3	Serum withdrawal.....	96
4.1.4	Rationale	98
4.1.5	Aims of Chapter	99
4.2.	Results	99
4.2.1	Treatment of SH-SY5Y cells with agonistic anti-Fas antibody.....	99
4.2.2	TNF α treatment of SH-SY5Y cells	103
4.2.3	Rotenone	104
4.2.4	Serum withdrawal.....	108

4.3.	Discussion.....	121
4.3.1	Death receptor-mediated apoptosis	121
4.3.2	Rotenone-mediated apoptosis	122
4.3.3	Serum withdrawal-induced apoptosis.....	122
4.3.4	Conclusion	125
 OVEREXPRESSION OF MAO-A IN HUMAN NEUROBLASTOMA CELLS		128
5.1.	Introduction.....	129
5.1.1	Increased MAO levels in humans - physiological relevance.....	129
5.1.2	Changes in MAO expression in <i>in vitro</i> cell culture systems.....	130
5.1.3	Increased MAO expression following genetic manipulation.....	130
5.1.4	Rationale	131
5.1.5	Aims of Chapter	131
5.2.	Results	132
5.2.1	Characterisation of SH-SY5Y cells overexpressing MAO-A.....	132
5.2.2	Characterisation of newly cloned MAO-A+ (1A9, working clone).....	134
5.2.3	Characterisation of sub-cultured MAO-A+ stable SH-SY5Y cells (1A9 working clone).....	137
5.2.4	Treatment of MAO-A+/1A9 SH-SY5Y stable clones with apoptotic inducers 147	
5.3.	Discussion.....	150
5.3.1	Development of a stable SH-SY5Y cell line over expressing MAO-A	150
5.3.2	Consequences of MAO-A overexpression.....	152
5.3.3	Response of MAO-A+ SH-SY5Y cells to stress.....	156
5.3.4	Conclusion	157
 THE EFFECT OF KNOCKDOWN OF MAO-A EXPRESSION IN NEUROBLASTOMA CELLS.....		158
6.1.	Introduction.....	159
6.1.1	Reduced MAO in humans-physiological relevance	159
6.1.2	Reduced MAO in <i>in vitro</i> culture systems.....	161
6.1.3	MAO knockdown by genetic manipulation.....	162
6.1.4	miRNA technology.....	163
6.1.5	Rationale	164
6.1.6	Aims of Chapter	165

6.2.	Results	166
6.2.1	Characterisation of MAO-A knockdown SH-SY5Y cells.....	166
6.2.2	Characterisation of working MAO-A knockdown clone 10D8.....	168
6.2.3	Effect of MAO-A knockdown on apoptotic induction.....	174
6.3.	Discussion.....	181
6.3.1	Stable MAO-A knockdown in SH-SY5Y cells.....	181
6.3.2	Characteristics of stable MAO-A knockdown clone 10D8	182
6.3.3	The effect of MAO-A knockdown in selected apoptotic models.....	183
6.3.4	Conclusion	186
CONCLUSIONS AND FUTURE DIRECTIONS.....		187
7.1.	Main findings	188
7.1.1	STS	188
7.1.2	Serum withdrawal.....	189
7.1.3	Overexpression	189
7.1.4	Knockdown	190
7.1.5	Rotenone and mitochondrial regulation.....	190
7.2.	Wider significance in relation to the development and treatment of PD.....	192
7.3.	Future directions.....	193
7.3.1	Expanding insights into relevance of MAO-A overexpression and knockdown.....	193
7.3.2	The role of MAO-A in rotenone-induced cell death	193
7.3.3	The relationship between MAO and other mitochondrial proteins	194
REFERENCES		194
APPENDIX		231

LIST OF FIGURES

Figure 1. 1 Ribbon diagrams of the crystal structures of human MAO-A and –B elucidated by Binda <i>et al.</i> 2002, DeColibus <i>et al.</i> 2005.	4
Figure 1. 2 Catalytic mechanism of amine oxidation by MAO	5
Figure 1. 3 Chemical structures of some substrates of MAO-A and –B	6
Figure 1. 4 Chemical structure and specificity of some MAO inhibitors.....	7
Figure 1. 5 A schematic diagram of the MAO-A promoter	10
Figure 1. 6 The Fenton reactions	16
Figure 1. 7 Schematic representation of the electron transport chain (Abou-Sleiman <i>et al.</i> 2006)	17
Figure 1. 8 Schematic representation of the MAO-dependent pathway for suppression of mitochondrial electron flow and subsequent recovery (Cohen <i>et al.</i> 1997).	18
Figure 1. 9 MAPK phosphorylation cascade (From www.cellsignal.com).....	21
Figure 1. 10 Protein kinase signalling and MAO gene expression	24
Figure 1. 11 An overview of the mitochondrially mediated apoptotic pathway.....	28
Figure 1. 12 Schematic of mitochondrial permeability transition (Abou-Sleiman <i>et al.</i> 2006)	29
Figure 1. 13 An overview of mitochondrial signalling (Pagliarini 2006).....	30
Figure 2. 1 Overview of cloning procedure	53
Figure 2. 2 Stable over expression of MAO-A in SH-SY5Y cells.....	55
Figure 2. 3 Overview of cloning procedures used for knockdown of MAO-A using BLOCK-iT miRNA expression vector kit	58
Figure 3. 1 Chemical structure of staurosporine from <i>Streptomyces staurosporeus</i>	63
Figure 3. 2 Chemical structures of Decyl TPP and MitoQ	66
Figure 3. 3 MAO-A is predominant in SH-SY5Y human neuroblastoma cells.....	69
Figure 3. 4 Concentration of STS required to reduce the cell viability of SH-SY5Y Cells	70
Figure 3. 5 STS induces apoptotic morphologies in SH-SY5Y cells.....	71
Figure 3. 6 STS induces loss of cell viability in SH-SY5Y cells.....	72
Figure 3. 7 Caspase-3 is activated following STS exposure in SH-SY5Y cells.	72
Figure 3. 8 The intrinsic but not extrinsic pathway is active in STS-induced apoptosis	73
Figure 3. 9 Caspase-8 and -9 mRNA is detectable in SH-SY5Y cells	74
Figure 3. 10 Changes in MAO and caspase-3 activities following STS treatment	75
Figure 3. 11 STS-induced apoptosis causes increased MAO-A protein.....	76
Figure 3. 12 MAO-A mRNA expression levels are unaffected by STS.....	76
Figure 3. 13 Inhibition of MAO-A reduces caspase-3 activity in STS-induced apoptosis..	77

Figure 3. 14 Inhibition of MAO-A reduces caspase-9 activation in STS-induced apoptosis	78
Figure 3. 15 Inhibition of MAO-A reduces loss of cell viability in STS-induced apoptosis	79
Figure 3. 16 Effect of clorgyline on translocation of GAPDH to the nucleus following STS insult.....	80
Figure 3. 17 Staurosporine induces changes in MAPK signalling and Bcl-2 levels: attenuation by clorgyline.....	81
Figure 3. 18 Effect of MAO inhibitor clorgyline and antioxidants on ROS production in Staurosporine exposed SH-SY5Y cells	82
Figure 3. 19 ROS co-localised with intact mitochondria in STS-induced apoptotic SH-SY5Y cells.....	83
Figure 3. 20 Effect of DTTP and MitoQ concentration on caspase-3 activity.....	84
Figure 3. 21 ROS in STS treated SH-SY5Y cells: Effect of mitochondrially directed antioxidant MitoQ.....	84
Figure 3. 22 Overview of STS-induced apoptosis: role of MAO-A	91
Figure 4. 1 Fas and TNF receptor mediated apoptosis	95
Figure 4. 2 Chemical structure of rotenone and location of mitochondrial complex I.....	96
Figure 4. 3 Mechanisms of serum withdrawal-induced apoptosis	98
Figure 4. 4 MTT reduction in SH-SY5Y cells following treatment with AAF	101
Figure 4. 5 The effect of agonistic anti-Fas antibody on SH-SY5Y morphology.....	102
Figure 4. 6 Agonistic anti-Fas antibody does not induce apoptosis in SH-SY5Y cells	103
Figure 4. 7 AAF does not activate caspase-8 or caspase-9	104
Figure 4. 8 MTT reduction in SH-SY5Y cells following treatment with TNF α	104
Figure 4. 9 TNF α does not induce caspase-3 mediated apoptosis in SH-SY5Y cells.....	105
Figure 4. 10 MTT reduction following rotenone exposure in SH-SY5Y cells	106
Figure 4. 11 Effect of rotenone on cell morphology and caspase-3 activity.....	107
Figure 4. 12 Effect of rotenone on MAO activity	108
Figure 4. 13 Effect of rotenone on ROS levels	108
Figure 4. 14 Apoptotic morphologies of SH-SY5Y cells following serum withdrawal ...	109
Figure 4. 15 Serum withdrawal induced caspase-3 mediated apoptosis in SH-SY5Y cells	110
Figure 4. 16 Serum withdrawal caused increased MAO activity	111
Figure 4. 17 Serum withdrawal caused increased MAO-A mRNA expression.....	111
Figure 4. 18 Serum withdrawal caused increased MAO-A protein levels.....	112
Figure 4. 19 The effect of MAO inhibitors on the apoptotic morphology of SH-SY5Y cells following serum withdrawal.....	113
Figure 4. 20 Effect of MAO inhibition on cell viability following serum withdrawal	114

Figure 4. 21 The effect of MAO inhibition on serum withdrawal-induced caspase-3 activation.....	115
Figure 4. 22 The effect of MAO inhibition on serum withdrawal-induced DNA fragmentation.....	115
Figure 4. 23 Effect of MAO inhibition on caspase-9 activation induced by serum withdrawal.....	116
Figure 4. 24 Serum withdrawal induces subtle elevation of ROS.....	117
Figure 4. 25 Effect of serum withdrawal on MAPK phosphorylation.....	118
Figure 4. 26 Effect of MAPK inhibitors on levels of phosphorylated MAPK proteins	119
Figure 4. 27 Effect of MAPK inhibitors on MAO Activity and mRNA expression.....	120
Figure 4. 28 Possibilities for reduced caspase-8 function in SH-SY5Y cells.....	122
Figure 4. 29 The role of MAO in serum withdrawal-induced apoptosis.....	127
Figure 5. 1 MAO-A mRNA levels and catalytic activities are increased in MAO-A+ SH-SY5Y clones	132
Figure 5. 2 Cell morphologies of mock transfected and MAO-A+ SH-SY5Y stable clones	133
Figure 5. 3 MAO-A protein levels in mock transfected and MAO-A+ SH-SY5Y cells...	134
Figure 5. 4 MAO-A protein in MAO-A+/1A9 stable clones	135
Figure 5. 5 MAO-A in MAO-A+/1A9 cells is localised to mitochondria.....	136
Figure 5. 6 Growth and doubling times of wild type, mock/2D8 and MAO-A+/1A9 cells	137
Figure 5. 7 MTT reduction in wild type, mock/2D8 and MAO-A+/1A9 cells.....	138
Figure 5. 8 ATP levels in wild type, mock/2D8 and MAO-A+/1A9 cells	138
Figure 5. 9 Changing cell morphologies of MAO-A+/1A9 SH-SY5Y cells after long term culture.....	139
Figure 5. 10 Changes in morphology during long term culture following cloning of MAO-A+/1A9 cells.....	140
Figure 5. 11 Cytoskeletal proteins and GAPDH in wild type, mock/2D8 and MAO-A+/1A9 cells	141
Figure 5. 12 Basal caspase-3 activities are reduced during long term culture of MAO-A+/1A9 cells.....	142
Figure 5. 13 MAO-A protein levels in MAO-A+/1A9 cells over a 6 month culture period	143
Figure 5. 14 Production of ROS is increased in MAO-A+/1A9 cells	144
Figure 5. 15 Bcl-2 levels in mock/2D8 and MAO-A+/1A9 SH-SY5Y clones	145
Figure 5. 16 Phosphorylated JNK and transcription factor c-jun in mock/2D8 and MAO-A+/1A9 cells.....	146
Figure 5. 17 Effect of apoptotic inducers on cell viability in wild type, mock transfected and over expressing MAO-A stable clones.....	147

Figure 5. 18 ROS production in mock/2D8 and MAO-A+/1A9 SH-SY5Y cells following STS and serum deprivation treatments	149
Figure 5. 19 Cellular effect of H ₂ O ₂ concentration (modified from Giorgio <i>et al.</i> 2007) .	152
Figure 5. 20 Proposed effect of MAO-A overexpression on SH-SY5Y cells in long term culture	155
Figure 5. 21 Overview of biochemical changes in SH-SY5Y cells overexpressing MAO-A	156
Figure 6. 1 An overview of miRNA gene silencing	163
Figure 6. 2 MAO-A mRNA and catalytic levels are decreased in MAO-A- SH-SY5Y clones	166
Figure 6. 3 Morphology of stable miRNA SH-SY5Y clones	167
Figure 6. 4 MAO-A protein levels in MAO-A knockdown clone 10D8	168
Figure 6. 5 MAO-A protein detected by dot blotting in MAO-A knockdown SH-SY5Y and controls.....	169
Figure 6. 6 Growth and doubling times of wild type, negative miRNA control and MAO-A- clones	170
Figure 6. 7 MTT reduction in MAO-A knockdown SH-SY5Y cells and controls	171
Figure 6. 8 Cytoskeletal and GAPDH proteins in MAO-A knockdown SH-SY5Y cells and controls.....	172
Figure 6. 9 ROS levels in untreated MAO-A knockdown SH-SY5Y and negative miRNA control	173
Figure 6. 10 Effect of apoptotic inducers on cell viability of MAO-A knockdown SH-SY5Y and controls.....	174
Figure 6. 11 Effect of apoptotic inducers on ATP levels in MAO-A knockdown SH-SY5Y and controls	175
Figure 6. 12 Effect of STS treatment on caspase-3 activity and apoptotic morphology in MAO-A knockdowns.....	177
Figure 6. 13 Effect of rotenone treatment on caspase-3 activity and apoptotic morphology in MAO-A knockdowns.....	178
Figure 6. 14 Effect of serum withdrawal on caspase-3 activity and apoptotic morphology in MAO-A knockdowns.....	179
Figure 6. 15 Hypothetical schematic of MAO's ability to enhance rotenone-induced cell death.....	185
Figure 7. 1 Overview of role of MAO in mitochondrial dysfunction	185

LIST OF TABLES

Table 1. 1 Reactive oxygen species (Halliwell and Gutteridge 2007)	15
Table 1. 2 Some characteristics of p38	23
Table 1. 3 Some reported cellular targets of H ₂ O ₂ signalling	25
Table 1. 4 Some substrates and functions of important caspases.....	27
Table 1. 5 Evidence for apoptosis in AD and PD.....	31
Table 2. 1. Details of commonly used experimental treatments in this thesis	42
Table 2. 2 Primer combinations used for qRT-PCR.....	49
Table 2. 3 Primer combination for conventional PCR.....	51
Table 2. 4 Oligonucleotide sequences encoding human MAO-A pre-miRNA.....	56
Table 2. 5 Useful information for miRNA experiments	58
Table 3. 1 General Characteristics of the SH-SY5Y Human Neuroblastoma Cell Line	64
Table 5. 1 Effect of serum deprivation and rotenone treatment on MTT reduction.....	148
Table 6. 1 Overview of some human conditions where MAO is reduced.....	159
Table 6. 2 A summary of the effects of MAO-A knockdown in SH-SY5Y cells on their response to different apoptotic inducers	180

CHAPTER 1

GENERAL INTRODUCTION

GENERAL INTRODUCTION

1.1. MONOAMINE OXIDASE

Monoamine oxidase (amine: Oxygen oxidoreductase [deaminating] [flavin containing] EC 1. 4. 3. 4 [MAO]) is an enzyme that catalyses the oxidative deamination of a wide range of biogenic and dietary amines to their corresponding aldehydes. The enzymatic reaction requires molecular oxygen (O₂) and produces hydrogen peroxide (H₂O₂) as a by-product, a simplified schematic of which is shown below.



In addition, MAO requires a flavin-adenosine-dinucleotide (FAD) co-factor and insertion into the outer mitochondrial membrane (OMM) for its activity. The primary substrates of MAO in the brain are neurotransmitters such as adrenaline, noradrenaline (NA), dopamine (DA), serotonin (5-HT) and β -phenylethylamine (PEA). There are two isoforms of MAO, coded for by two separate genes, termed MAO-A and MAO-B, which are characterised by their substrate and inhibitor specificities. MAO plays a central role in neurotransmitter metabolism and has been implicated in a range of human conditions including Parkinson's disease (PD).

1.1.1 A brief history

- **1928**-Mary Hare termed the amine deaminating enzyme she discovered in rabbit liver, tyramine oxidase. The name was later modified to monoamine oxidase to reflect its substrate specificity following related studies in neurotransmitter metabolism (Blashko *et al.* **1937**).
- **1966**-Gorkin proposed that there were two different MAO variants and MAO was solubilised and purified from rat liver (Youdim and Sourkes).
- **1968**-Johnston characterised two MAO isoforms (MAO-A and -B) by their substrate and inhibitor specificities.
- **1972**-Knoll and Magyar developed the MAO-B inhibitor Deprenyl. This inhibitor was later to become a mainstay treatment for Parkinson's disease (PD).
- **1977**-Achee and Gabay found that MAO was attached to the OMM.
- **1983**- Cohen proposed that the production of hydrogen peroxide by MAO could damage dopaminergic neurons. Savov proposed that this damage was caused by the lipid peroxidation of mitochondrial membranes.

- **1983**-Langston and co-workers showed that the synthetic compound, 1-methyl-4-phenyl-1, 2, 3, 6-tetrahydropyridine (MPTP) produced PD-like symptoms in man and the conversion of MPTP to its active form *in vivo* was found to occur *via* MAO-B (Markey, **1984**).
- **1988**-Bach and others confirmed the presence of two MAO isoforms, coded for by two separate genes by cloning human cDNA from liver. The organisation of the genes was described by Grimsby *et al* in **1991**.
- **1995**-Cases and colleagues engineered the first MAO knockout mouse.
- **1996**-Hauptmann and colleagues found that MAO generated H₂O₂ caused oxidative damage to mitochondrial DNA.
- **2001**-DeZutter and Davis described the MAO-A gene as a target for pro-apoptotic signalling.
- **2002**-The crystal structure of MAO-B was published by Binda *et al*.
- **2005**- The crystal structure of MAO-A was published by Colibus *et al*.

1.1.2 Structure and catalytic mechanism

1.1.2.1 Structure

The translated protein sequences of MAO-A and MAO-B cDNA show that the two enzymes differ in size, with MAO-A consisting of 527 amino acid residues (Mr 59700 Da) and MAO-B comprising 520 amino acid residues (Mr 58800 Da; Brown *et al.* 1980). Three-dimensional modelling of MAO-A and -B suggested that the overall tertiary structures and active sites are similar, both isoforms sharing 70 % amino acid homology (Geha *et al.* 2002). The overall structure of the monomers of human MAO-A is similar to that of human MAO-B and rat MAO-A, with the only significant structural difference being the conformation of the cavity shaping loop (DeColibus *et al.* 2005). Differences in quaternary structure were shown by elucidation of both MAO-A and -B crystal structures. Human MAO-B and rat MAO-A crystallise as a dimers (Binda *et al.* 2002, Ma *et al.* 2004), whereas human MAO-A crystallises as a monomer (DeColibus *et al.* 2005). The main difference between rat MAO-A and human MAO-B is in the structure of their active site cavities in the area opposite to the flavin coenzyme, which is responsible for their differing substrate and inhibitor affinities (Youdim *et al.* 2006).

A flavin co-factor, covalently linked to the enzyme by a cysteinyl thioester is required for both MAO-A and -B activities (Erwin and Hellerman 1967). Glu³⁴ and Tyr⁴⁴ are required for the initial binding of FAD and Gly²²⁶ and Asp²²⁷ are required for catalytic activity of

MAO-B (Zhou 1998). In MAO-A, Cys⁴⁰⁶ is important in FAD binding and Phe²⁰⁸ and Ile³³⁵ are crucial at the active site for substrate binding (DeColibus *et al.* 2005). Tyr⁴⁴⁴ and Tyr⁴⁰⁷ in MAO-A and Tyr³⁹⁸ and Tyr⁴³⁵ in MAO-B may form an aromatic sandwich that stabilises substrate binding (Geha *et al.* 2002). Both MAO-A and -B both contain a redox-active disulfide at the catalytic centre in addition to the flavin redox-active group (Sablin and Ramsay 1998) and both enzymes follow the same catalytic mechanisms. Significant differences in structure are attributed to differences in active sites that govern substrate specificity (Edmondson *et al.* 2007).

MAO is tightly bound to the outer mitochondrial membrane (Achee and Gabay 1977). In MAO-B amino acid residues 489-515 in the C-terminal form a transmembrane helix, 27 amino acids long (Binda *et al.* 2002) and in MAO-A amino acid residues 463-506 form the C-terminal membrane region which is 43 amino acids long (DeColibus *et al.* 2005). The insertion of MAO into the outer mitochondrial membrane has been suggested to occur via the recruitment of ubiquitin and energy generated by ATP (Zhaung and McCauley 1989, Zhaung *et al.* 1992). Recent work by Cruz and Edmondson (2007) showed that the entrance to the active site of MAO-A is situated at the mitochondrial surface. They suggested that the negatively charged surface may act to attract the protonated amine substrates towards the cavity and aid in deprotonation upon entering the active site.

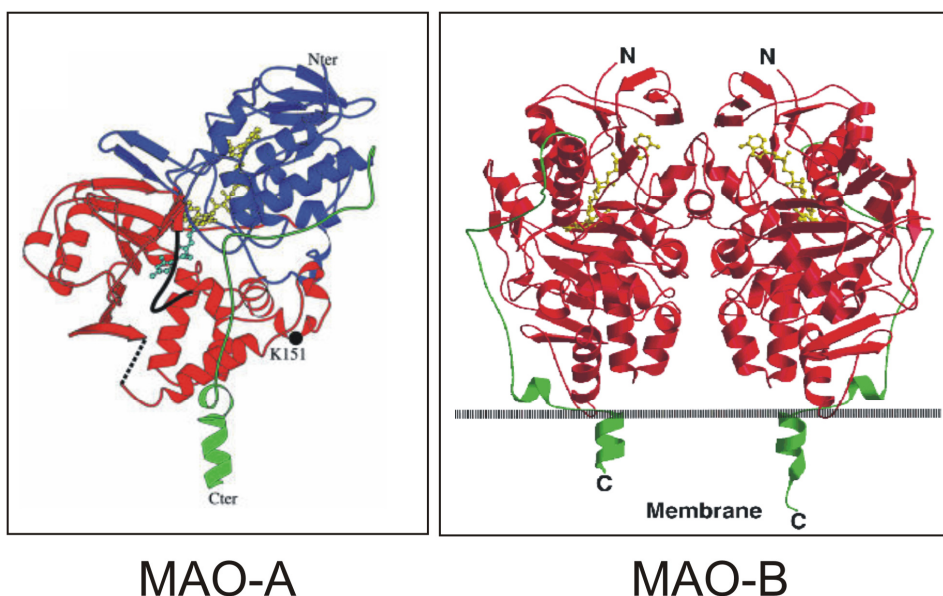


Figure 1. 1 Ribbon diagrams of the crystal structures of human MAO-A and -B elucidated by Binda *et al.* 2002, DeColibus *et al.* 2005.

MAO-A monomer, showing FAD binding domain (blue), substrate binding domain (red), C-terminal tail (green), clorgyline (cyan) and FAD (yellow, DeColibus *et al.* 2005). MAO-B dimer showing FAD (yellow) and C-terminal tail (green, Binda *et al.* 2002).

1.1.2.2 Catalytic mechanism

The oxidative deamination of amines by MAO is a two step catalytic reaction, which involves the formation of a intermediate imine, which quickly dissociates to form an aldehyde product (Berry *et al.* 1994). Step by step; the amine substrate in the presence of oxidised MAO, forms the intermediate imine and MAO is reduced. In the presence of oxygen, MAO is re-oxidised; hydrogen peroxide is produced (via the oxidation of reduced FAD (FADH₂) to the FAD cofactor). Finally, in the presence of water, the imine is converted to aldehyde and ammonia products. The mechanism has been simplified somewhat since other complex events occur during the reaction, described further by Ramsay and co-workers (1991 and 1998). The production of H₂O₂ by MAO and the ensuing biochemical effects were a primary concern in this work and therefore the characterised reaction of MAO shown below is adequate for the scope of this thesis.

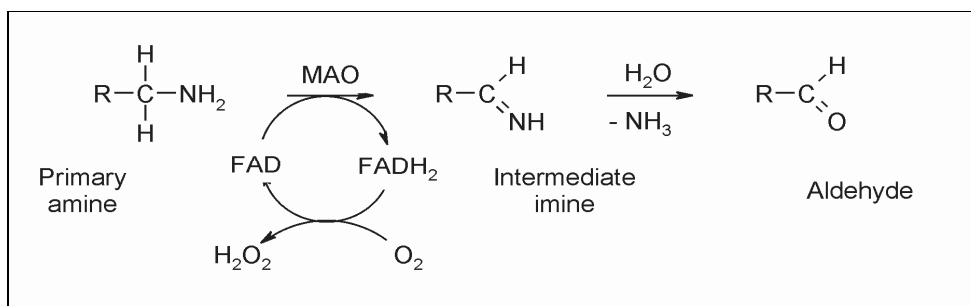


Figure 1. 2 Catalytic mechanism of amine oxidation by MAO

MAO catalysis is undertaken at the mitochondria where the enzyme is transported following its release from the polysomes. Following studies on MAO-A synthesised from reticulocytes and rat liver mitochondrial extracts, MAO-A was suggested to exist in a soluble but inactive form when it is released from the polysomes, but then binds to the OMM in the presence of ubiquitin and ATP and becomes active (Zhaung *et al.* 1992). However, the involvement of ubiquitin has never been confirmed and the question regarding whether MAO is active outside the OMM *in vivo* remains unanswered.

1.1.3 Isoenzyme classification

MAO specificity is relatively low compared to some enzymes, and substrates include all primary, secondary and tertiary monoamines attached to a free carbon chain (Berry *et al.* 1994). The existence of two forms of MAO was proposed on the foundation that there were different substrate and inhibitor affinities in *in vitro* enzyme assays (Johnston 1968). MAO-A preferentially deaminates 5-HT and NA and is inhibited by low concentrations of clorgyline, whilst MAO-B prefers benzylamine (BA) and β -PEA and is inhibited by low

concentrations of L-deprenyl (Gerlach and Riederer 1993). The substrates DA, tryptamine, octopamine and tyramine can be deaminated by both isoforms, although in human brain DA has a higher affinity for MAO-B (Riederer and Youdim 1986). Substrates described as being specific for one form or another however, can still be metabolised by either isoform *in vivo* and this depends on three parameters: concentration, affinity and turnover. Cellular compartmentation of MAO may also be responsible for determining substrate specificity (Waldmeier 1987). For example, in neurons where there is very little if any MAO-B, the metabolism of DA will be undertaken largely by MAO-A. Yet in extra-neuronal cells such as astrocytes (which are MAO-B rich) the proportion of DA deaminated by MAO-A decreases.

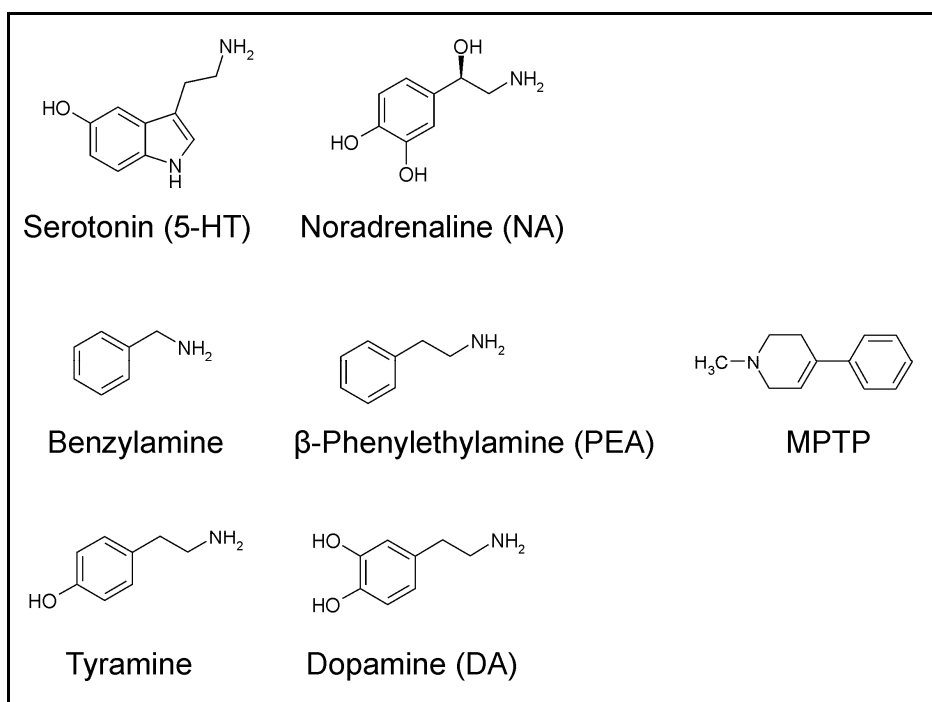


Figure 1.3 Chemical structures of some substrates of MAO-A and -B

Top-some preferred substrates of MAO-A. *Middle*-some preferred substrates of MAO-B and *Bottom*-some substrates of both MAO isoforms.

1.1.4 MAO inhibitors

As previously described, MAO-A and -B are commonly characterised by their specific and irreversible inhibition by low concentrations of the inhibitors clorgyline and deprenyl respectively. The therapeutic use of deprenyl in PD and the anti-apoptotic properties of propargylamines are discussed further in sections 1.2.2.2 and 3.3. The MAO inhibitors clorgyline and tranlycypromine (TCP) were used in this work and some preliminary studies were undertaken using moclobemide (Figure 1. 4). These MAO inhibitors are used clinically for the treatment of depression and the anti-depressant properties of MAO

inhibitors result from the selective inhibition of MAO-A in the central nervous system (CNS), which leads to increased levels of DA, NA and serotonin 5-HT (Youdim *et al.* 2006). Clorgyline is a highly specific and irreversible inhibitor of MAO-A and belongs to a group of MAO inhibitors known as the propargylamines because they contain a propargyl moiety. This inhibitor initially binds MAO-A reversibly, but then becomes oxidised by the enzyme to become active, covalently binding to the active site via the FAD cofactor, thus rendering it permanently unavailable for amine metabolism (Foley *et al.* 2000). Clorgyline has previously been shown to protect against apoptosis (DeZutter and Davis 2001) and serum withdrawal-induced loss of cell viability (Ou *et al.* 2006). However, irreversible MAO-A inhibitors are not often used clinically because of the “cheese effect”, so called because of potentiation of the sympathomimetic action of dietary tyramine (Youdim and Finberg 1987) and cheese contains lots of tyramine. The Inhibitors TCP and moclobemide are still in clinical use. Moclobemide does not contain a propargyl group and is a reversible and competitive inhibitor of MAO-A (Ramsay 1998). TCP is a non-selective MAO inhibitor that does not contain the propargyl moiety, but interacts irreversibly with the flavin group. TCP is effective in the treatment of phobic anxiety and atypical depressions such as hysteria and bulimia for which they are superior to amine re-uptake inhibitors (Youdim *et al.* 2006).

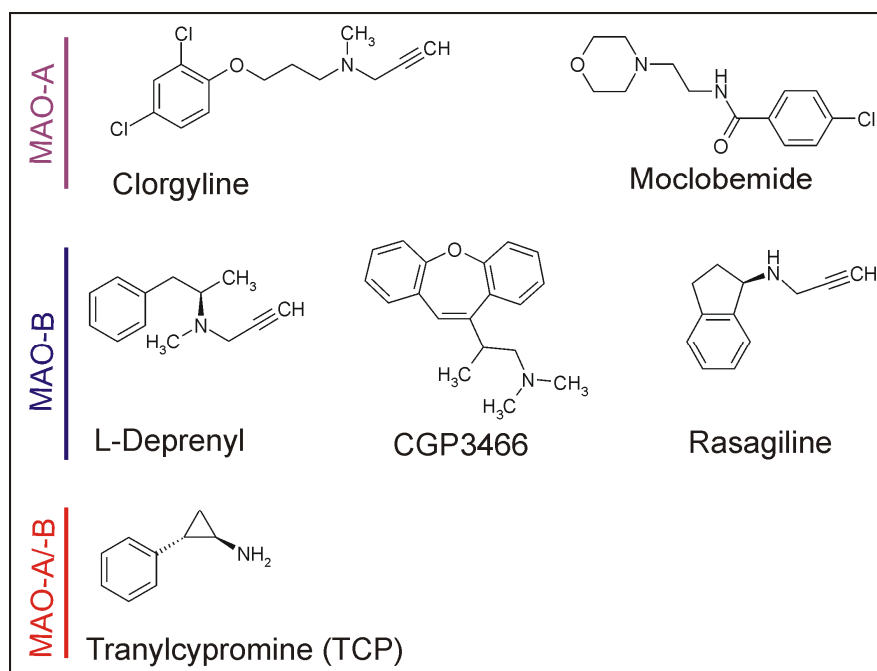


Figure 1. 4 Chemical structure and specificity of some MAO inhibitors

1.1.5 Distribution and physiological significance of MAO

The physiological functions of MAO are primarily the metabolism of amines and secondly, the regulation of neurotransmitter levels and intracellular amine stores (Billett 2004). MAO enzymes are widely distributed in various peripheral organs and the expression of the isoenzymes depends on distribution, development, ageing and hormonal environment (Bompart *et al.* 2001). MAO-B mainly acts on small exogenous amines, whereas MAO-A carries out the degradation of bulkier endogenous amine neurotransmitters (Binda *et al.* 2002). In mammals, MAO has been identified in all cell types excluding erythrocytes (Berry *et al.* 1994). In the majority of tissues MAO-A and -B isoforms seem to co-exist (Westlund 1988). However, some tissues only express single forms of MAO, namely platelets and lymphocytes (Bond and Cundall 1977), which only express MAO-B and placenta, which only expresses MAO-A (Sivasubramaniam *et al.* 2002). The highest levels of MAO-A activity in humans are found in the liver, lung and intestines (Tipton 1973) whereas the highest levels of MAO-B are found in brain and liver (Glover and Sandler 1986, Tipton 1973). The ratio of MAO-A/MAO-B in the human brain depend on age (Fowler *et al.* 1980a).

The distribution of MAO in human brain has been examined by means of immunohistochemistry (Westlund 1988, Finch *et al.* 1995), which revealed that MAO-A is found predominantly in adrenergic and noradrenergic neurons and MAO-B in serotonergic and histaminergic neurons as well as astrocytes. In 1996, Saura and others used quantitative enzyme radiography and *in situ* hybridisation to study the cellular distribution of MAO-A and -B in tissue sections of human brain. They concluded that sites of synthesis are the noradrenergic neurons of the locus coeruleus for MAO-A and the serotonergic neurons of the raphe and histaminergic neurons of the posterior hypothalamus for MAO-B. Neurons of the substantia nigra pars compacta (SNpc) contain small amounts of MAO-A and no MAO-B (Westlund 1988).

Within neurons, MAO regulates the levels of neurotransmitters released upon synaptic firing (Holschneider *et al.* 1998). Termination of a neurotransmitter's action depends on their reuptake into the nerve terminals, their dilution by diffusion out of the synaptic junction and their metabolic transformation. Uptake of neurotransmitters by glial cells and their metabolism via MAO-B also serves to regulate neurotransmitter action. In the gastrointestinal system, the circulatory system and the liver, MAO also serves a protective function to oxidise ingested amines and prevent them acting as false neurotransmitters. MAO has a similar function at the blood-brain barrier (Holschneider and Shih 2000). It has

been hypothesised that the existence of two MAO isoforms may be important in maintaining the specificity of function of catecholaminergic and serotonergic neurons, for example, MAO-A may help eliminate serotonin in dopaminergic and noradrenergic neurons whilst MAO-B may eliminate dopamine and phenylethylamine from serotonergic neurons (Westlund 1988). A secondary function of limiting these neurotransmitters may be the resulting altered release of hormones; hence MAO may function indirectly as a regulator of neuroendocrine function (Holschneider and Shih 2000).

1.1.6 MAO Genetics

In 1979, Cawthon and Breakefield suggested that MAO-A and MAO-B were coded for by two separate genes, following peptide mapping studies. Their functional differences became more apparent when it was shown that the two isoforms had conformational differences in their active site (Chen *et al.* 1985). Successful MAO-A and MAO-B cDNA clones from human liver showed that molecular attributes were positively allocated to two different genes and the amino acid sequence of both MAO isoforms were published (Bach *et al.* 1988). The primary amino acid sequences for MAO-A and -B show approximately 70% homology and similar hydrophobicity indices (Bach *et al.* 1988). The FAD binding site was revealed to be in the same position for both MAO-A and -B (Bach *et al.* 1988).

Both MAO genes are located on the X chromosome (Breakefield *et al.* 1980, Kochersperger *et al.* 1986). Later, by utilising full length MAO-A and -B cDNA clones and data from mapping studies in humans with Norrie's disease, the MAO-A and -B genes were found to be close to each other and close to the DXS7 locus on the X chromosome at position Xp11.23 (Lan *et al.* 1989). The genes span at least 60 kb and have 15 exons with identical intron-exon organisation. Exon 12 codes for the covalent FAD binding site in both isoforms and is the most conserved exon, with MAO-A and -B sharing 93.9 % peptide identity (Grimsby 1991), suggesting a common ancestral gene. The two genes were shown to be arranged in a tail-to-tail configuration with CpG islands at the 5' end in each case and the 3' coding sequences separated by around 50 kb (Chen *et al.* 1992).

The promoter regions for MAO-A and -B genes have been characterised. The promoter fragments for both enzymes are GC rich and contain Sp1 binding sites (Zhu *et al.* 1992). Sp1 is a ubiquitous transcription factor shown to be involved in tissue specific regulation (Saffer *et al.* 1991).

Hotamisligil and Breakefield (1991) determined the coding sequence of mRNA for MAO-A. The MAO-A promoter shows bi-directional activity and a repeat element and a number

of repeats that have been related to differential promoter activity. The core promoter region of MAOA contains two 90 bp repeats, each of which contains GC rich elements that are potential binding sites for Sp1 transcription factors, and lacks a functional TATA box (Zhu *et al.* 1994).

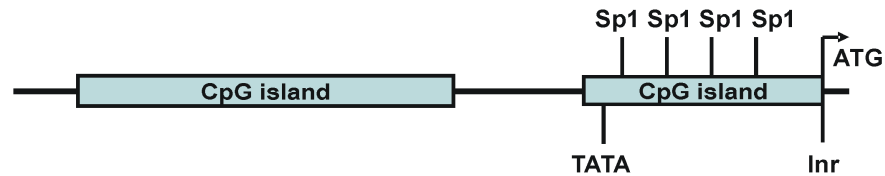


Figure 1. 5 A schematic diagram of the MAO-A promoter

These GC elements bind Sp1 but also a repressor, R1 (RAM2), which is able to inhibit MAO-A gene transcription (Chen *et al.* 2004a).

The human MAO-B gene is also under the control of GC elements (Wong *et al.* 2001). The MAOB core promoter region contains two sets of overlapping Sp1 sites which flank a CACCC element all upstream of a TATA box (Zhu *et al.* 1992).

1.2. NEURODEGENERATION

Due to the pharmacological importance of neurotransmitter metabolism, MAO has been the focus of extensive research with approximately 20,000 papers in the literature since the 1950s (Edmondson *et al.* 2007). Association of MAO expression with certain human conditions has been an immense area of research, with ageing, neurodegenerative diseases and affective disorders linked with MAO. The physiological relevance of both increased and decreased MAO expression is discussed further in chapter 5 (section 5.1) and chapter 6 (section 6.1) respectively. Since, neurodegeneration is of particular relevance to this thesis; this section aims to introduce several neurodegenerative diseases (specifically PD), their supposed aetiology and the role of MAO in their pathobiology.

1.2.1 Common pathobiology

The cause of neurodegenerative diseases (NDs) such as PD and Alzheimer's disease (AD) is extremely complex and the underlying mechanisms are still being elucidated. It is generally accepted that susceptibility to ND results from a combination of genetic, environmental and cumulative factors. Certain features are common to all ND and these include: loss of neuronal cells in key areas of the brain, dysfunction of key cellular mechanisms, protein damage, reduced protein clearance, cellular inclusions and increased

oxidative stress. Whether or not these factors are the cause and/ or the consequence of the diseases remains unknown.

The death of neuronal cells is ultimately responsible for the symptoms of neurodegenerative diseases. MAO is important in ND, not only because of its ability to regulate neurotransmitters (which are dysfunctional in ND), but also because it is thought to be involved in regulating cell death mechanisms. Atypical expression of MAO may have some implications in the aetiology of NDs and could provide a target for new therapies and/ or prevention of these diseases.

1.2.2 Parkinson's Disease

PD is a common neurodegenerative movement disorder first described in 1817 by James Parkinson, of which the progressive form of the disease affects 1-2 % of the population over the age of 65 (Mouradian 2002). The core clinical features of the disease include bradykinesia, tremor and rigidity (Ghandi and Wood 2005) and the primary pathology is characterised by degeneration of DA-containing neurons in the substantia nigra pars compacta (SNpc), where 80 % of dopaminergic neurons have been lost (McNaught 2001). Alongside neuronal loss, the presence of Lewy body inclusions are a pathological hallmark of PD and have been reported not only in the SNpc, but also in the cerebral cortex, anterior thalamus, hypothalamus amygdale and basal forebrain (Galvin *et al.* 1999).

1.2.2.1 Molecular pathogenesis of PD

The most common form of PD is the progressive or sporadic form, which is usually associated with old age, however, there are also genetic forms that exists, which can develop early in life (also known as early-onset PD, Mouradian 2002). Genetic mutations causing PD are rare, accounting for only 5-10 % of the overall PD population. However, the striking, consistent specific phenotype of both forms of PD has led researchers to believe that a common set of molecular mechanisms underlies PD (Ghandi and Wood 2005).

The supposition that sporadic PD may be a result of a combination of environmental toxins which cause *mitochondrial dysfunction* is supported by findings that mitochondrial complex I inhibitors such as rotenone (described in chapter 4, section 4.1) and MPTP reproduce PD features with dopaminergic neuronal loss *in vivo* (Burns *et al.* 1983) and *in vitro* (E.g. De Girolamo 2001, Caneda-Ferron *et al.* 2008). MPTP is a synthetic neurotoxin produced by attempts to synthesise the reverse ester of meperidine, an analogue of heroin (Langston *et al.* 1983). *In vivo* MPTP is oxidised in glial cells by MAO-B to the

intermediate MPDP⁺ which then auto-oxidises to form the active neurotoxin 1-methyl-4-phenylpyridinium (MPP⁺). MPP⁺ is then taken up by a dopamine transport mechanism into dopaminergic neurons (Song and Ehrich 1998). MPP⁺ accumulates in mitochondria (Murphy *et al.* 1995) and inhibits complex I of the mitochondrial electron transport chain (Nicklas *et al.* 1985) resulting in ATP depletion, the formation of free radicals and cell death.

The mitochondrial dysfunction hypothesis in PD is further supported by studies of rare familial forms of PD, where a variety of genetic mutations have been identified. It is the case, that many of the wild type proteins coded for by these genes are often mitochondrially localised and have putative roles in mitochondrial protection. For example, overexpression of the mitochondrial DJ-1 (mutated in some rare forms of PD) appears to protect cells against mitochondrial complex I inhibitors and oxidative stress (Canet-Aviles *et al.* 2004). Mutations in mitochondrial kinase, PINK1 and serine protease HtrA2/Omi both cause mitochondrial dysfunction leading to ND with PD features. It is now known that PINK1 and HtrA2 proteins interact to protect the mitochondria from stress (Plun-Favreau *et al.* 2007).

Mutations in certain genes encoding proteins involved in the **protein aggregation**, protein clearance and the ubiquitin-proteasome pathway are also associated with familial forms of PD. In brief, the **ubiquitin-proteasome pathway** (UPP) degrades unwanted, misfolded or damaged proteins via a cycle of events involving the tagging of proteins for degradation by ubiquitin, the action of certain ligases and finally proteolysis by the proteasome (For an overview see Hershko 1992). Dysfunction of the UPP in PD has been the focus of many publications over the last 20 years, yet there is limited evidence that the UPP is impaired in PD (McNaught *et al.* 2001). However, mutations in genes that code for components of the UPP, such as the E3 ligase Parkin, are known to cause early onset PD (Burke 2008). A recent study has shown that overexpression of wild type Parkin suppresses the expression of MAO-A and -B *in vitro* (Jiang *et al.* 2006), suggesting that MAO may be a target of signalling via regulatory pathways such as the UPS (see section 6.1).

The common underlying feature in PD aetiology is **oxidative stress**, which is the result of unregulated production of reactive oxygen species (ROS). High oxygen consumption, relatively low antioxidant levels and low regenerative capacity result in brain tissue being susceptible to oxidative damage (Barnham *et al.* 2004). In addition, elevated concentration of iron in the SNpc, can act as a catalyst in the Fenton reaction for the formation of

hydroxyl radicals from H₂O₂ (Gu *et al.* 1998). Oxidative damage may be a result of ageing and progression of the disease, but may also contribute further to its progression since oxidative stress is involved in cell signalling, cell death and inflammation (Dunnett and Bjorklund 1999).

1.2.2.2 MAO and PD

The oxidative degradation of DA catalysed by MAO generates hydrogen peroxide, a cellular toxin and a source of free radicals. Therefore MAO catalysis may be considered a major source of oxygen-derived toxic compounds in dopaminergic neurons. The increased turnover of DA in PD might explain the oxidative stress observed in the SNpc (Damier *et al.* 1996). Numerous studies have revealed increased MAO expression in PD (discussed in chapter 6, section 6.1). However there is still some debate over these findings, since the most of the work has been done on circulatory MAO-B in platelets.

The symptoms of PD can be alleviated by the administration of L-DOPA, a dopamine precursor, or similar drugs that manipulate striatal dopamine function such as dopamine agonists, dopamine transport blockers or inhibitors of dopamine degrading enzymes catechol-O-methyl transferase (COMT) and MAO-B (Dunnett and Bjorklund 1999). Since MAO activity may be indirectly elevated following administration of L-DOPA, it was thought that L-DOPA could be neurotoxic, indeed, some studies found that administration of L-DOPA caused oxidative stress (Lai and Yu 1997) and inhibited complex IV of the mitochondrial electron transport chain (Pardo *et al.* 1995) in human neuroblastoma cells *in vitro*. However, Mytilineou and colleagues (2003) showed that L-DOPA is toxic to dopamine neurons in an *in vitro* but not an *in vivo* model of oxidative stress. L-DOPA, often in conjunction with MAO-B inhibitors, continues to be the mainstay treatment for PD today. Since Knoll and Magyar developed L-deprenyl in the 1970s many new and better MAO inhibitors have been developed. Some propargylamine inhibitors are thought to have anti-apoptotic and neuroprotective effects that are not a result of MAO inhibition *per se*. For example, the MAO-B inhibitor Rasagiline is thought to protect neuronal apoptosis via a mechanism involving up-regulation of the anti-apoptotic protein Bcl-2, PKC and prevention of nuclear transcription of apoptotic proteins (Maruyama *et al.* 2000, Maruyama *et al.* 2002, Youdim *et al.* 2003). Currently in phase III trials for PD, the MAO inhibitors TCH346 and CGP3466 (see Figure 1. 4) are thought to delay or prevent PD by promoting neuronal survival. MAO inhibitors are now being seen as inhibitors of ND as well as simply slowing dopamine catabolism (Youdim *et al.* 2006).

1.2.3 Alzheimer's and other neurodegenerative diseases

1.2.3.1 Alzheimer's disease

Alzheimer's disease (AD) is distinct from PD, since it is mainly catecholaminergic neurons that are lost. AD is recognised as being the most common form of dementia, accounting for about 50-70 % of the late-onset cases of dementia (Hardy 1997). AD is typically a progressive disease that eventually leads to the degeneration of synaptic afferent systems, dendritic and neuronal damage, and the presence of large numbers of neuritic plaques and neurofibrillary tangles (Isacson *et al.* 2002). The plaques are largely extracellular lesions consisting of a peptide called amyloid. The neurofibrillary tangles are usually intracellular and consist of twisted bundles of the cytoskeletal protein tau (Hardy 1997). The key areas of the brain affected are those associated with thought, language and learning, namely the hippocampus, basal forebrain and cerebral cortex respectively (Highfield 2001). 20% of AD cases are thought to be a result of a genetic mutation (Highfield 2001). Genes identified to be dysfunctional in AD include the amyloid precursor protein (APP, which processes the formation of amyloid), and presenilins (Hardy 1997). There is some evidence that MAO levels are increased in AD (see chapter 5, section 5.1) and the MAO-B inhibitor deprenyl has been shown to be therapeutic in AD by reducing free radical production in the brain (Thomas 2000, Emilsson 2002, Riederer *et al.* 2004). Free radicals have been shown to increase abnormal cleavage of APP to produce increased β -amyloid, which in turn generates more free radicals (Emilsson 2002).

1.2.4 Huntington's disease and Pick's disease

1.2.4.1 Huntington's disease

Huntington's disease (HD) is caused by an abnormal polyglutamine expansion within the protein huntingtin and the characteristic hallmarks are inclusion bodies containing aggregated huntingtin protein in striatal neurons (Arrasate *et al.* 2004). The formation of these inclusion bodies is thought to be a coping mechanism in order to sequester the toxic mutant protein (Arrasate *et al.* 2004). The underlying causes of HD are not known but mitochondrial dysfunction and excitotoxicity have been proposed to be a major factor. DA toxicity mediated by MAO has been suggested to be involved in mitochondrial dysfunction (Jakel and Maragos 2000) in HD. Indeed, increased MAO-B activity in platelets of patients with HD has been observed (Mann *et al.* 1980)

1.2.4.2 Pick's disease

Pick's disease and the closely related frontotemporal dementia are rare dementias, with a frequency of around 1 % that of AD. The principal pathologies include gross depletion of neurons in the frontal lobe and distinctive inclusions known as Pick's bodies. Alfons Pick described the clinical features in 1892 and the inclusion bodies were first described by Alois Alzheimer in 1911 (Morris 1995). Although Pick's disease is degenerative, age is not a major factor, with onset ranging between 30-60 years of age (Wise *et al.* 1995). 20 % of cases are due to a genetic mutation that is autosomal dominant (Wise *et al.* 1995). The Pick's bodies contain tau proteins, ubiquitin and neurofilaments and resemble neurofibrillary tangles. The molecular mechanisms underlying this disease are unknown at present; however MAO-A and -B activities were found to be increased in different areas of Pick's diseased brains following *post mortem* (Sparks *et al.* 1991), therefore MAO inhibitors may be therapeutic.

1.3. FREE RADICALS AND OXIDATIVE STRESS

A free radical is any chemical species capable of independent existence that contains one or more unpaired electrons (Halliwell and Gutteridge 2007). Reactive oxygen species (ROS) is a collective term that includes not only oxygen radicals but some non-radical derivatives of O₂, such as H₂O₂. Reactive is a relative term; superoxide (O₂^{•-}) and H₂O₂ are highly selective in their reactions with biological molecules, whereas the hydroxyl radical (OH[•]) is highly reactive, attacking everything around it (Halliwell and Gutteridge 2007).

Radicals	Non-radicals
Superoxide	Hydrogen peroxide
Hydroperoxyl	Peroxynitrite
Hydroxyl	Peroxynitrous acid
Peroxyl	Nitrosoperoxycarbonate
Alkoxy	Hypochlorous acid
Carbonate	Hypobromous acid
Carbon dioxide	Ozone

Table 1. 1 Reactive oxygen species (Halliwell and Gutteridge 2007)

1.3.1 Hydrogen peroxide

Hydrogen peroxide is continually produced in many tissues *in vivo* and the steady state concentration in the cell is thought to be approximately 10⁻⁷ M (Giorgio *et al.* 2007). H₂O₂ is only a weak oxidising or reducing agent and is generally poorly reactive. Indeed, this probably allows it to play a role in signal transduction (Toledano *et al.* 2004). However, H₂O₂ is capable of inactivating some enzymes directly, usually by oxidation of sulfhydryl groups essential for catalysis and these enzymes include caspases and some protein

phosphatases. H_2O_2 can also oxidise certain keto-acids such as pyruvate and 2-oxoglutarate (Halliwell and Gutteridge 2007). Although there are few examples of the direct actions of H_2O_2 , cellular damage by H_2O_2 can be immense because H_2O_2 can react with iron or copper to form more damaging species such as OH^\bullet via the Fenton reaction (Halliwell and Gutteridge 2007).

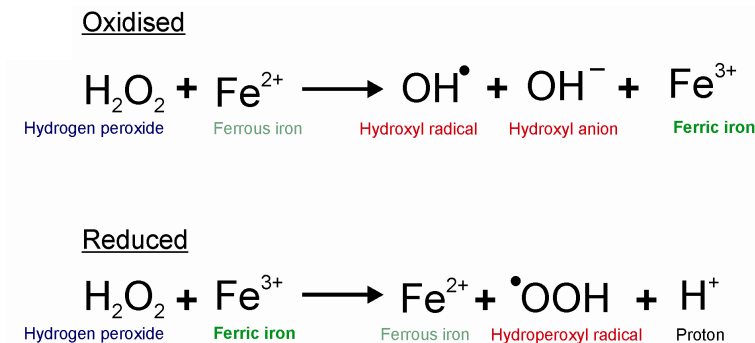


Figure 1. 6 The Fenton reactions

The production of H_2O_2 in the cell arises from the activity of certain enzymes including xanthine oxidase, urate oxidase, glucose oxidase and superoxide dismutase (SOD). Mitochondria are a major source of H_2O_2 , harbouring both MAO and the electron transport chain (ETC).

1.3.2 Mitochondrial ROS

The ETC is a well documented source of H_2O_2 from deprotonating O_2^\bullet . The ETC can generate O_2^\bullet from O_2 . During mitochondrial respiration, oxidative phosphorylation creates a flux of electrons through the ETC. The flux creates a proton gradient across the inner mitochondrial membrane (IMM) known as the protomotive force (Abou-Sleiman *et al.* 2006), which is used for the synthesis of ATP. Electrons are extracted from reduced substrates and are transferred to O_2 through the enzymatic steps involving the complexes I to IV. Cytochrome c ensures the complete reduction of O_2 to water. O_2^\bullet is generated if O_2 interacts with electrons upstream of complex IV, particularly complexes I and III (Giorgio *et al.* 2007).

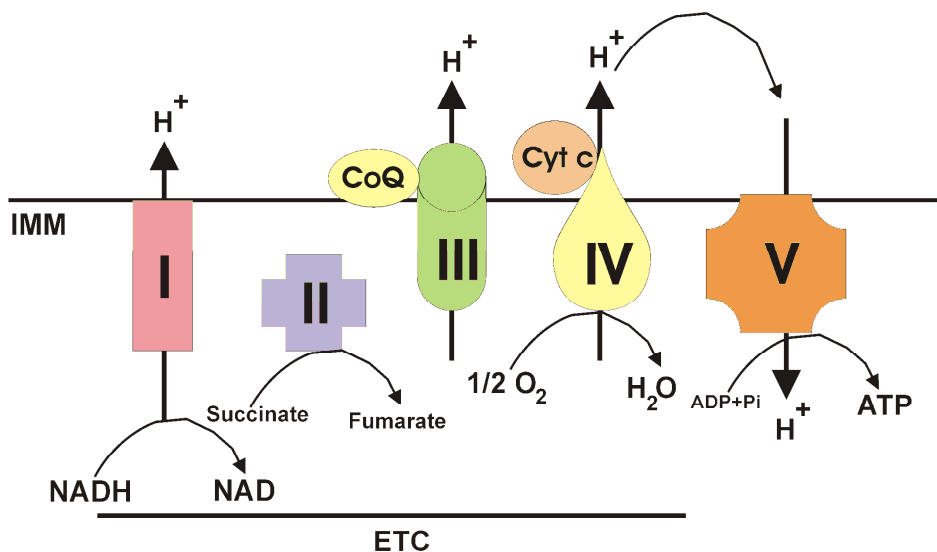


Figure 1. 7 Schematic representation of the electron transport chain (Abou-Sleiman *et al.* 2006)

The membrane spanning complexes of the ETC comprise complex I (NADH-ubiquinone reductase), which oxidises NADH, complex II (succinate ubiquinone oxidoreductase) which oxidises FADH₂, complex III (ubiquinol cytochrome c oxidoreductase) and complex IV (cytochrome c oxidase). The hydrophobic electron carriers coenzyme Q10 (CoQ) and cytochrome c (Cyt c) are also shown.

The high rate of O₂[•] production at the IMM is functionally related to the localisation of SOD in the matrix, which defines the steady state concentration of O₂[•]. The contribution of H₂O₂ at the OMM by MAO to cytosolic and mitochondrial steady state H₂O₂ concentrations is thought to have been underestimated and the steady state concentration of H₂O₂ in the mitochondrial matrix, from MAO activity alone has been calculated to be around 10⁻⁷ M (Cadenas and Davies 2000).

1.3.2.1 Mitochondrial damage

The generation of O₂[•] and H₂O₂ by the ETC in close proximity to active pools of copper and iron in the mitochondrial membranes can result in the formation of OH[•] via the Fenton reactions. OH[•] can attack the deoxyguanosine base of mitochondrial DNA (mtDNA) leading to mutations (Cadenas and Davies 2000). The production of H₂O₂ by MAO-mediated oxidation of tyramine in rat brain mitochondria elicited significant induction of mtDNA single strand breaks (Hauptmann *et al.* 1996). MAO-catalysed oxidation of DA and production of H₂O₂ inhibit active mitochondrial respiration and causes mitochondrial membrane permeabilisation resulting in mitochondrial swelling (Berman and Hastings 1999, see section 1.5). Uncontrolled, O₂[•] and H₂O₂ cause oxidative inactivation and proteolytic degradation of mitochondrial proteins (Cohen *et al.* 1997, Cadenas and Davies 2000). Indeed, subtle elevation of MAO-B levels *in vitro*, resulted in inhibition of α -ketoglutarate dehydrogenase and loss of mitochondrial flux (Kumar *et al.* 2003).

Metabolism of monoamines by MAO, by intact rat brain mitochondria suppressed pyruvate- and succinate-dependent electron transport, which was reversed by MAO inhibition (Cohen *et al.* 1997).

1.3.3 Antioxidant defences

The cell has a sophisticated antioxidant defence system that normally works in parallel with ROS production to eliminate excess free radicals and maintain steady state concentrations of H_2O_2 and other ROS.

1.3.3.1 Glutathione system

Cellular redox potential is largely determined by glutathione (GSH), a tripeptide of glutamate, cysteine and glycine, which is synthesised from its constituent amino acids in the cytosol of virtually all mammals (Domenicotti *et al.* 2003). Upon oxidative stress GSH may be oxidised to GSSG (oxidised glutathione) through the glutathione peroxidase (GPx) reaction. Oxidative stress in the cell results in an decreased in the GSH to GSSG ratio (Jahngen *et al.* 1997). Increased GSSG level often results in the covalent modification of sulfhydryl groups, which is known as glutathiolation. Enzymes that contain active site sulfhydryls are particularly vulnerable, and damage to proteins involved in both the ETC and UPP by glutathiolation has been reported (Cohen *et al.* 1997, Jahngen *et al.* 1997 respectively). PD is characterised by reduced GSH in the SNpc, including DA-containing neurons in this brain region (Pearce *et al.* 1997). Glutathione depletion triggers increases in both ROS and activity of PKC- δ , which leads to apoptosis and growth arrest in human neuroblastoma cells (Domenicotti *et al.* 2003). MAO-generated H_2O_2 is detoxified within the mitochondria by GPx and the resulting glutathiolation causes suppression of SH-dependent electron transport.

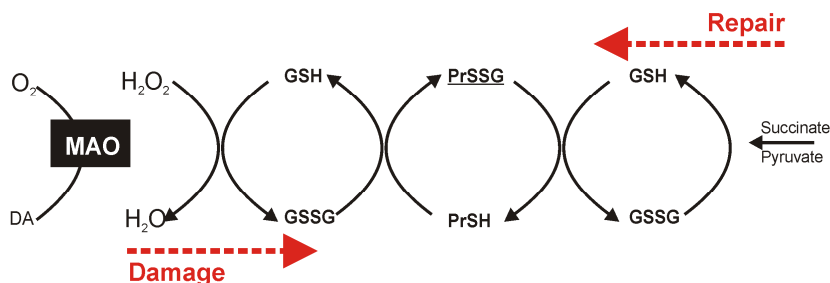


Figure 1. 8 Schematic representation of the MAO-dependent pathway for suppression of mitochondrial electron flow and subsequent recovery (Cohen *et al.* 1997).

Formation of GSSG forms disulfide linkages (Pr-SSG) with cysteine residues of proteins associated with the IMM resulting in suppression of ETC. This inhibition is relieved by reduction of GSSG by GSSG reductase, reversing the reaction that forms PrSSG (Cohen *et al.* 1997).

1.3.3.2 Superoxide dismutase and catalase

SOD exists as three isoforms, including a mitochondrial isoform that is important in converting $O_2^{\bullet-}$ to O_2 and H_2O_2 . The nuclear expression of mitochondrial SOD is known to be regulated by mitochondrial redox state (Kim 2005). Mutations in cytoplasmic forms of SOD are involved in 20 % of familial cases of amyotrophic lateral sclerosis (ALS, a neurodegenerative disorder), implicating antioxidant dysfunctions in ND aetiology (reviewed by Anderson 2004).

Catalase is only present in the cytosol and is an antioxidant enzyme that is capable of rapidly decomposing high concentrations of H_2O_2 but is inhibited by high concentrations of L-DOPA and dopamine in rat neuronal cells (Han and Cohen 1996), suggesting that DA toxicity or treatment with L-DOPA in PD may be damaging to cytosolic antioxidant defences. Antioxidants such as ascorbic acid (vitamin C) and α -tocopherol (vitamin E) also play an important role in detoxification (Schulz *et al.* 2000, see chapter 3, section 3.1).

1.3.4 Free radical production by MAO in neurons

DA is capable of autooxidation forming oxygen radicals, and products of DA such as quinones and neuromelanin. Most of the DA released into the synapse is stored in vesicles to be reutilised. However, some DA does not reach the vesicles but encounters MAO, where it is metabolised. MAO oxidation of dopamine results in increase in H_2O_2 , which is detoxified by GSH. In PD the neuronal levels of DA are low in the striatum. However, turnover of DA may increase during the disease process or during L-Dopa treatment (Adams *et al.* 2001).

Metabolism of monoamine substrates by MAO can result in the formation of a number of reactive oxygen species, primarily H_2O_2 , but also OH^{\bullet} , hydroperoxyl radical, aminium radical and iminium radical (Adams *et al.* 2001). MAO activity also yields aldehyde which can interact with aldehyde dehydrogenase to produce 3, 4-dihydroxyphenylacetic acid (DOPAC). Complex I activity oxidises NADH to NAD. NAD is used by aldehyde dehydrogenase in the oxidation of the aldehyde DOPAL (Adams *et al.* 2001). Reduced complex I activity may result in decreased catabolism of MAO metabolites. Moreover, levels of the toxic MAO-A metabolite, 3,4-Dihydroxyphenylglycolaldehyde (DOPEGAL) were increased in the locus ceruleus of AD brains (Burke *et al.* 1999), further implicating MAO derived toxic species in mechanisms of neuronal cell death.

1.4. CELL SIGNALLING

Cells communicate using a diverse network of signalling pathways which rely on transduction through proteins or hormones for example. For the scope of this thesis three important signalling modules will be discussed here; these include (1) protein kinase signalling, with emphasis on the mitogen activated protein kinase (MAPK) phosphorylation cascades, (2) apoptotic signalling (see section 1.5) and briefly (3) H₂O₂ as a signalling molecule.

1.4.1 Protein kinase signalling

Kinase enzymes transfer phosphate groups from high energy molecules such as ATP to specific residues of a substrate.

1.4.1.1 Protein kinase C

Protein kinase C (PKC) is so called because it is Ca²⁺ dependent. Rise in cytosolic Ca²⁺ levels triggers PKC translocation from the cytosol to the inner plasma membrane, where it interacts with membrane lipid, phosphatidyl serine, Ca²⁺ and diacylglycerol for activation (Alberts *et al.* 1994). Active PKC phosphorylates serine / threonine residues on target proteins such as MAPK and I κ B (which release NF κ B).

1.4.1.2 Phosphatidylinositol 3'-kinase and Akt/PKB

Phosphatidylinositol 3'-kinase (PI3-K) is important in regulating cell proliferation since it is activated by binding of growth factors to cell receptors (Brazil *et al.* 2004). It phosphorylates phosphatidylinositol at the 3' position hence the name. PI3-K activates Akt/PKB because Akt/PKB requires the formation of phosphatidylinositol (3,4,5)-triphosphate (PIP₃) in order to translocate to the plasma membrane where it is phosphorylated and activated (Alberts *et al.* 1994). Akt/PKB signalling is critical for cell cycle progression, apoptosis and transcription regulation. Akt/PKB controls the cell cycle at G1/S by blocking cell cycle inhibitors (Brazil *et al.* 2004). Activation of Akt/PKB can be inhibited by PTEN and can bind to extracellular regulated kinase (ERK) to regulate apoptosis (Brazil *et al.* 2004). Akt/PKB inhibits Raf (a MAP kinase kinase kinase [MEKKK]) important in MAPK signal transduction and blocks apoptosis by inhibiting BAD (Brazil and Hemmings 2001).

1.4.1.3 Ras signalling

Ras is a G-protein, a regulatory hydrolase that cycles between an active and an inactive form. Ras is attached to the cell membrane and a crucial factor in transducing mitogenic

signals as a result of ligand-receptor binding (Alberts *et al.* 1994). Active Ras activates Raf (a MEKKK), which triggers a cascade of phosphorylation known as the MAPK pathway.

1.4.2 Mitogen activated protein kinase (MAPK) signalling

MAPK pathways are activated by a wide range of signals including growth factors, mitogens, cytokines and stress. The general structure of the pathway is a three tier serine/threonine phosphorylation cascade where upstream MAP kinase kinase kinase (MAPKKK) activate MAP kinase kinase (MAPKK), which activate MAP kinase. Three well characterised MAPK pathways have been the focus of immense study. The MAPK targets of these pathways are extracellular regulated kinase (ERK), c-jun terminal regulated kinase (JNK) and p38. It is generally thought that ERK1/2 is activated by mitogenic/survival stimuli and that JNK and p38 are activated by stressful/pro-death stimuli. However, it is more likely that it is the balance between the pathways which is important, since lack of ERK1/2 stimulation may activate JNK/p38 (Xia *et al.* 1995, Wang *et al.* 1998). MAPK signalling pathways play a central role in survival/growth signalling and cell death pathways. JNK and p38 are important effectors in apoptosis in brain during neurodegeneration (Mielke and Herdegen 2000). Cellular stressors that may activate these pathways may include deprivation of growth factors, ionising radiation, free radicals and ROS, hypoxia, heat shock (Mielke and Herdegen 2000).

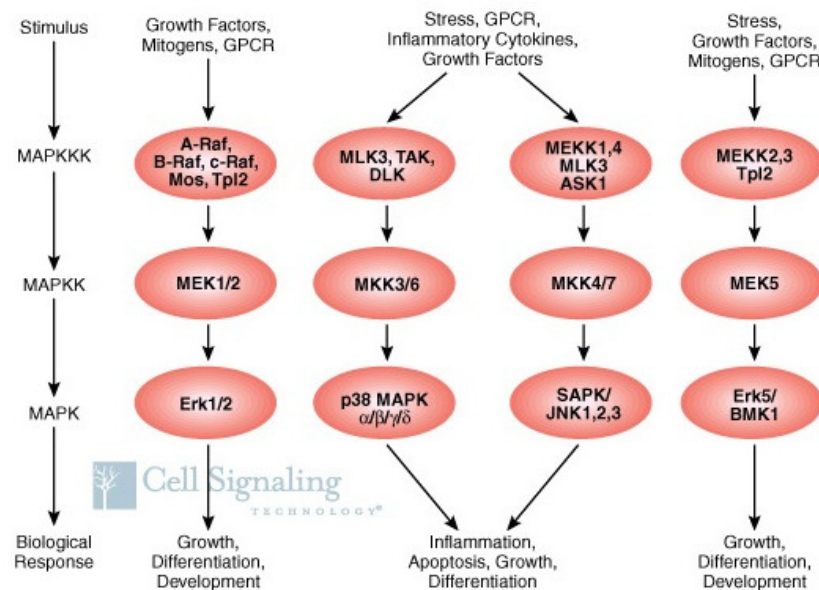


Figure 1. 9 MAPK phosphorylation cascade (From www.cellsignal.com)

1.4.2.1 ERK MAPK

ERK1/2 refers to the classical 44 and 42 kDa isoforms respectively, which are referred to in this thesis as ERK. The regulation of a large number of cellular processes is dependent upon the activation of ERK. ERK is localised in the cytoplasm and upon stimulation, detaches from its cytosolic anchor and translocates to the nucleus (Yung *et al.* 2000). In the nervous system ERK is critical for neuronal differentiation, plasticity and may modulate neuronal survival (Hetmen and Gozdz 2004). Mice lacking ERK fail to develop and die at embryonic stage 10.5 (Nishimoto and Nishida 2006). ERK plays a pivotal role in mitogenic signalling and apoptosis induced by withdrawal of growth factors and death receptors. Targets of ERK are mainly transcription factors or signalling molecules involved in pro-survival. Two examples include the targeting of transcription factors that transcribe cell cycle factors (Molnar *et al.* 1997) and inhibition of the pro-death protease caspase-9 by phosphorylation at a key threonine site (Allan *et al.* 2003). In contrast, ERK can be compartmentalised to restrict access to downstream targets and therefore can favour cell death in neurons following oxidative stress (Chu *et al.* 2004). The mechanism by which ERK promotes cell death is not known, however the balance between ERK (ERK1/2) and ERK5 may be important (Nishimoto and Nishida 2006). Ishikawa and Kitamura (1999) proposed that ERK has a dual role in the control of cell survival, since transient up-regulation of ERK participates in the induction of apoptosis, whereas basal, constitutive activity of ERK is required for maintenance of cell survival.

1.4.2.2 JNK MAPK

The JNK protein kinases are encoded by three genes that are expressed ubiquitously. The genes encode JNK proteins with or without a COOH-terminal extension, thereby forming a 46 kDa and a 55 kDa isoform (Davis 2000). The JNK pathway is activated by a large group of MAPKKK and activation of JNK has been reported following activation the Rho GTPase family, in response to cytokines and death receptors (Davis 2000). Commonly reported JNK substrates include the transcription factors c-jun and ATF-2, which regulate a range of cellular responses including cell proliferation, apoptosis and embryonic development (Dunn *et al.* 2002). JNK has a crucial role in phosphorylating substrates involved in cell death, for example the tumour suppressor p53, Fas ligand and mitochondrial proteins that are involved in cytochrome-c dependent death signalling (Davis 2000, Tournier *et al.* 2000). JNK signalling is important in neuronal survival (Harris *et al.* 2002). Phosphorylated JNK was found in cortical neurons with neurofibrillary tangles in Lewy body dementia, cytoplasmic granules in the vicinity of

Lewy bodies and α -synuclein deposits (Ferrer *et al.* 2001). In a mouse model of PD, JNK-mediated induction signalling was required for neurodegeneration in mice (Hunot 2003) and DA-induced apoptosis in an *in vitro* PD model (Luo *et al.* 1998). JKK1, an upstream activator of JNK, is activated in AD brains (Zhu *et al.* 2003) and the amyloid β -peptide 17-42, a major constituent in AD senile plaques, activates JNK and caspase-8 leading to cell death (Wei *et al.* 2002).

1.4.2.3 p38 MAPK

The p38 MAP kinases are activated by cellular stresses including ROS and cytokines (Enslin 1998) and play an important role in the regulation of gene expression (Hazzlan *et al.* 1996). The first p38 isoform to be identified was originally described as a 38 kDa polypeptide that underwent tyrosine phosphorylation in response to osmotic shock and was named p38 α . There are now four known p38 isoforms: p38 α , β , γ , and δ , which are differentially activated (Alonso *et al.* 2000). Activation of the p38 pathway results in the phosphorylation of various substrates. p38 can directly phosphorylate and activate a number of transcription factors including ATF-2, CREB, Elk-1, CHOP and MEF2C. Moreover, p38 can indirectly (via phosphorylation of the kinase MAPKAP-2 and Mnk1/2) phosphorylate tau protein in AD (Mielke and Herdegen 2000). Activation of the p38 pathway is strongly associated with activation of cell death pathways and inhibitors of p38 promote neuronal survival *in vitro* (Horstmann *et al.* 1998). Conversely, p38 is known to prevent apoptosis from occurring during cellular differentiation by activating the transcription factor MEF2 (Okamoto *et al.* 2000).

p38 seems to play a major role in gene regulation since it can also regulate gene expression at the post transcription level by stabilising mRNA in a mechanism involving adenosine and uridine rich elements (AREs) (Clark *et al.* 2003).

P38 Activated by	P38 Regulated by	P38 Substrates
MKK3 MKK6 TAK1 MEKK2 and 3 ASK1 TRAF 2, 5, 6 RIP	Rho family GTPases Heterotrimeric G proteins Adapter coupled proteins coupled to TNF receptors	MAPKAP kinases-2, 3, and 5 Myosin light chain Tyrosine hydroxylase PRAK MSK1/2 Tau MnK1/2 PLA2 Transcription factors: ATF-2, CREB, Elk-1, MEF2, CHOP, STAT1, MAX, c-Myc, HMG-14 and Histone -H3

Table 1. 2 Some characteristics of p38
(Enslin 1998, Woodgett 2000)

1.4.3 Regulation of MAO expression by protein kinase signalling

As previously described, the MAO-B gene can be regulated by Sp1 and Sp3 transcription factors (Wong *et al.* 2001). In 2002, Wong and colleagues described the activation of MAO-B gene expression via c-jun and Egr-1 transcription factors. In the promoter region of the MAO-B gene between -246 and -225 bp there are overlapping sequences that are recognised by Sp1, Sp3 and Egr-1 transcription factors. Phorbol 12-myristate 13-acetate (PMA) is known to increase Egr-1 and c-jun expression. PMA treatment increased MAO-B but not MAO-A gene expression. A PKC inhibitor blocked the PMA dependent activation of MAO-B and co-transfection with dominant forms of Ras, Raf-1, MEKK1, MEK1, MEK3, MEK7, ERK2, JNK1 and p38 inhibited the PMA-dependent activation of the MAO-B promoter (Wong *et al.* 2002). This study provided evidence that PKC and MAPK signalling pathways are important in PMA-induced MAO-B gene expression.

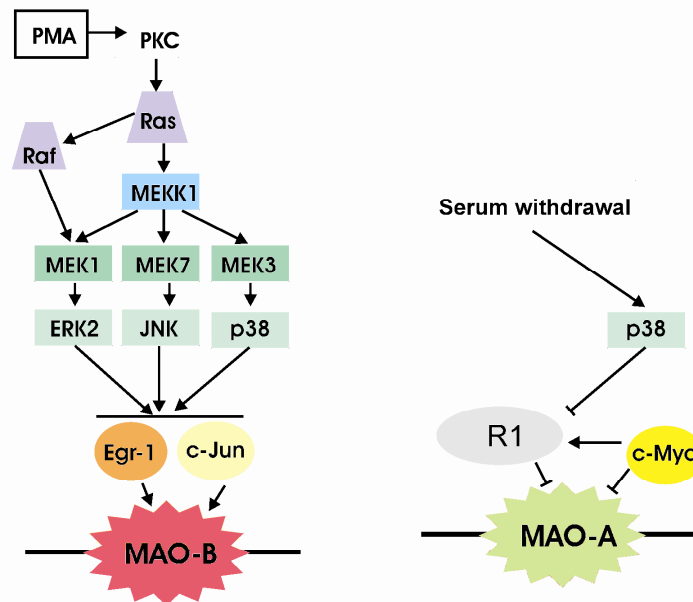


Figure 1. 10 Protein kinase signalling and MAO gene expression

Left panel-PMA induced PKC which in turn activates Ras and Raf and MEKK1 kinase. MEK1, 7 and 3 are phosphorylated, activating ERK2, JNK and p38 MAP kinases. Downstream targets of MAPK pathway are transcription factors Egr-1 and c-jun which induce gene transcription (Wong *et al.* 2002). *Right panel*-Serum withdrawal activates p38 MAPK which induces MAO-A gene transcription by inhibiting the repressor R1. The transcription factor c-Myc can repress MAO-A gene transcription directly, or indirectly by up regulating R1 expression (DeZutter and Davis 2001, Ou *et al.* 2006).

The MAO-A gene is under the control of the p38 MAPK signalling pathway in apoptosis induced by nerve growth factor (NGF) withdrawal. MAO-A gene expression was increased following NGF withdrawal and this was prevented by inhibition of the p38 signal transduction pathway (DeZutter and Davis 2001). In 2006, Ou and co-workers confirmed that the p38 MAPK signalling pathway was involved in regulating MAO-A expression

during apoptosis induced by serum deprivation. They also reported that JNK and ERK MAPK pathways were not involved in the regulation of MAO-A gene expression. The transcription factor c-Myc (involved in cell proliferation) was shown to induce expression of the MAO-A repressor R1 and inhibit MAO-A expression.

1.4.4 H₂O₂ as a signalling molecule

ROS can act as second messengers in signal transduction in a variety of cell types (Finkel 1998). H₂O₂-initiated cysteine-based redox signalling is tightly controlled by specialised H₂O₂ sensors in *Saccharomyces cerevisiae* (Toledano *et al.* 2004), suggesting that microbial H₂O₂ sensors are archetypal redox signalling modules. H₂O₂ functions as a signalling molecule in intracellular and oncogenic growth signalling. Induction of cell **proliferation** by growth factor binding correlates with transient increases in intracellular H₂O₂, mediated by MAPK and NF-κB pathways (Giorgio *et al.* 2007, Halliwell and Gutteridge 2007). H₂O₂ under certain conditions induces **senescence** (a permanent state of growth arrest) and at high concentrations is a potent inducer of apoptosis (Giorgio *et al.* 2007, Halliwell and Gutteridge 2007). Induction of senescence can occur via inactivation of caspases (Allan *et al.* 2003, Halliwell and Gutteridge 2007) and via the p53 checkpoint (Giorgio *et al.* 2007). **Apoptosis** is triggered by activation of various cell signalling pathways including MAPK pathways (Tan *et al.* 1998). H₂O₂ has a dose dependent effect, where generally low levels of H₂O₂ promote survival and high levels promote death (Yoon *et al.* 2002).

1.4.4.1 Targets of H₂O₂

Target(s)	Model	Reference
Growth factor signalling	Yeast and animal cells	Stone and Yang 2006
Modification of Gα _i and Gα _o proteins	Rat cardiomyocytes (primary culture)	Nishida <i>et al.</i> 2000
Reversible glutathionylation of ETC proteins	Isolated mitochondria from rat brains	Cohen <i>et al.</i> 1997
Reversible glutathionylation of complex I of the ETC	Isolated mitochondria from rat liver	Taylor <i>et al.</i> 2003
Reversible glutathionylation of α-ketoglutarate dehydrogenase	Mitochondria isolated from rat heart	Nulton-Persoson <i>et al.</i> 2003
Dopamine transport	Rat PC12 cells	Huang 2003
ERK, JNK and p38 pathways	Rat smooth muscle cells (primary culture)	Guyton <i>et al.</i> 1996
	Human cervical	Wang <i>et al.</i> 1998
Dual regulation of Caspase-3	Mouse (Jurkat) cells	Hampton and Orrenius 1997
Transforming growth factor (TFG-β)-induced increase in gene expression	Human mesangial cells	Inglesias-DeLaCruz <i>et al.</i> 2001
MAPK p38 in hypoxia	Mouse fibroblast cells	Emerling 2005
Cell proliferation via PI3-K/PKB pathway	Human hepatoma cells	Liu <i>et al.</i> 2002

Table 1. 3 Some reported cellular targets of H₂O₂ signalling

1.4.4.2 Targets of H₂O₂ generated by MAO

MAO-B produced H₂O₂ induces ERK-dependent cell mitogenesis in rat embryonic kidney cells (Vindis *et al.* 2000) and in rat renal epithelial cells (Vindis *et al.* 2001). Activation of ERK by H₂O₂ produced by MAO in rat renal epithelial cells leads to activation of apoptosis, which is reversible following MAO inhibition (Bianchi *et al.* 2003). Apoptosis induced by MAO-generated H₂O₂ has been reported to involve a common oxidative stress pathway which begins with H₂O₂ activating the JNK MAPK pathway, which through NFκB and c-jun signals increased p53 expression. Active p53 activates pro-apoptotic Bax which induced cytochrome-c release, activation of caspase-3 and execution of apoptosis (Del Rio and Velez-Pardo 2002).

1.5. CELL DEATH

The molecular definition of cell death historically has been distinguished in mammalian cells by morphological criteria. Type I cell death (known as *apoptosis*) is defined by characteristic changes in the nuclear morphology, including chromatin condensation and fragmentation; minor changes in cytoplasmic organelles; and overall cell shrinkage, blebbing of the plasma membrane and formation of apoptotic bodies. All these changes occur before plasma membrane integrity is lost. Type II cell death (known as *autophagy*) is characterised by the accumulation of double-membrane- autophagic vacuoles in the cytoplasm. Type III cell death (known as *necrosis*) lacks the characteristics of type I and II but can also be defined by early plasma membrane rupture and dialation of cytoplasmic organelles, particularly mitochondria (Golstein and Kroemer 2006). Necrotic cells swell and are internalised by a mechanism where only parts of the cell are taken up by the phagocytes (Golstein and Kroemer 2006), which often causes inflammation. Apoptotic cells usually shrink and are engulfed by phagocytes. Apoptosis is under the tight control of unique signalling pathways, which involve the activation of specialised proteases.

1.5.1 Apoptosis

Apoptosis (sometimes known as programmed cell death) comprises two major signalling pathways known as the mitochondrially mediated pathway (or intrinsic pathway) and the death receptor-mediated pathway (or extrinsic pathway). Apoptosis can also arise from the endoplasmic reticulum (ER) which is known as the stress-ER pathway.

1.5.1.1 Caspases

Caspases (cysteine-aspartate-specific proteases) are a family of proteins that initiate and execute the apoptosis. Caspases are highly specific in their substrate specificity since they cleave after aspartic acid residues (Hengartner 2000). At least 14 different caspases have been identified in mammals (Ashe and Berry 2003). Caspases stop the control processes that protect the cell from death and activate other caspases in a cascade of protease activity. Caspases are responsible for the executing the downstream processes that ultimately dismantle the cell via cleavage of a variety of substrates. Caspases cleave key components of the cytoskeleton, the nucleus, protein kinases and survival factors. Caspases can also activate degradation systems by activating nucleases, serine proteases, calpains and the proteasome. Caspases 1, 4, 5, 11, 12, 13 and 14 are responsible for cytokine activation and the inflammatory response, with the exception of caspase-12 which is involved in the stress-ER pathway. Caspases 2, 8, 9 and 10 are involved in the initiation of the apoptotic cascade and caspases 3, 6 and 7 are common to all apoptotic pathways since their activation represents the point of apoptotic execution, committing the cell to die and are therefore often described as executioners.

Caspase	Substrate(s)	Function
1	Pro-IL-1 β	Cytokine activation
2	α II spectrin, golgi-160, PKC	Apoptotic initiator associated with piddosome formation
3	Poly(ADP) ribose polymerase (PARP), DNA-PK, lamins, Fodrin, PKC and recruits serine proteases, calpains, proteasomes, DNaseI, NUC18, CAD and Pak1.	Central effector caspase responsible for the cleavage Of important proteins including JNK. Important in mediating apoptosis in the nervous system
4	PARP (closely related to caspase1)	Cytokine activation, maturation of caspase-1 Induces apoptosis at high concentrations
5	PARP (closely related to caspase1)	Cytokine activation and apoptosis at high concentrations
6	Caspase-3 and therefore substrates of caspase-3 but less active (~150 fold less)	Effector caspase via caspase-3
7	Same as caspase-3	Effector caspase important in receptor mediated apoptosis and mediator of cytotoxic T-cell killing
8	PARP, Bid and all known caspases including caspase-3	Apoptotic initiator essential in death receptor-induced apoptosis
9	Effector caspases	Apoptotic initiator essential for the formation of the apoptosome in the mitochondrially mediated pathway and under the control of ERK
10	Same as caspase-8	Apoptotic initiator activated through death effector domains (DEDs) and associated with death receptor-mediated pathway
12	Other caspases including caspase-9	Cytokine activation and essential in stress-ER pathway

Table 1. 4 Some substrates and functions of important caspases

(Bortner *et al.* 1995, Cohen 1997, Hengartner 2000, Nakagawa and Yuan 2000, Lassus *et al.* 2002, Salvesen 2002, Allan *et al.* 2003, Ashe and Berry 2003, Enemoto *et al.* 2003, Zhivotovsky and Orrenius 2005).

1.5.2 Mitochondria-mediated apoptosis

1.5.2.1 Bcl-2 family proteins

The mitochondrial outer membrane harbours the protein Bcl-2 and other anti-apoptotic members of the Bcl-2 family of proteins such as Bcl_{xL}. These are central regulators of apoptosis by integrating diverse signals from inside and outside the cell. They regulate apoptosis by opposing the pro-apoptotic Bcl-2 family members such as Bax, Bak and Bad. Bcl-2 family proteins control mitochondrial membrane permeability. The OMM can become perforated and proteins sequestered inside the mitochondria are then allowed to leak into the cytoplasm and participate in apoptotic signalling. Bcl-2 localises to other membranes including the nuclear envelope and the ER membrane, where it continues to protect the mitochondria (Thomenius and Distelhorst 2003). Bcl-2 localises to other membranes because it lacks a signal that directs other Bcl-2 family proteins such as Bcl_{xL} to the mitochondrial surface (Kaufmann *et al.* 2003). The localisation of Bcl-2 may be an important factor in regulating the survival/apoptotic balance. Regulation of pro- and anti-apoptotic Bcl-2 family members also involves the action of BH3-only proteins which act as sensors for apoptotic stimuli. Following stimulus, a BH3-only protein is modified and travels to the OMM where via its BH3 domain interacts with anti-apoptotic Bcl-2 proteins causing OMM perforation or interacts with pro-apoptotic family members stimulating their oligomerisation (Kaufmann *et al.* 2003). Bcl-2 can also change its conformation to inhibit Bax oligomerisation (Dlugosz *et al.* 2006), which is triggered by active Bid (Figure 1. 11).

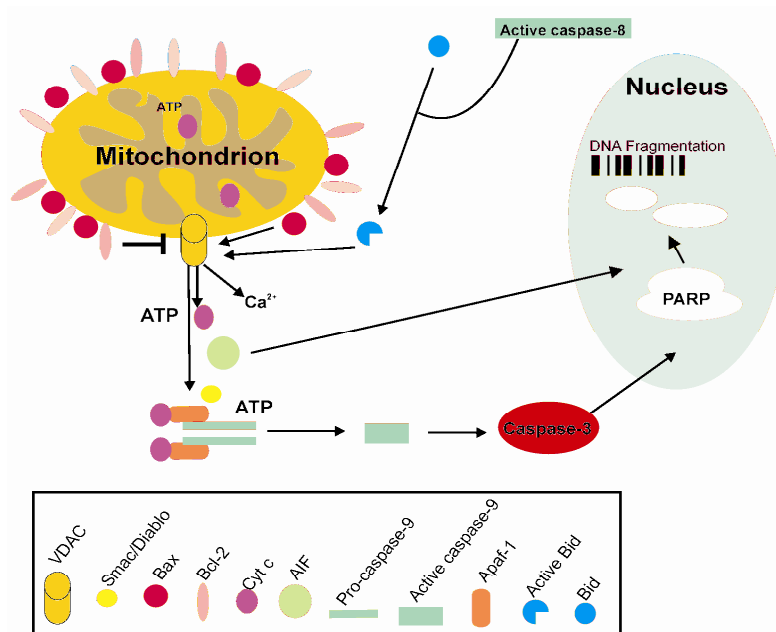


Figure 1. 11 An overview of the mitochondrially mediated apoptotic pathway

1.5.2.2 Mitochondrial membrane pore opening

The release of cytochrome c (Cyt-c) from the IMM is essential for the formation of the apoptosome (Figure 1. 11). Release of apoptosis inducing factor (AIF) from the mitochondria is also important since it translocates to the nucleus where it binds to DNA and promotes chromatin condensation (Figure 1. 11). AIF functions independently of caspases (Joza *et al.* 2001, Cande *et al.* 2002).

Prior to release of mitochondrial proteins, the mitochondrial membranes undergo morphological changes that resemble events associated with mitochondrial fission and fragmentation (Youle and Karbowski 2005, Arnoult 2006). However there is some debate as to whether these processes are essential for mitochondrial outer membrane permeability (MOMP). The alternative model proposes MOMP to be initiated at the IMM. Signals such as increased Ca^{2+} or ROS promote mitochondrial permeability transition (MPT) involving a permeability transition pore (PTP) complex. Major components of the PTP complex include the OMM located voltage-dependent anion channel (VDAC), the IMM protein called adenine nucleotide translocator (ANT) and cyclophilinD (CypD), which is resident in the matrix (Garrido *et al.* 2006). MOMP does not always occur through the PTP, osmotic swelling and rupture of the IMM can also release IMM proteins into the cytosol. Bcl-2 family members are also known to form low selectivity channels by undergoing oligomerisation (Hengartner 2000).

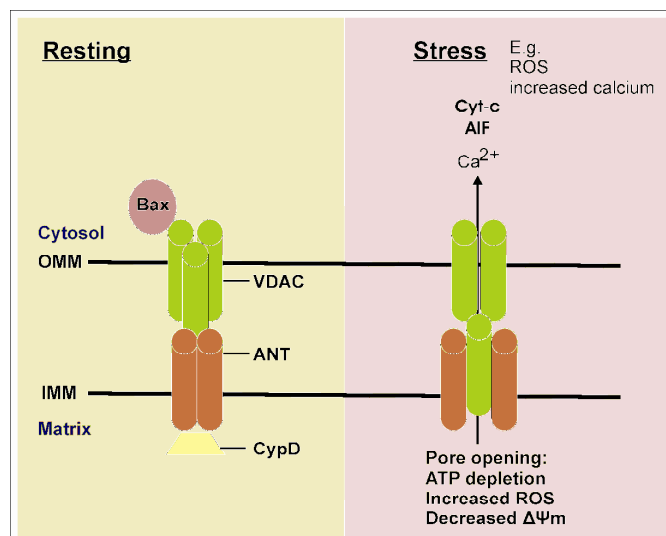


Figure 1. 12 Schematic of mitochondrial permeability transition (Abou-Sleiman *et al.* 2006)

1.5.2.3 Formation of the apoptosome and caspase activation

Once released from the mitochondria, Cyt-c interacts with the C-terminal domain of Apaf-1 and in the presence of ATP cause a conformational change in Apaf-1 that allows it to

undergo self oligomerisation into two complexes that recruit caspase-9 via its N-terminal caspase activation-recruitment domain (CARD) and allows the catalytic activation of caspase-9 that can then proceed to activate caspase-3 and -7 (Bratton and Cohen 2001).

1.5.2.4 Regulation by phosphorylation and apoptotic inhibitors

Mitochondria are primary control centres for energy production and survival/ death and recent studies have reported that phosphorylation by mitochondrial kinases, phosphatases and phosphoproteins is important in the regulation of mitochondrial processes. Some of these events have been characterised and include the phosphorylation of Bad by protein kinase A, the phosphorylation and dephosphoylation of pyruvate dehydrogenase, phosphorylation and inhibition of cytochrome c oxidase (Pagliarini 2006). Mitochondrially mediated apoptosis is also regulated by ‘inhibitor of apoptosis’ proteins (IAPs which suppress apoptosome formation). The mitochondrial proteins HtrA2/Omi and Smac regulate IAPs (Orrenius *et al.* 2003). Figure 1.13 shows an overview of mitochondrial signalling.

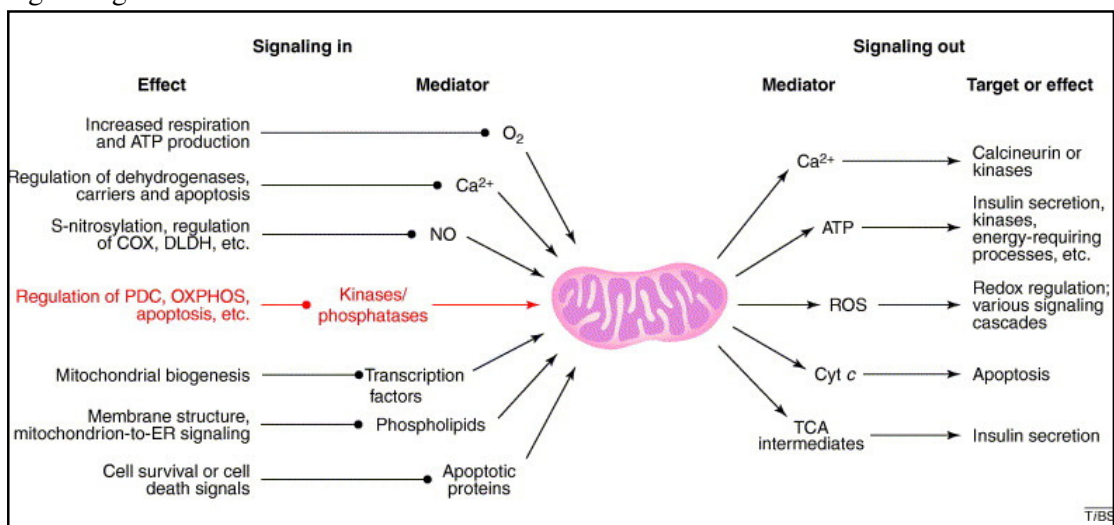


Figure 1. 13 An overview of mitochondrial signalling (Pagliarini 2006)

1.5.3 Death receptor-mediated apoptosis

Death receptor-mediated apoptosis is introduced in chapter 4, section 4.1.

1.5.4 Calcium and apoptosis

Cellular Ca²⁺ import through the plasma membrane largely occurs via receptor-operated, voltage sensitive and store-operated channels. Inside the cell, Ca²⁺ can interact with Ca²⁺ binding proteins or become sequestered into the ER or mitochondria. The cytoplasmic Ca²⁺ concentration is maintained by uptake into the ER and by extrusion into the extracellular space. Ca²⁺ release by the ER is regulated by phospholipase C. Mitochondria take up Ca²⁺

through a uniport transporter and can be released by either: reversal of uniporter Ca^{2+} exchange (through the PTP) and calmodulin regulated release (Orrenius *et al.* 2003). Mitochondrial Ca^{2+} fluxes are integrated parts of cellular signalling and uptake of Ca^{2+} by the mitochondria stimulates Ca^{2+} sensitive matrix dehydrogenases of the ETC. Ca^{2+} has two roles in apoptosis, one is by contributing to the calcineurin-catalysed phosphorylation of Bad and the other is regulation of OMM permeabilisation. As described previously, VDAC forms part of the PTP and VDAC becomes activated by a high concentration of Ca^{2+} . Opening of the PTP causes a rapid flux of Ca^{2+} into the cytoplasm. Depletion of intracellular calcium stores is toxic to neuronal cells (Nguyen *et al.* 2002). There is some evidence that Ca^{2+} may interact or play a role in Bcl-2 family function via Ca^{2+} mediated events that take place at the ER (Orrenius *et al.* 2003).

1.5.5 Apoptosis and neurodegeneration

A universal pathology in all neurodegenerative disease is the loss of neurons in key areas of the brain. Cell death is an important feature in the development of the nervous system and deficit of death in some circumstances can give rise to cancers. Apoptosis might serve to remove damaged or dysfunctional neurons as a protective mechanism and this may explain the evolution of mechanisms to regulate the cellular response to stress. It appears that the complexity of cell death signalling reflects the necessity for fine tuning the cellular response to deal with stressors accordingly.

Alzheimer's disease	Parkinson's disease
Altered expression of apoptosis-related genes (Bcl-2 family members, DNA response genes, p53) are found in neurons associated with plaque formation in AD brains (De La Monte <i>et al.</i> 1998, Mattson <i>et al.</i> 1998)	Bcl-XL is required for the proper development of the mouse SNpc (Savitt <i>et al.</i> 2005)
Neurons from caspase-2 and caspase-12 knockout mice are protected against β -amyloid induced apoptosis (Nakagawa and Yuan 2000, Troy <i>et al.</i> 2000)	Caspase-3 is a vulnerability factor and final effector in apoptotic death of dopaminergic neurons in PD (Hartmann <i>et al.</i> 2000)
Mutant presenelin-1 expression causes mitochondrial dysfunction and sensitises cells to apoptotic insults (Guo <i>et al.</i> 1999)	Mutations in the anti-apoptotic mitochondrial kinase PINK1 cause PD-like symptoms (Plun-Favreau <i>et al.</i> 2007)
Activation of caspase-3 and -9 and subsequent cleavage of tau leads to the formation of neurofibrillary tangles (Rohn <i>et al.</i> 2002)	Mutations in anti-apoptotic DJ1 cause early onset PD (reviewed by Burke 2008)

Table 1. 5 Evidence for apoptosis in AD and PD

1.6. OVERALL AIMS OF THESIS

The overall purpose of the work was to investigate the role of MAO in neuronal cell death. The first approach was to develop a variety of apoptotic models *in vitro* that would reflect the different types of apoptosis evident in neuronal cells *in vivo*. Three types of apoptotic cell death were induced in a human neuroblastoma cell line:

- (i) *Classic mitochondria-mediated* apoptosis was induced by the PKC inhibitor staurosporine;
- (ii) Chronic deprivation of serum was used to induce apoptosis associated with the *withdrawal of survival signals*, which include protein kinase signalling and up-regulation of pro-apoptotic genes;
- (iii) Mitochondrial *complex I inhibition* by rotenone was used to induce cell death that is associated with mitochondrial dysfunction and mimic the cell death observed in PD.

The role of MAO in these death processes was investigated by monitoring the levels of MAO mRNA, protein and catalytic activity. To uncover the mechanisms by which MAO may be involved in cell death, MAPK signalling pathways, Bcl-2 levels, ROS levels and caspase activation were examined in the presence and absence of two unrelated MAO inhibitors.

The second approach was to study the effects of MAO overexpression and knockdown in human neuroblastoma cells. The MAO status and general viability of the transfected cells was assessed and cell growth, ROS production, caspase activity and MAPK/apoptotic signalling components were monitored to verify the relevance of MAO in these cellular processes.

Finally, neuroblastoma clones with stable alterations in MAO expression were exposed to the three apoptotic inducers (described above) to confirm the role of MAO in different types of neuronal cell death.

CHAPTER 2

MATERIALS AND METHODS

MATERIALS AND METHODS

2.1. MATERIALS

Materials are listed with the company from which they were purchased.

2.1.1 Cell culture

2.1.1.1 Reagents

Dulbecco's Modified Eagles Medium (DMEM), Hank's buffered salt solution (HBSS), foetal bovine serum (FBS), penicillin/streptomycin, L-glutamine and trypsin-versene solution, all from Cambrex Biosciences (now Lonza), Berkshire, U.K.

DMEM/Ham's F12 medium, Roswell Park Memorial Institute (RPMI) – 1640 medium, MEM non-essential amino acid solution and 0.4 % (v/v) trypan blue solution, all from Sigma-Aldrich Chemical Company, Poole, UK.

G418 sulphate (50mg ml⁻¹), Blastocidin (50 mg) and 1 X Dulbecco's PBS (without Ca and Mg) from PAA Laboratories, Pasching, Austria.

2.1.1.2 Plastic ware

All plastic ware was supplied by Starstedt, Nümbrecht, Germany, except cryo-vials and Lab-Tek CC chamber slides which were purchased from NUNC, Roskilde, Denmark.

2.1.2 General laboratory reagents

All laboratory reagents were of the highest quality and purchased from Sigma-Aldrich Chemical Company, Poole, U.K, unless otherwise stated.

2.1.3 Specialised laboratory reagents

Specialised laboratory reagents are listed and were purchased from Sigma Aldrich Chemical Company, Poole, U.K unless otherwise stated.

1-methyl-4-phenyl pyridinium iodide (MPP⁺), 2', 7'-Dichlorodihydrofluorescein diacetate (DCDHF, Alexis Biochemicals, Nottingham, U.K), 3-(4, 5-dimethylthiazol-2-yl)-2, 5-diphenyltetrazolium bromide (MTT), 3, 3'-Diaminobenzidine (DAB). 3-[(3-Cholamidopropyl)dimethylammonio]-1-propanesulfonate (CHAPS). 3MM chromatography paper (Fisher Scientific, Leicestershire), UK. 5-bromo-4-chloro-3-indolyl-phosphate (di-sodium salt) (BCIP, Melford Laboratories Ltd, Ipswich, UK) and ¹⁴C-labelled tyramine hydrochloride.

(A) Acetyl-Asp-Glu-Val-Asp-7-amido methyl Coumarin. Acrylogel 3 solution Electran (containing 2.5 % NN'-methylenebisacrylamide, final ratio 29:1:0.9 (VWR International Ltd, Poole, UK), all-trans Retinoic acid. ascorbic acid (vitamin C).

(B) BCA protein assay reagent. Bio-Rad protein assay dye reagent concentrate (Bio-Rad Laboratories Ltd, Hemel Hempstead, UK).

(C) Caspase-8 fluorogenic assay kit (Calbiochem, Nottingham, U.K).

(D) Dimethylsulfoxide (DMSO, Fisher Scientific UK Ltd, Loughborough, UK), Dithiothreitol (DTT, Melford Laboratories Ltd, Ipswich, UK), 3-hydroxytyramine [3,4-Dihydroxyphenethylamine (dopamine)] and Dual colour precision plus protein standards, (Bio-Rad Laboratories, CA, U.S.A).

(E) ECL Western blotting detection reagents (Amersham Pharmacia Biotech UK Ltd, Bucks, UK).

(F) Folin and Ciocalteu's phenol reagent (Fisher Scientific UK, Leicestershire, UK) and FluroMAO monoamine oxidase A and B detection kit (Cell Technology Inc, Mountain view, CA, U.S.A).

(G) GBX developer/replenisher, GBX fixer/replenisher.

(I) Igepal CA-630 and Interleukin-4 (IL-4) human cytokine (PeproTech, New Jersey, U.S.A).

(L) Levodopa-carbidopa (Sinemet®) was a kind gift from Bristol Myers-Squibb, New York, U.S.A.

(M) MitoQ was a kind gift from Michael Murphey, University of Cambridge, U.K. Mitotracker (Molecular probes, Invitrogen, Karlsruhe, Germany) and MPP⁺ Iodide.

(N) N-acetylcysteine (NAC), Nitro Blue Tetrazolium (NBT, Melford Laboratories Ltd, Ipswich, UK) and Nitrocellulose (0.22 µM pore size, Genetic Research Instrumentation, Essex, UK).

(P) Phenylmethylsulfonyl fluoride (PMSF), Pre-stained SDS molecular weight standard markers (SDS-7B), Protease inhibitor cocktail (for use with mammalian cell and tissue cultures) and Protein-G sepharose fast flow (recombinantly expressed in *E. coli*).

(R) Rotenone

(T) TNFα (210-TA-010/CF) Human tumour necrosis factor alpha was purchased from R and D Systems, Abingdon, U.K.

(S) Sodium-orthovanadate.

(V) Vectashield mounting medium and Vectashield mounting medium with propidium iodide (Vector Laboratories Ltd, Peterborough, UK).

(X) XAR-5 Kodak film.

2.1.4 MAO inhibitors

- Clorgyline
- L-Deprenyl
- Moclobemide was a kind gift from F. Hoffmann-La Roche Ltd, Basel, Switzerland

2.1.5 Kinase inhibitors

- CEP-11004 mixed lineage kinase inhibitor, Cephalon Inc, Frazer, U.S.A.
- PD98059 MEK inhibitor, Calbiochem, Nottingham, U.K.
- SB202190 p38 MAPK inhibitor, Calbiochem, Nottingham, U.K.
- Staurosporine, Sigma Aldrich Chemical Company, Poole, U.K.

2.1.6 Antibodies

2.1.6.1 Primary antibodies

Anti-ERK 1 (K-23) antibody, Anti-phospho ERK 1/2 (E-4) antibody, Anti-phospho JNK (G-7) antibody, Santa Cruz Biotechnology, California, U.S.A

Monoclonal Bcl-2 antibody (clone Bcl-2-100), SAPK/JNK, c-jun, Cleaved caspase-3 (Asp175-clone 5A1), PARP (Cat #9542) and phospho p38 (Thr180/Tyr182, Cat #9211) were all purchased from Cell Signalling Technologies, MA, U.S.A.

Total p38 antibody, New England Biolabs, Ipswich, MA, U.S.A

Caspase-8 mouse monoclonal antibody (clone 1-1-37), caspase-9 mouse monoclonal antibody (clone 962-22), Anti-Fas (clone CH11) human activating monoclonal antibody, Upstate Biotechnology (now part of Millipore), MA, U.S.A.

Cytochrome c oxidase 1 (C-20), cytochrome c (7H8), GAPDH (6C5), Santa Cruz Biotechnology Inc, CA, U.S.A.

2.1.6.2 Secondary antibodies

Purchased from DAKO Ltd, Cambridge, U. K.

- Goat anti-mouse immunoglobulins alkaline phosphatase conjugated
- Goat anti-mouse immunoglobulins horseradish peroxidase conjugated
- Goat anti-rabbit immunoglobulins alkaline phosphatase conjugated
- Goat anti-rabbit immunoglobulins horseradish peroxidase conjugated
- Rabbit anti-mouse immunoglobulins FITC conjugated
- Rabbit anti-mouse immunoglobulins TRITC conjugated

Donkey Anti-goat immunoglobulins TRITC-conjugated was purchased from Molecular probes, Invitrogen, Karlsruhe, Germany.

2.1.7 Molecular biology

2.1.7.1 Reagents

Purchased from Sigma Aldrich Chemical Company, Poole, U.K unless otherwise stated.

100 bp DNA ladder and 1kb DNA ladder (Promega, Southampton, U.K).

(A) Advantage 2 polymerase kit (Takara Bio Europe, St-Germain, France). Ampicillin ready made solution (100 mg/ ml).

(C) Competent bacterial cells (TOP10, Invitrogen, Karlsruhe, Germany) and (XL1, Stratagene, CA, U. S. A).

(D) Deoxynucleotide triphosphates (dNTPs, Promega, Southampton, U.K).

(L) Miller LB Agar (Miller) Miller LB Broth (Miller)

(O) Oligonucleotides were purchased from Biotex, Berlin, Germany, Invitrogen, Karlsruhe, Germany and Sigma Aldrich Chemical Company, Poole, U.K. Oligo (dT)₁₅ was purchased from Promega (Southampton, U.K).

(R) RNAsin (Promega, Southampton, U.K), RNase Zap and RNase OUT ribonuclease inhibitor (Ambion, Austin, U.S.A).

(S) Superscript II reverse transcriptase (Invitrogen, Karlsruhe, Germany), Sybr green supermix (Bio-Rad Laboratories, CA, U.S.A).

(T) TURBO DNA free and Tri Reagent (Ambion, Austin, U.S.A).

(V) Vectors pCR2.1 and pcDNA3.1(-) Invitrogen were a kind gift from Harmut Kuhn's laboratory, University Medicine Berlin-Charité, Berlin, Germany.

2.1.7.2 Restriction enzymes

Bam HI, Bss HII and Eco RI were purchased from Promega, Southampton, U.K.

Hind III, Msc I, Bgl II, Not I, Sal I, Spe I and Xho I were purchased from New England Biolabs, Ipswich, MA, U.S.A.

2.1.7.3 Kits

RNeasy Mini kit, Qias shredder, Qiaprep spin miniprep kit, Qiagen plasmid Midi kit, Qiaquick gel extraction kit, DNeasy tissue kit, and Qiaquick PCR purification kit were all purchased from Qiagen, Hilden, Germany.

BLOCK-iT Pol II miR RNAi Expression Vector Kit and TOPO TA Cloning kit were purchased from Invitrogen, Karlsruhe, Germany.

Cell line Nucleofector Kit V was purchased from Amaxa GmbH, Cologne, Germany.

2.1.8 Specialised equipment

- Aida Software, Raytest GmbH, Straubenhardt, Germany.
- ATTO HorizBlot, ATTO corporation, Japan.
- Biometra Agagel, standard horizontal gel electrophoresis apparatus, Thistle Scientific, Glasgow, U.K.
- Bio-Rad mode 680 microplate reader, Bio-Rad Laboratories, CA, U.S.A.
- Bio-Rad Power Pac 300, Bio-Rad Laboratories, CA, U.S.A.
- Bio-Rad Trans-Blot electrophoretic transfer system, Bio-Rad Laboratories, CA, U.S.A.
- Fluorescence/Luminometer, MWG Biotechnology,
- GeneTools/GeneSnap gel analysis/quantification system, Syngene, Cambridge, UK.
- iCycler Real time PCR machine, Bio-Rad Laboratories, CA, U.S.A.
- iCycler Real time PCR Quantification Software, Bio-Rad Laboratories, CA, U.S.A.
- LAS-3000 image analyser, Fuji Film Co. Ltd., Tokyo, Japan.
- Leica CLSM confocal laser microscope, Leica, Germany.
- MC6 centrifuge 230V including rotor, strip rotor and adapter sets, Starstedt, Nümbrecht, Germany.
- MIKRO 22R microfuge, Hettich, Germany.
- Mini-PROTEAN II system, Bio-Rad Laboratories, CA, U.S.A.
- NEB Cool cooling rack, New England Biolabs, Ipswich, MA, U.S.A.
- Nikon Digital Net camera DN100, Nikon, Japan.
- Nikon Eclipse TS 100 inverted microscope, Nikon, Japan.
- Nucleofector™ device, Amaxa GmbH, Cologne, Germany.
- PCR cap strips (ultra clear, strips of 8) and PCR tubes (ultra clear, strips of 8) were purchased from Biorline, London, U.K.
- Pharmacia electrophoresis power supply EPS 500/400, Pharmacia, UK.
- Sanyo Incubators
- Shakers for bacteria
- Shakers for blots
- Sanyo Harrier 18/80 refrigerated centrifuge, Sanyo Gallenkamp PLC, Leicestershire, UK.
- Soniprep 150, MSE scientific instruments, UK.
- Walker class II microbiological safety cabinet, Walker safety cabinets Ltd, Derbyshire, UK.

2.2. TISSUE CULTURE METHODS

2.2.1 Cell culture

Wild type human SH-SY5Y neuroblastoma cells were purchased from The European Collection of Animal and Cell Cultures (ECACC), which were characterised in our laboratory by Dr Katy Beck and referred in her PhD thesis (K. E. Beck, 2004) as 'ECACC new clone'. In this work the ECACC new clone cells will now be referred to as SH-SY5Y or wild type SH-SY5Y. Hybridoma cells secreting anti-MAO-A antibody 6G11-E1 and anti-MAO-B antibody 5A11-2F4 were made in the laboratory of Prof. Ellen Billett. Human U937 cells were a kind gift from the laboratory of Prof. Hartmut Kuhn, University Medicine Berlin-Charité, Berlin, Germany. Stably transfected SH-SY5Y clones that were routinely used in this work are referred to as mock (clone 2D8), MAO-A+ (clone 1A9), neg (clone 2G11) and MAO-A- (clone 10D8L).

2.2.1.1 Maintenance of SH-SY5Y cells

Cell culture was carried out in a class II safety cabinet using aseptic techniques. Cells were cultured in 25 cm² (T25), 75 cm² (T75) and 175 cm² (T175) flasks in Dulbecco's Modified Eagles Medium (DMEM) HAMs-F12 containing 10% (v/v) foetal bovine serum, 2mM L-glutamine, 1% (v/v) non-essential amino acid solution, 100 U/mL penicillin and 100 µg/mL streptomycin at 37°C in a 5% CO₂ humidified atmosphere until 70-90 % confluent.

2.2.1.2 Sub-culture of SH-SY5Y cells

Growth medium was removed and the cell monolayer rinsed twice with Dulbecco's PBS to remove traces of serum. Cells were detached using trypsin (100 µg/ml)/versene (40 µg/ml) in Dulbecco's PBS at 37°C. Growth medium ten times the volume of trypsin solution was added to quench the action of trypsin. The suspension was centrifuged at 300 × g for five minutes. Supernatant was removed and the pellet resuspended in 1 ml fresh growth medium. A volume of cell suspension (depending on requirement) was transferred to an appropriate sterile flask containing fresh growth medium and incubated as described in section 2.1.1.1.

2.2.1.3 Viable cell counting and seeding

A 1:10 dilution of cell suspension, prepared during sub-culture was made in trypan blue solution 0.4% (v/v). A cell count was performed in four fields (each 1 mm²) on a haemocytometer (0.1 mm depth chamber) using light microscopy. Cell number was calculated as follows:

$$\text{Cell number / ml} = \text{mean cell number} \times 10^4 \times \text{dilution factor}$$

Once the required number of cells was seeded, cells were incubated as described in 2.1.1.1.

2.2.1.4 Cryo-preservation of cells

Cells underwent long-term storage in the vapour phase of liquid nitrogen in freezing medium containing, 95 % (v/v) foetal bovine serum and 5 % (v/v) sterile dimethyl sulfoxide (DMSO). Two million cells were pelleted by centrifugation at 300 × g for 5 minutes, the supernatant discarded and the pellet resuspended in 1 ml of freezing medium and transferred to a cryovial (on ice). The vial was then rapidly transferred to a -70°C freezer overnight before transferring to liquid nitrogen storage for the long term.

2.2.1.5 Resuscitation of cryo-preserved cells

Cells inside the cryovial were thawed rapidly in a 37°C water bath and immediately transferred to a sterile tube containing 10 mL fresh growth medium. The cell suspension was centrifuged at 300 × g for 5 minutes. Supernatant was removed and the cell pellet resuspended in 1 ml fresh growth medium (using a Pasteur pipette) before transfer to a T25 flask containing growth medium and incubated as described in section 2.1.1.1.

2.2.1.6 Hybridoma cells

Hybridoma cells were routinely maintained as described above for SH-SY5Y except the growth medium was RPMI-1640. Hybridoma cells do not require trypsin for detachment from the flask; instead they are detached by gentle squirting of media down the monolayer. For collection of antibody, dead cells in suspension were centrifuged at 300 × g for 5 minutes and the supernatant only (which contains the antibody) is kept in a sterile container at + 4 °C.

2.2.1.7 Mock /2D8 and MAO-A+/1A9 stably transfected SH-SY5Y cells

Stable transfection with pcDNA3.1(-) vector confers resistance to the antibiotic G418 sulphate (geneticin), which is required in the growth medium at all times. The correct concentration of G418 sulphate was determined (see appendix) and used at a final concentration of 700 µg/ml in SH-SY5Y growth medium. Cells were maintained as described for SH-SY5Y with the exception of the addition of G418 sulphate in the growth medium. It is not necessary to have G418 sulphate in media used for sub-culturing.

2.2.1.8 Neg/2G11) and MAO-A-/10D8 stably transfected SH-SY5Y cells

Transfection with Pol II miR RNAi expression vectors confers resistance to the antibiotic blasticidin. Therefore, blasticidin is required in the growth medium at all times. The correct concentration of blasticidin was determined (see appendix) and used at a final concentration of 6 µg/ml in SH-SY5Y growth medium. Cells were maintained as described for SH-SY5Y with the exception of the addition of blasticidin in the growth medium. It is not necessary to have blasticidin in media used for sub-culturing.

2.3. BIOCHEMICAL METHODS

2.3.1 Assessment of cell viability

2.3.1.1 MTT reduction assay

MTT is a substrate that is taken up by cells and reduced by mitochondrial and endoplasmic reticulum dehydrogenase enzymes, to yield a purple formazan product that accumulates within cells depending on cell integrity (Cookson *et al.* 1995). Cells were seeded in 96-well plates at a density of 20,000 cells/well and grown to 70-80 % confluence. MTT stock solution in PBS was added to each well to give a final concentration 0.5 mg/ml and incubated for 30 min. The media containing the MTT was removed and the formazan crystals solubilised in 100 µl of dimethylsulfoxide (DMSO) and absorbance measured at 595 nm with a microtitre plate reader.

2.3.1.2 Trypan blue exclusion assay (estimation of viable cell number for sub-culture)

Trypan blue is taken up by dead cells (where the cell membrane is no longer intact) where it stains the cytoplasm, causing the cells to shine blue when observed by light microscopy. Viable cells however, exclude trypan blue and remain colourless (or white) and can be counted using a haemocytometer (see cell counting, page 39).

2.3.1.3 Trypan blue exclusion assay (For estimation of viable cell number following treatment with apoptotic inducers)

Growth medium following treatment was removed and kept to one side in a sterile tube. The remaining cells were detached by trypsinisation and transferred to the tube containing the floating cells. The cell suspension was centrifuged at $300 \times g$ for 5 minutes, the supernatant discarded and the cell pellet resuspended in 1 ml growth medium. A small aliquot of this cell suspension was transferred to a sterile 1.5 ml tube containing a volume of trypan blue solution (0.4 % [v/v]). Cells were counted in a haemocytometer chamber as described in section 2.1.1.3. Cell counts were performed on at least two independent cell populations exposed to the same treatment conditions for each experiment.

2.3.1.4 Trypan blue exclusion assay (For estimation of viable cell number from 24-well plates for cell growth studies)

A cell count was performed as described in section 2.2.1.3 and 100,000 cells seeded per well of a 24 well plate in duplicate. The original cell suspension was then re-counted for accuracy. At each time point, the medium was removed from each well and the monolayer rinsed with Dulbecco's PBS. 100 μ l trypsin (100 μ g/ml)/versene (40 μ g/ml) in Dulbecco's PBS at 37°C was added to detach the cells (with gentle squirting down the monolayer). The action of trypsin was quenched with 1 ml growth medium and the cell suspension transferred to a sterile Eppendorf tube. The cells were pelleted by centrifugation at $300 \times g$ for 5 minutes. The supernatant was discarded and the cell pellet resuspended in 50 μ l of trypan blue solution (0.5 % trypan blue solution diluted 1:1 with growth medium). Viable cells in the cell suspension were counted in a haemocytometer chamber as described in section 2.1.1.3. The total number of viable cells per well at each time point were plotted on a graph as cell number \pm S.D. To calculate doubling time the following equation was applied:

$$\text{doubling time} = [t2 - t1] \times \left[\frac{\log 2}{\log \left(\frac{q2}{q1} \right)} \right]$$

Where ***t2*** is the time (in hours) at point two on the linear part of the graph, ***t1*** is the time (in hours) at point one on the linear part of the graph, ***q2*** is the cell number at time point 2, ***q1*** is the cell number at time point 1 (Jones *et al.* 1998).

2.3.1.5 ATP assay

The ViaLight HS kit is based upon the measurement of ATP by luminescence, utilising the luciferase enzyme which catalyses the formation of light from ATP and luciferin. Cells were cultured in 96-well plates and once confluent, assayed for ATP levels according to the manufacturer's instructions. ATP standards were prepared in the range of 0.5-5000 pmoles/assay and results were expressed as mean ATP pmoles/ μg total protein \pm S.D.

2.3.2 Treatment of SH-SY5Y cells

SH-SY5Y cells were treated with a number of toxins and other reagents alongside an appropriate control. Experimental conditions are described in figure captions in the results chapters. For quick reference, details of routinely used treatments are listed below in Table 2. 1.

Experiment	Control	Treatment	Final concentration	Time frame	Common end point
Staurosporine induced apoptosis	SFM	STS	1 μM	0-6 h	3 h
Serum withdrawal induced apoptosis	GM	Extensively wash monolayer with PBS and replace media with SFM	N/A	24-96 h	72 h
Rotenone induced apoptosis	GM	Rotenone	0.5 μM	3-72 h	24-48 h
MPP ⁺ induced apoptosis	GM	MPP ⁺	1 mM	1-72 h	24-48 h
Dopamine induced apoptosis	GM	Dopamine	500 μM	1-72 h	24-48 h
BSO treatment	GM	BSO	2 mM	1-72 h	72 h
Levodopa treatment	GM	Sinemet preparation	100 μM	1- 72h	72 h
Inhibition of ERK	Inhibitor alone	PD98059	20 μM	N/A	N/A
Inhibition of JNK	Inhibitor alone	Cep	1 μM	N/A	N/A
Inhibition of p38	Inhibitor alone	SB202190	10 μM	N/A	N/A
MAO Inhibition	Inhibitor alone	Clorgyline/tran-ylcypromine	1 μM	2 h pre-incubation	N/A
Treatment with antioxidants	antioxidant alone	NAC/Vit C	1 mM	N/A	N/A

Table 2. 1. Details of commonly used experimental treatments in this thesis

2.3.3 Cell extraction

Following the experimental period, treatment medium was poured into a sterile centrifuge tube (as it may contain apoptotic cells that are no longer attached to the monolayer), the monolayer rinsed using sterile PBS or DMEM and the adherent cells removed by trypsinisation. Trypsinised cells were quenched with growth media and combined with the treatment medium (containing floating cells). The cell suspension was centrifuged for 5 minutes at $300 \times g$. The supernatant was discarded and the cell pellet washed by re-suspending it in 1 ml sterile PBS, transferred into a sterile 1.5 ml tube and re-centrifuged for 5 minutes at $300 \times g$. The supernatant was discarded and any remaining supernatant around the cell pellet removed using a 20-200 μ l pipette. The cell pellet was stored at -20°C (short term) and -80°C (long term).

2.3.4 Estimation of total protein in cell extracts

The protein content of samples was estimated by one of three methods, depending on compatibility of the constituents of the buffer that the samples remain in following assay.

2.3.4.1 Mini Lowry

This Lowry method (Lowry *et al.* 1951) is based on Biuret and Folin and Ciocalteu reactions. Interference can occur with a number of substances (importantly detergents) and the method has a limited pH range (strong acids interfere).

A calibration graph was obtained using bovine serum albumin (BSA) as standard protein 0-100 μ g. Protein standards and test samples were diluted appropriately to a final volume of 100 μ l (where both standards and sample contain the same amount of the buffer that then sample is resuspended in). The working Lowry reagent was freshly prepared on the day as 2 % (w/v) NaCO_3 , 1 % (w/v) CuSO_4 , 2.7 % NaK tartrate in 0.1 M NaOH. 1 ml of working Lowry reagent was added to each standard and sample, mixed and incubated at room temperature (RT) for 15 min. 100 μ l Folin and Ciocalteu reagent (diluted 1:1 with distilled water, dH_2O) was added, mixed and incubated at RT for a further 30 min. The solutions were mixed again and the absorbencies measured spectrophotometrically on a multi-plate reader at 750 nm.

2.3.4.2 Bio-Rad protein assay

The Bio-Rad protein assay is based on the Bradford method, a colorimetric protein assay, where an absorbance shift in the coomassie dye changes from red to blue upon binding of the protein. The main advantages of the Bio-Rad assay are it is less susceptible to

interference from detergents (SDS \leq 0.1 %, Triton X-100 \leq 0.1%). The disadvantages however, are that the assay is linear over a shorter range of protein concentration and therefore samples may need to be diluted several times to make sure that the sample is within the range of the linear calibration graph. The Bio-Rad assay was performed in accordance with the manufacturer's instructions.

2.3.4.3 Bicinchoninic acid assay

The bicinchoninic acid assay (BCA) is based on the Lowry and Bradford method (Smith *et al.* 1985). The main advantage of the method is its compatibility with many chemicals and detergents. The BCA assay was performed according to the manufacturer's instructions (Sigma Aldrich Chemical Company, Poole, U.K).

2.3.5 Biochemical Assays

2.3.5.1 Caspase-3 fluorogenic assay

Caspase-3 activity was monitored using a fluorescence-based assay with Ac-DEVD-AMC as substrate. 500,000 cells were seeded in 25 cm² flasks. On reaching 70-80% confluence, the cells were treated for the appropriate times for each experimental condition. Following treatment cells were harvested as described in section 2.2.4. Cell pellets were resuspended in 200-300 μ l lysis buffer (50 mM HEPES, 5mM CHAPS and 5 mM DTT, pH 7.4) and incubated on ice for 20 min. The lysates were centrifuged at 200g at 4°C for 5 min to remove cell debris. The assay was prepared in triplicate. 30 μ l of cell lysate was transferred to a black 96-well plate and made up to 80 μ l with assay buffer (20 mM HEPES pH7.4, 0.1% [w/v] CHAPS, 5 mM DTT and 2mM EDTA). Reactions were initiated by the addition of Ac-DEVD-AMC to a final concentration of 200 μ M in a total reaction volume 100 μ l. Fluorescence was measured (excitation 450 nm and emission 360 nm) every 5 min for 3 h at 37°C. Data were normalised for protein content, which was determined by the Lowry method and expressed as Δ fluorescence units/min/ μ g total protein.

2.3.5.2 Monoamine oxidase activity assay

2.3.5.2.1 Radioassay

Monoamine oxidase activity was monitored using a radiometric assay with ¹⁴C-labelled tyramine hydrochloride as substrate, based on the method of Russell and Mayer (Russell and Mayer, 1983) with modifications. Treated cells were harvested as described in section 2.2.4 and the pellet resuspended in 200 μ l potassium phosphate buffer (20 mM K₂HPO₄, 20 mM KH₂PO₄, pH 7.4) and 30 μ l aliquots transferred to scintillation vials, in triplicate.

Samples were made up to 200 μ l with potassium phosphate buffer and then incubated at 37°C for 5 min. Sample blanks were prepared in parallel containing, in addition, 200 μ l 0.5 M HCl. To each sample 20 μ l 1 mM 14 C-labelled tyramine hydrochloride (1 mCi/mmol) was added and incubated for 1 h at 37°C. The reaction was stopped by the addition of 200 μ l 0.5 M HCl. Finally, 3 ml scintillant (1:1 Ethyl acetate: toluene, 1 % [w/v] PPO) was added to each vial, and a sample of the organic phase containing the product transferred into a scintillation vial. MAO activity was measured in a liquid scintillation counter (Cambera-Packard, Schwadorf, Germany). Preliminary assays were undertaken to ensure that MAO activity was linear beyond the 1 h time point. Data were normalised for protein content, which was determined either by the Lowry method (Lowry et al. 1951) or BCA method and rates expressed as pmoles/min/mg protein.

2.3.6 Immunohistochemistry

Human liver sections (4 μ m) fixed in 2 % (v/v) para-formaldehyde in PBS for 4 h, cryo-protected in 15 % sucrose solution for 72 h and incubated at -20°C for 20 min, were permeabilised with 0.5 % (v/v) Triton X-100 in PBS for 5 min at room temperature then washed in PBS. Slides were blocked for 20 min with 20 % (v/v) normal swine serum in PBS and then incubated overnight in monoclonal antibody, anti-MAO-A (6G11-E1) or anti-MAO-B (3F12-G10-2E3) (tissue culture supernatants), or PBS as a negative control at room temperature. The slide was washed in PBS and then incubated with secondary antibody; horseradish peroxidase conjugated anti-mouse immunoglobulin G (dilution 1:100) in 5 % v/v normal swine serum in PBS for 30 min at room temperature. The slide was washed in PBS and antibody binding revealed by incubation in DAB substrate for 40 min and stopped with excessive washing in cold water.

2.3.7 Immunocytochemistry

SH-SY5Y cells grown on Lab-Tek (NUNC, Roskilde, Denmark) chamber slides were fixed in 90 % (v/v) ice cold methanol in TBS and incubated at -20°C for 20 min, were permeabilised with 0.5 % (v/v) Triton X-100 in PBS for 5 min at room temperature then washed in PBS. Slides were blocked for 20 min with 20 % (v/v) normal swine serum in PBS and then incubated overnight in monoclonal antibody, anti-MAO-A (6G11-E1) or anti-MAO-B (3F12-G10-2E3) (tissue culture supernatants), or PBS as a negative control at room temperature. The slide was washed in PBS and then incubated with secondary antibody; horseradish peroxidase conjugated anti-mouse immunoglobulin G, followed by DAB as described in 2.3.6.

2.3.8 Immunofluorescence

SH-SY5Y cells grown on Lab-Tek (NUNC, Roskilde, Denmark) chamber slides were fixed in 90 % (v/v) ice cold methanol in TBS and incubated at -20°C for 20 min, were permeabilised with 0.5 % (v/v) Triton X-100 in PBS for 5 min at room temperature then washed in PBS. Slides were blocked for 20 min with 20 % (v/v) normal swine serum in PBS and then incubated overnight in primary antibody (for dilution of primary antibody for immunocytochemistry, see vendors recommendation), or PBS as a negative control at room temperature. The slide was washed in PBS and then incubated with secondary antibody; FITC/TRITC-conjugated anti-mouse, rabbit or goat immunoglobulin G (dilution 1:1000) in 5 % v/v normal swine serum in PBS for 30 min at room temperature. The slide was washed in PBS and air dried. Slides were mounted using Vectashield (with or without propidium iodide) and antibody binding revealed by confocal microscopy.

2.3.9 Detection of ROS

2.3.9.1 Short term treatments (e. g. STS)

Cells were grown to ~70-80 % confluence on Lab-Tek (NUNC, Roskilde, Denmark) chamber slides prior to pre-treatment for 2 h with antioxidants or inhibitors if required. Media were removed and replaced with DMEM containing 100 μ M DCDHF and incubated at 37°C for 50 min. Following incubation the dye was removed and replaced with Hanks buffered salt solution (HBSS) alone or HBSS + treatment. Changes in DCDHF fluorescence were immediately monitored using a Leica CLSM inverted confocal laser scanning microscope. Increase in cytosolic dichloro-fluorescein (DCF) fluorescence reflected elevated intracellular ROS production. Images in each independent experiment were taken using the same laser power, gain and objective.

2.3.9.2 Long term treatments (e.g. serum withdrawal/ rotenone)

Cells were grown to ~50 % confluence on Lab-Tek (NUNC, Roskilde, Denmark) chamber slides prior to treatment for the required time (in the presence or absence of antioxidants or inhibitors). Media were removed and replaced with DMEM containing 100 μ M DCDHF and incubated at 37°C for 50 min. Following incubation the dye was removed and replaced with HBSS alone or HBSS + original treatment. Changes in DCDHF fluorescence (Excitation 502 nm, Emission 523 nm) were immediately monitored using a Leica CLSM inverted confocal laser scanning microscope. Increase in cytosolic dichloro-fluorescein (DCF) fluorescence reflected elevated intracellular ROS production. Images in each independent experiment were taken using the same laser power, gain and objective.

2.3.10 Mitotracker

Mitotracker Red CMXRosamine (Molecular Probes, Invitrogen, Karlsruhe, Germany) is a specialised dye taken up by active mitochondria and can be used for live confocal microscopy, but also remains in fixed cells and can be used for conventional confocal microscopy. For live confocal microscopy, Mitotracker was added to each well in DMEM at a final concentration of 100 nM and incubated at 37°C for 30 min. The medium containing the Mitotracker was removed and replaced with HBSS either alone or containing treatment. Mitotracker fluorescence (Excitation 579 nm, Emission 599 nm) were immediately monitored using a Leica CLSM inverted confocal laser scanning microscope. Images in each independent experiment were taken using the same laser power, gain and objective.

2.3.11 Gel electrophoresis and Western blotting

Cells were extracted into extraction buffer (50 mM Tris, 5 mM EDTA, 150 mM NaCl, 1 mM sodium orthovanadate, 2 mM PMSF, 1 % [w/v] SDS, and 0.2 % [v/v] protease inhibitor cocktail) and immediately boiled for 5 min. Equal protein aliquots (80-100 µg for analysis of MAPK proteins and 20 µg for all others proteins) per sample were subjected to electrophoresis on a 12 % (v/v) SDS-polyacrylamide gel. Separated proteins were transferred onto a nitrocellulose membrane and equal protein loading assessed by staining with 0.05 % (w/v) copper phthalocyanine in 12 mM HCl, checked by immunodetection of total ERK, total JNK or total P38. Blotted membranes were blocked for 1 h in either 3-5 % (w/v) dried skimmed milk (depending on primary antibody, method may vary, see vendors recommendations) in TBS or PBS containing 0.1 % (v/v) Tween-20 and incubated overnight at 4°C with primary antibody diluted in 3-5 % (w/v) dried skimmed milk (Due to the presence of phosphatases in milk, all phospho protein primary antibodies were diluted in 3-5 % [w/v] BSA). Membranes were washed and incubated for 2 h at room temperature with peroxidase-conjugated anti-mouse or anti-rabbit immunoglobulin G (dilution 1:1000). Antibody binding was revealed with the ECL Western blotting detection reagent (Pierce, Rockford, Illinois, and U.S.A). Digital images were captured using a LAS-3000 image-analyser (Fuji Film Co. Ltd., Tokyo, Japan), and band intensity quantified using Aida software (Raytest GmbH, Straubenhardt, Germany).

2.3.12 Dot blotting

Treated cells were harvested as described in section 2.2.4 and resuspended in 150 µl MAO extraction buffer (50 mM Tris, 150 mM NaCl, 5 mM EDTA, 1 mM Na orthovanadate, 0.5

% [w/v] Triton X-100, 2 mM PMSF and 0.2 % [v/v] protease inhibitor cocktail) and incubated on ice for 20 min. Samples were centrifuged for 10 min at 300×g at 4°C. The supernatants were sonicated (3× 3 second pulses at 60 Hz). Equal protein samples, in triplicate, were loaded onto a Dot blot manifold and bound to a nitrocellulose membrane filter. Membranes were blocked for 1 h in 3 % (w/v) dried skimmed milk in TBS containing 0.1 % Tween-20 and incubated overnight in monoclonal antibody anti-MAO-A 6G11-E1 (tissue culture supernatant) at 4°C. Membranes were washed and incubated for 2 at room temperature with phosphatase-conjugated anti-mouse immunoglobulin G (dilution 1:1000). Antibody binding was revealed in substrate buffer (0.75 M Tris, pH 9.5) containing 0.13 mM nitroblue tetrazolium and 0.29 mM bromochloroindolyl phosphate. Digital images were captured using a LAS-3000 image-analyser (Fuji Film Co. Ltd., Tokyo, Japan), and band intensity quantified using Aida software (Raytest GmbH, Straubenhardt, Germany).

2.4. MOLECULAR BIOLOGY METHODS

Basic methods used in molecular biology, such as purification of nucleic acids, assays of nucleic acid concentration in solution, agarose gel electrophoresis, ligation and transformation have been achieved using standard methods provided by the manufacturer. Sequencing was carried out by MWG Biotechnology.

2.4.1 Preparation of RNA and reverse transcription

For monitoring of MAO mRNA expression, SH-SY5Y cells were harvested as described in section 2.3.3, homogenised using Qiashredder (Qiagen, Hilden, Germany) and RNA isolated using the RNeasy mini kit (Qiagen, Hilden, Germany). DNase digestion when required was performed using the TURBO DNase free kit (Ambion, Austin, U.S.A) according to the manufacturer's instructions.

The conversion of the resulting RNA into cDNA was carried out by reverse transcription using the M-MLV (Moloney murine Leukaemia-Virus) reverse transcriptase (Superscript II, Invitrogen, Karlsruhe, Germany). RNA was denatured for 5 min at 70°C and cooled immediately on ice. The reverse transcription reaction was started as follows: 1-3µg total RNA; 50 mM Tris-HCL, pH 8.2; 8 mM MgCl₂; 1 mM DTT; 100 µg/ml BSA; 30 units RNasin; 0.166 mM dNTPs; 150 mM Oligo-dT₁₅-primer and 50 units Superscript II reverse transcriptase. The reaction was incubated for 90 minutes at 37°C and finally deactivated at 70°C for 15 min.

2.4.2 Real-Time-PCR (qRT-PCR)

Primer	Sequence 5'-3'	Fragment size
GAPDH		
GAPDH-forward	CCA TCA CCA TCT TCC AGG AGC GA	520 bp
GAPDH-reverse	GGA TGA CCT TGC CCA CAG CCT TG	
MAO-A		
MAO-A-forward	GCC CTG TGG TTC TTG TGG TAT GT	368 bp
MAO-A-reverse	TGC TCC TCA CAC CAG TTC TTC TC	

Table 2. 2 Primer combinations used for qRT-PCR

Real time PCR allows the quantification of DNA molecules in a given sample. The kinetics of DNA amplification were measured by continuously measuring the fluorescence intensity of a dye (Sybrgreen) that intercalates with double stranded DNA as it is being synthesised. Quantification of DNA was obtained on a Bio-rad iCycler following manufacturer's instructions. The qRT-PCR reaction contained 5 µl (1 X) Bio-Rad Sybrgreen supermixes (which contain reaction buffer, dNTPs, MgCl₂ and Taq polymerase), 0.6 µl (5 µM) primer combination (containing forward primer and backwards primers), 3.4 µl PCR grade water plus of the following PCR templates, 1 µl cDNA (RT product) or 1 µl DNA standard (see below). A template free mix was used as a control. DNA was amplified using the following program:

Denaturing:	95°C	3 min
PCR cycle	94°C	20 s
	65°C	30 s
	72°C	30 s and measurement of fluorescence
		Repeating of the PCR cycle 45 times
Meltcurve	60°C	1 min
		60-99°C in 0.5°C increments
		(at each step wait 5 s and measure the fluorescence)

The *melting curves* are a control of the homogeneity of the PCR amplification. A unique PCR product melts at a given temperature. The first derivative of the fluorescence signal plotted against temperature should show only one peak if only one specific product is formed. The *analysis* of PCR curves was achieved on Bio-Rad iCycler software. Standard dilutions of the studied gene sequences were used to quantify the relative amount of transcription. The gene-specific external *Standards* necessary for the exact quantification

were prepared as follows: The desired DNA fragments (cDNA obtained from human brain tissue, Invitrogen, Karlsruhe, Germany) containing each primer combination was amplified using Advantage II polymerase mix according to the manufacturer's directions. The amplified DNA was separated by electrophoresis on a 1% agarose/1X TAE-gel. The corresponding bands were cut out of the gel, purified using the Qiaquick gel extraction kit (Qiagen, Hilden, Germany) and used as a template for re-amplification using Advantage II polymerase mix. The resulting PCR product was purified using Qiagen PCR purification kit and the DNA concentration determined. The PCR fragments were cloned into pCR2.1 vector and transformed into TOP10 *E.coli* using the TOPO-TA cloning kit according to the manufacturer's instructions (Invitrogen, Karlsruhe, Germany). Restriction digestions (see section 2.4.4) were performed on prepared DNA (QIAprep Spin Miniprep kit, Qiagen, Hilden, Germany) expressed from the bacterial clones to check for the presence of the insert and the DNA sequences of positive clones verified. Following confirmation by sequencing that DNA sequences were free from mutations, the pCR2.1 TOPO vector was subjected to quantitative restriction digestion to yield the linearised vector including the insert (which was checked by agarose electrophoresis). Following purification of the linearised vector, the concentration of DNA was determined. In order to calculate the number of double-stranded DNA molecules per μl of this solution (termed original solution or UL) the following calculation is applied:

$$\frac{c \left(DNA \left[g / \mu l \right] \right)}{\left(Fragment \ length \left[bp \right] \right) \times M_r} \times N_A = Molecules / \mu l$$

c..... Concentration

N_A..... 6.022×10^{23} molecules / mol Avogadro's number

M_r.....660 g / mol \times bp (molecular mass of double stranded DNA)

The correct standard dilutions were prepared based on this calculation which was used for the determination of molecular count in the samples. The expressed standard dilutions in the range from 1 to 10^8 molecules were used as a DNA template for qRT-PCR. The iCycler software calculated the absolute amount of transcription with regards to the pre-defined standard solution series. For **quantification** of the relative amounts of DNA transcription (mRNA levels), RNA was prepared from SH-SY5Y cells, the RNA reversely transcribed (see section 2.4.1) to cDNA and the single strands of cDNA used as a PCR

template for the qRT-PCR. Amount of transcript obtained were normalised to the amount of transcription of the housekeeping gene GAPDH.

2.4.3 Conventional PCR

Conventional (semi-quantitative) RT-PCR was performed using the Advantage 2 polymerase kit according to the manufacturer's recommendations (Takara Bio Europe, St-Germain, France). A template free PCR-mix was used as a control in each reaction. DNA was amplified using the following program.

Denaturing:	95°C	3 min
26-34 PCR cycles	95°C	0.5 min
	68°C	1 min
	68°C	2 min

Primer	Sequence 5'-3'	Fragment size
GAPDH		
GAPDH-forward	CCA TCA CCA TCT TCC AGG AGC GA	520 bp
GAPDH-reverse	GGA TGA CCT TGC CCA CAG CCT TG	
MAO-A		
MAO-A-forward	GCC CTG TGG TTC TTG TGG TAT GT	368 bp
MAO-A-reverse	TGC TCC TCA CAC CAG TTC TTC TC	
MAO-B		
MAO-B-forward	ACT CGT GTG CCT TTG GGT TCA G	317 bp
MAO-B-reverse	TGC TCC TCA CAC CAG TTC TTC TC	
Caspase-8		
Caspase-8-forward	GAT GAT GAC ATG AAC CTG CTG	323 bp
Caspase-8-reverse	GCA TCC AAG TGT GTT CCA TTC C	
Caspase-9		
Caspase-8-forward	TTG GTG ATG TCG AGC AGA AAG	276 bp
Caspase-8-reverse	AGT GAG CCC ACT GCT CAA AGA	

Table 2. 3 Primer combination for conventional PCR

2.4.4 Restriction endonuclease digestion reactions

Restriction endonuclease digestions using the appropriate restriction endonucleases were performed for the analysis of DNA sequences; from plasmids to confirm successful cloning or the presence of a particular sequence. All digestions were carried out according to the recommendation of the manufacturer.

2.4.5 Overexpression of MAO-A in SH-SY5Y cells

Human MAO-A was stably over expressed in the human neuroblastoma (SH-SY5Y) cell line by cloning human MAO-A cDNA into the expression vector (pcDNA3.1-, Invitrogen, Karlsruhe, Germany), which was then transformed into competent bacteria. The expressed plasmid DNA was purified using DNA mini and DNA midi kits (Qiagen, Hilden, Germany) and transfected into SH-SY5Y cells by electroporation (Amaxa, Cologne, Germany). Stable SH-SY5Y clones were selected by their resistance to geneticin (G418) which is conferred by the plasmid vector pcDNA3.1

2.4.5.1 TOPO Cloning

First human MAO-A DNA was amplified using PCR primers specific to a homologous region of human MAO-A cDNA (underlined sequence shown in Figure 2. 2A) and containing the restriction endonuclease sites of XhoI/NotI at their respective 5' end. The template used for the PCR reaction was cDNA previously prepared by reversely transcribing RNA purified from SH-SY5Y cells.

TOPO TA[®] cloning is a highly efficient one step cloning strategy for the insertion of amplified PCR products into a plasmid vector (Invitrogen, Karlsruhe, Germany). During PCR amplification *Taq* polymerase has a nontemplate-dependent terminal transferase activity that adds a single deoxyadenosine (A) to the 3' end of PCR products. The linearised pCR2.1 vector has single, overhanging 3' deoxythymidine (T), which allows the PCR product to ligate efficiently with the vector (Invitrogen Corporation, 2006). Topoisomerase I activates and guides the unravelling of DNA by binding to duplex DNA at specific sites and cleaves the phosphodiester backbone after 5' CCCTT. The energy released from the cleaved bond is conserved by the formation of a covalent bond between the 3' phosphate of the cleaved strand and the tyrosyl residue (Tyr-274) of topoisomerase I. The reaction can be reversed and the topoisomerase enzyme released (Simply, topoisomerase cuts one duplex DNA strand, passes the other through it and reanneals the cut strand). Figure 2. 1B (step1) illustrates the cloning of human MAO-A cDNA into the pCR2.1 vector.

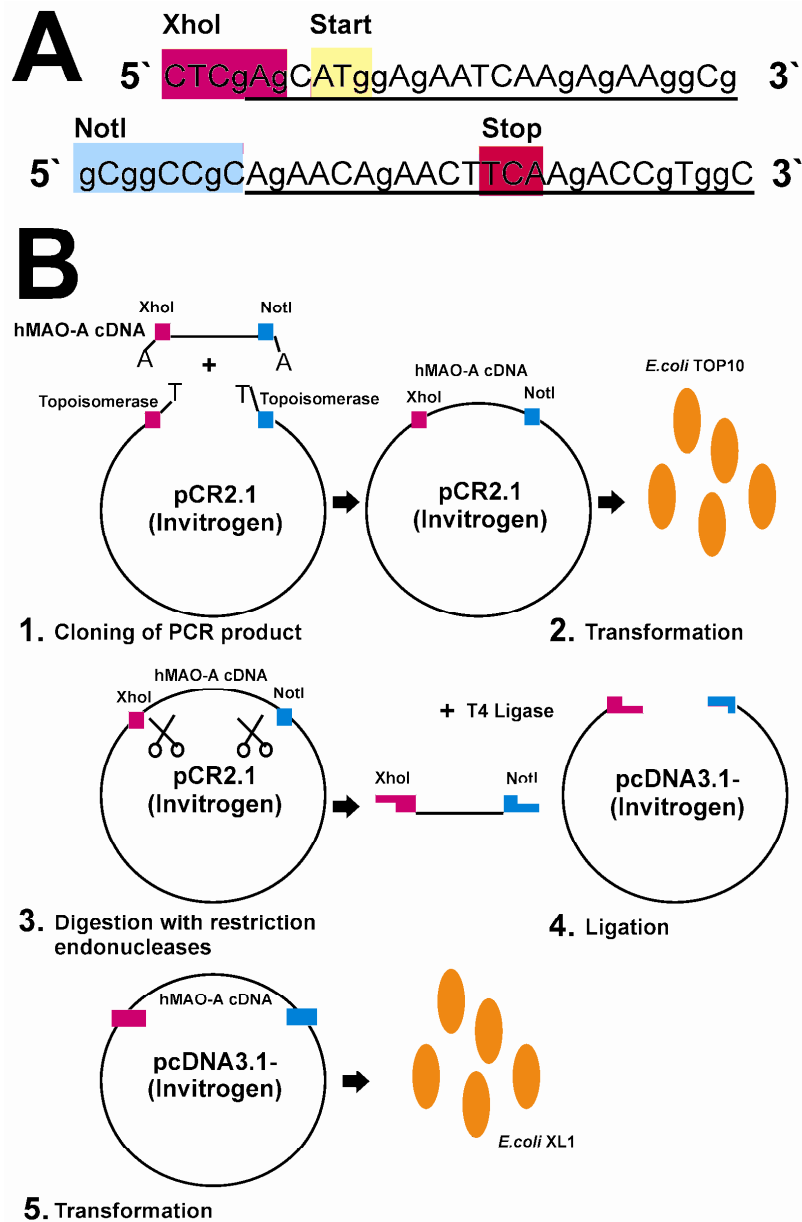


Figure 2. 1 Overview of cloning procedure

(A) PCR primers for amplification of human MAO-A DNA for cloning into pcDNA2.1 (Invitrogen, Karlsruhe, Germany) via XhoI/NotI restriction sites. *Top sequence* shows forward primer and *Bottom sequence* shows reverse primer, where the underlined region in both cases is homologous to human MAO-A cDNA. (B) A step by step overview of cloning human MAO-A into pcDNA3.1(-) (Invitrogen, Karlsruhe, Germany). Cloning of the PCR product (MAO-A cDNA) directly into the pcDNA3.1(-) expression vector is not viable. Therefore MAO-A cDNA was first cloned via the TOPO TA system (Invitrogen, Karlsruhe, Germany) into pCR2.1 vector (*step 1.*), transformed into competent *E. coli* for expression (*step 2.*), purified, the hMAO-A insert cut out again using restriction endonucleases (*step 3.*) and ligated with the pcDNA3.1(-) expression vector via the action of T4 ligase (*step 4.*). Complete pcDNA3.1(-) containing the human MAO-A DNA insert was then transformed into competent *E. coli* cells (*step 5.*), grown and expressed plasmid DNA purified using DNA mini or midi kits (Qiagen, Hilden, Germany).

The cloned pCR2.1 vector was transformed into competent bacteria (*E. coli* TOP10 cells). Isolated bacterial clones allowed to grow overnight yielded significant amounts of bacterial plasmid DNA, which is purified and sequence analysed by sequential sequence reactions

and from a clone devoid of mutations, plasmid DNA is purified and restriction digestion of the pCR2.1 vector performed (Figure 2. 1B step 2). Digestion with specific restriction endonucleases results in the MAO-A insert being cut out from the vector backbone (Figure 2. 1B step3). The MAO-A insert is a 1.6 kb fragment which can be excised and distinguished from the large empty vector fragment (3.9 kb) by agarose gel electrophoresis. The excised DNA fragments are purified and sent for sequencing to check for mutations. Meanwhile the eukaryotic expression plasmid pcDNA3.1(-) containing a human COX2 insert (a kind gift from the laboratory of Professor Hartmut Kuhn, University Medicine Berlin-Charité, Berlin, Germany) was digested using restriction endonucleases to remove the COX2 insert. Human MAO-A DNA (see above) was then used in the ligation step, combining the MAO-A insert with the pcDNA3.1(-) vector using the T4 ligase enzyme (Figure 2. 1B, step 4). The complete pcDNA3.1(-) vector can now be transformed into competent bacterial cells for the collection of expressed plasmid DNA (Figure 2. 1B, step 5).

2.4.5.2 Stable transfection

For transient transfection studies, the intact pcDNA3.1(-) plasmid containing the MAO-A insert was transfected. For stable transfection the plasmid was linearised using restriction endonuclease BglII which cuts the plasmid vector only once without interfering with either the MAO-A coding sequence or the neomycin resistance gene.

SH-SY5Y cells were transfected with 1 µg of pcDNA3.1(-) containing the hMAO-A insert or 1 µg of the empty pcDNA3.1(-) vector via electroporation using the Amaxa nucleofection system (Figure 2. 2). The method of electroporation using the Amaxa nucleofactor was optimised for SH-SY5Y cells following the manufacturer's instructions. Electroporated SH-SY5Y cells were seeded in 6-well tissue culture plates in normal growth medium, which was replaced after 24 hours. 48 hours post-transfection, cells were passaged and seeded at 25% confluence in growth medium containing G418 sulphate (geneticin) at a concentration of 700 µg/ml (as previously determined by titration, see appendix). The media was replaced every 3-4 days until resistant foci were visible (Figure 2. 2). Resistant cells were diluted in 96 well plates at a density of 0.5 cell/well (Invitrogen Corporation, 2006). Single clones were expanded and assayed for MAO-A expression.

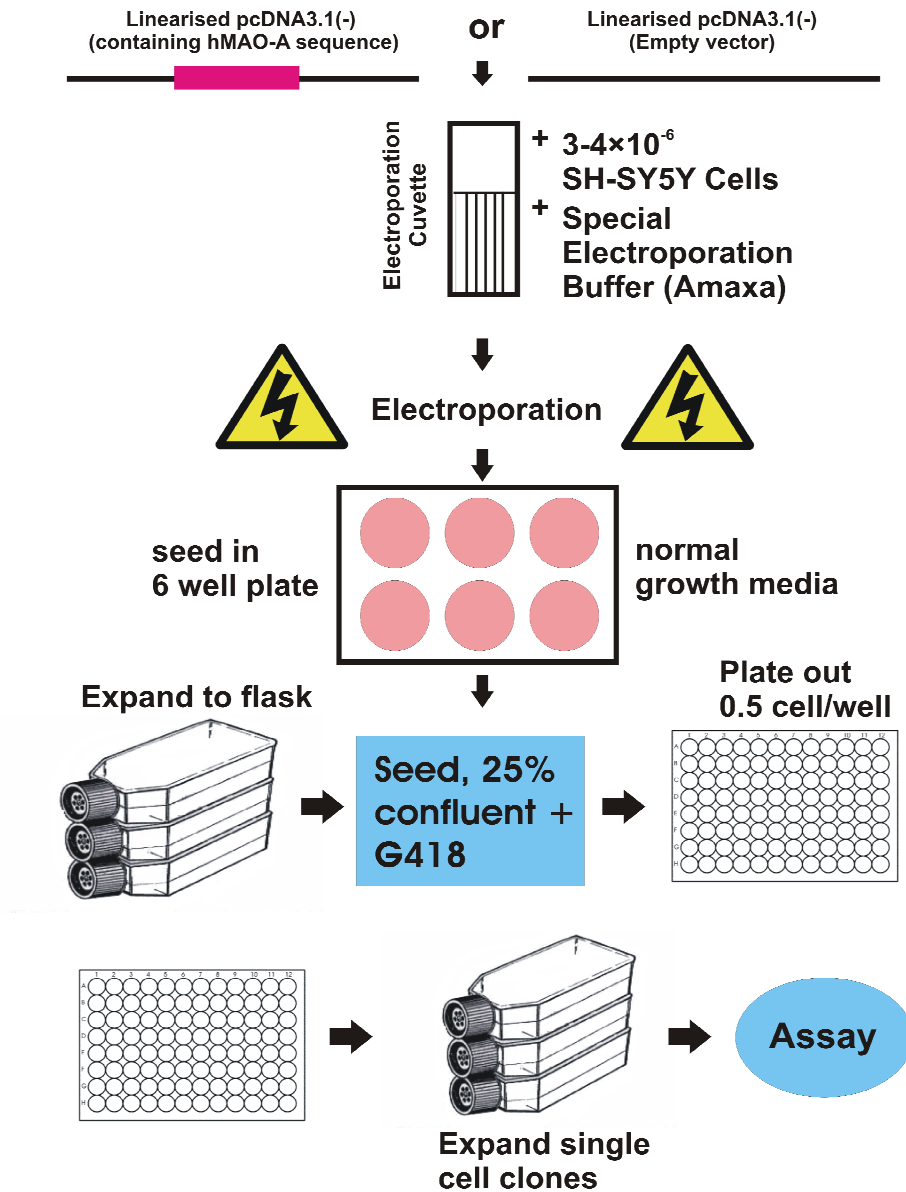


Figure 2. 2 Stable over expression of MAO-A in SH-SY5Y cells

Flow chart-Stable transfection method using electroporation. Method development work was carried out to achieve optimal transfection conditions for SH-SY5Y cells. 1 μ g plasmid DNA was mixed with 3-4 million SH-SY5Y cells re-suspended in a special electroporation buffer (supplied by Amaya GmbH) and electroporated. The cells were seeded equally between a 6-well plate, in normal growth medium for 24 hours. After 48 hours a viable cell count is performed and the cells seeded into flasks at 25% confluence in selective growth medium (normal growth medium containing G418 sulphate). The media is changed every 3-4 days until resistant foci are visible (this may take some weeks). Resistant cells are then serially diluted to seed (in theory) half a cell per well in >10X 96-well plates. Once confluent, cells from each well are studied using light microscopy to ensure that the colony of cells has arisen from a single cell. Stable clones are then expanded for assay.

2.4.6 MAO-A knockdown in SH-SY5Y cells

A description of RNAi technology can be found in chapter 6, section 6.1. Initially pre-designed human MAO-A siRNAs made by Santa Cruz Biotechnology were used to knock down MAO-A expression. However these experiments were unsuccessful. miRNA technology was then chosen to knock down MAO-A in the cells since this technique was thought to be advantageous over siRNA or shRNA technologies.

Human MAO-A was stably knocked down in the human neuroblastoma (SH-SY5Y) cell line by means of the BLOCK iT Pol II miR expression vector technology (Invitrogen, Karlsruhe, Germany). The pcDNA6.2-GW/miR expression vector facilitates the generation of an expression clone containing one or more double stranded oligonucleotide encoding a pre-miRNA sequence directed against MAO-A mRNA. The resulting expression construct was transformed into competent bacteria and the expressed plasmid DNA purified and transfected into SH-SY5Y cells by electroporation. Stable SH-SY5Y clones were selected by their resistance to the antibiotic Blasticidin.

2.4.6.1 Cloning procedure

An overview of the cloning procedure is shown in Figure 2. 3. Two single stranded DNA oligonucleotides encoding pre-miRNA for human MAO-A were designed using online resources provided by Invitrogen (BLOCK-iT RNAi Designer).

Oligonucleotide name	Oligonucleotide sequence (5'-3')	Fragment size
Sh-hMAO-A_617 forward	TGC TGC CAT TTG TCA GCA TGT TGA GCG TTT TGG CCA CTG ACT GAC GCT CAA CAC TGA CAA ATG G	64 bp
Sh-hMAO-A_617 reverse	CTT GCC ATT TGT CAG TGT TGA GCG TCA GTC AGT GGC CAA AAC GCT CAA CAT GCT GAC AAA TGG C	
Sh-hMAO-A_1544 forward	TGC TGA TTG AAG ACC TCC CTA GCT GCG TTT TGG CCA CTG ACT GAC GCA GCT AGA GGT CTT AAA T	64 bp
Sh-hMAO-A_1544 reverse	CCT GAT TTA AGA CCT CTA GCT GCG TCA GTC AGT GGC CAA AAC GCA GCT AGG GAG GTC TTA AAT C	

Table 2. 4 Oligonucleotide sequences encoding human MAO-A pre-miRNA

For each of the two oligonucleotide sequences designed (617 and 1544) the following procedure was applied. The single stranded DNA oligonucleotides were annealed to

generate a double stranded (ds) DNA oligonucleotide following the manufacturer's instructions. A small amount of the annealed product was run on a 4 % agarose, 1 X TAE gel to confirm successful annealing (the presence of one 64 bp dsDNA fragment). The dsDNA oligonucleotide was diluted, cloned into the pcDNA 6.2-GW/miR vector and transformed into competent bacterial cells according to the manufacturer's instructions. Restriction digests were performed to confirm successful cloning and DNA from positive bacterial clones were sent for sequencing following quantitative digestion using the restriction enzyme MScI. Following confirmation that the DNA sequence was free from mutations, transient transfections of SH-SY5Y cells with the DNA from a '617 Sh-hMAO-A sequence containing' clone, from a '1544 Sh-hMAO-A sequence containing' clone and the negative control plasmid DNA (Negative control plasmid DNA was prepared according to the instructions of the manufacturer) were performed. Both RNA and total extracts from these cells were taken for qRT-PCR and catalytic activity assays to determine the level of MAO-A knockdown. Sufficient knockdown was not achieved. Therefore, miRNA chaining of both sh-hMAO-A inserts (617 and 1544) and cloning into one pcDNA 6.2-GW/miR vector was performed to achieve a more efficient knockdown. The miRNA chaining procedure was performed by a number of quantitative digestion steps and cloning which is described in Figure 2. 3. Instructions for miRNA chaining are provided in the BLOCK iT Pol II miR manual (Invitrogen, Karlsruhe, Germany). As before restriction endonuclease digests were performed to confirm successful cloning following transformation into bacteria and the plasmid DNA from a positive clone containing the chained miRNA insert was sent for sequencing. Following confirmation that DNA was free from mutation, transient transfections were performed using purified plasmid DNA. Data suggested significant knockdown of MAO-A mRNA after 48 h. 1 µg of the chained (clone 10) DNA was used to stably transfect SH-SY5Y cells by electroporation as suggested by the manufacturers (see Figure 2. 2). The antibiotic blasticidin was used for the selection procedure.

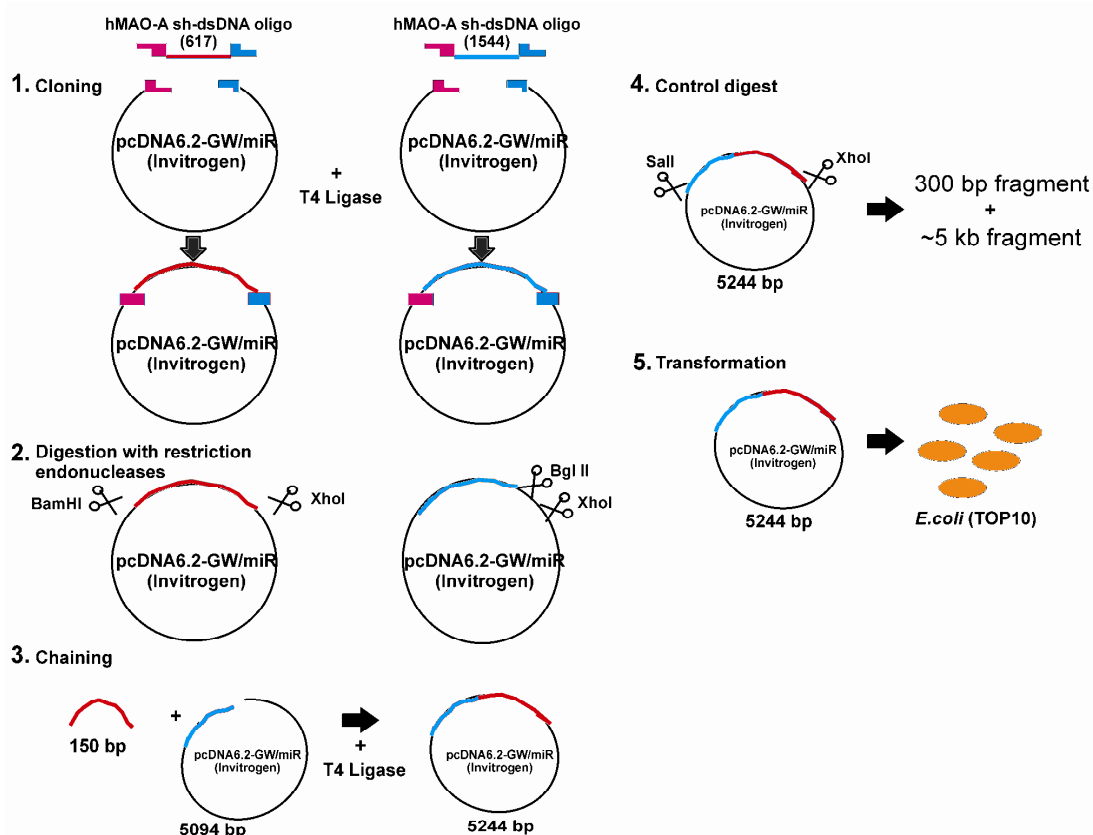


Figure 2. 3 Overview of cloning procedures used for knockdown of MAO-A using BLOCK-iT miRNA expression vector kit

In order to achieve better cloning efficiency, a second round of stable transfection was performed using the linearised vector. 1µg of the chained DNA was linearised with the restriction endonuclease BssHII. Linearisation was confirmed by agarose gel electrophoresis. The linearised plasmid was purified (Qiagen PCR purification kit) then used for the transfection of the cells. MAO-A- stable clones used in this thesis were a result of this transfection.

Name of sh- oligo' sequence	Number given to the successful clone used	DNA purified and DNA stock made by Midi-prep?	Glycerol stocks of bacterial clone?	Amount of plasmid DNA used for transfection and time point for extraction or stable cloning
617	4	Yes (Midi-prep)	Yes	1 µg, 48 h
1544	7	Yes (Midi-prep)	Yes	1 µg, 48 h
N/A (chained 617 and 1544)	10	Yes (Mini-prep)	Yes	1 µg, 48 h

Table 2. 5 Useful information for miRNA experiments

CHAPTER 3

THE ROLE OF MAO IN MITOCHONDRIA-MEDIATED NEURONAL APOPTOSIS

THE ROLE OF MAO IN MITOCHONDRIA-MEDIATED NEURONAL APOPTOSIS

3.1. INTRODUCTION

Oxidative deamination of amines by MAO produces H_2O_2 as one of the reaction's by-products. This is a key contributor to increased steady state concentrations of ROS (Cadenas and Davies 2000) which cause oxidative damage to mitochondrial DNA (Hauptmann *et al.* 1996), the electron transport system and antioxidant defence systems (Cohen and Kesler 1999). Thus elevated MAO activities are likely to cause damage to the cell, according to the ROS theory of cell death. The damaging effects of H_2O_2 and its involvement in cell death processes are well known (Cadenas and Davies 2000, Chandra *et al.* 2000). More recently, H_2O_2 has been shown to be an essential redox signalling molecule (Toledano *et al.* 2004), a mitogen in cell survival/proliferation (Sohal and Weindruch 1996, Vindis *et al.* 2000, Yoon *et al.* 2002) and involved in G protein activation (Nishida *et al.* 2000) and MAPK signalling (Guyton *et al.* 1996 Finkel 1998, Wang *et al.* 1998, Crossthwaite *et al.* 2002, Ruffels *et al.* 2003).

3.1.1 Previous work

The role of MAO in neuronal cell death has been the focus of three recent publications. Induction of apoptosis in rat PC12 cells was paralleled by an increase in MAO-A expression (DeZutter and Davis 2001), mediated by the stress activated p38 MAPK signal transduction pathway. On the contrary, MAO-A has been found to be a target of a dopaminergic toxin, N-methyl-R-salsolinol, and in this case inhibition of MAO appears to lead to apoptosis in human SH-SY5Y cells (Yi *et al.* 2006a). Most recently, Ou and co-workers (Ou *et al.* 2006) have reported that growth factor deprivation led to concomitant reduction in the transcription factor repressor R1 (RAM2/CDCA7L/JPO2), increase in MAO-A expression and activity in human SH-SY5Y cells, and a reduction in oxidoreductase activity (MTT assay used as a means of cell viability).

3.1.2 An *In Vitro* Model of Neuronal Apoptosis

3.1.2.1 SH-SY5Y human neuroblastoma cell line

Whilst animal models are extremely useful with regard to pathological changes occurring as a result of apoptosis in a physiological setting, their use is often limited for a number of reasons, notably species differences and ethical issues.

Studies on Parkinson's disease and other neurodegenerative diseases have greatly benefited from the use of *post mortem* samples. However, human *post mortem* brain samples are not only extremely difficult to obtain (due to strict ethical regulations) and their value usually restricted because of *post mortem* delay (the period between death and harvesting) or samples are derived from individuals in the final stages of the disease, subjected to intervention with numerous drugs (which themselves may affect the final pathology). It is worth noting that although it is well established that neuronal cells die progressively in neurodegenerative diseases (Friedlander and Yuan 1998), the type of cell death may vary between conditions. Nevertheless there is a wealth of evidence suggesting that apoptotic type cell death occurs predominantly in chronic neuronal diseases such as Huntington's disease, Parkinson's disease, ALS, Alzheimer's disease and dementia, whilst acute brain injury such as ischemic stroke is thought to involve a combination of apoptotic and necrotic cell death (reviewed by Friedlander 2003).

In vitro experiments allow investigation of biochemical and molecular events in a specific cell type in a controlled environment. The SH-SY5Y human neuroblastoma cell line was previously characterised in our group (Beck 2004).

Human neuroblastoma is a cancer of early childhood and arises from the neural crest (Ciccarone *et al.* 1989). The neuroblastoma cell line SK-N-SH was established from the metastatic bone tumour of a young female (Biedler *et al.* 1973) and thrice cloned to produce the SH-SY5Y cell line (Biedler *et al.* 1973). The SH-SY5Y cell line has been further characterised by Ross (Ross *et al.* 1983) and then Ciccarone (Ciccarone *et al.* 1989) who described the cell line as possessing three morphologically distinct cell types, the N type is neuroblast-like, having small cell bodies and short neurite processes, poorly adherent but able to form aggregates. The S type is epithelial/fibroblast like, larger and flatter than the N type and is highly substrate adherent. Finally the I type is an intermediate cell type, expressing properties of both the N and S type (Ross *et al.* 1983). SH-SY5Y cells undergo spontaneous bi-directional phenotypic and biochemical interconversion between the neuroblast and fibroblast like types, termed transdifferentiation (Ross *et al.* 1983). The

previously reported general characteristics of the SH-SY5Y cell line are presented in Table 3. 1

GROWTH	BIOCHEMICAL	KARYOTYPE
High cell densities at stationary phase (Ross <i>et al.</i> 1983)	Uptake mechanisms for noradrenaline (Ross <i>et al.</i> 1983; Ciccarone <i>et al.</i> 1989), epinephrine, dopamine, MPP ion and other neurotransmitters	Abnormalities (+7 position) on chromosome 9 and chromosome 22 (Ross <i>et al.</i> 1983)
Extensive multi-layering of cells (Ross <i>et al.</i> 1983)	Biosynthetic enzymes for neurotransmitter synthesis (Ciccarone <i>et al.</i> 1989)	Complex duplication of the long arm of chromosome 1 (Ross <i>et al.</i> 1983)
Formation of dense focal aggregates (Ross <i>et al.</i> 1983)	Contains three neurofilaments (200 kDa, 150 kDa and 68 kDa, Ciccarone <i>et al.</i> 1989)	
	Dopamine rich (Song <i>et al.</i> 1996; Song and Ehrich, 1998)	
	Expresses dopamine uptake receptor (Song <i>et al.</i> 1996; Song and Ehrich, 1998)	
	Contain MAO enzymes (Song and Ehrich, 1998)	

Table 3. 1 General Characteristics of the SH-SY5Y Human Neuroblastoma Cell Line

The most important characteristics of SH-SY5Y cells with regards to this work are that they contain MAO enzymes, are able to synthesise dopamine and have neuronal characteristics. The existence of MAO activities in the SH-SY5Y cell line were revealed when Song and others were investigating the uptake and metabolism of the neurotoxins MPTP and MPP⁺ (Song *et al.* 1996, Song and Ehrich 1998). The nature of the MAO isoforms was not determined in these studies. Zhu *et al.*, (1992), had showed that MAO-A mRNA expression was predominant over MAO-B mRNA expression (Zhu *et al.* 1992); nevertheless MAO-B mRNA expression was detected, later confirmed by Yi and co-workers (2006a).

3.1.2.2 Neuronal apoptosis induced by staurosporine

Staurosporine (STS) is an alkaloid produced by *Streptomyces staurosporeus* that possesses inhibitory activity against fungi and yeasts but has no significant effect on bacteria (Meksuriyen and Cordell 1988). STS is a potent inhibitor of a broad-spectrum of protein

kinases, including protein kinase C (PKC), cAMP-dependent kinases and receptor protein kinases (Boix *et al.* 1997). Its chemical structure contains an indole carbozole chromophore, which characterises a family of protein kinase inhibitors that act by blocking the ATP binding site of protein kinases (Hidaka and Kobayashi 1992). STS is widely employed as an inducer of apoptosis in many mammalian cell types (Kruman and Guo 1998) and is of particular interest in cancer chemotherapy (Meksuriyen and Cordell 1988).

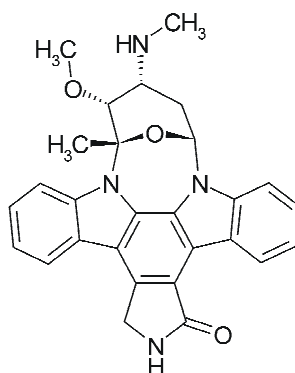


Figure 3. 1 Chemical structure of staurosporine from *Streptomyces staurosporeus*

Numerous morphological changes typical of STS induced apoptosis have been observed in neuronal cell lines, the most common being cell body shrinkage and chromatin condensation (Koh *et al.* 1995). It appears that STS-induced apoptosis in neurons is triggered by disruption of the cell cycle (Gong *et al.* 1994) and a rapid and prolonged elevation of intracellular free calcium (Ca^{2+}) levels, since calcium chelators have been shown to protect rat PC12 cells from STS-induced apoptosis (Kruman and Guo 1998). Accumulation of mitochondrial ROS occurs in the early phase of apoptosis and treatment with free radical scavengers protects PC12 cells from apoptosis (Kruman and Guo 1998). There is some controversy regarding the depletion of the anti-apoptotic protein Bcl-2; which has been claimed to be both essential (Kruman and Guo 1998, Tieu *et al.* 1999) and non-essential (Yuste *et al.* 2002) for STS-mediated apoptosis. Zhang and colleagues have shown that overexpression of Bcl-2 in a melanoma cell line protects from STS-induced early phase but not late phase apoptosis (Zhang *et al.* 2004). Increased free calcium levels and ROS (and possibly the depletion of Bcl-2) cause early activation of caspases including caspase-3 (Kruman and Guo 1998). Activation of caspases in PC12 cells by STS is followed by increased lipid peroxidation, loss of mitochondrial membrane potential and finally nuclear changes (Kruman and Guo 1998), including DNA laddering (Koh *et al.* 1995). STS treatment of SH-SY5Y cells has been reported to be associated with activation of the upstream initiator caspase-9 (mitochondrial apoptotic pathway) and caspase-3 but

not with activation of initiator caspase-8 (receptor mediated apoptotic pathway, Lopez and Ferrer 2000). Collectively, the evidence to date shows that STS is a potent inducer of apoptotic cell death and importantly this toxin is of particular relevance to this project since it induces the intrinsic apoptotic pathway (associated with the mitochondria and its function).

3.1.2.3 Caspases in SH-SY5Y cells

For a good model of neuronal apoptosis that will accurately reflect *in vivo* mechanisms of neuronal apoptosis, molecular components of the apoptotic signalling cascades should be present and inducible in SH-SY5Y cells. The activation of the executioner caspase-3 following STS exposure in SH-SY5Y is well documented (Enari *et al.* 1998, Lopez and Ferrer 2000, Tang *et al.* 2000) and STS treated cells are often used as a positive control for commercial caspase-3 activity assay kits (O' Brian *et al.* 2003). Although staurosporine is known to activate caspase-3, its essentiality in STS-induced apoptosis has been argued, with several studies claiming that STS-induced apoptosis (measured by down stream events such as DNA laddering) can still occur in the presence of Z-VAD-fmk (a caspase-3 inhibitor, Deas *et al.* 1998, Janicke *et al.* 1998). Nonetheless, as indicated earlier caspase-3 has been shown to be activated in SH-SY5Y cells following STS treatment (McGinnis 1999a, McGinnis 1999b, Lopez and Ferrer 2000). The upstream initiator caspase-9 is known to exist and be activated following apoptotic stimuli in SH-SY5Y cells (Lopez and Ferrer 2000, Xia *et al.* 2001). However, the presence and activation of the initiator caspase-8 in these cells is the focus of some debate. Lopez and Ferrer found no evidence of caspase-8 activation following STS treatment in SH-SY5Y cells (Lopez and Ferrer 2000). Numerous publications have suggested that caspase-8 protein is not expressed in SH-SY5Y cells because of gene silencing due to methylation (Eggert *et al.* 2001, Harada *et al.* 2002). Hopkins and co-workers were unable to show caspase-8 mRNA, protein expression or caspase-8 activity in control SH-SY5Y (which the authors class as N-type neuroblastoma) cells or in cells that were induced to undergo receptor-mediated apoptosis induced by the death ligand TRAIL (Hopkins *et al.* 2002). They did however find expression of caspase-8 in S-type human neuroblastoma cells. Hopkins and co-workers suggested that the caspase-8 gene was not deleted in the SH-SY5Y (N-type) cells, since caspase-8 expression was seen when the cells were made sensitive to TRAIL using the chemotherapy drug doxyrubicin (Hopkins *et al.* 2002). The authors concluded that caspase-8 expression was merely silenced in malignant neuroblastoma and that this correlated to tumour severity. Conversely, although no activation of caspase-8 was found

in SH-SY5Y cells following treatment with A β protein (Wei *et al.* 2002), the full length caspase-8 proform protein was detected and levels reduced during A β -induced apoptosis. Recently, caspase-8 proform protein only was detected by Miller and colleagues in undifferentiated SH-SY5Y cells (Miller *et al.* 2006), suggesting that variable findings in SH-SY5Y cells reflect clonal differences.

In summary, staurosporine is thought to activate caspase-9 but not caspase-8 in SH-SY5Y cells. Whether or not caspase-8 protein exists and can be activated by staurosporine in the SH-SY5Y clone used in our laboratory should be investigated.

3.1.3 Antioxidants

3.1.3.1 Vitamin C and N-Acetyl-L-cysteine

Vitamin C (L-ascorbate) is an essential nutrient and an important antioxidant *in vivo*, protecting against cancer and other diseases by scavenging ROS (Halliwell 1999). It is widely believed that vitamin C protects against cardiovascular diseases and some forms of cancer (Halliwell 1999). However, Podmore and colleagues (1998) suggested that vitamin C could damage DNA. The toxicity of vitamin C is still debated and is probably dependant on concentration. It is known to stimulate free radical reactions *in vitro* under certain conditions by reducing Fe (III) to Fe (II, Halliwell 1999). N-Acetyl-L-cysteine (NAC) is a powerful antioxidant known to protect against apoptosis (Mayer and Noble 1994). NAC is an aminothioliol antioxidant in its own right and a synthetic precursor of intracellular cysteine and glutathione (Zandwijk 1995). The thiol reducing agent glutathione plays an essential role in the cell's antioxidant defence system. Glutathione serves as a sulfhydryl buffer, cycling between its reduced thiol form (GSH) and an oxidised form (GSSG) and plays a key role in cell detoxification by reacting with hydrogen peroxide and organic peroxides (Stryer 1996). In addition, enzymes such as glutathione peroxidase and glutathione-S-transferase play key roles in detoxification. Nonetheless, reduction of total glutathione levels and oxidised glutathione levels are the earliest known biochemical indicators of nigral degeneration in the human brain (Anderson 2004).

3.1.3.2 MitoQ

MitoQ (mitoquinone) is an antioxidant, similar in structure to coenzyme Q10, which is specifically targeted to the mitochondria by covalent attachment to a lipophilic triphenylphosphonium cation (Figure 3. 2). Because of the large mitochondrial membrane potential, the cations accumulate within mitochondria up to 1,000 fold compared to non-

targeted antioxidants such as coenzyme Q10 or its analogues (Antipodean Pharmaceuticals 2007). Once there MitoQ is reduced to its active ubiquinol form, which has been used to prevent mitochondrial oxidative damage, reduce ROS-induced apoptosis (Kelso *et al.* 2000) and demonstrate the involvement of mitochondrial ROS in cell signalling pathways (James *et al.* 2004). MitoQ was invented at The University of Otago, New Zealand by Robin Smith and Michael Murphy (the latter now at The University of Cambridge, U.K). MitoQ is being developed by Antipodean Pharmaceuticals and is currently in phase II clinical trails for Parkinson's disease. The experimental control used alongside MitoQ is a compound called decyltriphenylphosphonium bromide (DTPP), which contains the TPP⁺ moiety (the cationic moiety that drives the compound to the mitochondria) but has only weak antioxidant properties (Figure 3. 2).

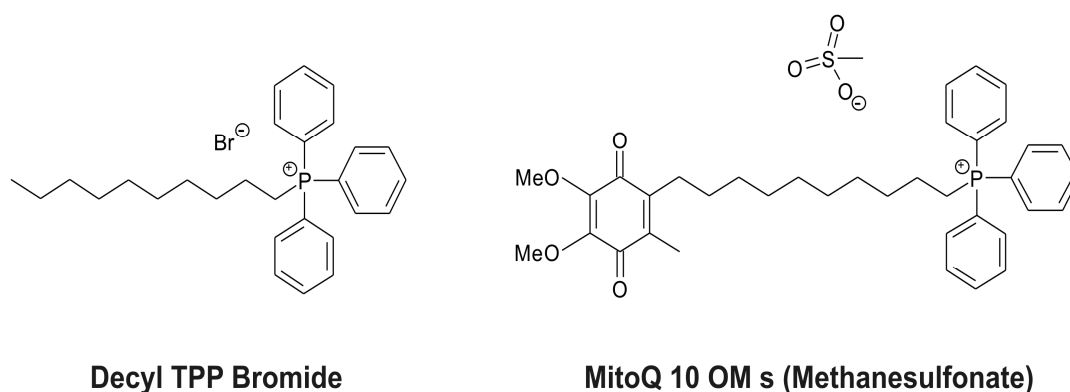


Figure 3. 2 Chemical structures of Decyl TPP and MitoQ

Left panel shows the chemical structure of Decyltriphenylphosphonium bromide (Decyl TPP or DTPP), the control compound often used in conjunction with MitoQ. DTPP consists of a lipophilic triphenylphosphonium cation moiety attached to a compound with very mild antioxidant properties. *Right panel* shows the chemical structure of MitoQ, which comprises the lipophilic triphenylphosphonium cation moiety linked with a quinone group antioxidant.

3.1.4 Aims of Chapter

Human neuroblastoma cells (SH-SY5Y) display a neuronal phenotype, have neurotransmitter uptake mechanisms and are dopamine rich, providing an excellent human neuronal cell model.

The aims of this chapter of the thesis were:

- **To determine the MAO status of human neuroblastoma cells**

MAO activity levels were measured by titration with MAO-A and -B specific inhibitors *in vitro*. To support the MAO activity data, expression of the MAO isoforms were investigated at the protein and messenger RNA level. Analysis of MAO proteins involved the use of MAO isoform-specific monoclonal antibodies made in our

laboratory, which were previously characterised (Church *et al.* 1994, Rodriguez *et al.* 2000, Sivasubramaniam *et al.* 2002, Billett and Mayer 1986). Analysis of MAO mRNA expression was carried out using oligonucleotide primers, designed to probe and bind to MAO-A or MAO-B specific cDNA sequences. This involved a conventional RT-PCR approach and secondly a more sensitive and quantitative RT-PCR method (real time- or q-RT-PCR).

- **To characterise apoptotic cell death induced by staurosporine in human neuroblastoma cells**

The concentration of STS commonly used to induce apoptotic cell death in SH-SY5Y cells ranges between 0.5 μ M-1 μ M (Boix *et al.* 1997; Lopez and Ferrer, 2000; Yuste *et al.* 2002). An initial titration of STS to determine its effect on cell viability and cell morphology was undertaken to ensure induction of apoptotic cell death and not differentiation. A time course of cell viability (MTT assay) and execution of apoptosis (caspase-3 activation assay) was monitored. Caspase-3 is a well established biochemical marker of apoptosis (Hartmann *et al.* 2000, Ashe and Berry 2003). Caspase-3 is common to all apoptotic pathways, representing the point where the execution of apoptosis begins, committing the cell to die. Activation of upstream caspases-8 and -9 were assessed to determine whether the receptor-mediated or mitochondrially mediated route was predominant in STS-induced apoptosis. Finally, expression of caspase-8 and -9 at the mRNA level and protein level was investigated using conventional PCR, quantitative PCR and western blotting to confirm the presence of these apoptotic components in our SH-SY5Y clone.

- **To assess the role of MAO in STS-induced apoptosis**

The objectives were to monitor changes in MAO catalytic activity, protein and mRNA expression levels during STS-induced apoptosis. To confirm the relevance of MAO in the apoptotic cascade, caspase-3 activation, cell viability (MTT reduction), changes in morphology and upstream caspase activation were measured during STS-induced apoptosis with or without MAO inhibition. To improve the validity of the data two unrelated MAO inhibitors were used.

- **To define how MAO mediates apoptosis**

MAPK phosphorylation cascades are activated following oxidative stress (Finkel 1998) and are involved in the activation of MAO-B expression (Wong *et al.* 2002) and in pro-apoptotic MAO-A expression (DeZutter and Davis, 2001). The Bcl-2 family of

proteins are critical in apoptotic signalling because of their anti- and –pro-apoptotic effects at the mitochondrial surface. To investigate the mechanism of involvement of MAO in STS induced apoptosis, changes in MAO were related to production of ROS, activation of caspases, Bcl-2 levels and MAPK signalling pathways.

3.2. RESULTS

3.2.1 Characterisation of apoptotic model

3.1.1.1 MAO isotype status of SH-SY5Y cells

MAO activity was measured *in vitro* in SH-SY5Y cell homogenates following titration with specific and irreversible inhibitors of MAO-A (clorgyline) and MAO-B (deprenyl) (Figure 3. 3A). Complete inhibition of MAO activity was achieved with 10^{-8} M clorgyline or 10^{-5} M deprenyl (Figure 3. 3A), suggesting MAO-A prevalence in this cell line. MAO-A but not MAO-B protein was detected in SH-SY5Y cells (Figure 3. 3B) using immunohistochemical analysis with monoclonal antibodies specific to MAO-A and MAO-B. In contrast, control human liver sections exhibited positive staining for both MAO-A and –B (Figure 3. 3B).

Conventional RT-PCR revealed an intense signal for MAO-A indicating strong expression of the MAO-A messenger (Figure 3. 3C). In contrast, no signal was observed for the MAO-B messenger. Finally, using the more sensitive approach of qRT-PCR, average MAO-A mRNA expression of 2.58 ± 1.00 molecules/1000 molecules GAPDH was measured, whereas MAO-B mRNA levels were insignificant (0.0006 ± 0.0005 molecules/1000 molecules GAPDH, data not presented). Since, approximately 4000 fold more MAO-A mRNA than MAO-B mRNA was detected using quantitative RT-PCR, it appears that only the MAO-A isoform is present in SH-SY5Y cells.

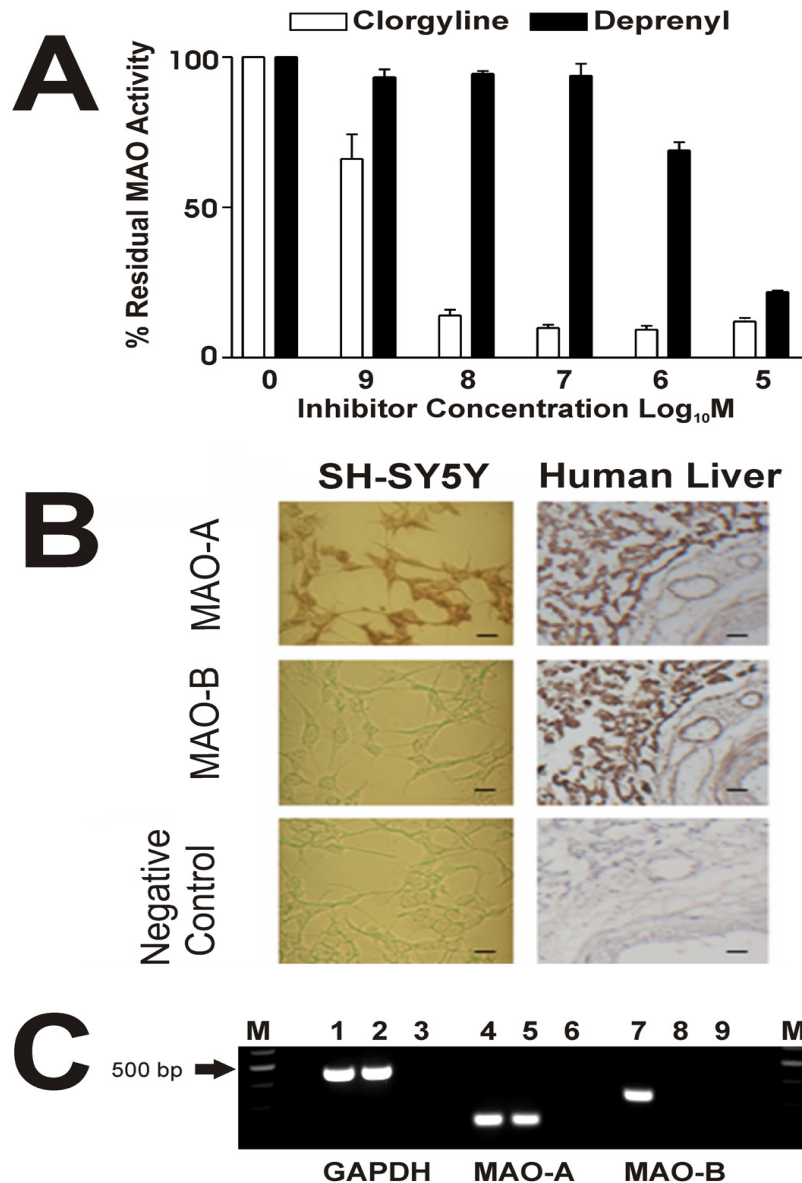


Figure 3.3 MAO-A is predominant in SH-SY5Y human neuroblastoma cells

(A) MAO activity in SH-SY5Y cells was measured following addition of 0, 10^{-9} , 10^{-8} , 10^{-7} , 10^{-6} , 10^{-5} M clorgyline or deprenyl via a radiometric method using ^{14}C -Tyramine as a substrate. MAO activity was determined in the presence or absence of the inhibitors and expressed as % residual activity. (B) SH-SY5Y cells and human liver sections were probed using MAO-A (6G11-E1) and MAO-B (3F12/G10/2E3) specific primary antibodies (see section M&M) using 3, 3'-Diaminobenzidine as substrate for the secondary antibody. Control sections were incubated in the absence of MAO-specific antibodies but subjected to the same conditions. MAO immunoreactivity is represented by dark brown/red staining. The images shown are from a representative experiment. Scale bar represents 20 μm . (C) Agarose gel showing positive PCR controls (lanes 1, 4 and 7), SH-SY5Y samples (lanes 2, 5 and 8) and negative PCR controls (lanes 3, 6 and 9) for GAPDH, MAO-A and MAO-B gene expression.

3.1.1.2 Cell viability

Initially, we used the MTT reduction assay (which is a measure of cell viability / proliferation) to obtain a dose response to STS administered to the cells in serum free

medium (Figure 3. 4). At 1 h following STS insult no loss of cell viability was observed. After 16 h, doses of 0.5 and 1 μM STS significantly reduced cell viability (~25% reduction to ~50% reduction, respectively). By 24 h 0.05 μM STS reduced cell viability by ~40% and higher concentrations reduced cell viability by ~60% (Figure 3. 4).

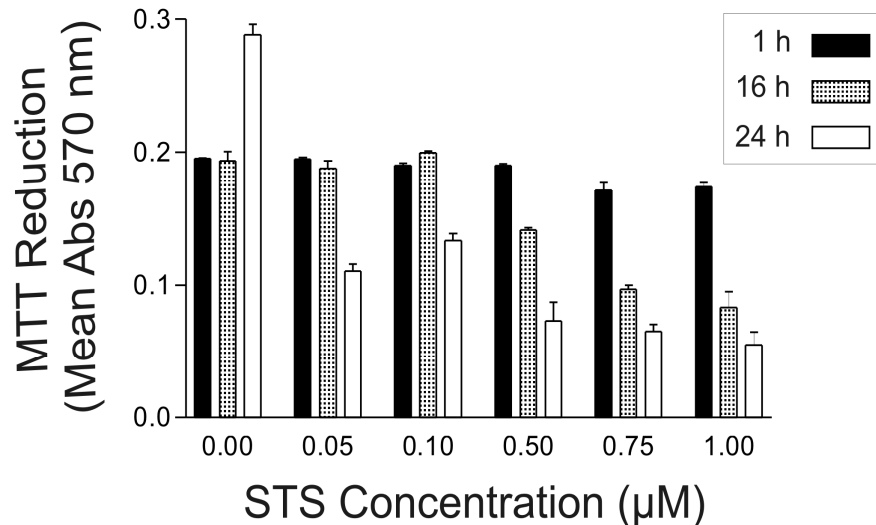


Figure 3. 4 Concentration of STS required to reduce the cell viability of SH-SY5Y Cells

Cell viability was measured in SH-SY5Y cells over 24 h, following the addition of 0.05, 0.1, 0.5, 0.75, and 1 μM STS or no STS. MTT reduction was determined and expressed as mean absorbance values at 570 nm \pm SEM. Replicates in assay=12 and n=2.

The concentration of STS commonly used to induce apoptotic cell death in SH-SY5Y cells ranges between 0.5 μM -1 μM (Boix *et al.* 1997, Lopez and Ferrer 2000, Yuste *et al.* 2002). A 1 μM concentration of STS was chosen for further studies on cell morphology. Images of cells were taken following exposure to 1 μM STS over a 3 h period (Figure 3. 5). Control cells were exposed to serum free medium only (-STS) and show the normal SH-SY5Y neuronal phenotype which is: flat, elongated, approximately 20-30 μm in length with limited neurite-like structures over this short time course. Serum free medium was used as the vehicle and control for all experiments using STS. Following the addition of STS, the cells immediately show classical hallmarks of apoptosis which are: shrinkage, rounding, surface blebbing, shininess and nuclear condensation. These characteristics are evident after as little as 0.5 h in STS and are also present after 1 and 3 h (Figure 3. 5).

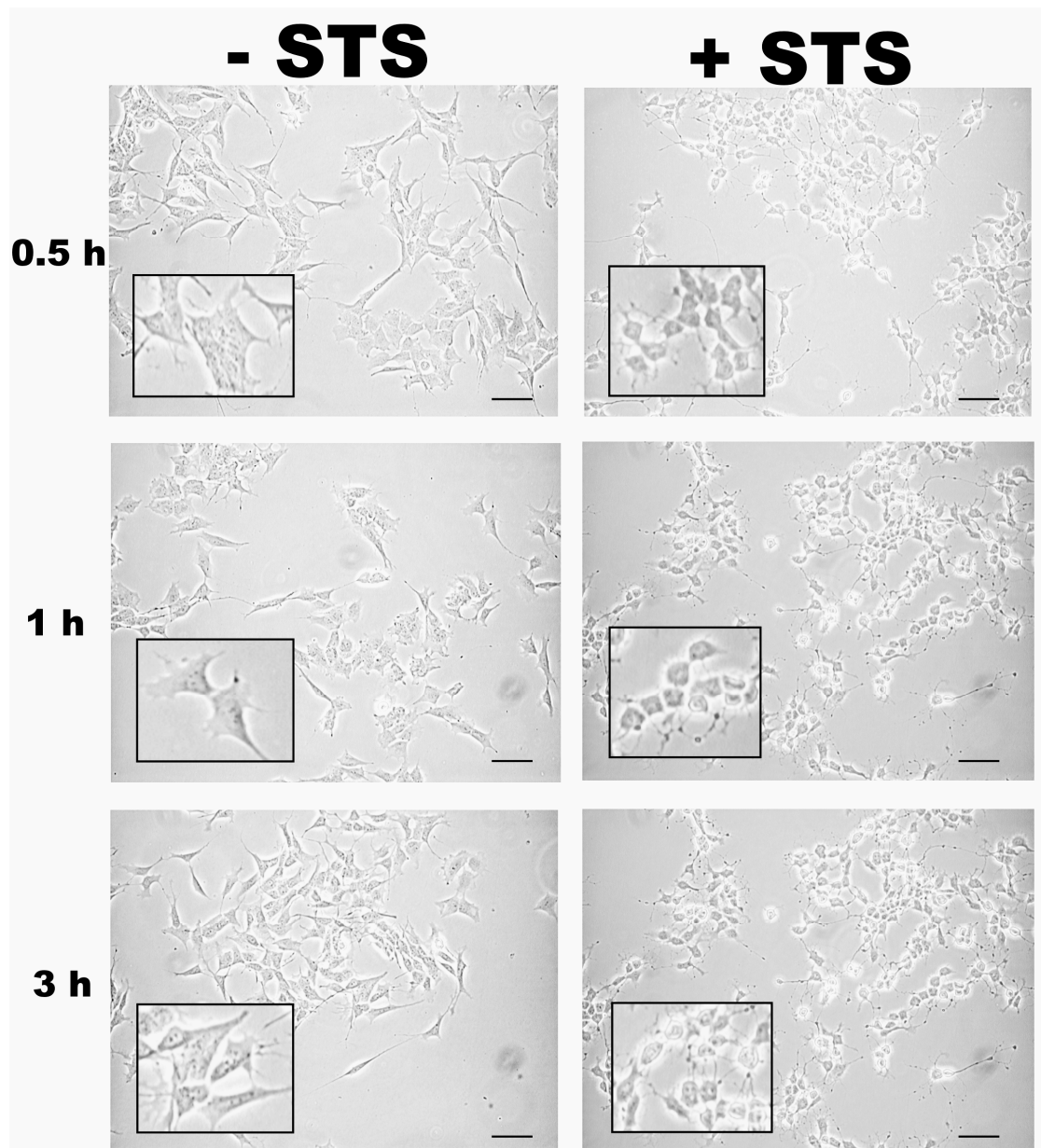


Figure 3. 5 STS induces apoptotic morphologies in SH-SY5Y cells

SH-SY5Y cells were exposed to 1 μ M STS for up to 3 h. Cell morphologies were visualised using a Nikon eclipse TS100 microscope. Photomicrographs ($\times 10$ objectives, taken on Nikon DN100 digital camera) are shown at 0.5 h, 1 h and 3 h post-treatment and are representative of 3 independent experiments. Scale bar represents 20 μ m. Photomicrographs have been enlarged in each case and a small area shown inset.

To further monitor cell viability following exposure to 1 μ M STS, MTT reduction was measured again, but over a 6 h period. Cell viability is only significantly reduced following 4 h exposure to STS (Figure 3. 6).

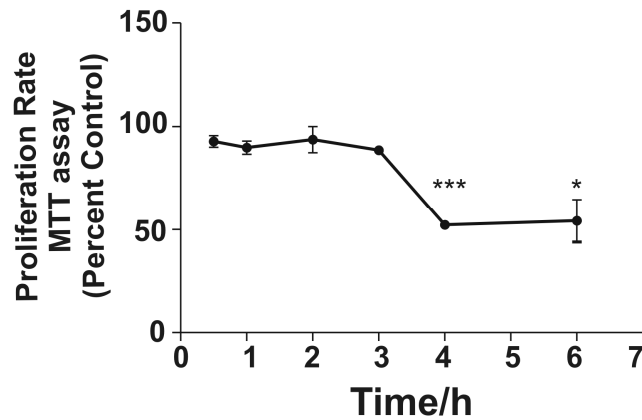


Figure 3. 6 STS induces loss of cell viability in SH-SY5Y cells

Cell viability was measured in SH-SY5Y cells over 6 h, following the addition of 1 μ M STS using the MTT reduction assay. MTT reduction is expressed as mean percent cell viability compared to control \pm S. D, where replicates in assay=12 and n=3. Treated samples were statistically compared to untreated controls using the Student's t-test where * p <0.05 and *** p <0.001.

3.1.1.3 Apoptotic markers

Since the MTT reduction assay only measures loss of cell metabolism it was necessary to investigate whether apoptotic cell death was occurring following exposure to 1 μ M STS. Treatment with 1 μ M STS consistently resulted in caspase-3 activation (around twenty fold of control levels, peaking at around 3 h, Figure 3. 7), before returning to baseline levels.

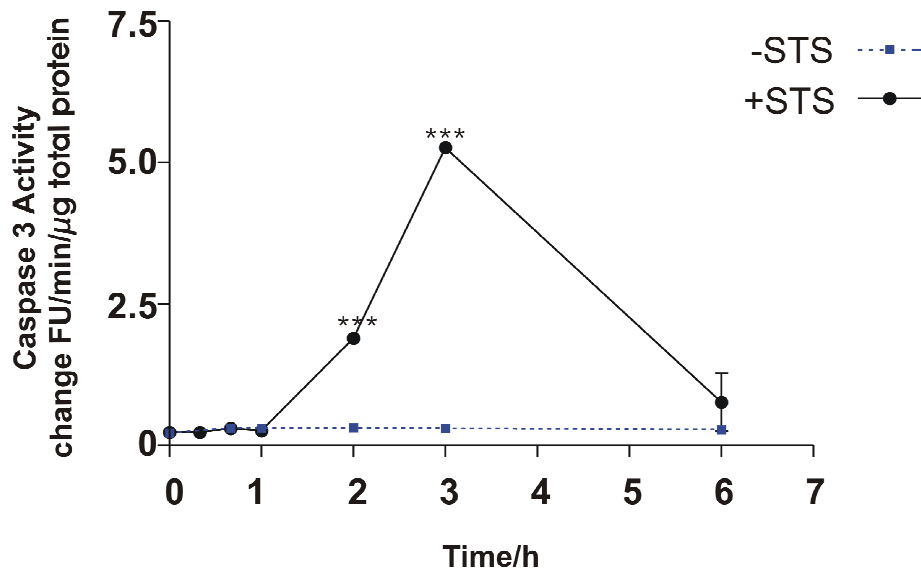


Figure 3. 7 Caspase-3 is activated following STS exposure in SH-SY5Y cells.

Following addition of 1 μ M STS, Caspase-3 activity was measured to monitor the apoptotic time course, using Acetyl-Asp-Glu-Val-Asp-7-Amidomethylcoumarin as substrate and expressed as change FU/min/ μ g protein. All data represent triplicate values from three independent experiments (n=3) and are expressed as mean \pm S.D. Treated samples were statistically compared to untreated controls using the Student's t-test where *** p <0.001.

To further characterise the apoptotic cell death pathways in this model, activation of upstream initiator caspases was assessed. Throughout the apoptotic time course induced by

STS, caspase-9 was consistently activated (detected after 1 h STS exposure and remaining active for the following 5 h, Figure 3. 8A). However, no activation of caspase-8 was detected, despite the presence of the caspase-8 proform (Figure 3. 8B) in both untreated and treated cells, confirming the presence of procaspase-8 protein in our clone.

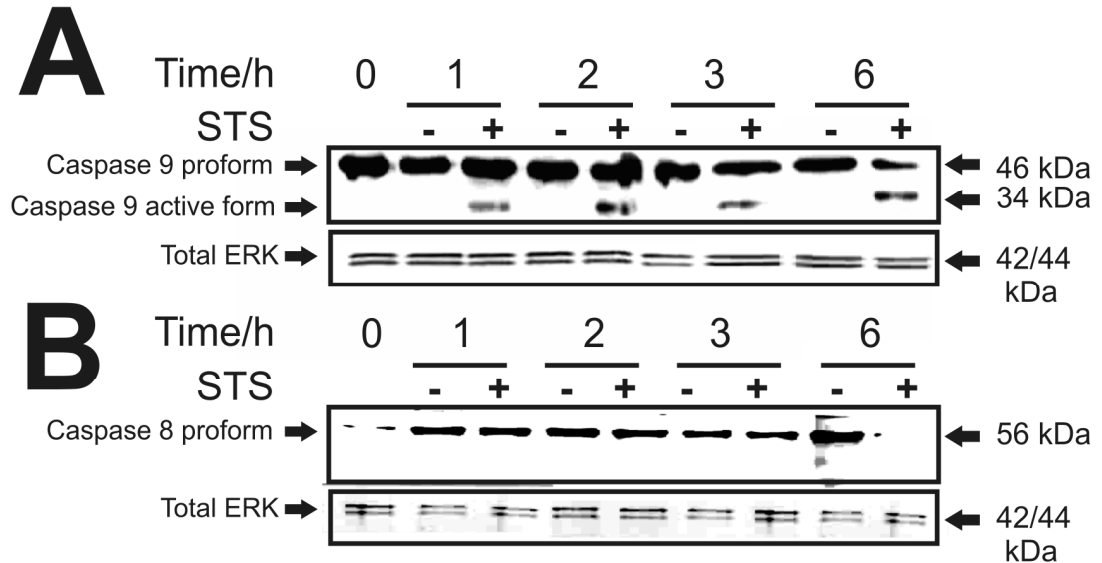


Figure 3. 8 The intrinsic but not extrinsic pathway is active in STS-induced apoptosis

(A) Western blot analysis of caspase-9 activation (pro-form / active form) in cell extracts of SH-SY5Y cells exposed to 1 μ M STS over a 6 h period. Equal protein aliquots (20 μ g) were separated on a 12 % (v/v) acrylamide SDS-PAGE gel prior to transfer to nitrocellulose membranes. The blot was probed with anti-caspase-9 antibody (2 μ g/ml) which detected both the pro-form (46 kDa) and the active-form (34 kDa). (B) Western blot analysis of caspase-8 activation (pro-form / active form) in cell extracts of SH-SY5Y cells exposed to 1 μ M STS over a 6 h period. Equal protein aliquots (50 μ g) were separated on a 12 % (v/v) acrylamide SDS-PAGE gel prior to transfer to nitrocellulose membranes. The blot was probed with anti-caspase-8 antibody (2 μ g/ml) which detected the pro-form (56 kDa) but not the active-form (28 kDa). Equal loading in both cases was checked by probing for total ERK (1: 1000 dilution). The Western blots shown are representative of three separate experiments.

To confirm caspase-8 and caspase-9 expression in SH-SY5Y, conventional RT-PCR and the more sensitive qRT-PCR approach were applied to detect mRNA expression in both SH-SY5Y and U937 cells (Figure 3. 9). The human U937 cell line used in our laboratory was used as a positive control for caspase-8 expression since it is known to contain caspase-8 and is sensitive to Fas ligand stimulation (Niikura *et al.* 2002). Figure 3. 9 shows the presence of both caspase-8 and caspase-9 mRNA expression in SH-SY5Y and U937 cells (see chapter 4).

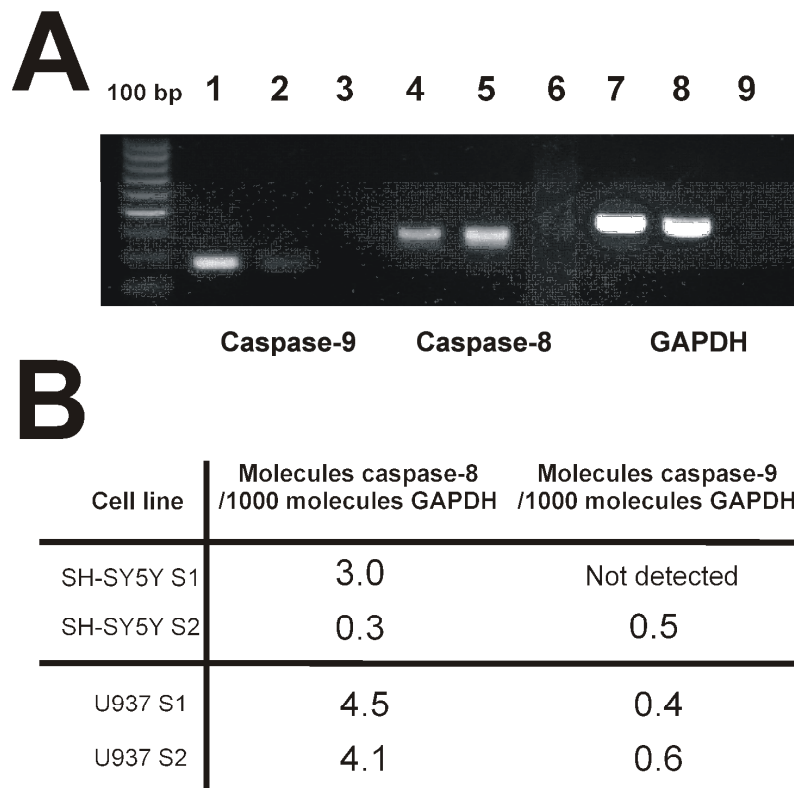


Figure 3. 9 Caspase-8 and -9 mRNA is detectable in SH-SY5Y cells

(A) Agarose gel showing SH-SY5Y samples (lanes 1,4 and 7), U937 samples (lanes 2, 5 and 8) and negative PCR controls (lanes 3, 6 and 9) for caspase-9, caspase-8 and GAPDH gene expression. (B) Quantitative RT-PCR data expressed as single values for each independent SH-SY5Y or U937 cell sample (sample 1, S1 and sample 2, S2).

3.2.2 Changes in MAO in STS-induced apoptosis

Peak caspase-3 activation following exposure to 1 μ M STS (approximately 3 h, Figure 3. 7) was preceded by a significant (two- to -threefold) increase in MAO catalytic activity (Figure 3. 10) which peaked at around 1 h and remained high during the subsequent 5 h period.

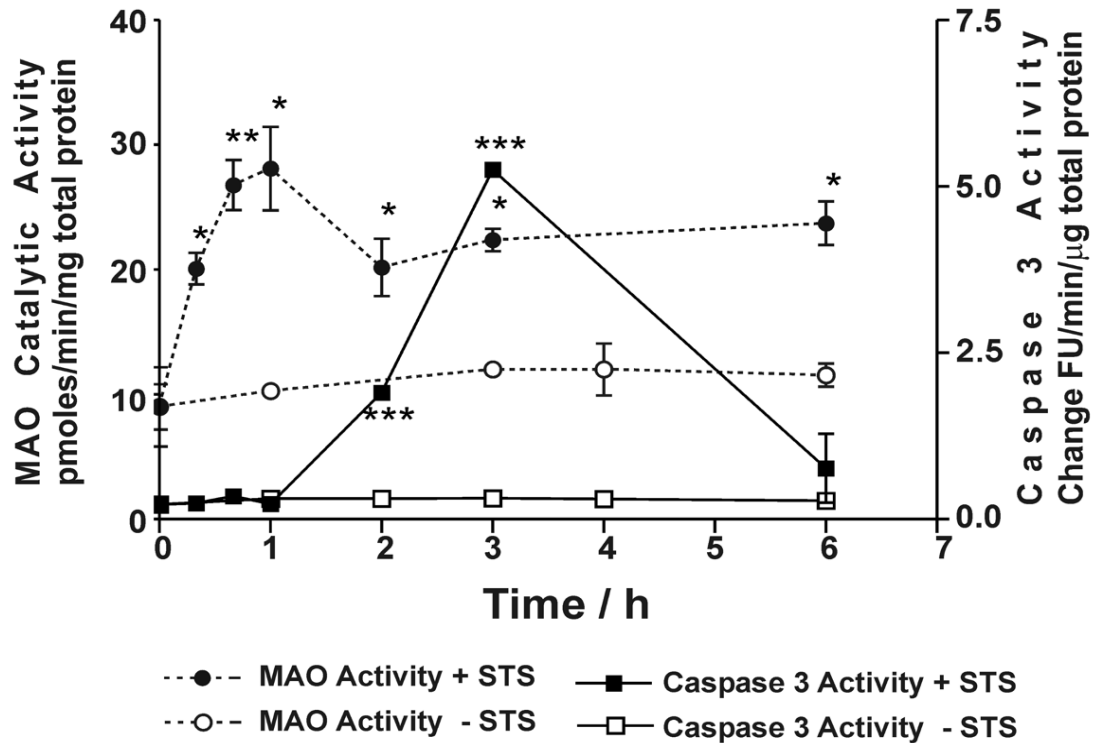


Figure 3.10 Changes in MAO and caspase-3 activities following STS treatment

Following addition of 1 μM STS, MAO activity was measured in SH-SY5Y via a radiometric method, using ^{14}C -Tyramine as a substrate. MAO catalytic activity was expressed as pmoles/min/mg protein. Caspase-3 activation was measured to monitor the apoptotic time course, using Acetyl-Asp-Glu-Val-Asp-7-Amidomethylcoumarin as substrate and expressed as $\Delta\text{FU}/\text{min}/\mu\text{g}$ protein. All data represent triplicate values from three independent experiments ($n=3$) and are expressed as mean \pm S.D. Treated samples were statistically compared to untreated controls using the Student's t-test where * $p<0.05$, ** $p<0.01$, *** $p<0.001$.

Increased MAO activity was associated with a significant but transient increase in MAO-A protein (two- to threefold, Figure 3.11). MAO-A protein levels were significantly elevated in a time dependent manner, reaching maximal activity at 1 h post STS treatment (Figure 3.11). MAO-A protein levels then return back to control level over the following 2 h (Figure 3.11).

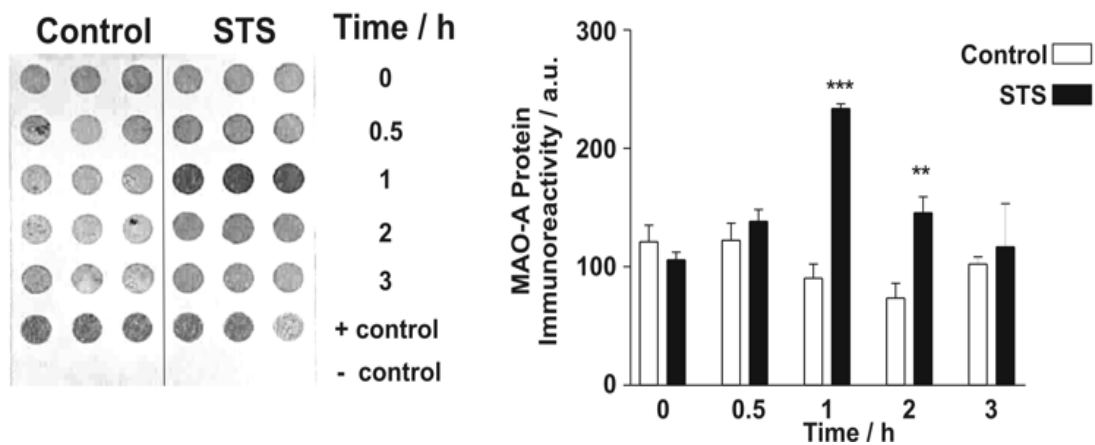
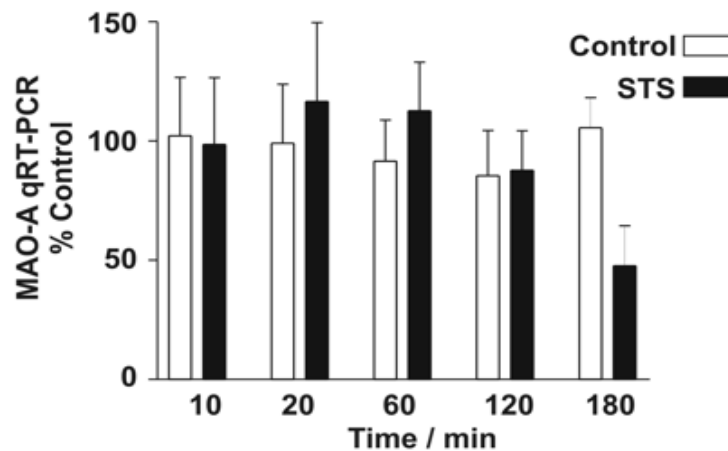


Figure 3. 11 STS-induced apoptosis causes increased MAO-A protein

Left panel shows a dot blot of MAO-A protein levels following STS exposure. Equal protein homogenates were loaded on to a nitrocellulose membrane and probed with a MAO-A specific antibody. Mitochondrial outer membranes from human liver are the positive control and no primary antibody was the negative control. *Right panel*. Quantification of dot blots. Blots were digitised and densitometry was performed to quantify relative MAO-A protein levels in all blots. These data represents values from four separate experiments ($n=4$) and expressed as mean arbitrary units (a.u.) \pm S. D. Statistical analysis of treated cells in comparison to untreated controls was carried out using the Student's t test, where ** $p<0.01$, *** $p<0.001$.

To determine whether the increased MAO-A protein levels were a result of increased MAO-A mRNA expression, quantitative RT-PCR analyses were performed. No significant changes in MAO-A mRNA levels were detected following 1 μ M STS over a 3 h apoptotic time course (Figure 3. 12).

**Figure 3. 12 MAO-A mRNA expression levels are unaffected by STS**

MAO-A mRNA expression was measured by qRT-PCR following the addition of 1 μ M STS for 3 h. Data represent duplicate values from three independent experiments ($n=3$). Values are expressed as means (% untreated control) \pm S.D. Statistical analysis of treated cells in comparison to untreated controls was performed using the Student's t-test, where no data was significant at $p<0.05$.

3.2.3 Relevance of MAO in STS induced apoptosis

Two unrelated MAO inhibitors, clorgyline and tranylcypromine, inhibit *in situ* MAO activity in SH-SY5Y cells in the presence and absence of STS during a 4 h time period (Figure 3. 13). Caspase-3 activity was measured following inhibition of MAO-A in this apoptotic model to investigate the relevance of MAO in the apoptotic cascade. Both clorgyline and tranylcypromine significantly reduced caspases-3 activation by 50 % and 35 % respectively (Figure 3. 13B).

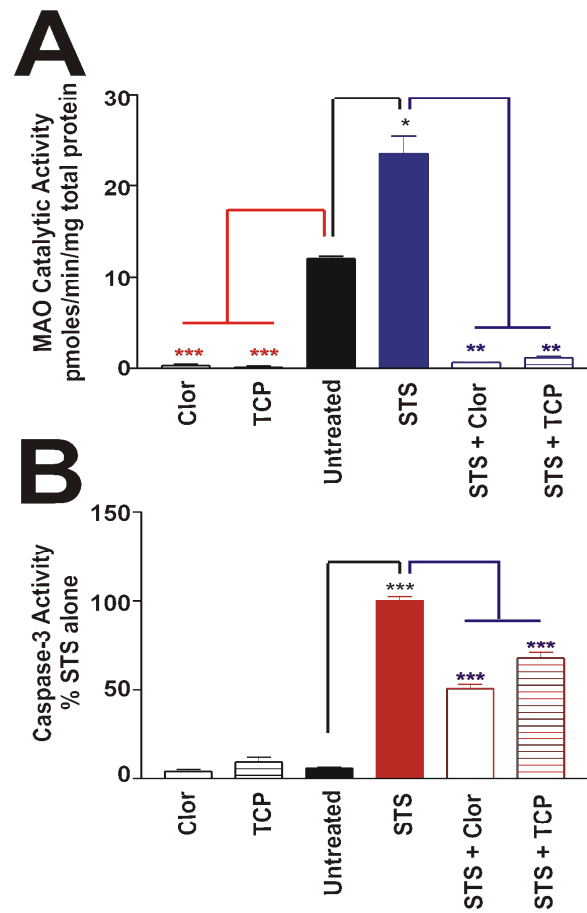


Figure 3. 13 Inhibition of MAO-A reduces caspase-3 activity in STS-induced apoptosis

(A) MAO activity was measured in untreated SH-SY5Y cells, and in cells at 3 h following the addition of 1 μ M clorgyline (Clor), 1 μ M tranylcypromine (TCP), 1 μ M STS, 1 μ M STS + 1 μ M clorgyline (STS+Clor) or tranylcypromine (STS+TCP), using 14 C-Tyramine as a substrate. Changes in MAO activity were determined and expressed as experimental mean pmoles/min/mg protein \pm S.D. (B) Caspase-3 activity was measured in untreated SH-SY5Y cells, and in cells at 3 h following the addition of 1 μ M clor, 1 μ M TCP, 1 μ M STS, 1 μ M STS + 1 μ M clorgyline or 1 μ M tranylcypromine, using Acetyl-Asp-Glu-Val-Asp-7-amidomethylcoumarin as a substrate. Caspase-3 activity was expressed as mean Δ FU/ min/ μ g protein (% STS alone) \pm S.D, where n=3. MAO/Caspase activities from STS+MAO inhibitor treated cells were compared to activities from cells exposed to STS alone using the Student's t-test, where ** $p < 0.01$, *** $p < 0.001$. MAO/Caspase activities from STS treated cells were compared to activities from untreated cells using the Student's t-test, where * $p < 0.05$, *** $p < 0.001$. MAO/Caspase activities from MAO inhibitor treated cells were compared to activities from untreated cells using the Student's t-test, where *** $p < 0.001$.

Activation of the upstream initiator caspases-9 during STS induced apoptosis was significantly reduced to ~50% by clorgyline (Figure 3. 14).

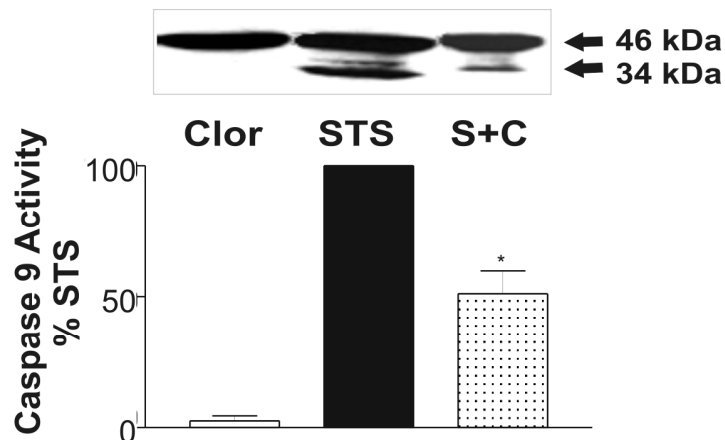


Figure 3. 14 Inhibition of MAO-A reduces caspase-9 activation in STS-induced apoptosis

Top. Activation of caspase-9 (pro-form/active form) was assessed in extracts of SH-SY5Y cells exposed for 3 h to 1 μ M STS in the presence or absence of 1 μ M clorgyline. Equal protein aliquots (20 μ g) were separated on a 12 % (v/v) acrylamide SDS-PAGE gel prior to transfer to nitrocellulose filters. Western blots were probed with anti-caspase-9 antibody (2 μ g/ml). *Bottom.* Western blots were digitised and densitometry was performed to quantify relative caspase-9 proform and active protein levels. These data represents values from three separate experiments (n=3) and expressed as mean caspase-9 activity (by dividing the active band intensity by the proform band intensity) \pm S. D. Statistical analysis of STS treated cells in comparison to STS + clorgyline treated cells was carried out using the Student's t test, where * p<0.05.

Inhibition of MAO-A also improved the viability of STS treated cells. STS reduced cell viability (measured using MTT assay) by around 10%. The MAO inhibitors clorgyline and tranylcypromine reduced this effect, which was significant after 1 h (Figure 3. 15A). Morphological observations also demonstrated that inhibition of MAO-A improved cell viability. Figure 3. 15B shows that after 3 h exposure, STS treatment results in a typical apoptotic phenotype, with cells being shrunk and rounded [panels (a and d)]. The addition of clorgyline and tranylcypromine at the same time as STS significantly improved the condition of the cells, with axonal outgrowths being evident [compare panels (b and c) with, respectively, panels (e and f)].

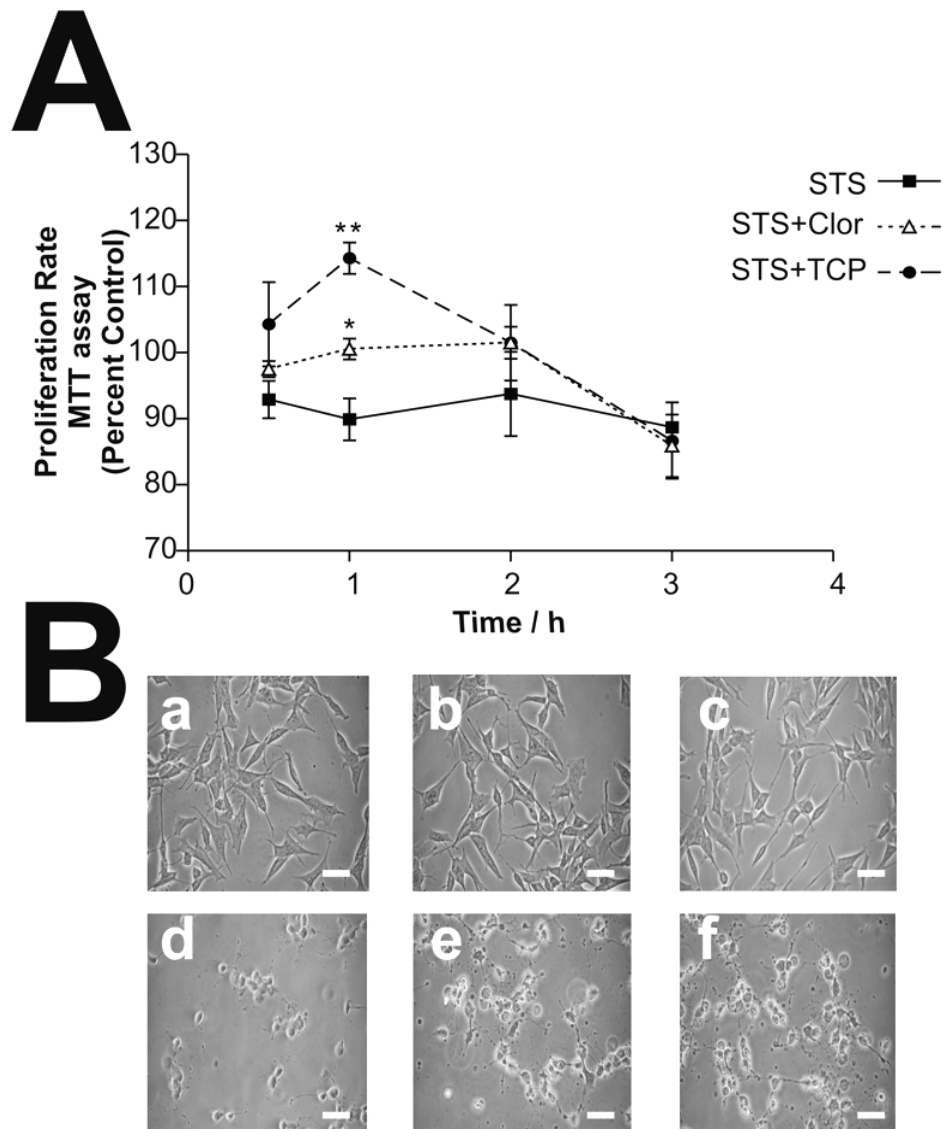


Figure 3.15 Inhibition of MAO-A reduces loss of cell viability in STS-induced apoptosis

(A) Cell viability (proliferation rate/MTT reduction) was measured in SH-SY5Y cells over 3 h, following the addition of serum free medium, clorgyline 1 μM, tranlycypromine 1 μM, STS 1 μM, STS 1 μM + clorgyline 1 μM (STS+Clor) or STS 1 μM + tranlycypromine (STS+TCP) using the MTT reduction assay. MTT reduction was determined and expressed as mean percent cell viability compared to control \pm S. D, where replicates in assay=12 and n=3. MTT reduction in the presence of STS and the MAO inhibitor was compared to MTT reduction with STS alone using the Student's t-test, where * = $p < 0.05$ and ** = $p < 0.01$. (B) SH-SY5Y cells were exposed to serum free medium [a], 1 μM clorgyline [b], 1 μM tranlycypromine [c], 1 μM STS [d], 1 μM STS + 1 μM clorgyline [e] or 1 μM STS + 1 μM tranlycypromine [f]. Cells were visualised using a Nikon eclipse TS100 microscope. Photomicrographs ($\times 20$ objectives, taken on Nikon DN100 digital camera) are shown at 3 h post-treatment and are representative of 3 independent experiments. Scale bars represent 30 μm.

To support MAO-A inhibition data, the location of glyceraldehyde-3-phosphate dehydrogenase (GAPDH) in STS treated cells and those concomitantly treated with clorgyline was investigated. As discussed later (section 3.3), GAPDH translocates to the nucleus during apoptosis (Chuang *et al.* 2005). The effect of clorgyline on the translocation of GAPDH induced by STS was revealed using confocal microscopy (Figure 3.16). In

control cells GAPDH remains in the cytosol, whereas in STS treated cells, at least some GAPDH translocates to the nucleus (Figure 3. 16). Addition of clorgyline had no effect on GAPDH translocation to the nucleus in STS treated cells (Figure 3. 16).

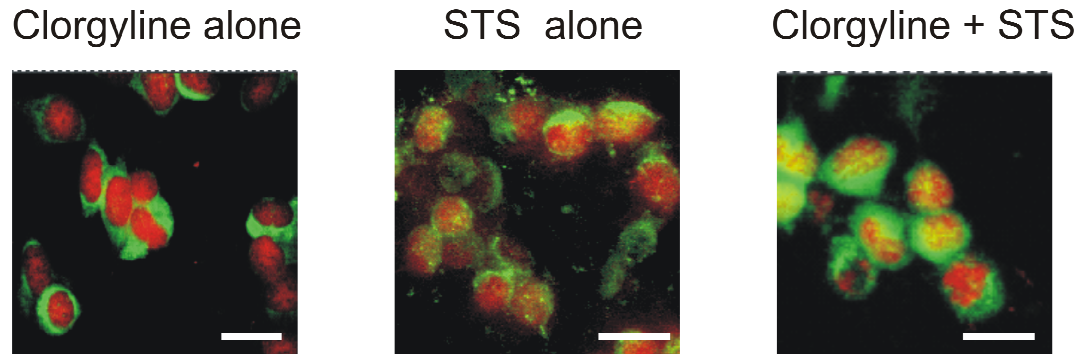


Figure 3. 16 Effect of clorgyline on translocation of GAPDH to the nucleus following STS insult

SH-SY5Y cells were then exposed to 1 μ M clorgyline alone, 1 μ M STS alone or 1 μ M clorgyline + 1 μ M STS for 3 h. Cells were probed with a primary antibody specific to GAPDH and the presence of GAPDH (green fluorescence) revealed using a secondary antibody coupled to FITC. Nuclei (shown in red) were detected by counterstaining with propidium iodide. The presence of GAPDH in the nucleus is shown by the yellow signal. Images were visualised using a CLSM Leica microscope. Scale bar represents 20 μ m

3.2.4 MAO enhanced apoptosis: mechanism of action

To examine the potential involvement of MAPK signalling in MAO-enhanced apoptosis, the levels of phosphorylated (activated) ERK, JNK and p38 during STS-induced apoptosis were examined. As shown in Figure 3. 17A, STS treatment resulted in sustained increases in the levels of phosphorylated JNK and p38 compared with controls and a transient reduction in phosphorylated ERK followed by increased phosphorylation of ERK, all starting at approximately the same time as MAO activation (Figure 3. 17). Inhibition of MAO-A with clorgyline attenuated these effects, reducing these levels of phosphorylated p38, JNK and ERK back to control levels.

As presented in Figure 3. 17B, STS induced depletion of Bcl-2 levels and clorgyline alone had no effect on Bcl-2 levels, using the time zero data as a control. When the cells were exposed to clorgyline and STS together, Bcl-2 protein expression was maintained at the control level (Figure 3. 17B).

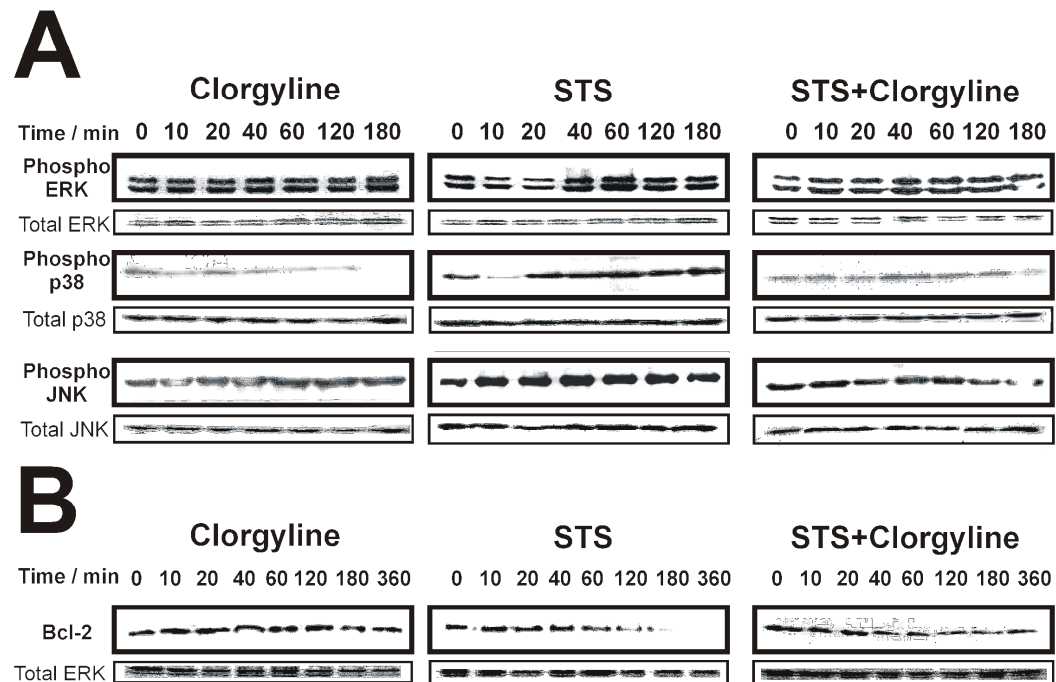


Figure 3. 17 Staurosporine induces changes in MAPK signalling and Bcl-2 levels: attenuation by clorgyline

Equal protein aliquots (80 μ g for MAPK proteins and 20 μ g for Bcl-2) of cells extracts from SH-SY5Y cells exposed to 1 μ M clorgyline, 1 μ M STS or 1 μ M STS + 1 μ M clorgyline for a 3 h period were separated on a 12 % (v/v) acrylamide SDS-PAGE gel prior to transfer to nitrocellulose membranes. Blots were probed with antibodies directed to pERK (1:1000 dilution), pJNK (1:500 dilution) and pP38 (1:1000) (A) or by anti-bcl-2 antibody (1:750) (B) Equal loading was checked by probing for total ERK (1:1000 dilution), total JNK (1:750 dilution) and total p38 (1:1000 dilution). Blots shown are representative of three separate experiments.

MAO-A produces H_2O_2 as a by-product of its enzymatic action and therefore MAO derived ROS might contribute to apoptotic signalling in this cell model. Hence antioxidants may mimic the effects of MAO-A inhibition in apoptotic signalling. Exposure of SH-SY5Y cells to 1 μ M STS resulted in the production of high levels of ROS (Figure 3. 18A). This effect was lessened by concomitant treatment with 1 μ M clorgyline or the antioxidant NAC (1mM, Figure 3. 18B). However, 1 mM vitamin C was less effective (Figure 3. 18B). NAC but not vitamin C significantly protected cells from caspase-3 activation following STS insult (Figure 3. 18C). These data indicate that MAO-generated oxidative stress is involved in apoptotic signalling.

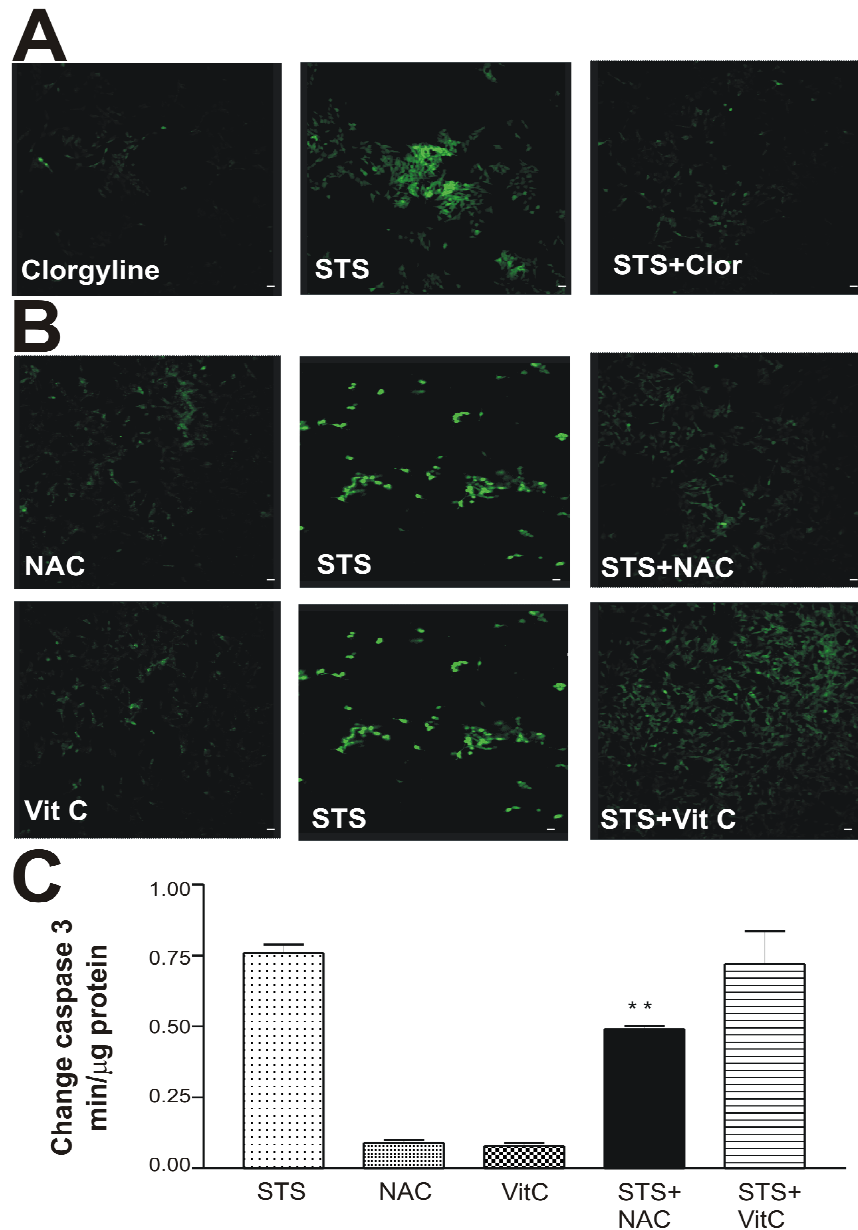


Figure 3. 18 Effect of MAO inhibitor clorgyline and antioxidants on ROS production in Staurosporine exposed SH-SY5Y cells

(A) Cells were exposed to 1 μ M clorgyline, 1 μ M STS or 1 μ M STS + 1 μ M clorgyline. DCDHF fluorescence was monitored over a 4 h period and visualised using a CLSM Leica microscope. Photomicrographs are shown at 2 h post-treatment, are laser power matched and are representative of 3 independent experiments. Scale bar represents 20 μ m. (B) Cells were exposed to 1 mM antioxidant alone, 1 μ M STS or 1 μ M STS + 1 mM antioxidant. DCDHF fluorescence was monitored over a 4 h period and visualised using a CLSM Leica microscope. Photomicrographs are shown at 2 h post-treatment and are laser power matched and are representative of 3 independent experiments. Scale bar represents 20 μ m (C) The effects of antioxidants NAC and vitamin C on caspase-3 activity were measured following treatment for 2 h using Acetyl-Asp-Glu-Val-Asp-7-Amidomethylcoumarin as a substrate. Caspase 3 activity was expressed as mean Δ FU/min/ μ g protein \pm S.D, where $n=3$. Statistical analysis of antioxidant treatment in the presence of STS was compared to STS treatment alone using the Student's t-test where ** $p<0.01$.

In order to investigate whether increased ROS produced by MAO at the mitochondrial surface could influence mitochondrial function, ROS produced following STS insult was

detected in live cells that were stained for active mitochondria using Mitotracker-Red™. Figure 3. 19 shows ROS as green and intact mitochondria as red (brightly stained area). Co-localisation of ROS and mitochondria is seen as orange-yellow (depending on levels). The merge shows that a considerable amount of ROS produced following STS insult is in the mitochondria or in close vicinity (Figure 3. 19).

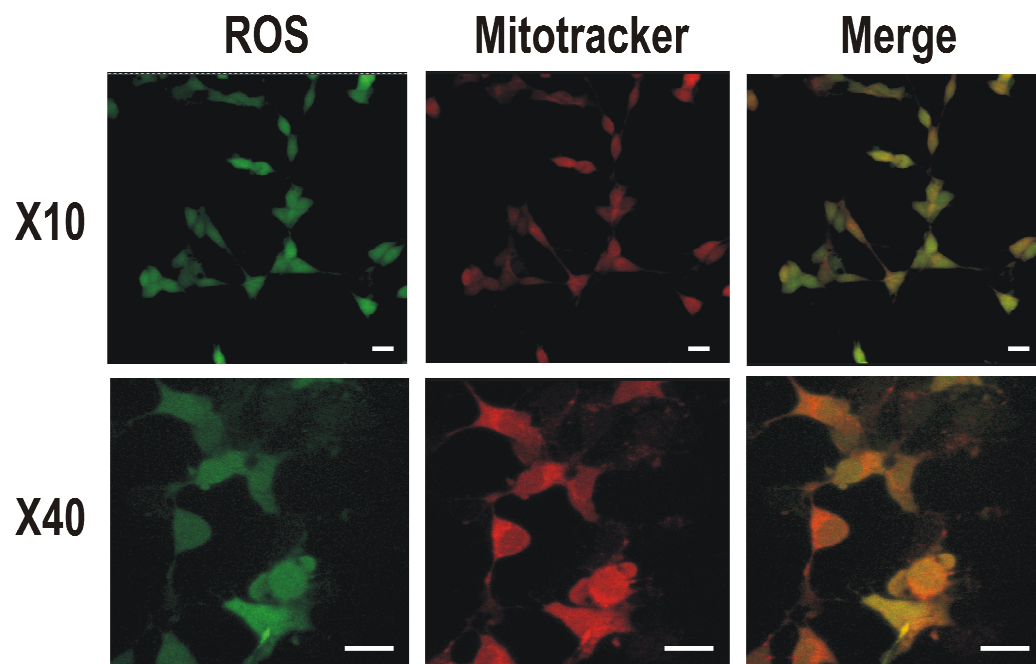


Figure 3. 19 ROS co-localised with intact mitochondria in STS-induced apoptotic SH-SY5Y cells
SH-SY5Y cells incubated with DCDHF (dye fluorescing in presence of ROS, green) and mitotracker red (dye fluorescing in intact mitochondria, red) were then exposed to 1 μ M STS and visualised using a CLSM Leica microscope. Photomicrographs are shown at 1.5 h post-STS treatment. Scale bar represents 20 μ m.

To further confirm that ROS produced by MAO during STS-induced apoptosis was in the mitochondria. MitoQ and the control compound DTPP were assessed for their anti-apoptotic properties. Figure 3. 20 demonstrates that MitoQ reduces caspase-3 activity in STS-treated cells at a 100 nM concentration. In addition, 100 nM MitoQ significantly reduces ROS production in STS-treated cells; this was not the case for DTPP (Figure 3. 21).

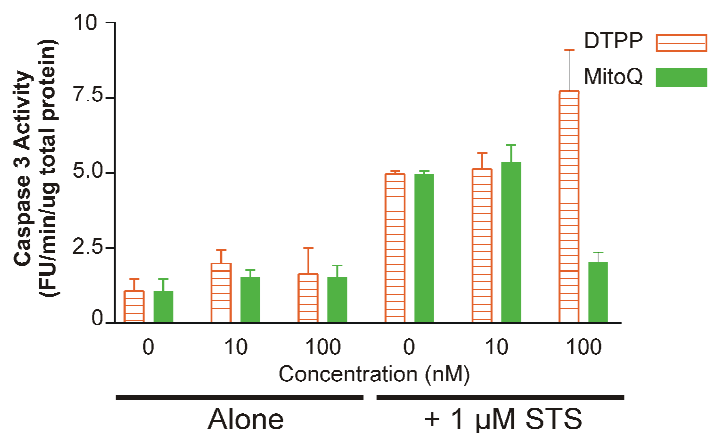


Figure 3. 20 Effect of DTTP and MitoQ concentration on caspase-3 activity

Following addition of 50, 200 and 500 nM DTTP alone, MitoQ alone, DTTP + 1 μ M STS, or MitoQ + 1 μ M STS, caspase-3 activity was measured in SH-SY5Y using Acetyl-Asp-Glu-Val-Asp-7-Amidomethylcoumarin as substrate and expressed as caspase-3 activity (% untreated control). All data represent triplicate values from three independent experiments ($n=3$) and are expressed as mean \pm S.D.

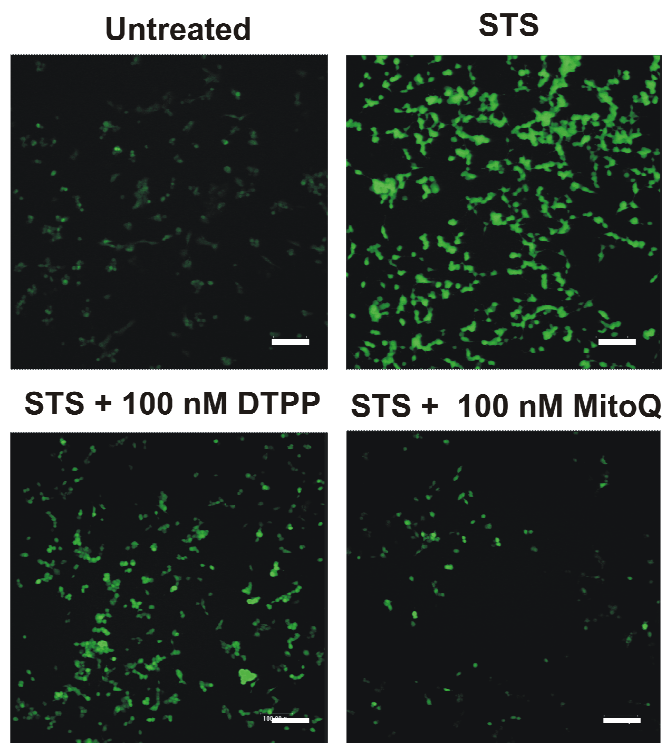


Figure 3. 21 ROS in STS treated SH-SY5Y cells: Effect of mitochondrially directed antioxidant MitoQ

Cells exposed to 1 μ M STS, 1 μ M STS + 100 nM DCTP (compound directed to mitochondria with only weak antioxidant properties), 1 μ M STS + 100 nM MitoQ (antioxidant directed to mitochondria) or untreated cells were monitored for DCDHF fluorescence, visualised using a CLSM Leica microscope. Photomicrographs are shown at 1.5 h post-treatment and are representative of 2 independent experiments. Scale bar represents 100 μ m.

3.3. DISCUSSION

3.3.1 Development of an *in vitro* model of neuronal apoptosis

SH-SY5Y cells contain solely MAO-A mRNA, MAO-A protein and MAO-A catalytic activity (Figure 3. 3). These data confirm previous claims on MAO isoform mRNA expression in these cells (Zhu *et al.* 1992, Yi *et al.* 2006a).

In SH-SY5Y cells, STS activates caspase-9 (Figure 3. 8) and -3 (Figure 3. 7) and thus initiates the intrinsic apoptotic pathway. In contrast, the extrinsic route, which depends on agonist binding to cell surface death receptors, is unaffected (Figure 3. 8), despite the cells containing procaspase-8 protein and caspase-8 mRNA (Figure 3. 9). These data are consistent with previously reported data obtained in a similar cellular model (Lopez and Ferrer 2000). It is not clear whether lack of caspase-8 activation in the STS model of apoptosis is due to the receptor-mediated pathway not being required or whether caspase-8 (although present) is non-functional. Loss of caspase-8 function may be a direct cause of malignancy and may be a consequence of gene silencing resulting from the cloning process or due to the loss of death receptor function, or both. Nevertheless, the activation of the mitochondrial apoptotic pathway in this model is of special interest considering the mitochondrial localisation of MAO in the outer mitochondrial membrane. This model of neuronal cell death may be useful for research on conditions such as PD for a number of reasons: SH-SY5Y cells contain MAO-A and neurotransmitter uptake systems, the neuroblastoma cells die by apoptosis, the apoptotic pathway is associated with mitochondrial function, mitochondrial dysfunction being a major factor in neurodegenerative disease aetiology (reviewed by Schapira 2006).

3.3.2 The role of MAO in STS-induced neuronal apoptosis

MAO activity increased significantly prior to activation of caspase-3 (Figure 3. 10) and increased ROS induced by STS was reduced by MAO inhibition (Figure 3.18), signifying that increased oxidative stress resulting from increased MAO catalytic activity is involved in early apoptotic events upstream of apoptotic execution. Increased ROS in STS-induced apoptosis may also be linked to a rapid increase in Ca^{2+} levels (Kruman and Guo 1998) and Ca^{2+} has very recently been shown to selectively increase the catalytic activity of MAO-A in protein extracts from mouse neurons (Cao *et al.* 2007). Increased MAO activity at the mitochondrial surface will result in increased formation of H_2O_2 , which if removal pathways are inactive or overloaded is converted to the highly damaging hydroxyl radical,

which is capable of inducing intense oxidative stress in mitochondria, (Mathai and Sitaramam 1994).

MAO inhibition significantly reduced caspase-3 activation (Figure 3. 13) and loss in cell viability (Figure 3. 15), confirming that MAO-generated ROS was involved in STS-induced apoptosis. To improve the reliability of the experimental data, two independent MAO inhibitors were used. Clorgyline preferentially inhibits MAO-A, but is structurally related to the MAO-B inhibitor deprenyl and other propargyl deprenyl analogues such as *N*-propargyl-1 (*R*)-aminoindan (rasagiline) and the compound CGP3466 (now in clinical trials for PD). The propargylamine-containing deprenyl analogues are reported to possess neuroprotective and anti-apoptotic properties (Tatton *et al.* 1994, Akao *et al.* 2002, Sharma *et al.* 2003, Holt *et al.* 2004), although this is not always the case (Ferber *et al.* 1998). These neuroprotective properties, rather than being a result of MAO inhibition, are thought to be due to the inhibition of pro-apoptotic translational machinery (Tatton *et al.* 1994, Kragten *et al.* 1998, Berry and Boulton 2000), induction of anti-apoptotic Bcl-2 proteins (Akao *et al.* 2002, Maruyama *et al.* 2002) and hydroxyl radical scavenging activity (Sharma *et al.* 2003). It has been suggested that the key event in these processes is the specific binding of propargylamines to glyceraldehydes-3-phosphate dehydrogenase (GAPDH), which has been implicated in apoptosis (reviewed by Chuang *et al.* 2005). The mechanism by which GAPDH promotes apoptosis is still unclear, however early work showed that GAPDH overexpression induced programmed cell death (Tajima *et al.* 1999), depletion of GAPDH mRNA inhibited apoptosis (Chuang and Ishitani 1996) and GAPDH was instrumental in cell transport (Robbins *et al.* 1995). Importantly, GAPDH translocates to the nucleus during apoptosis (Chuang *et al.* 2005) and here it is thought to be involved in translational control, DNA replication, DNA repair and nuclear tRNA transport (Sirover 2005); propargylamines are thought to inhibit translocation of GAPDH to the nucleus and hinder its pro-apoptotic activities. Clorgyline has previously been shown to protect against apoptosis (Malorni *et al.* 1998, DeZutter and Davis 2001), serum withdrawal-induced loss in cell viability (Ou *et al.* 2006) and MPTP-induced neurotoxicity (De Girolamo 2001). Whether or not the protective effects are due solely to MAO inhibition has not been fully confirmed. Nevertheless, in the present study, clorgyline had no effect on Bcl-2 levels in control cells (Figure 3. 17B) and did not inhibit translocation of GAPDH to the nucleus (Figure 3. 16).

To verify the effects of clorgyline in STS-induced apoptosis were a result of MAO inhibition, a second MAO inhibitor that did not contain the propargyl moiety was needed.

Initially the MAO-A inhibitor moclobemide was chosen. It was found that a high concentration of this inhibitor (at least 1 mM) was required to inhibit MAO *in vitro* and *in situ*, and that non-toxic concentrations did not inhibit MAO (see appendix, Figure A1.1). Therefore, TCP was chosen as a second MAO inhibitor as it contains no propargyl moiety, but interacts irreversibly with the flavin group and inhibits both MAO-A and MAO-B. TCP also protects cells from STS-induced apoptosis and since MAO-B is absent in our cell model, this confirms that MAO-A is functional in apoptosis induced by STS. Although links between MAO and mitochondrial damage have previously been made (Berman and Hastings 1999, Cohen and Kesler 1999, Kumar *et al.* 2003, Alves *et al.* 2007) and mitochondrial function is vital in apoptotic signalling, a direct role for MAO-A in apoptosis has only been claimed by DeZutter and Davis 2001 and, very recently by Ou *et al.* 2006. However, these authors have not linked the apoptotic effects to ROS production by MAO-A activity.

Reactive oxygen species formation was substantially increased following STS treatment (Figure 3. 18A) and inhibition of MAO by clorgyline and treatment with the antioxidant NAC reduced STS-induced ROS to a similar extent (Figure 3. 18B). The fact that both clorgyline and NAC also reduced caspase-3 activation (Figure 3. 13 and Figure 3. 18C) indicates that ROS produced by MAO are activating apoptosis. The antioxidant vitamin C was also used but was less effective than NAC or clorgyline in reducing STS-induced ROS and caspase-3 activation (Figure 3. 13 and Figure 3. 18C). The reason for this may be related to the fact that vitamin C, although a potent antioxidant, is considered to be toxic in some circumstances, especially in the presence of metal ions and H₂O₂ (reviewed by Halliwell 1999). Use of Mitotracker-Red™ and DCDHF together in live cells revealed that the majority of ROS produced following STS insult was localised in mitochondria (Figure 3. 19). This again supports the importance of MAO-generated oxidative stress at the mitochondrial surface in this model. The role of mitochondrial ROS was further supported by the fact that the novel antioxidant MitoQ also reduced ROS production in the presence of STS (Figure 3. 21), whilst the same concentrations of its control compound DTTP was less effective (Figure 3. 21).

3.3.3 Effects of STS on MAO expression

The nature of an apoptotic inducer (or trigger) of death signalling has a profound impact on the apoptotic mechanisms. Nonetheless, apoptosis is thought to be the predominant form of

neuronal cell death in chronic neurodegenerative disease (Friedlander 2003, Emerit *et al.* 2004). Thus the fact that MAO has an active role in this process is of high significance.

MAO protein levels were increased following STS exposure (Figure 3. 11), albeit transiently, and without a concomitant increase in MAO-A mRNA levels (Figure 3. 12). This implies that in this apoptotic model, increases in MAO protein are due to post-transcriptional events. The exact mechanism has not been addressed here, but this could be attributed to a number of scenarios. Reduction in MAO protein degradation is feasible since protein degradation pathways (the ubiquitin-proteasome system in particular) are likely to be overloaded or impaired following such stress (discussed in Ciechanover and Brundin 2003). Indeed mitochondrial complex I inhibition by rotenone (Shamoto-Nagai *et al.* 2003) and MPP⁺ (Caneda-Ferron *et al.* 2008) in SH-SY5Y cells inactivates the proteasome and importantly, caspase activation was shown to inhibit proteasome function during Jurkat cell apoptosis (Sun *et al.* 2004). Exactly how MAO is degraded is unknown, however the proteasome is particularly sensitive and preliminary data indicate STS induced loss of chymotrypsin-like proteasome activity, which was reduced following MAO inhibition (see appendix, Figure A1.2). An increase in MAO protein levels, without increased mRNA expression, could also result from increased translation of existing MAO-A mRNA following STS insult. Post-translational modifications, such as the addition of functional groups or conformational change can in turn contribute to protein function.

Since increased MAO catalytic activity is maintained throughout the apoptotic time course whilst MAO-A protein is increased only transiently, the increased MAO-A protein may not be exclusively responsible for the increases in catalytic activity of MAO. The catalytic turnover of an enzyme can be affected by a number of factors. In the case of MAO-A catalysis, the availability of its flavin cofactor, the requirement for metal ions (such as copper) and disruption of negative feedback mechanisms could be involved. Another consideration for the control of MAO-A catalytic activity is its special relationship with the mitochondrial membrane. MAO is an integral membrane protein and only following its insertion into the outer mitochondrial membrane (which requires ATP and ubiquitin), can it become catalytically active (Zhuang *et al.* 1992). Very recent work by Cao and co-workers showed increased MAO-A catalytic activity in hippocampal cells exposed to increased free calcium, which was not paralleled by increased MAO-A mRNA expression or MAO protein levels (Cao *et al.* 2007), supporting the suggestion that MAO can be more active without more enzyme being made.

In contrast, transcriptional activation of the MAO-A gene was seen following withdrawal of nerve growth factor in rat PC12 cells (DeZutter and Davis 2001; which has been related to stress MAPK activation and apoptotic signalling). In addition, Ou *et al.* (2006) recently found that MAO-A mRNA expression is induced following serum starvation, mediated by a reduction in the expression of the transcriptional repressor R1.

These very different findings suggest that there are various regulatory mechanisms of cell death that could regulate MAO-A activity, dependent on the inducer.

3.3.4 Regulation of apoptosis by MAO

Bcl-2 is an anti-apoptotic protein that plays a central role in mitochondrially mediated apoptosis and survival as a result of its strong influence on the balance of pro- and anti-apoptotic proteins that also reside on the mitochondrial surface. Depletion of Bcl-2 is thought to be one of the first initiators of the intrinsic apoptotic cascade, as this shifts the balance of Bcl-2 family proteins in favour of apoptosis, triggering the release of cytochrome *c* from the mitochondria (Hengartner 2000). STS treatment resulted in depletion of Bcl-2 in this model (Figure 3. 17B), which was prevented by clorgyline, suggesting that MAO acts upstream of changes in Bcl-2. This is contrary to the situation in serum deprivation, where MAO appears to act downstream of Bcl-2 (see Chapter 4 and Ou *et al.* 2006). These differences may again reflect the different apoptotic inducers used and further work needs to be carried out to clarify the relationship between MAO and Bcl-2.

The highly conserved MAPK cascades are among the pathways often used to transduce mammalian stress signals (Robinson and Cobb 1997). They have been extensively described as being crucial in regulating stress/survival responses and hence play an important and universal role in mechanisms of cell death. Following STS-induced apoptosis, ERK (generally thought to be activated by pro-survival stimuli and influenced by JNK/p38) was eventually activated, coinciding with increases in MAO activity (Figure 3. 10 and Figure 3. 17A). Activation of p38 and JNK (generally thought to be activated by stressful stimuli and influenced by ERK) occurred slightly before activation of ERK (Figure 3. 17A). MAO inhibition by clorgyline attenuated the activation of these pathways to control levels (Figure 3. 17A). Thus MAPK signalling modules are involved in STS-induced apoptosis and ROS generated by MAO are involved in initiating these pathways (as MAO inhibition reduced MAPK activation). Indeed, H₂O₂ has previously been shown to activate MAPK proteins (Guyton *et al.* 1996). Whether or not the MAO gene is also a target of the MAPK pathways as described by DeZutter and Davis (2001) and Wong *et al.*

(2002) was not addressed in the present chapter, but would seem unlikely given that MAO-A mRNA levels were unchanged following STS treatment. However, in this model MAPK signalling might be recruited to transmit pro-apoptotic stress signals following STS exposure.

In this apoptotic model it is likely that MAO exerts its pro-apoptotic effects mainly by influencing the major stress/survival signalling pathways such as MAPK pathways via its production of reactive oxygen species, most likely as a result of H₂O₂ production but the effects of other reaction products such as aldehyde and ammonia may also be considered. The targets of MAPK pathways activated during STS-induced apoptosis could include a wide range of transcription factors, ultimately targeting specific genes involved in cell death/survival. MAPK signalling also involves a large amount of cross talk with other signalling pathways that could be recruited such as PKC or Ras and MAPK pathways may play a role in many cellular responses such as receptor desensitisation and cytokine signalling. It should be noted that MAO generated oxidative stress could have a direct influence on apoptosis by its action at the mitochondrial surface. Not only by influencing the balance of pro-apoptotic and anti-apoptotic Bcl-2 family proteins that also reside there, but by directly compromising the integrity of mitochondrial function directly. This is possible since MAO-generated ROS can pass through the mitochondrial outer membrane, directly damaging the electron transport system (Cohen *et al.* 1997, Berman and Hastings 1999) and mitochondrial DNA (Hauptmann *et al.* 1996). Certainly, ATP levels are significantly reduced in SH-SY5Y cells over expressing MAO-A (Chapter 5, Figure 5.9).

3.3.5 Conclusion

Data in this chapter suggest a dynamic role for MAO-A in STS-induced neuronal apoptosis, driven by the ability of MAO to generate oxidative stress at the mitochondrial surface. The data supports the hypothesis that MAO plays a key role in the modulation of apoptotic signalling in response to biological stressors. Here the stressor STS initiated classical apoptosis, having severe and rapid consequences on the cell (Figure 3.22). The nature of the inducer and its rapid effects may explain why there were no changes in MAO-A at the gene level and opens up questions regarding the role of MAO in neuronal apoptosis in the broader sense. It is likely that MAO can act as an enhancer of cell death (in addition to its role as a deaminating enzyme) but that the mechanisms involved depend on the nature of the stressor, enabling MAO to fine tune death/survival responses. These findings may have wider implications for the therapeutic use of the dopamine precursor,

levodopa, in PD, predisposition to neurodegenerative diseases and mechanism of acute apoptotic cell death associated with brain damage and stroke.

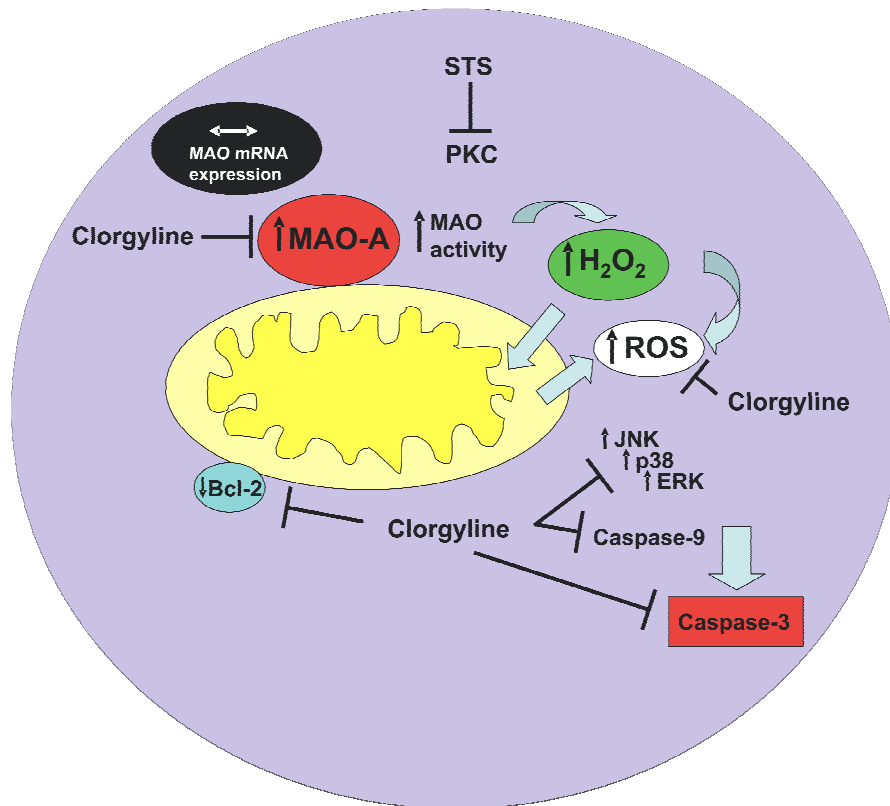


Figure 3. 22 Overview of STS-induced apoptosis: role of MAO-A

STS inhibits PKC which triggers an array of stressful stimuli within the cell. Whilst MAO-A mRNA expression remains unaffected, MAO-A protein and catalytic activity are greatly increased, generating amplified levels of its catalytic product H₂O₂. In turn, free radical levels are elevated (which can be reduced by MAO-A inhibition). Bcl-2 levels are depleted and levels of phosphorylated (activated) MAPK signalling components JNK, ERK and p38 are increased. The upstream apoptotic caspase-9 is cleaved (activated) and finally the executioner caspase-3 is activated, initiating the final stages of apoptosis. Inhibition of MAO-A protects cells from apoptotic commitment (caspase-3) and also reduces activation of upstream apoptotic components (MAPK, Bcl-2 and caspase-9), confirming the relevance of MAO in the apoptotic cascade.

CHAPTER 4

THE ROLE OF MAO-A IN SELECTED MODELS OF APOPTOSIS

THE ROLE OF MAO-A IN SELECTED MODELS OF NEURONAL APOPTOSIS

4.1. INTRODUCTION

Cell death mechanisms are extremely varied and how cells respond to stress both *in vitro* and *in vivo* depends on many factors including the nature of the stressor and the cell type. Data in chapter 3 indicate MAO may be involved in modulating cell death in STS-treated SH-SY5Y cells. The present chapter addresses whether the role of MAO in cell death is universal or whether it is only evident in specific types of cell death.

4.1.1 Receptor-mediated apoptosis

Receptor-mediated apoptosis is characterised by the interaction of extracellular ligands with cell surface receptors, which induces the formation of death inducing signalling complex (DISC), activating caspase-8 (Hengartner 2000). Receptor-mediated apoptosis is distinct from mitochondrially-mediated apoptosis, since the apoptotic trigger arises from events on the cell surface rather than events at the mitochondria. Intracellular events that occur following ligand-receptor binding are somewhat complicated by the large amount of cross-talk between signalling pathways. For example, caspase-8 often activates the intrinsic pathway, whereas caspase-9 seldom activates caspase-8.

4.1.1.1 Fas / Fas ligand system

Fas (also known as CD95) is a member of the tumour-necrosis receptor family of death receptors, which can induce apoptosis or conversely, deliver growth signals (Desbarats *et al.* 2003). Fas receptor-mediated apoptosis is summarised in Figure 4. 1. Caspase-8 cleavage is characteristic of Fas-induced apoptosis (Nagata 1997, Hengartner 2000). SH-SY5Y cells express the cell-surface Fas receptor (Desbarats *et al.* 2003) and express Fas mRNA (Russo *et al.* 2004). However, numerous publications have reported that SH-SY5Y cells do not undergo caspase-8 mediated apoptosis due to gene silencing (see section 3.1.2.3).

4.1.1.2 TNF α

Tumour necrosis factor alpha (TNF α) is secreted by immune cells including monocytes macrophages and T lymphocytes. TNF α is a pro-inflammatory cytokine playing a key role

in host defence responses against injury and infection (Alberts *et al.* 1994) and acts by binding to two distinct cell surface receptors known as TNF receptor 1 and -2 (Kamata *et al.* 2005). TNF α activates and can be activated by the gene regulatory protein NF- κ B (Alberts *et al.* 1994) and is known to increase oxidative stress in target cells (Halliwell and Gutteridge 2007). SH-SY5Y cells have been reported to undergo apoptosis in response to TNF α (Kenchappa *et al.* 2004, Kweon *et al.* 2004).

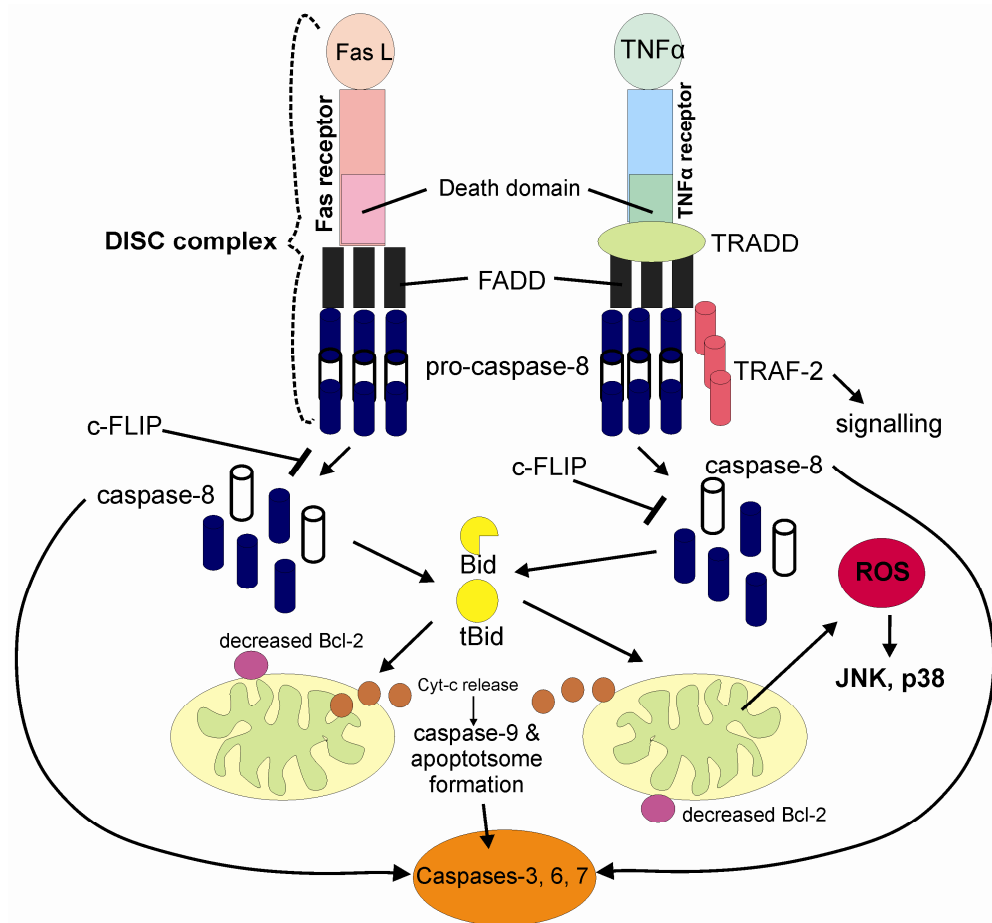


Figure 4. 1 Fas and TNF receptor mediated apoptosis

Fas system-Fas engagement by Fas ligand (FasL), or by antibodies directed against Fas, initiates receptor clustering and binding of the intracellular death domain of Fas to an adapter protein known as FADD, coupling Fas to the caspase cascade via formation of DISC (Thomas *et al.* 2002, Desbarats *et al.* 2003). Caspase-8 cleavage is characteristic of Fas-induced apoptosis (Nagata 1997, Hengartner 2000). Apoptosis mediated by caspase-8 is then amplified through the mitochondrial release of cytochrome c, thus activating caspase-9 and the formation of the apoptosome (Kuwana *et al.* 1998). *TNF system*- TNF receptors initiate activation of caspase-8 in a similar manner to Fas receptors, except for an extra adapter protein called TRADD that together with FADD and pro-caspase-8 forms the DISC. Activation of ROS production by TNF α appears to involve mitochondria (Hughes *et al.* 2005). TNF α induced ROS is known to cause JNK activation, p38 activation, loss of Bcl-2, cytochrome-c release and caspase-3 cleavage resulting in apoptosis in Cos-7 cells and mouse models (Grethe *et al.* 2004, Kamata *et al.* 2005).

4.1.2 Complex I inhibitors

The neurotoxin MPP⁺ is used both *in vitro* and *in vivo* to induce Parkinson-like features and its effect on SH-SY5Y cells has previously been extensively characterised (Itano 1995, Song and Ehrich 1998, Fall and Bennett 1999). MPP⁺ is a neurotoxin that causes increased oxidative stress and inhibition of mitochondrial complex I in SH-SY5Y cells (Fall and Bennett 1999). The pro-toxin MPTP is a substrate of MAO, being converted to the active toxin MPP⁺ by MAO (Song and Ehrich 1998). Unfortunately, MPP⁺ significantly inhibits MAO activity (Singer and Ramsay 1993, Tipton and Singer 1993). Therefore another mitochondrial complex I inhibitor, rotenone, was required to mimic PD cell death. Rotenone is a naturally occurring chemical obtained from the roots of several plant species belonging to the genus *Lonchocarpus* (lancepod) from the family *fabaceae* (pea, Tomlin 2000) and is commonly used in the U.K as a pesticide (British Crop Protection Council, 2001). Following experiments in rats, rotenone was shown to inhibit complex I of the mitochondrial electron transport chain (Heikkila *et al.* 1985, Sherer *et al.* 2003b). Long term exposure to rotenone reproduces features of PD including selective nigrostriatal degeneration and α -synuclein-positive inclusions in rats (Betarbet *et al.* 2000, Sherer *et al.* 2003a). In SH-SY5Y cells, rotenone causes dose-dependent ATP depletion, oxidative damage and cell death (Sherer *et al.* 2003b). Thus, rotenone is an excellent toxin to use *in vitro* to mimic oxidative stress in PD.

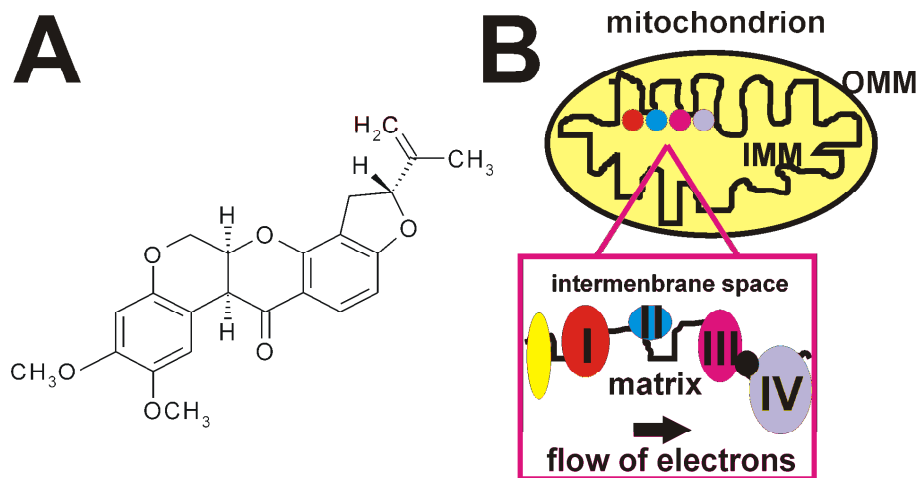


Figure 4. 2 Chemical structure of rotenone and location of mitochondrial complex I

(A) Chemical structure of rotenone. (B) Location of complex I of the mitochondrial respiratory chain (electron transport chain). Mitochondrial redox carriers or complexes I, II, III and IV (labelled) span the inner mitochondrial membrane (IMM), with the exception of complex II that sits on the IMM. The yellow complex represents ATP synthase and the black complex represents cytochrome c. Rotenone inhibits the action of complex I of the respiratory chain. Modified from (Stryer 1996, Abou-Sleiman *et al.* 2006).

4.1.3 Serum withdrawal

Neuronal cells require growth factors for development and survival including a range of polypeptides and glycoproteins that act transiently and are tightly controlled by the cell. They act locally by binding to receptors on target cell surfaces, exerting effects at low concentrations. Absence or withdrawal of growth factors in neuronal cells (normally supplied by the addition of serum to the growth medium) leads to apoptosis; this has been demonstrated in rat PC12 cells following serum deprivation (DeZutter and Davis 2001) and in human neuroblastoma (SH-SY5Y) cells following serum withdrawal (Macleod *et al.* 2001).

4.1.3.1 Serum withdrawal in human neuroblastoma

Neuroblastoma cells express insulin-like growth factor (IGF) and NGF receptors (Pahlman *et al.* 1995) and primary cultured low stage tumour cells were shown to be dependent on NGF for their survival and differentiation (Nakagawara *et al.* 1993). In contrast, neuroblastoma cell lines are established from high-stage, highly malignant tumours and are arrested in their differentiation (Pahlman *et al.* 1995). Differentiation of SH-SY5Y cells can be achieved *in vitro* via addition of phorbol ester (TPA, Pahlman *et al.* 1981) and retinoic acid (Pahlman *et al.* 1984, Beck 2004). Growth factors alone act as mitogens in SH-SY5Y cells but do not induce differentiation. However, brain-derived neurotrophic factor (BDNF) in combination with retinoic acid causes fully differentiated and neuron-like SH-SY5Y cells (Encinas *et al.* 2000) and growth factors added to SH-SY5Y cells alongside phorbol ester treatment enhance TPA-induced differentiation (Pahlman *et al.* 1995).

In contrast, complete removal of growth factors normally supplied in tissue culture media to neuroblastoma cell lines is lethal. Differentiated SH-SY5Y cells undergo apoptotic cell death in response to serum withdrawal (Macleod *et al.* 2001, Iglesias *et al.* 2003) and serum withdrawal causes reduced proliferation and loss of cell viability in undifferentiated human neuroblastoma cells (Ou *et al.* 2006). In SH-SY5Y cells, caspase-3 activation has been suggested to follow serum withdrawal by detection of total caspase-3 protein levels (Ou *et al.* 2006), caspase-3-like Ac-DEVD-amc fluorescent substrate cleavage and detection of caspase-3 processing (Macleod *et al.* 2001). Activation of caspase-3 in both PC12 and SH-SY5Y neuroblastoma following serum withdrawal occurs as an early event (within the first 24 h) and ranges between ~2-3 fold control level (Macleod *et al.* 2001, Vaghefi *et al.* 2004).

4.1.3.2 Mechanisms involved in serum withdrawal-induced neuronal apoptosis

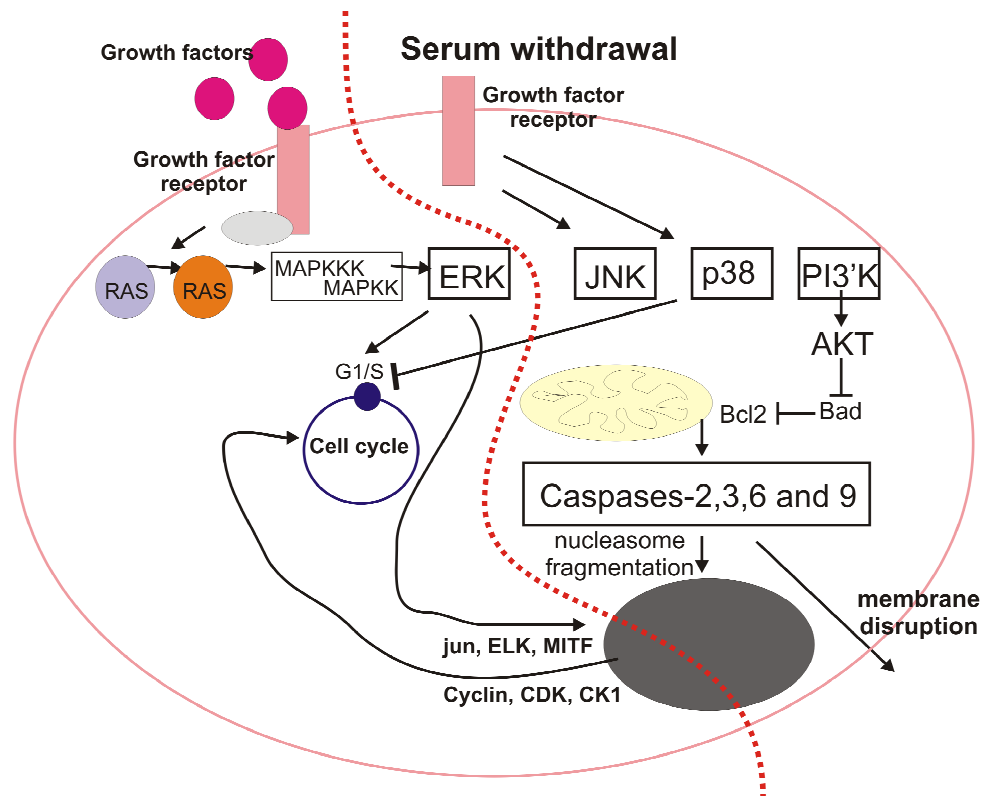


Figure 4. 3 Mechanisms of serum withdrawal-induced apoptosis

Apoptosis following serum withdrawal is characterised by membrane disruption (Vaghefi et al. 2004), DNA/nucleosome fragmentation (DeZutter and Davis 2001, Vaghefi et al. 2004) and reduced cell viability (Macleod et al. 2001, Vaghefi et al. 2004). Serum withdrawal-induced apoptosis is caspase dependent (Vaghefi et al. 2004) and caspases -2, -3, -6 and -9 have all been shown to be involved (DeZutter and Davis 2001, Dowds and Sabban 2001, Macleod et al. 2001, Vaghefi et al. 2004). The ERK/MAPK cascade mediates growth factor-supported survival in PC12 cells, retinal ganglion cells, cerebellar granule neurons and cortical neurons (Xia et al. 1995, Poser et al. 2003). The phosphatidylinositol 3 (PI3)-kinase pathway (Yao and Cooper 1995) and the action of cyclic AMP (Poser et al. 2003) are also thought to be involved in mediating serum withdrawal-induced apoptosis. Apoptosis induced by withdrawal of trophic factors has been shown to be mediated by p38 MAPK in rat neurons (Xia et al. 1995, Kummer et al. 1997, DeZutter and Davis 2001) and in human neuroblastoma (Ou et al. 2006). Growth factors in serum stimulate progression of the cell cycle in mouse fibroblasts (NIH-3T3) and p38 MAPK is required for its inhibition at G₁/S (Molnar et al. 1997).

4.1.3.3 Role of MAO in serum withdrawal-induced apoptosis

Generation of free radicals via monoamine oxidation by MAO was the focus of a great deal of publications during the 1990s and into the 2000s and many links were made between MAO, mitochondrial dysfunction and neurodegeneration. Nevertheless, the first evidence for a direct role of MAO in apoptosis was in 2001, when following serum withdrawal (NGF withdrawal) in rat PC12 cells, MAO-A mRNA, protein and activity were increased (DeZutter and Davis 2001). Increased expression of MAO following serum withdrawal was reduced by inhibition of p38 MAPK by the inhibitor PD169316 (DeZutter

and Davis 2001), suggesting that the pro-apoptotic expression of MAO was mediated by the p38 signal transduction pathway. The involvement of MAO in serum withdrawal induced apoptosis was confirmed when MAO inhibition reduced both nucleosome fragmentation and the appearance of apoptotic nuclei (DeZutter and Davis 2001). Very recently Ou *et al* (2006) provided evidence for the mechanism by which MAO may be regulated to enhance apoptosis. Following serum withdrawal from human neuroblastoma cells, MAO-A expression (mRNA, protein and catalytic activity) is increased and R1 (a transcription factor repressor of the MAO-A promoter) expression is decreased. Although these data support the supposition that MAO plays a pro-apoptotic role and provides evidence for a mechanism, the authors have assumed that serum withdrawal induces apoptosis since no attempt was made to directly measure apoptosis. Indeed, apoptotic cell death was assumed on the basis of MTT assays (which give an indication of cell viability/proliferation through measurement of cell metabolism) and total caspase-3 levels rather than caspase-3 activity. Nonetheless, serum withdrawal in human neuronal cells induces increased expression of MAO-A and this involves the p38 MAPK signalling pathway, since the p38 inhibitor PD169316 reduced MAO-A protein levels and loss in cell viability (Ou *et al.* 2006). An important finding from this work is the elucidation that the novel transcription factor repressor R1 is a target of the p38 stress-MAPK signalling pathway following serum withdrawal.

4.1.4 Rationale

When work commenced on this chapter of the thesis, MAO at that time had only been shown to have a direct involvement in apoptotic cell death in rat neuronal cells following serum deprivation (DeZutter and Davis 2001). The staurosporine-induced model of human neuronal apoptosis (chapter 3) allowed the investigation of MAO in a very potent, fast, mitochondrially-mediated and highly oxidative type of apoptosis. MAO modulates staurosporine-induced neuronal cell death by heightening the oxidative environment via its production of reactive species following increased catalytic activity. MAPK and caspase cascades may be involved in transducing MAO mediated pro-apoptotic signals, however the MAO gene was not up-regulated and therefore not a target of apoptotic or stress signalling pathways.

This chapter aims to elucidate whether MAO has a universal role in apoptotic signalling in human neuroblastoma cells. This was achieved by the use of a number of apoptotic inducers including serum withdrawal.

4.1.5 Aims of Chapter

- **To develop different *in vitro* models of apoptosis in SH-SY5Y cells**

SH-SY5Y cells were exposed to an analogue of Fas ligand (Fas activating antibody), the cytokine TNF α or the complex I inhibitor rotenone and also subjected to withdrawal of growth factors. Cells were monitored for biochemical and morphological changes characteristic of apoptosis in order to confirm whether or not the cells are sensitive to each treatment. If apoptotic cell death was confirmed, a time course of apoptosis was characterised.

- **To investigate the role of MAO in different apoptotic models**

Once an apoptotic time course had been characterised, changes in the expression of MAO-A mRNA, protein and catalytic activity were monitored. To confirm the relevance of MAO-A in receptor mediated apoptosis, the effect of MAO-A inhibition on the apoptotic cascade/cell status would be investigated.

- **To assess the signalling mechanisms involved in MAO-mediated apoptosis induced by serum withdrawal**

Caspase activation of ROS and changes in MAPK signalling pathways were measured using western blotting and confocal microscopy. To study the involvement of MAP kinases ERK, JNK and p38 in controlling MAO-A expression during apoptosis, specific MAPK inhibitors were used in conjunction with the apoptotic inducer.

4.2. RESULTS

4.2.1 Treatment of SH-SY5Y cells with agonistic anti-Fas antibody

SH-SY5Y cells were exposed to an agonist of Fas, which is an analogue of Fas ligand, an agonistic anti-Fas antibody (AAF). Recommended concentrations of AAF for use in the human jurkat cell line range between 10-50 ng/ml, based on a previous publication (Dotti et al. 2005) and vendors recommendation (Millipore, C.A, U.S.A). Doses 15-250 ng/ml AAF did not induce loss of cell viability in SH-SY5Y cells over a 24 h time course (Figure 4. 4).

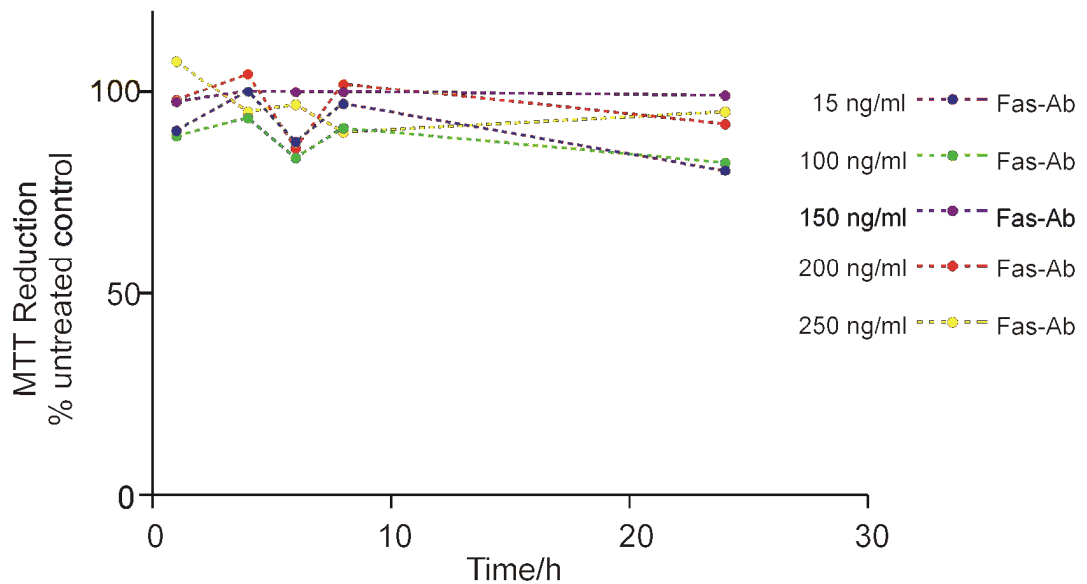


Figure 4. 4 MTT reduction in SH-SY5Y cells following treatment with AAF

Cell viability was measured in SH-SY5Y cells over 24 hours, following the addition of 15, 100, 150, 200 and 250 ng/ml human AAF (Fas-Ab). MTT reduction was determined and expressed as mean MTT reduction % untreated control (SFM). Replicates in assay=12 and n=2.

High doses of AAF did not induce apoptotic morphologies in SH-SY5Y cells in 6 h (Figure 4. 5) or 24 h (Figure 4. 6A). To compare agonistic AAF response in SH-SY5Y cells to the response in rat glioma cell line (C6), cells were exposed to 500 ng/ml AAF for 24 h. C6 cells showed some apoptotic morphologies such as cell shrinking and rounding (Figure 4. 6B). Nevertheless, SH-SY5Y cells remain viable following high doses of AAF and caspase-3 activity (Figure 4. 6C) remained unchanged over a 72 h time course.

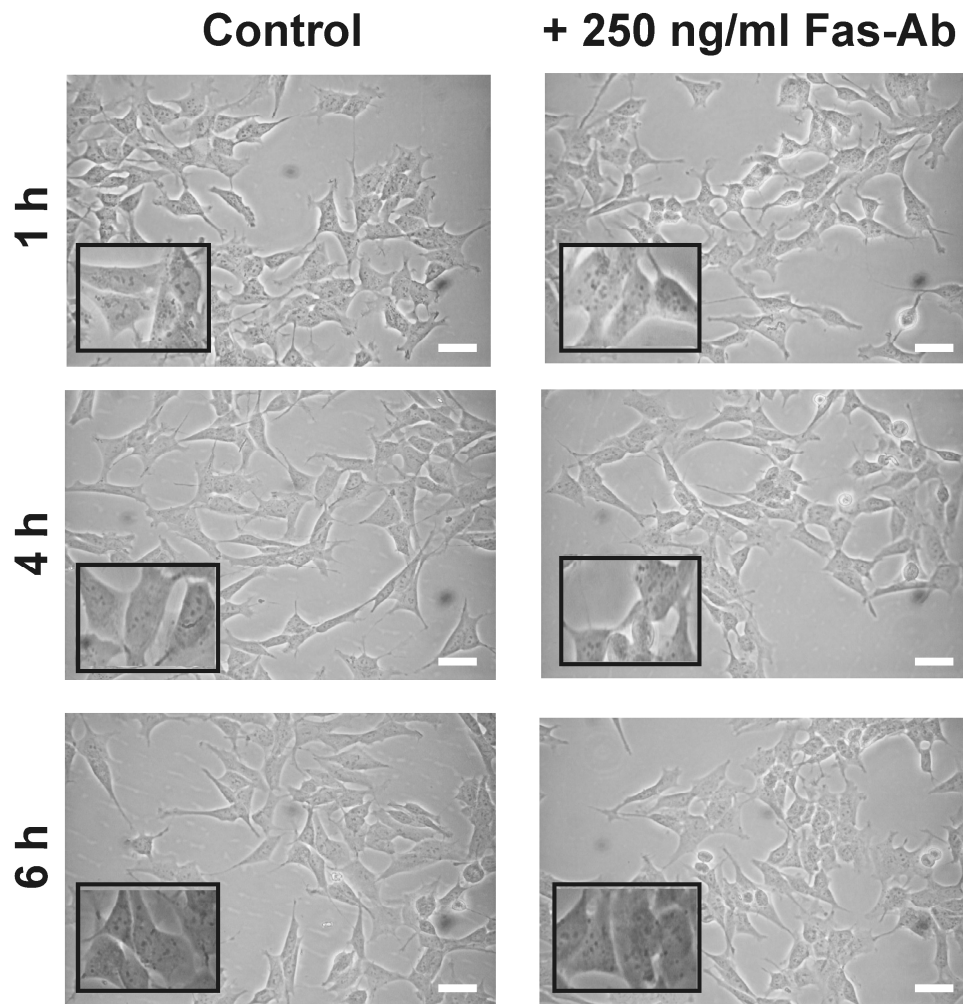


Figure 4. 5 The effect of agonistic anti-Fas antibody on SH-SY5Y morphology

SH-SY5Y cells were exposed to 250 ng/ml agonistic anti-Fas antibody (Fas-Ab) for up to 6 h. Morphologies of the cells were visualised using a Nikon eclipse TS100 microscope. Photomicrographs ($\times 20$ objectives, taken on Nikon DN100 digital camera) are shown at 1 h, 4 h and 6 h post-treatment and are representative of 3 independent experiments. Scale bar represents 20 μm . Photomicrographs have been enlarged in each case using Corel draw software and show ~ 4 representative cells enlarged by $\sim 300\%$.

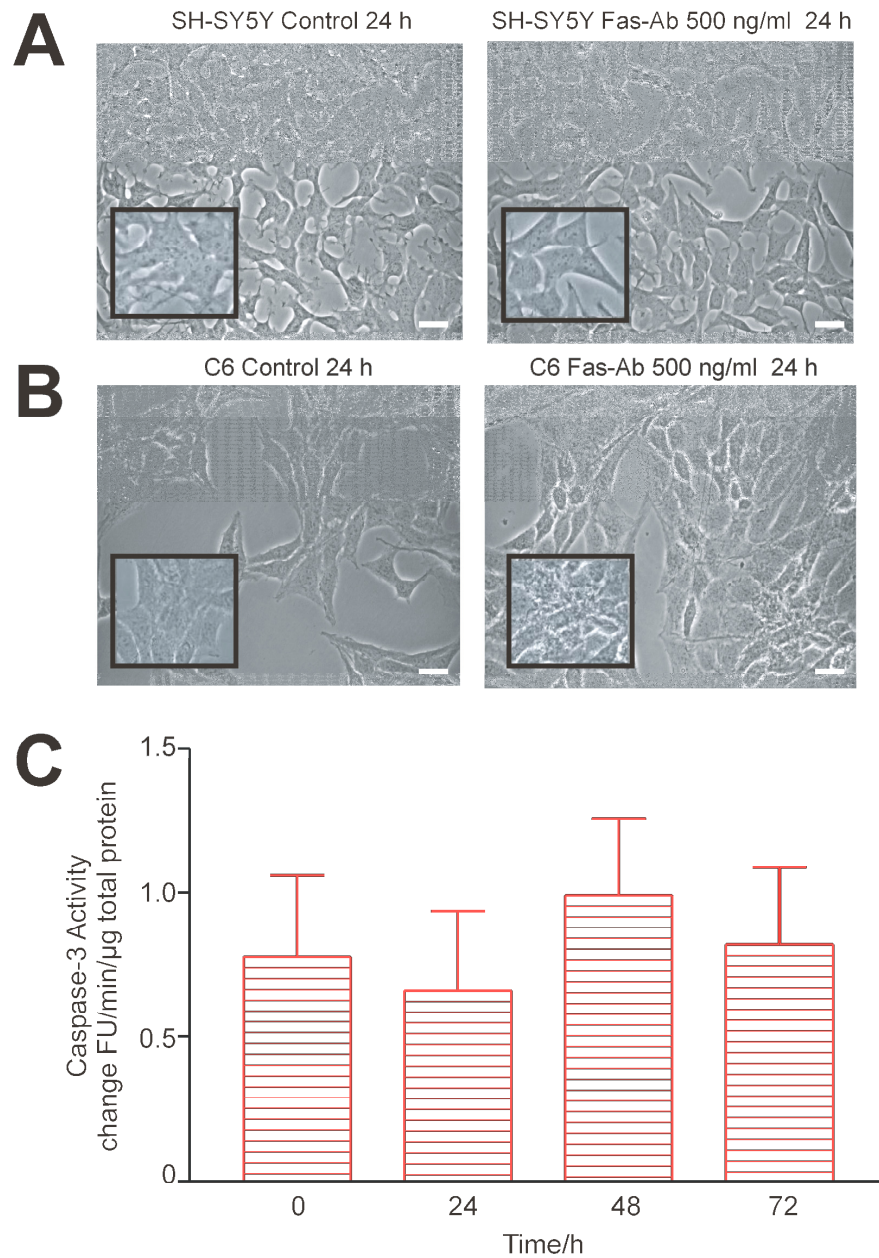


Figure 4.6 Agonistic anti-Fas antibody does not induce apoptosis in SH-SY5Y cells

(A) SH-SY5Y cells or (B) C6 cells were exposed to 500 ng/ml agonistic anti-Fas antibody (Fas-Ab) for 24 h. Morphologies of the cells were visualised using a Nikon eclipse TS100 microscope. Photomicrographs ($\times 20$ objectives, taken on Nikon DN100 digital camera) and are representative of 3 independent experiments. Scale bar represents 20 μ m. Photomicrographs have been enlarged in each case using Corel draw software and show ~ 4 representative cells enlarged by $\sim 300\%$. (C) SH-SY5Y cells were exposed to 500 ng/ml Fas-activating antibody (Fas-Ab) for 24 h Caspase-3 activation was measured using Acetyl-Asp-Glu-Val-Asp-7-Amidomethylcoumarin as substrate and expressed as mean change FU/min/ μ g protein \pm SEM. All data represent triplicate values from two independent experiments ($n=2$).

Loss of caspase-8 proform (58 kDa) was observed in SH-SY5Y cells exposed to Fas antibody for 4 and 6 h. However, the active form of caspase-8 (28 kDa) was not detected in either SH-SY5Y cells (Figure 4.7, *middle panel*) or in positive control U937 cells that undergo apoptosis following TNF α exposure (Figure 4.7, *left panel*). Activation of

caspase-9 was not detected in SH-SY5Y cells following Fas antibody exposure over a 6 hr time course (Figure 4.7, *right panel*).

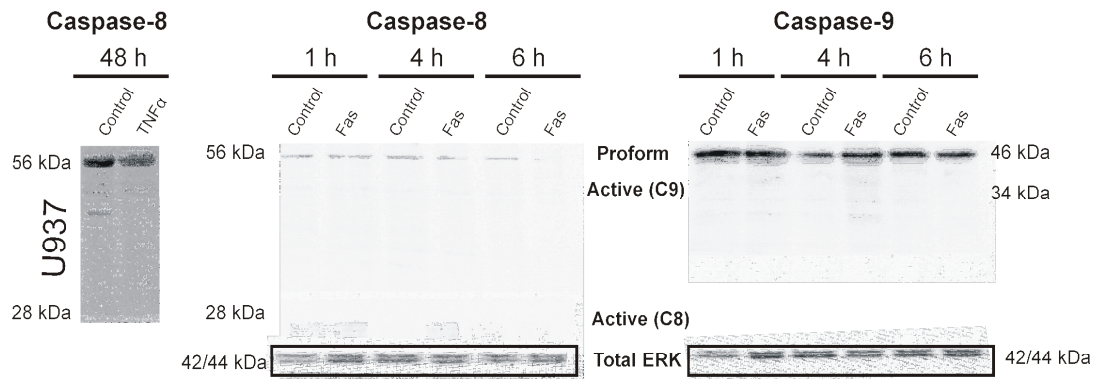


Figure 4.7 AAF does not activate caspase-8 or caspase-9

Western blot analysis of caspase-8 and -9 activation (pro-form / active form) in cell extracts of SH-SY5Y cells exposed to 500 ng/ml agonistic anti-Fas antibody over a 6 hour period or U937 cells exposed to 10 ng/ml TNF α for 48 h. Equal protein aliquots (20 μ g) were separated on a 12 % (v/v) acrylamide SDS-PAGE gel prior to transfer to nitrocellulose membranes. The blots were probed with either, anti-caspase-8 antibody (2 μ g/ml) which recognises the pro-form (56 kDa) and the active-form (28 kDa) and anti-caspase-9 antibody (2 μ g/ml) which recognises the pro-form (46 kDa) and the active-form (34 kDa). Equal loading in each case was checked by copper stain for total protein or by probing for total ERK (1: 1000 dilution). The Western blots shown are representative of two separate experiments.

4.2.2 TNF α treatment of SH-SY5Y cells

Treatment with human TNF α caused no significant loss in cell viability of the cells over a 72 h period (Figure 4.9).

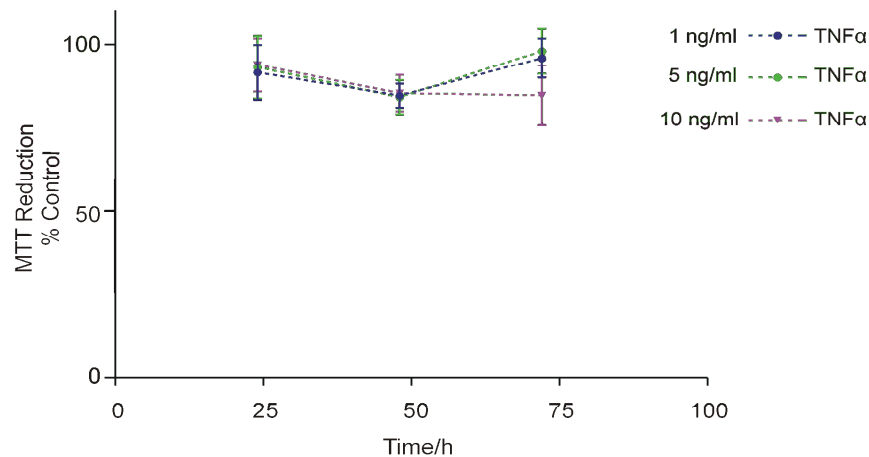


Figure 4.8 MTT reduction in SH-SY5Y cells following treatment with TNF α

Cell viability was measured in SH-SY5Y cells over 72 hours, following the addition of 1, 5 and 10 ng/ml human TNF α . MTT reduction was determined and expressed as mean MTT reduction % control (where control is SFM + 0.1 [v/v] BSA carrier) \pm S.D. Replicates in assay=12 and n=2.

SH-SY5Y cells exposed to TNF α appeared viable in cell culture and caspase-3 activity in SH-SY5Y cells remained unchanged over a 96 h period (Figure 4.9).

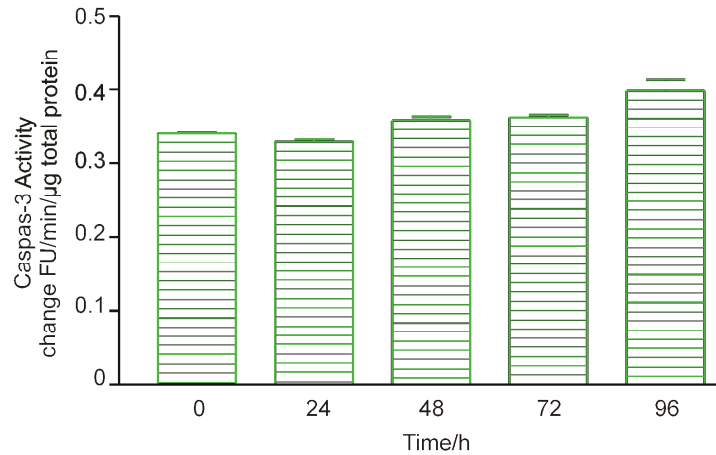


Figure 4. 9 TNF α does not induce caspase-3 mediated apoptosis in SH-SY5Y cells

SH-SY5Y cells were exposed to 10 ng/ml TNF α for 24 h. Caspase-3 activation was measured using Acetyl-Asp-Glu-Val-Asp-7-Amidomethylcoumarin as substrate and expressed as mean change FU/min/μg protein \pm S.D. All data represent triplicate values from two independent experiments (n=2).

4.2.3 Rotenone

SH-SY5Y cells were exposed to a range of rotenone concentration over a 48 h time course and assessed for MTT reduction as an indicator of cell viability. Rotenone reduced MTT viability in a concentration- and time-dependent manner (Figure 4. 10A). Rotenone concentrations of 0.5 μ M reduced cell viability by around 70% of untreated control levels by 48 h. SH-SY5Y cells were exposed to low concentration (0.5 μ M) rotenone over a 96 h period and MTT reduction measured several times (Figure 4. 10B). 0.5 μ M rotenone significantly reduced cell viability measured by MTT reduction throughout the 96 h time course.

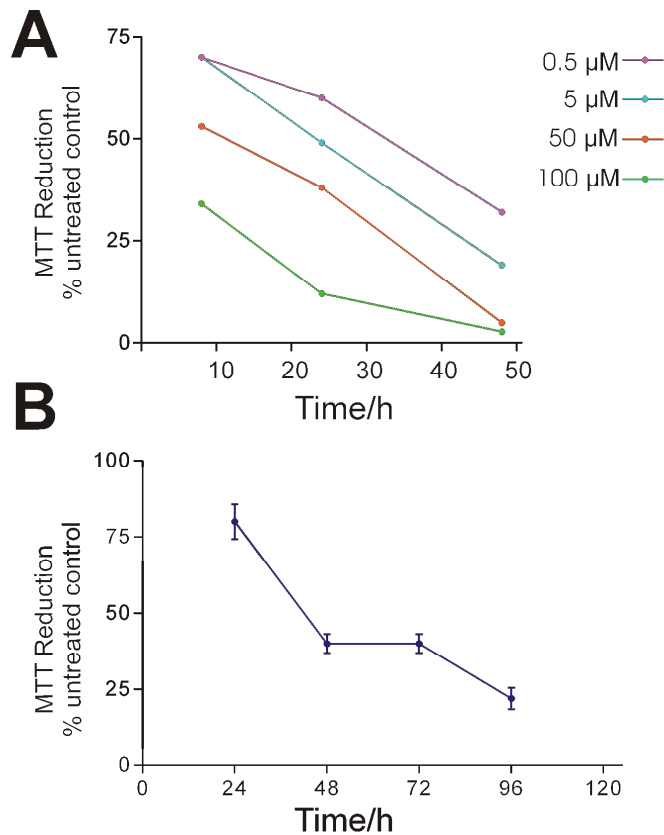


Figure 4. 10 MTT reduction following rotenone exposure in SH-SY5Y cells

(A) Cell viability was measured in SH-SY5Y cells over 48 hours, following the addition of 0.5, 5, 50 and 100 μM rotenone. MTT reduction was determined and expressed as mean MTT reduction % untreated control. Replicates in assay=12 and $n=1$. (B) Cell viability was measured in SH-SY5Y cells over 96 hours, following the addition of 0.5 μM rotenone. MTT reduction was determined and expressed as mean MTT reduction % control \pm S.D. Replicates in assay=12 and $n=7$. MTT reduction in untreated cells was statistically compared to MTT reduction in 0.5 μM rotenone treated cells over time using two way ANNOVA, where the effect of 0.5 μM rotenone on SH-SY5Y cells over the time course was significant at a confidence level of $p < 0.001$.

Cell morphology studies gave an insight into the time course of rotenone toxicity. Figure 4. 11 shows that following 48 h exposure to 0.5 μM rotenone, SH-SY5Y cells appear similar to untreated cells, with the exception of some floating cells (possibly apoptotic cells). Cells seem to then become extremely apoptotic very quickly peaking between 24-72 h on average. Caspase-3 is activated and peaks after 24 h rotenone treatment, with caspase-3 lower at 48 h than at 24 h. At 48 h, the cells appear to either be extremely apoptotic.

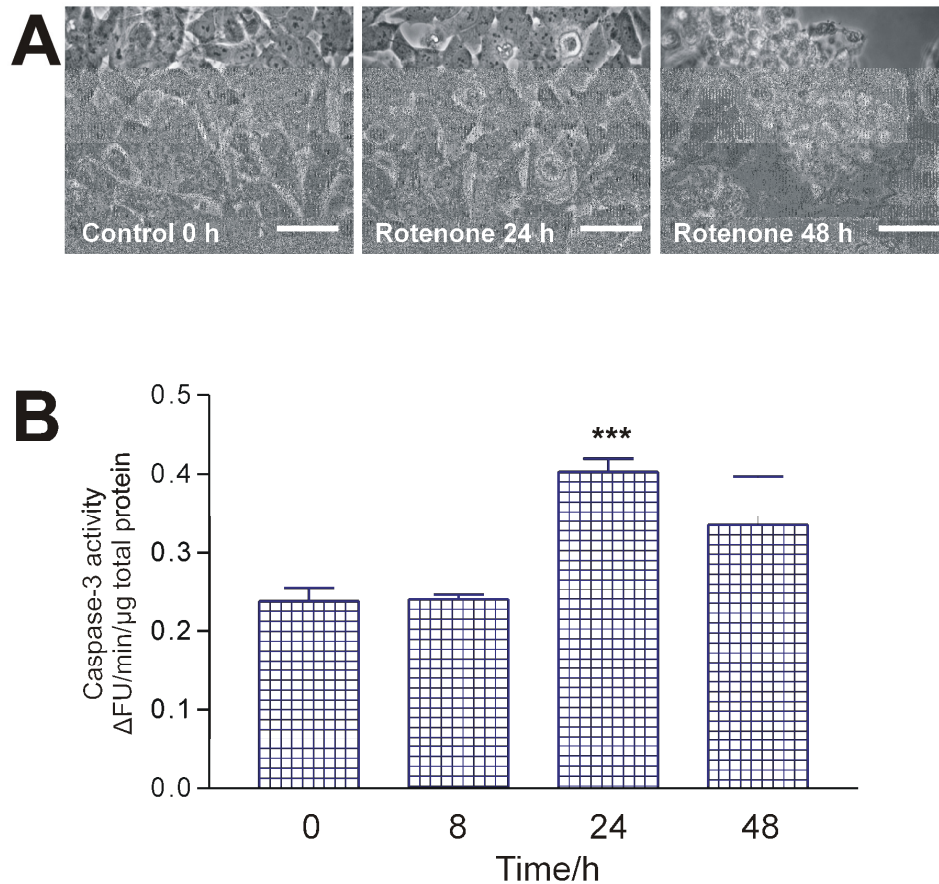


Figure 4. 11 Effect of rotenone on cell morphology and caspase-3 activity

(A) SH-SY5Y clones observed by phase contrast microscopy following 0.5 μ M rotenone treatment over a 48h period. Cells were visualised using a Nikon eclipse TS100 microscope. Photomicrographs (\times 40 objectives, taken on Nikon DN100 digital camera). Scale bar represents 20 μ M. (B) Caspase-3 activity measured using Acetyl-Asp-Glu-Val-Asp-7-Amidomethylcoumarin as substrate in SH-SY5Y cells following 0.5 μ M rotenone treatment over a 48h period and expressed as Δ FU/min/ μ g protein \pm S.D. Data represents values from four independent experiments over, where each extract was assayed in triplicate. Statistical analysis was performed using the Student's t-test to compare caspase-3 activity following rotenone treatment to untreated cells for each time point, where $n=4$ and ***= $p<0.001$.

MAO catalytic activity is increased following rotenone treatment, peaking after 24 h at around 2 fold of control level (Figure 4. 12).

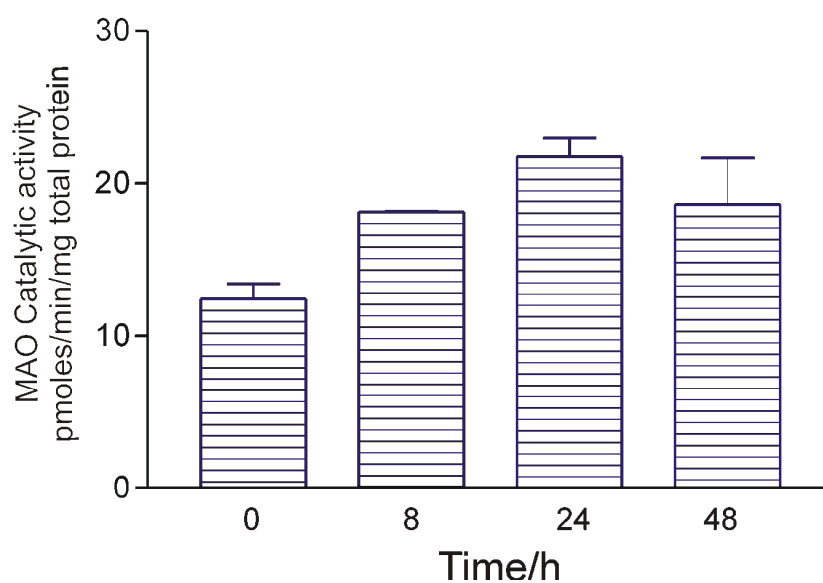


Figure 4. 12 Effect of rotenone on MAO activity

Following addition of 0.5 μM rotenone, MAO activity was measured in SH-SY5Y via a radiometric method, using ^{14}C -Tyramine as a substrate. MAO catalytic activity was expressed as pmoles/min/mg protein. Data represent triplicate values from two independent experiments ($n=2$) and are expressed as mean \pm S.D.

SH-SY5Y cells exposed to rotenone show subtle increases in ROS production. The cells were exposed to 0.5, 5 and 50 μM rotenone, but increasing the concentration of rotenone by 100 fold had no further effect on ROS levels.

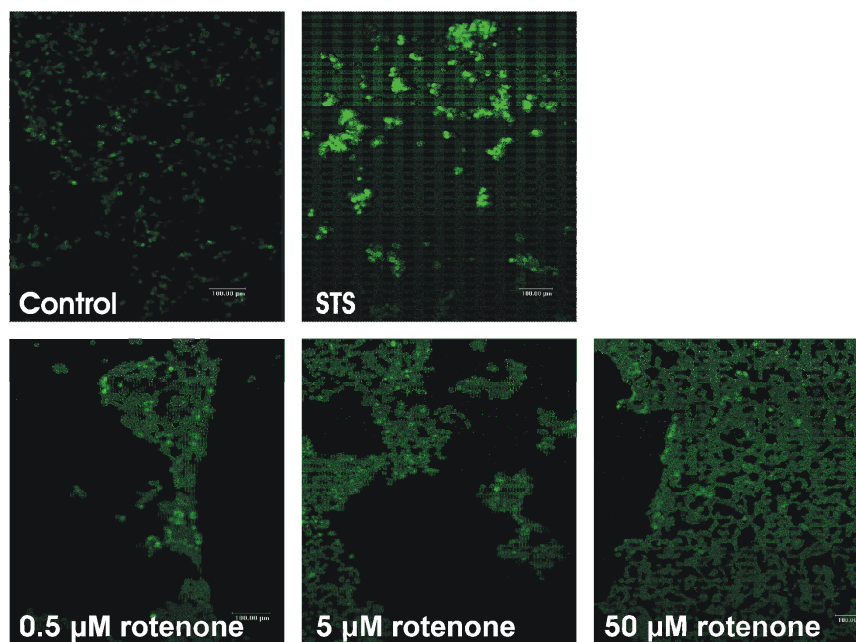


Figure 4. 13 Effect of rotenone on ROS levels

Cells were exposed to 0.5, 5 and 50 μM rotenone for 8 h and 1 μM STS as a positive control. DCDHF fluorescence was visualised using a CLSM Leica microscope. Photomicrographs are shown are laser power matched and are representative of 2 independent experiments. Scale bar represents 100 μm

4.2.4 Serum withdrawal

SH-SY5Y cells deprived of serum for 24 h show different morphologies to untreated cells. The cells become extended, elongated and develop neurite outgrowths typical of cellular differentiation. Some cells appear apoptotic in the population after 24 h serum withdrawal (Figure 4. 14). Following 48 h serum withdrawal half of the cell population shows apoptotic morphologies and this effect continues in a time dependent manner (Figure 4. 14).

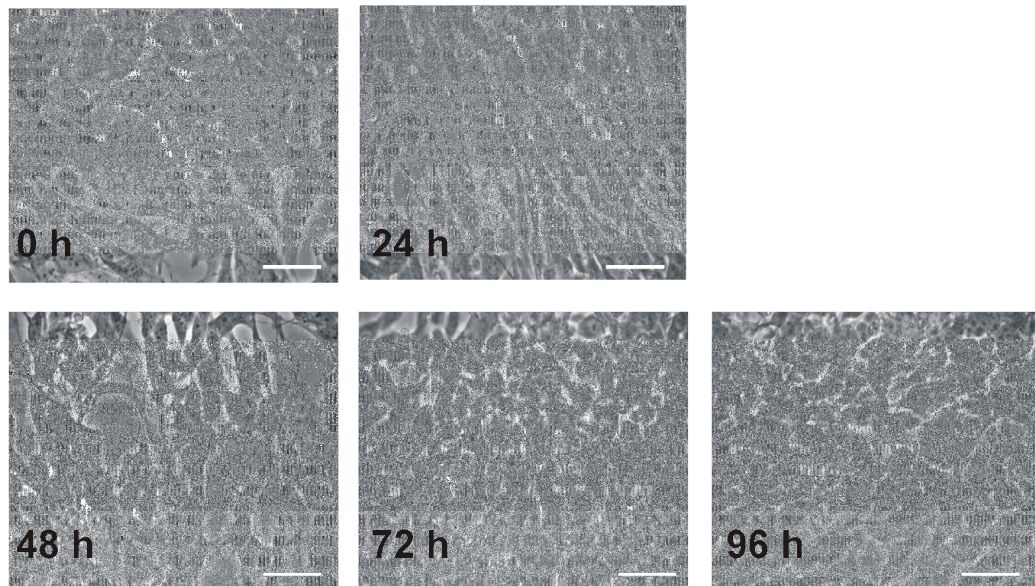


Figure 4. 14 Apoptotic morphologies of SH-SY5Y cells following serum withdrawal

SH-SY5Y cells were deprived of serum over a 96 h period. Morphologies were visualised using a Nikon eclipse TS100 microscope. Photomicrographs ($\times 40$ objectives, taken on Nikon DN100 digital camera) are shown at 0, 24, 48, 72 and 96 h post-treatment and are representative of 3 independent experiments. Scale bar represents 20 μm .

Caspase-3 activity is significantly increased after 24 h serum deprivation (by \sim two fold untreated control level). Caspase-3 activity remains increased until 72 and then begins to fall (Figure 4. 15).

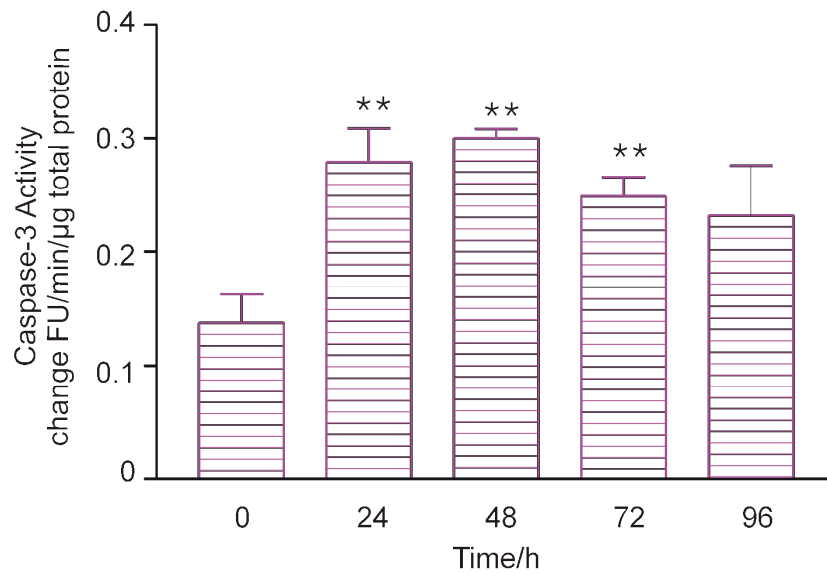


Figure 4. 15 Serum withdrawal induced caspase-3 mediated apoptosis in SH-SY5Y cells

SH-SY5Y cells were deprived of serum for a 96 h period. Caspase-3 activation was measured using Acetyl-Asp-Glu-Val-Asp-7-Amidomethylcoumarin as substrate and expressed as mean change FU/min/μg protein ± S.D. All data represent triplicate values from five independent experiments (n=5, except at 48 h, where n=3). Statistical analysis of serum deprived cells compared to untreated controls was carried out using the Student's t-test, where **p<0.01.

4.2.4.1 Relevance of MAO in serum withdrawal-induced apoptosis

MAO catalytic activity increases in a time dependent manner following serum withdrawal (Figure 4. 16) over a 96 h period (~2 fold untreated control). Expression of MAO-A mRNA is also increased ~two fold at 24 h and ~3 fold at 72 h and then decreases slightly by 96 h of serum deprivation (Figure 4. 17).

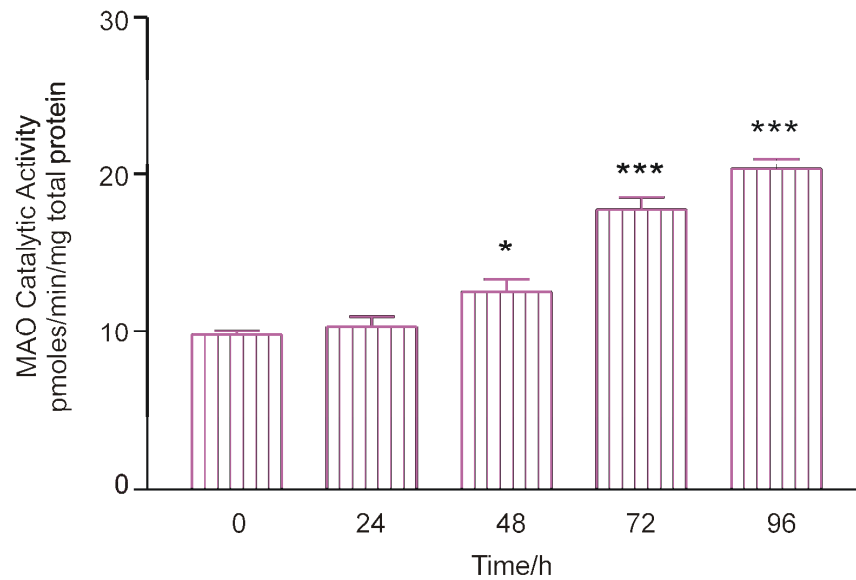


Figure 4. 16 Serum withdrawal caused increased MAO activity

Following deprivation of serum over a 96 h period, MAO activity was measured in SH-SY5Y via a radiometric method, using ^{14}C -Tyramine as a substrate. MAO catalytic activity was expressed as pmoles/min/mg protein. Data represent triplicate values from three independent experiments ($n=3$) and are expressed as mean \pm S.D. Serum deprived samples were statistically compared to untreated controls at time zero using the Student's t-test where * = $p<0.05$ and *** = $p<0.001$.

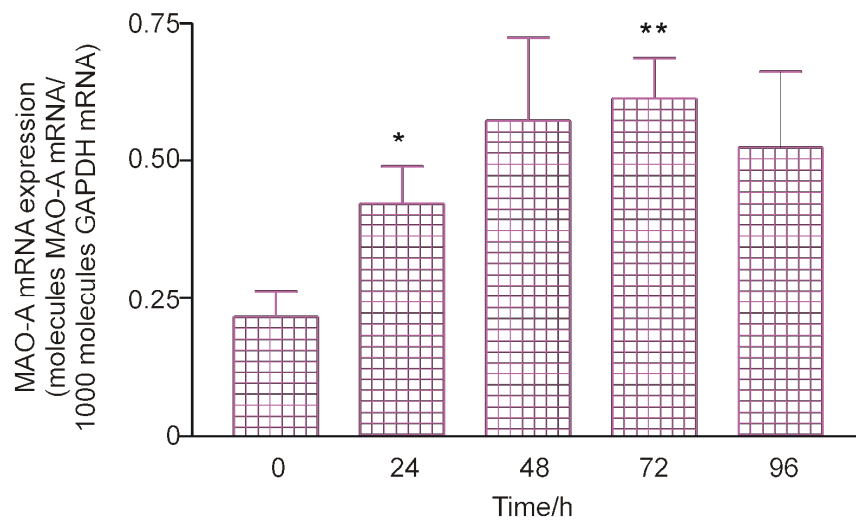


Figure 4. 17 Serum withdrawal caused increased MAO-A mRNA expression

MAO-A mRNA expression was measured by qRT-PCR following serum withdrawal over a 96 h period. Data represent duplicate values from three independent experiments ($n=3$). Values are expressed as molecules MAO-A mRNA / 1000 molecules GAPDH mRNA \pm S.D. Statistical analysis of serum deprived samples compared to untreated controls was performed using the Student's t-test, where * = $p<0.05$ and ** = $p<0.01$.

Finally, MAO-A protein levels are also elevated during serum withdrawal-induced apoptosis (Figure 4. 18). Dot blots revealed a time dependent increase in MAO-A protein

levels over the 96 h time course, peaking at 96 h (by more than 2 fold untreated control levels).

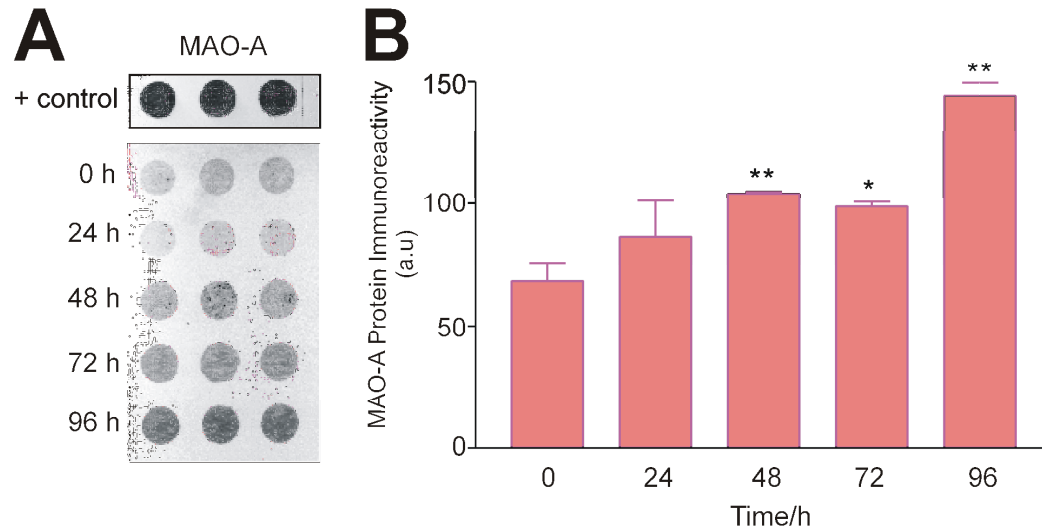


Figure 4. 18 Serum withdrawal caused increased MAO-A protein levels

(A) Representative dot blot of MAO-A protein following serum withdrawal. Equal protein homogenates were loaded on to a nitrocellulose membrane and probed with a MAO-A specific antibody. Mitochondrial membranes from human placenta (1 μ g) are the positive control. (B) Quantification of dot blots. Blots were digitised and densitometry was performed to quantify relative MAO-A protein levels in all blots. These data represents values from three separate experiments (n=3) and expressed as mean arbitrary units (a.u.) \pm S. D. Statistical analysis of treated cells in comparison to untreated controls was carried out using the Student's t test, where * = $p < 0.05$ and ** = $p < 0.01$.

4.2.4.2 Relevance of MAO-A in serum-withdrawal-induced apoptosis

The effect of MAO-A inhibition on changes in cell morphology, cell viability and apoptosis were assessed to determine the relevance of MAO-A in serum withdrawal-induced apoptosis. Cells deprived of serum in the presence of either tranylcypromine (TCP) or clorgyline appear less apoptotic (Figure 4. 19).

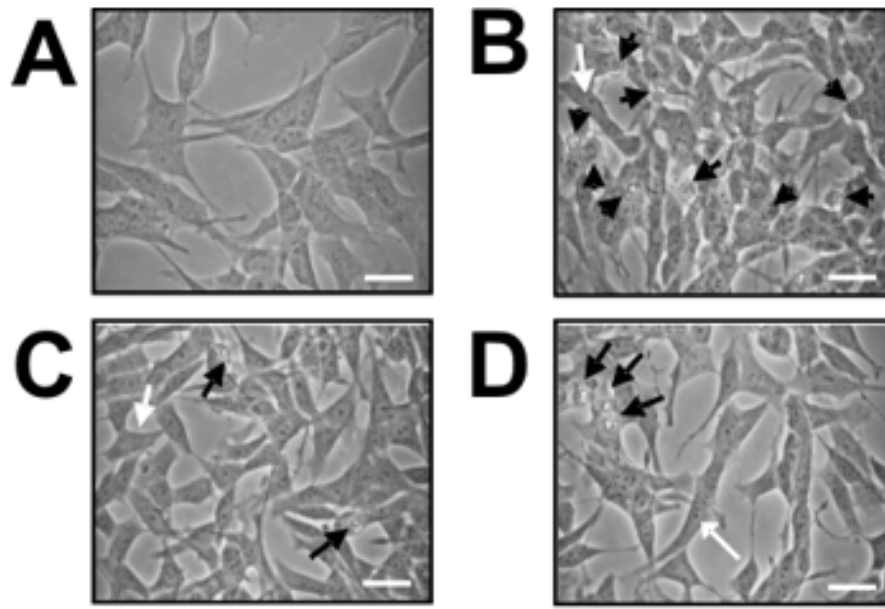


Figure 4. 19 The effect of MAO inhibitors on the apoptotic morphology of SH-SY5Y cells following serum withdrawal

The effect of MAO inhibitors tranylcypromine (TCP) and clorgyline on the apoptotic morphology of SH-SY5Y cells following serum withdrawal. Control SH-SY5Y cells (**A**) were exposed to serum withdrawal (**B**) and were treated concomitantly with 1 μ M tranylcypromine (**C**) or 1 μ M clorgyline (**D**). Cells were visualised using a Nikon eclipse TS100 microscope. Photomicrographs ($\times 40$ objectives, taken on Nikon DN100 digital camera) are shown at 48 hours post-treatment and are representative of 3 independent experiments. Scale bars represent 30 μ m. *Black arrows* indicate typical morphology of apoptotic cells (shrunken, rounded, shiny, condensed and surface blebs), whilst *white arrows* show examples of normal SH-SY5Y cell morphology (elongated and flattened with axon like outgrowths).

Serum withdrawal causes a significant loss of cell viability measured by MTT reduction over a 96 h time course, but concomitant treatment with TCP or clorgyline had no effect on MTT reduction throughout the 96 h period (Figure 4. 20A). On the other hand, loss of cell viability measured by trypan blue viable cell count was induced by serum withdrawal after 72 h and concomitant treatment with TCP and clorgyline significantly protected from loss of cell viability (Figure 4. 20B).

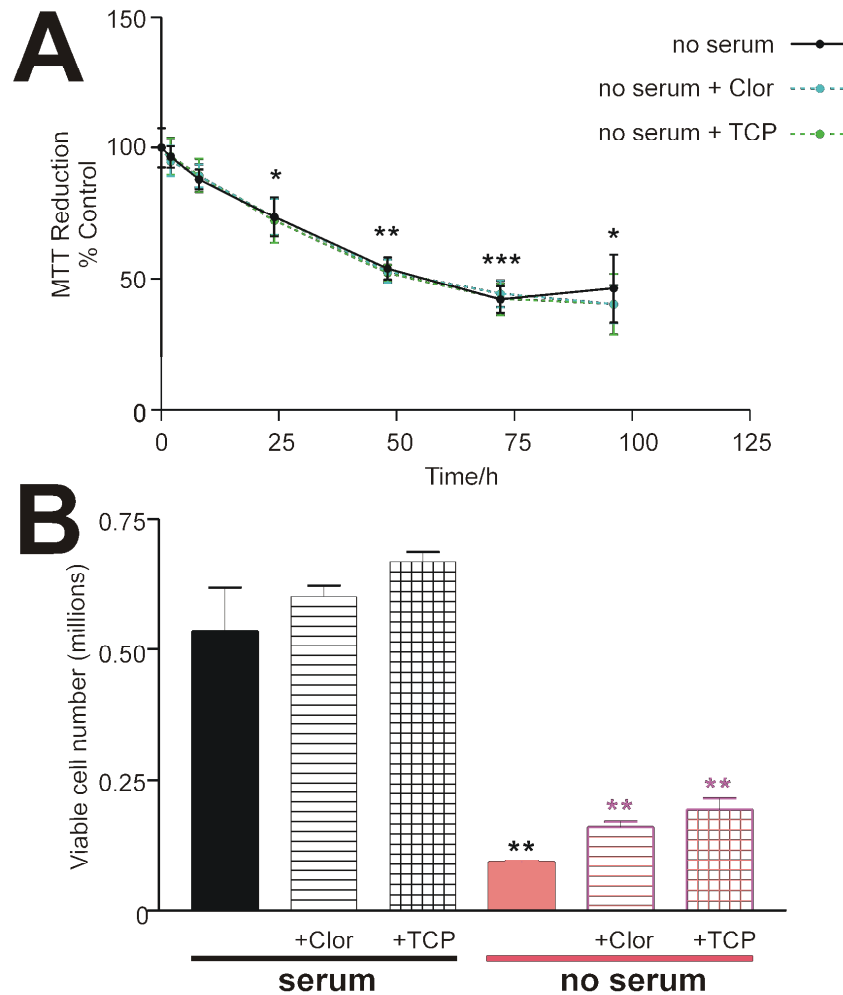


Figure 4. 20 Effect of MAO inhibition on cell viability following serum withdrawal

(A) Cell proliferation (MTT reduction) was measured in SH-SY5Y cells over a 96 h period, following serum deprivation or in serum deprived cells concomitantly treated with 1 μ M clorgyline (+clor), 1 μ M tranlycpromine (+TCP). MTT reduction was determined and expressed as mean MTT reduction % control (where control is cells in growth medium containing serum) \pm S.D. Replicates in assay=12 and n=4. MTT reduction in serum deprived cells was statistically compared to untreated controls using the Student's t-test, where * = $p < 0.05$, ** = $p < 0.01$ and *** = $p < 0.001$. Serum deprived MTT reduction was statistically compared to MTT reduction in serum deprived cells + Clor and + TCP, however there was no significant difference ($p < 0.05$). (B) Viable cells were seeded at equal density prior to treatment. Cell number in control cells, following serum withdrawal and in the presence and absence of clorgyline and TCP were counted at a 72 hour end point using trypan blue stain. Cell number was determined and expressed as mean cell number \pm S.D. Cell counts were performed in duplicate and n=3. Viable cell number following serum deprivation was statistically compared to untreated cell numbers using the Student's t-test, where ** = $p < 0.01$. Cell number following serum deprivation was statistically compared to cell number following serum + Clor and + TCP, where ** = $p < 0.01$.

Serum withdrawal induced caspase-3 activation was significantly reduced by TCP but not clorgyline (Figure 4. 21) following 48 h serum deprivation (Figure 4. 21).

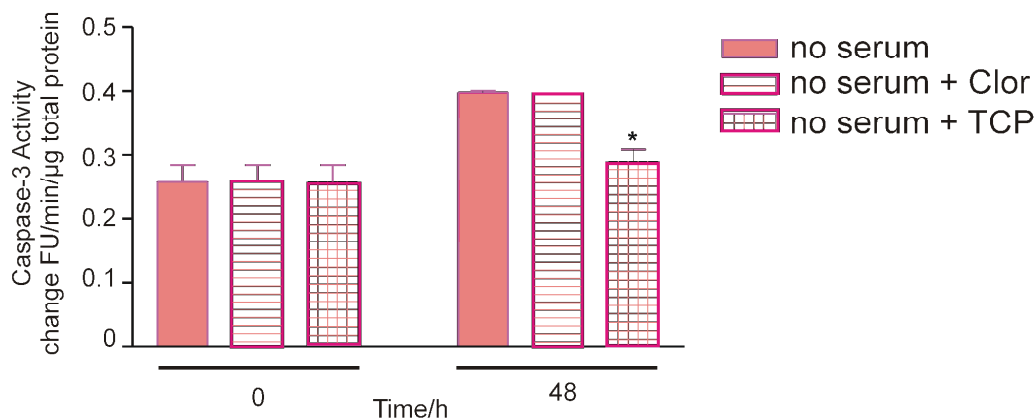


Figure 4. 21 The effect of MAO inhibition on serum withdrawal-induced caspase-3 activation

SH-SY5Y cells were deprived of serum for a 48 h period in the presence and absence of MAO inhibitors. Caspase-3 activation was measured using Acetyl-Asp-Glu-Val-Asp-7-Amidomethylcoumarin as substrate and expressed as mean change FU/min/ μ g protein \pm S.D. All data represent triplicate values from three independent experiments ($n=3$). Statistical analysis of serum deprived cells compared to serum deprived cells in the presence of MAO inhibitors was carried out using the Student's t-test, where $*p<0.05$.

DNA fragmentation in cells deprived of serum for 72 h was assessed with or without the presence of the MAO inhibitors. Extensive DNA fragmentation was observed in SH-SY5Y cells deprived of serum. Fragmentation of DNA was significantly reduced in the presence of clorgyline and even more so (almost back to control status) in the presence of TCP (Figure 4. 22).

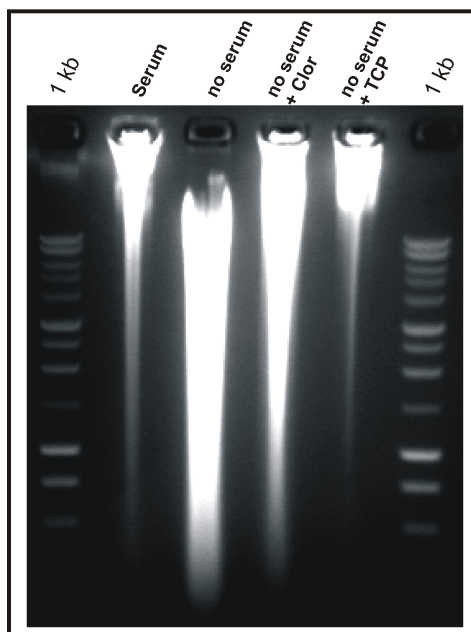


Figure 4. 22 The effect of MAO inhibition on serum withdrawal-induced DNA fragmentation

Serum was withdrawn for 72 h in the presence or absence of MAO inhibitors clorgyline (+Clor) or tranlycypromine (+TCP), DNA extracted and DNA fragmentation assessed by agarose gel electrophoresis.

4.2.4.3 Mechanism of MAO-A involvement in serum withdrawal-induced apoptosis

To investigate the mechanism of MAO-A involvement in serum withdrawal-induced apoptosis, caspase signalling pathways, MAPK signalling pathways and ROS production were considered.

Serum withdrawal caused cleavage (activation) of caspase-9 measured by reduced proform levels and increased active form levels (Figure 4. 23). Following deprivation for 96 h caspase-9 is substantially cleaved to its active form. Concomitant treatment with clorgyline delayed and reduced activation of caspase-9 (Figure 4. 23A). Quantification of caspase-9 activation following serum withdrawal is illustrated in Figure 4. 23B.

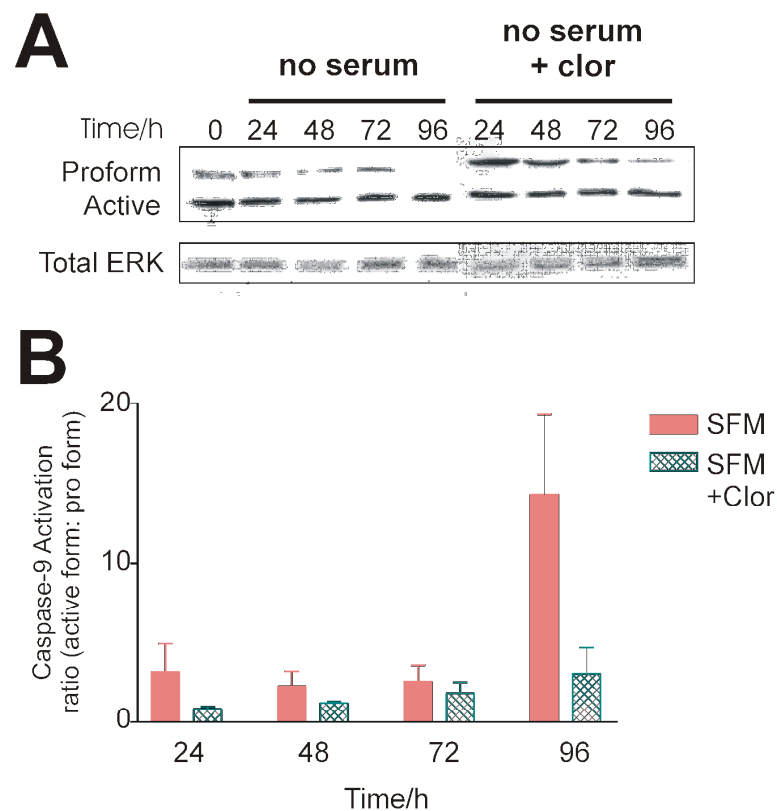


Figure 4. 23 Effect of MAO inhibition on caspase-9 activation induced by serum withdrawal

(A) Activation of caspase-9 (pro-form/active form) was assessed in extracts of SH-SY5Y cells deprived of serum in the presence or absence of 1 μ M clorgyline over a 96 h period. Equal protein aliquots (20 μ g) were separated on a 12 % (v/v) acrylamide SDS-PAGE gel prior to transfer to nitrocellulose filters. Western blots were probed with anti-caspase-9 antibody (2 μ g/ml). (B) Western blots were digitised and densitometry was performed to quantify relative caspase-9 proform and active protein levels. These data represents values from two separate experiments (n=2) and expressed as mean caspase-9 activity (by dividing the active C9 band intensity by the proform C9 band intensity) \pm standard error.

Caspase-8 proform levels remained unchanged following serum withdrawal in SH-SY5Y cells and the caspase-8 active form was not detected (data not shown). Numerous attempts were made to detect caspase-8 activation following serum withdrawal (and all other

treatments) using a fluorescent substrate-based caspase-8 activity kit from EMD Biosciences, New Jersey, U.S.A, however the kit was not sensitive enough to detect caspase-8 activation in any samples including positive controls provided by the company.

SH-SY5Y cells deprived of serum for 72 h show subtle increases in ROS production (Figure 4. 24). Concomitant treatment with clorgyline slightly reduced ROS production caused by serum withdrawal (Figure 4. 24).

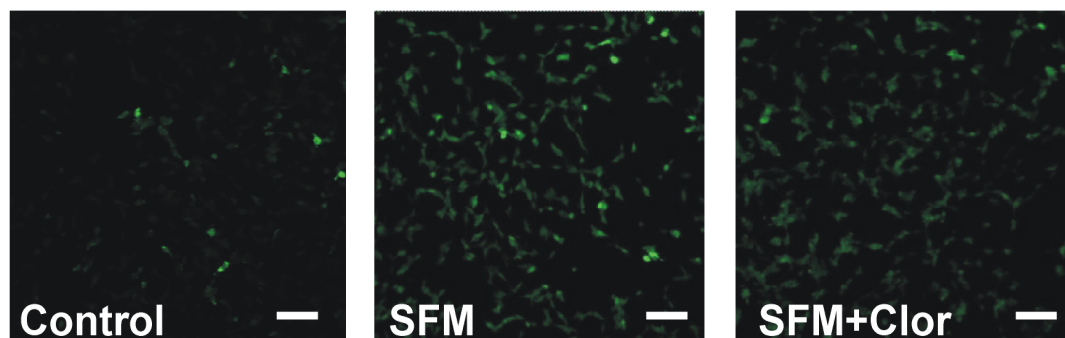


Figure 4. 24 Serum withdrawal induces subtle elevation of ROS

Cells were deprived of serum for 24 h (SFM) and in the presence of 1 μ M clorgyline (SFM+Clor). DCDHF fluorescence was visualised using a CLSM Leica microscope. Photomicrographs are shown are laser power matched and are representative of 3 independent experiments. Scale bar represents 100 μ m.

Serum withdrawal induces changes in MAPK signalling pathways detected by antibodies directed against the phosphorylated (activated) MAPK proteins ERK, JNK and p38. Following serum deprivation levels of phosphorylated (phospho) ERK are initially decreased, but levels rise and fall somewhat throughout the time course (Figure 4. 25A). Quantification of data from independent experiments indicates that the ERK response is generally reduced following serum withdrawal (Figure 4. 25B). JNK is activated immediately upon withdrawal of serum and remains active throughout the time course, peaking approximately at ~48-72 h according to mean quantified data (Figure 4. 25B). Figure 4. 25 shows that MAPK p38 is activated strongly following serum withdrawal, (peaking between 24-48 h according to quantified data).

In preliminary experiments (shown as representative blot in Figure 4. 25A), the MAO inhibitors clorgyline and TCP had no effect on phosphor ERK, JNK or p38 levels at 24 h.

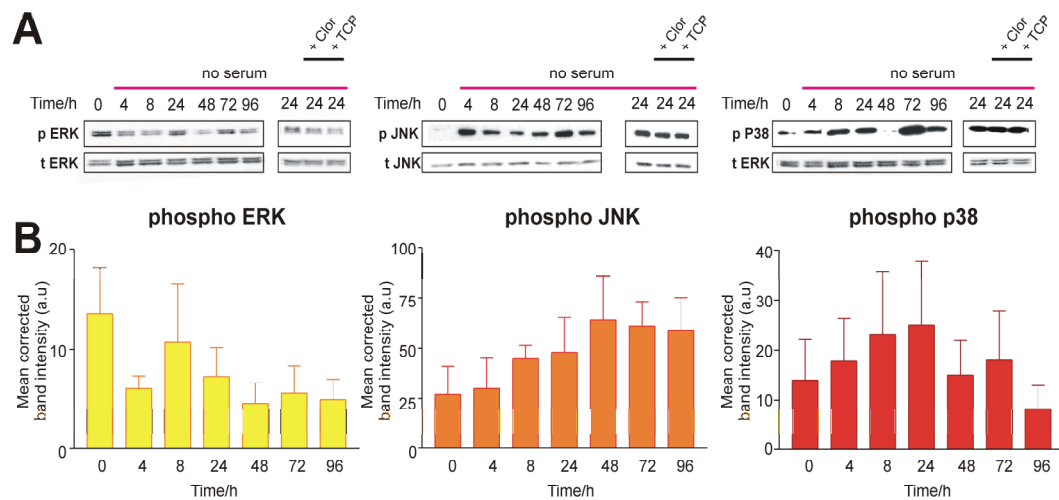


Figure 4. 25 Effect of serum withdrawal on MAPK phosphorylation

(A) Equal protein aliquots (80 μ g) of cells extracts from SH-SY5Y cells deprived of serum over a 96 h period or serum deprived cells in the presence or absence of 1 μ M clorgyline for a 24 h period were separated on a 12 % (v/v) acrylamide SDS-PAGE gel prior to transfer to nitrocellulose membranes. Blots were probed with antibodies directed to pERK (1:1000 dilution), pJNK (1:500 dilution) and pP38 (1:1000). Equal loading was checked by probing for total ERK (1:1000 dilution) or total JNK (1:750 dilution). Blots shown are representative of three separate experiments. (B) Western blots were digitised and densitometry was performed to quantify levels of pERK, pJNK and pP38. These data represents values from three separate experiments (n=3) and expressed as mean corrected band intensity \pm S. D.

Inhibitors of ERK, JNK and p38 MAP kinases were employed to investigate their involvement in MAO-mediated apoptosis induced by serum withdrawal. Inhibition of specific phosphorylated MAPK proteins by the inhibitors was assessed by western blotting. The ERK inhibitor PD98059 reduced levels of phosphorylated ERK in both untreated SH-SY5Y cells and following treatment with STS (Figure 4. 26 *top panel*). The JNK inhibitor Cep reduced phosphorylated JNK levels in untreated cells and following activation of JNK by STS (Figure 4. 26 *middle panel*). Phosphorylated p38 is detectable only following activation by stressors. STS treatment caused activation of p38 at 1 and 3 h. The p38 inhibitor SB202190 completely reduced phosphorylated p38 levels in STS treated cells (Figure 4. 26 *bottom panel*).

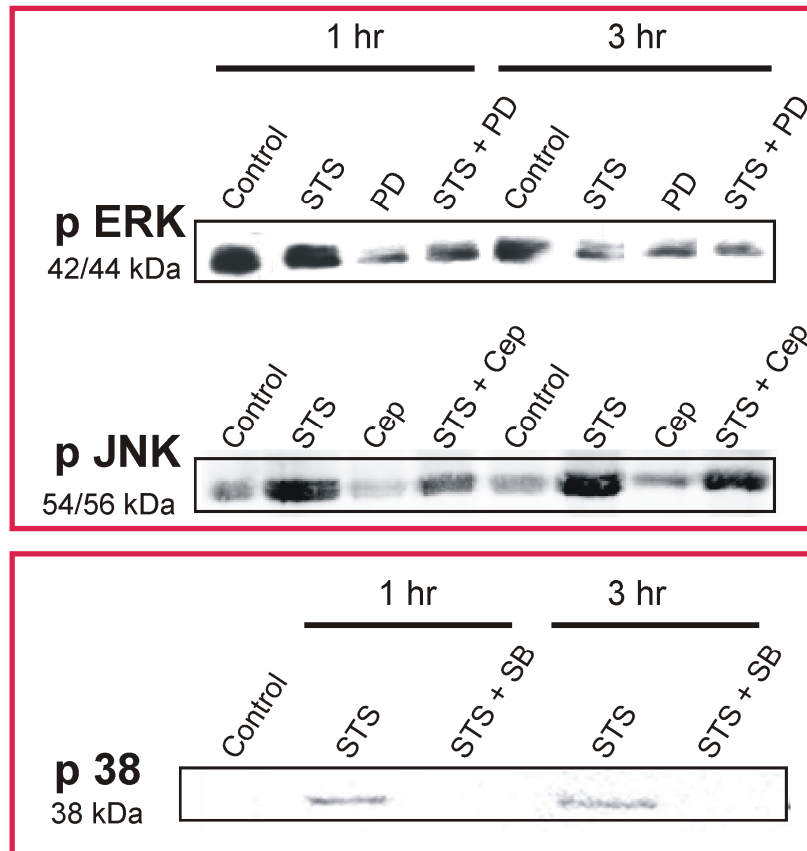


Figure 4. 26 Effect of MAPK inhibitors on levels of phosphorylated MAPK proteins

Equal protein aliquots (80 μ g) of cells extracts from SH-SY5Y cells treated with vehicle control, 20 μ M ERK inhibitor PD98059 (PD), 1 μ M JNK inhibitor Cep, 10 μ M P38 inhibitor SB202190 (SB) over a 3 h time period, 1 μ M STS, 1 μ M STS + 20 μ M PD98059, 1 μ M STS + 1 μ M Cep or 1 μ M STS + 10 μ M SB202190 over a 3 h time period were separated on a 12 % (v/v) acrylamide SDS-PAGE gel prior to transfer to nitrocellulose membranes. Equal loading was checked using copper stain for total protein (data not shown). Blots were probed with antibodies directed to pERK (1:1000 dilution), pJNK (1:500 dilution) and pP38 (1:1000). Representative blots from three separate experiments are shown.

MAO catalytic activity and mRNA expression are consistently increased in response to serum withdrawal in SH-SY5Y cells (Figure 4. 27A and B). After 96 h serum deprivation, MAO activity is increased ~2 fold compared to control cells. MAO activity was further increased in serum deprived cells concomitantly treated with the ERK inhibitor PD98059, although the increase was not statistically significant. Increased MAO activity induced by serum deprivation was reduced in the presence of the JNK inhibitor Cep (by ~33% of SFM alone) although this reduction was not statistically significant. Treatment of serum deprived cells with the p38 inhibitor SB202190, on the other hand, significantly reduced MAO activity to below control levels (Figure 4. 27A).

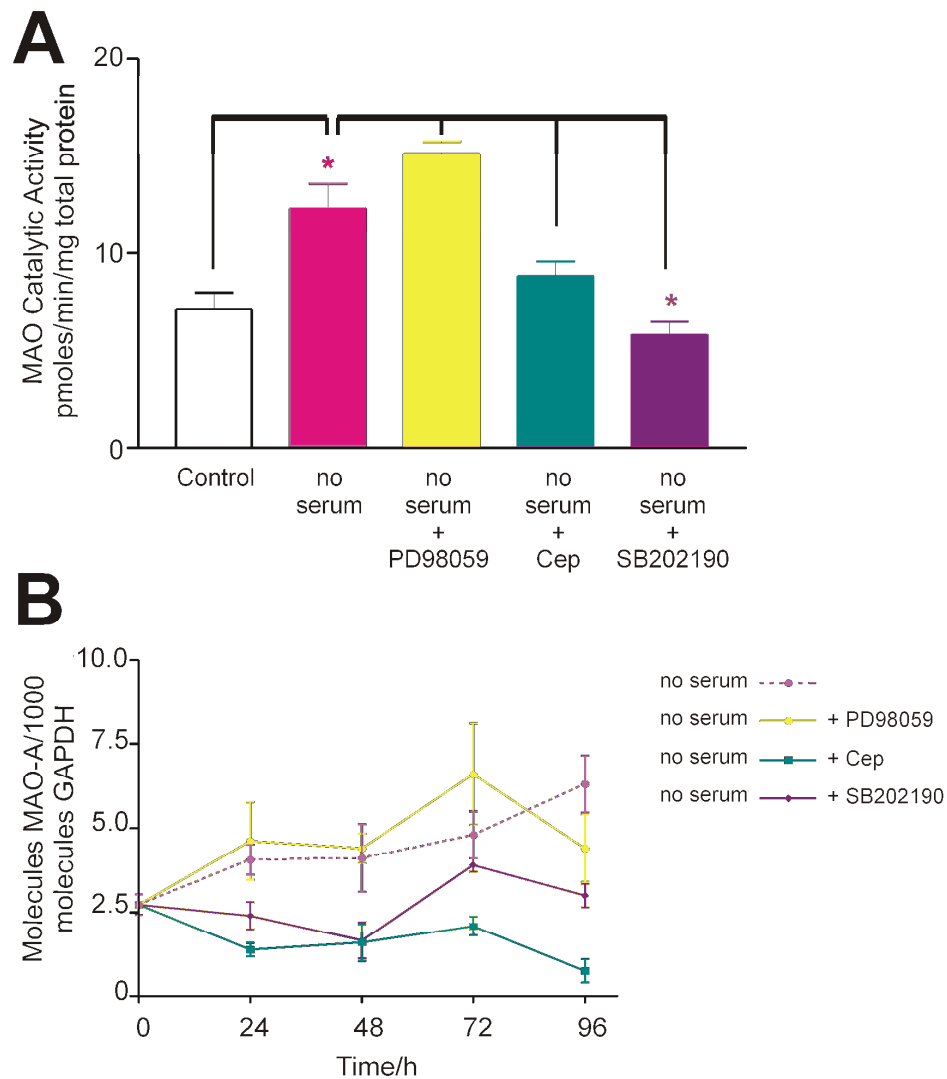


Figure 4. 27 Effect of MAPK inhibitors on MAO Activity and mRNA expression

(A) Following deprivation of serum for 96 h end point (peak MAO catalytic activity following serum withdrawal) in the presence or absence of either 20 μ M PD98059, 1 μ M Cep or 10 μ M SB202190, MAO activity was measured in SH-SY5Y via a radiometric method, using 14 C-Tyramine as a substrate. MAO catalytic activity was expressed as pmoles/min/mg protein. Data represent triplicate values from three independent experiments ($n=3$) and are expressed as mean \pm S.D. Serum deprived cells were statistically compared to control cells at 72 h using the Student's *t*-test, where * = $p<0.05$. Serum deprived samples were statistically compared to serum deprived samples in the presence of each MAPK inhibitor using the Student's *t*-test where * = $p<0.05$. (B) MAO-A mRNA expression was measured by qRT-PCR following serum withdrawal over a 96 h period in the presence and absence of MAPK inhibitors at the same concentration detailed above. Data represent mean values from two separate real time determinations, from one independent experiment ($n=1$). Values are expressed as mean molecules MAO-A mRNA / 1000 molecules GAPDH mRNA \pm SEM.

ERK inhibition had little effect on serum withdrawal-induced increased MAO-A mRNA levels over a 96 h time course (Figure 4. 27B). Conversely, JNK and p38 inhibition both greatly reduced MAO-A mRNA expression levels following serum withdrawal (Figure 4. 27B) back to untreated control levels (in the case of SB202190) or below control levels (in the case of Cep).

4.3. DISCUSSION

4.3.1 Death receptor-mediated apoptosis

AAF failed to induce changes in cell viability or morphology or caspase-3 activity even at high concentrations. In contrast, rat C6 cells showed early signs of apoptotic morphologies when challenged with AAF and preliminary data indicates that caspase-3 was activated (unpublished observations, data not shown); both suggestive that AAF was active.

Since apoptosis can occur independently of caspase-3 in SH-SY5Y cells (Racke *et al.* 2002) and receptor mediated apoptosis can activate multiple caspases (Bratton *et al.* 2000), including the executioner caspase-7, activation of the upstream caspases-8 and -9 were monitored in cells exposed to AAF. Caspase-9 was not activated by AAF in SH-SY5Y cells and there was some evidence that caspase-8 is activated by Fas ligand after 4 and 8 hours, since levels of the proform were reduced compared to control levels (Figure 4.7), but the active caspase-8 fragment was not detected.

Detection of the caspase-8 active fragment in SH-SY5Y cells was not achieved with this antibody or other commercial antibodies following any apoptotic treatment. Therefore, U937 cells treated with TNF α were used as a positive control for the antibody; these cells are known to undergo apoptosis with TNF α (unpublished observations of Dr C. Ufer, Nottingham Trent University). In these cells, loss of caspase-8 proform was evident but again the active form of caspase-8 was not detected (Figure 4.7). Exposure of SH-SY5Y cells to TNF α had no effect on cell viability (Figure 4. 8) or caspase-3 activity (Figure 4. 9). Detection of caspase-8 activation by a fluorescent substrate based assay was also attempted but the data were not reliable since results obtained with commercial standards were not convincing.

In view of the data obtained it was clear that the extrinsic pathway was not activated in SH-SY5Y cells and the work was discontinued. Nonetheless, these data have given support to previous research that has proposed similar unresponsiveness to receptor-mediated inducers in SH-SY5Y cells (Hopkins-Donaldson *et al.* 2000, Desbarats *et al.* 2003, Miller *et al.* 2006). Considering the loss of caspase-8 proform detected by western blotting following AAF (Figure 4.7), the presence of caspase-8 expression (chapter 3) and expression of Fas receptor in SH-SY5Y cells (Russo *et al.* 2004), a schematic of the proposed caspase-8 situation is shown below.

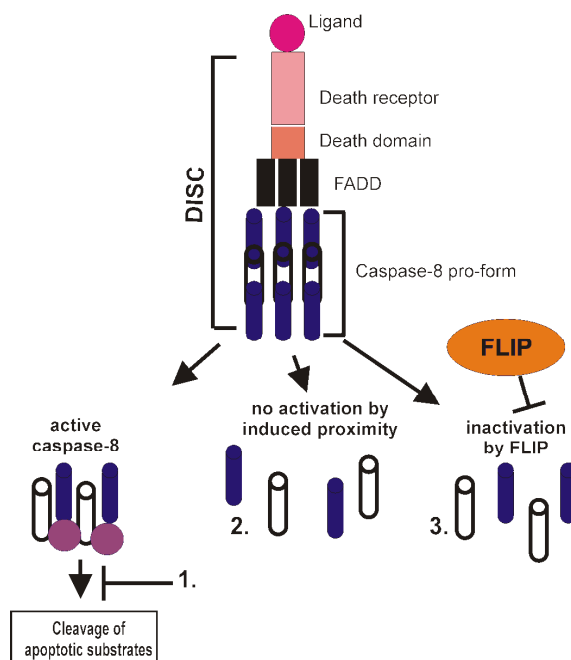


Figure 4. 28 Possibilities for reduced caspase-8 function in SH-SY5Y cells

Death receptors are activated following ligand binding and FADD and caspase-8 proform are recruited to form the death inducing signalling complex (DISC). Loss of proform indicates cleavage to the 28 kDa fragments. Recruitment or aggregation of multiple caspase-8 in close proximity somehow results in cross-activation (Hengartner 2000), however the mechanism of caspase-8 activation remains unclear. **1.** Activation may require unknown co-factors or proteases that are absent in SH-SY5Y cells, or events downstream of active caspase-8 in the apoptotic cascade are not functional. **2.** Induced proximity is thought to be a sophisticated and tightly regulated mechanism, yet the mechanisms are still unknown. It is possible that this mechanism of caspase-8 activation is dysfunctional in SH-SY5Y cells. **3.** Anti-apoptotic FLIP may inhibit caspase-8 function. Expression of FLIP is known to be regulated by ROS (Nitobe *et al.* 2003) and expression may be altered in SH-SY5Y cells because of malignancy. Finally, caspase-8L a novel inhibitory isoform of caspase-8 has been found in undifferentiated SH-SY5Y cells (Miller *et al.* 2006), which may act in a similar way to FLIP.

4.3.2 Rotenone-mediated apoptosis

4.3.2.1 Effects on cell viability and apoptosis

Rotenone had a potent effect on SH-SY5Y cells. Cell viability following rotenone treatment was reduced in a time and dose dependent manner (Figure 4. 10A). The lowest concentration of rotenone used (0.5 μ M) caused a significant loss of cell viability of approximately 25, 60 and 75 % after 24, 48 and 96 hours respectively (Figure 4. 10B). These data were complimented by the development of apoptotic cell morphologies following exposure to 0.5 μ M rotenone for 48 h (Figure 4. 11A), together with a 2 fold increase in caspase-3 activity (Figure 4. 11B).

Rotenone inhibits complex 1 of the ETC, and levels of ATP are likely to be strongly depleted. Apoptosis may only occur once ATP levels fall below a certain threshold, and this may explain the change in the cells' appearance between 24 and 48 hours (Figure 4.

11A). However, if ATP levels drop very low, the cells are likely to die by necrosis. Recent work in SH-SY5Y cells has suggested that ROS production is more relevant than ATP depletion in rotenone toxicity (Watabe and Nakaki 2006). Other effector caspases, such as -7 and -12, may also be activated in rotenone-induced apoptosis. Indeed, rotenone has been shown to induce both the mitochondrial (caspase-9) and the ER-dependent (caspase-12) apoptotic pathways in SH-SY5Y cells (Kitamura *et al.* 2002, Newhouse *et al.* 2004). Caspase-3 is thought to only account for about half of the caspase activity responsible for rotenone induced apoptosis in SH-SY5Y cells (Newhouse *et al.* 2004).

4.3.2.2 Role of MAO in rotenone-mediated apoptosis

Significantly, MAO activity was also increased following rotenone treatment, at approximately the same time as caspase-3 (Figure 4. 12), and this was associated with a small increase in ROS levels (Figure 4. 13). Unfortunately due to time restraints, the molecular basis of the increase in MAO activity was not studied further but, it is now acknowledged that this observation may be very important since increased MAO activity in response to complex I inhibition has not previously been reported. Indeed a role for MAO in cell death induced by complex I inhibition is plausible since inhibition of complex I causes increased oxidative stress and ATP depletion, mitochondrial dysfunction and cell death (Abou-Sleiman *et al.* 2006). ROS levels detected by confocal microscopy in live cells were increased in rotenone treated cells (Figure 4. 13). MAO activity will in theory generate more ROS within the cell but MAO's contribution to ROS levels was not assessed using MAO inhibition. The role of MAO in rotenone-induced apoptosis is further investigated in stable SH-SY5Y cells with reduced MAO-A (see chapter 6).

4.3.3 Serum withdrawal-induced apoptosis

Apoptotic morphologies and increased caspase-3 activity were evident in cell deprived of serum for 24 h, and following 48 h of serum withdrawal the cells were clearly apoptotic and caspase-3 activity had peaked. Caspase-9 was also activated, but maximum activation appeared to occur at 96 h. This was not expected since caspase-9 is upstream of caspase-3, indicating that apoptotic signalling following serum withdrawal is complex and may involve a diverse set of caspases and caspase interactions.

The response to serum withdrawal is a slow process, occurring over 4-5 days, during which the majority of the cells remained attached to the monolayer. These and published data suggest that neuronal cells undergo a slow but highly regulated and complex response to

the withdrawal of growth signals. The initial response will probably involve direct activation of PI3K, Akt, cytochrome c release, activation of upstream caspases and caspase-3.

Activation of caspase-3 alone is insufficient for apoptotic morphological changes in neuroblastoma cells (Racke *et al.* 2002) and therefore other systems, including up-regulation pro-apoptotic proteins and activation of caspases-6 and -7 may be important in this model. This model has particular relevance to human pathology in ageing and neurodegeneration, where neurons are exposed to low-level stress over a long time period.

4.3.3.1 Role of MAO in serum withdrawal-induced apoptosis

MAO expression was increased during serum withdrawal at the mRNA (Figure 4. 17), protein (Figure 4. 18) and activity level (Figure 4. 16). Increased MAO-A mRNA levels were apparent after 24 h and reached a maximum at 72 h. Increases in MAO-A protein levels and MAO activity follow, both reaching their highest values after 96 h. These changes were preceded by activation of caspase-3, suggesting that the MAO-A gene is down stream of caspase-3 activation.

MAO-A inhibition failed to reduce caspase-3 levels or loss of cell viability measured by MTT; however it did reduce apoptotic morphologies and loss of cell numbers. These data disagree with the work of Ou *et al* (2006) who reported that clorgyline increased cell viability and reduced caspase-3 levels in SH-SY5Y cells subjected to serum withdrawal. MAO inhibition by clorgyline has previously been shown to reduce nucleosome fragmentation using in rat PC12 cells (DeZutter and Davis 2001). In the present work, DNA fragmentation induced by serum withdrawal in SH-SY5Y cells was reduced by clorgyline and more so by TCP (Figure 4. 22), indicating that MAO-A is involved in later phases of serum withdrawal-induced apoptosis (72 h onwards) and that cell death can progress to downstream processes such as DNA fragmentation independently of caspase-3. Clorgyline reduced caspase-9 activation throughout the serum withdrawal time course (Figure 4. 23), suggesting that MAO-A is likely to promote apoptotic signaling via caspase-9.

4.3.3.1.1 Mechanism

Levels of ROS are elevated in serum deprived SH-SY5Y cells and concomitant treatment with clorgyline reduced ROS to control levels (Figure 4. 24), signifying that ROS production by increased MAO-A activity may be involved in death signaling following

serum withdrawal. Likely candidates for targets of elevated ROS produced by MAO in the cell include the diverse MAPK cascades.

Following serum deprivation, levels of phosphorylated ERK MAPK are decreased (Figure 4. 25). Active ERK is responsible for targeting transcription factors that will facilitate up-regulation of proteins required for progression of the cell cycle (Figure 4. 3). Loss of growth factor binding causes decreased activation of Ras and therefore decreased phosphorylation of the MAPK signaling module that ultimately phosphorylates ERK. Reduced ERK activation causes growth arrest and increased phosphorylation of the stress-activated MAPK proteins JNK and p38 (Figure 4. 25). Levels of phosphorylated JNK increase in a time dependent manner reaching maximal levels at 48-96 h (Figure 4. 25). Activation of p38 was also time dependent, but on average maximal levels were reached earlier at around 24 h (Figure 4. 25). These data suggest that as protective ERK levels deplete, MAPK signaling is tipped in favor of the stress response mediated by JNK and p38. Clorgyline has no effect on levels of active ERK, JNK or p38 MAPK at 24 h, suggesting that MAO-generated oxidative stress is not involved in activating MAPK signaling pathways at this point in the time course.

On the contrary, MAPK signaling pathways are involved in up-regulating MAO-A expression following serum deprivation. Inhibition of JNK and p38 greatly reduced the elevated MAO activities induced by serum withdrawal, whereas ERK inhibition may have further increased MAO activity (Figure 4. 27). Similar effects were seen on elevated MAO-A mRNA expression during serum withdrawal. However, JNK inhibition was more effective than p38 at reducing MAO-A expression, with expression levels reduced below control level (Figure 4. 27). Inhibition of the JNK signaling pathway by Cep has previously been reported to preserve metabolism and growth of serum deprived rat neurons (Harris *et al.* 2002) and inhibitors of p38 MAPK have previously been reported to promote neuronal survival in serum deprived rat neurons *in vitro* (Horstmann *et al.* 1998). MAO-A has been shown to be the target of p38 signal transduction following serum deprivation in rat neurons (DeZutter and Davis 2001) and human neuroblastoma involving regulation by the transcription repressor R1 (Ou *et al.* 2006). The MAO-B gene has previously been shown to be a target of MAPK signaling pathways following treatment with phorbol ester (PMA) in human hepatocytoma cells (Wong *et al.* 2002). MAO-B expression was increased following PMA exposure and the activation of MAO-B involved a PKC, MAPK dependent pathway that acted through JNK specifically and the transcription factors c-jun and Egr-1 (Figure 4. 27). Data in this chapter shows for the first time, that MAO-A is a target of both

JNK and p38 pro-apoptotic signaling pathways in human neuroblastoma cells, which is ROS and caspase-9 dependent. Data indicate that ROS generated by MAO are more involved in mitochondrial events than in activating MAPK, since clorgyline caused no changes in MAPK phosphorylation levels at 24 h. However, H₂O₂ generated by MAO in the cytosol may further enhance stress-signaling pathways but this event may occur later in the time course, when MAO activity is maximal (72-96 h).

4.3.4 Conclusion

MAO-A activity is increased in two selected models of apoptosis. MAO-A activity is increased in parallel to caspase-3 activation following complex I inhibition by rotenone. Rotenone will be discussed further in chapter 5 and 6. In serum withdrawal-induced apoptosis, MAO-A acts downstream of caspase-3. The role of MAO-A in serum withdrawal-induced apoptosis is shown in Figure 4. 29. Unlike STS-induced apoptosis, serum withdrawal is slower and allows the cell time to recruit pro-apoptotic proteins to enhance the death signals. The MAO-A gene is a target of both JNK and p38 MAPK pathways. The ensuing changes in oxidative levels generated by increased production of ROS by MAO-A may promote mitochondrial dysfunction, cytochrome-c release and activation of caspases. Together these data suggest that MAO is recruited by the cell to enhance apoptosis and depending on the nature of the stressor or inducer, MAO responds accordingly. Mechanisms by which MAO can be modulated to respond to cellular stress and/or survival signals may involve transcription factors, transcription and translation regulation at one end of the spectrum (slow or chronic responses) and post-translational modifications, enzyme maturation and regulation of enzyme rate as a rapid response.

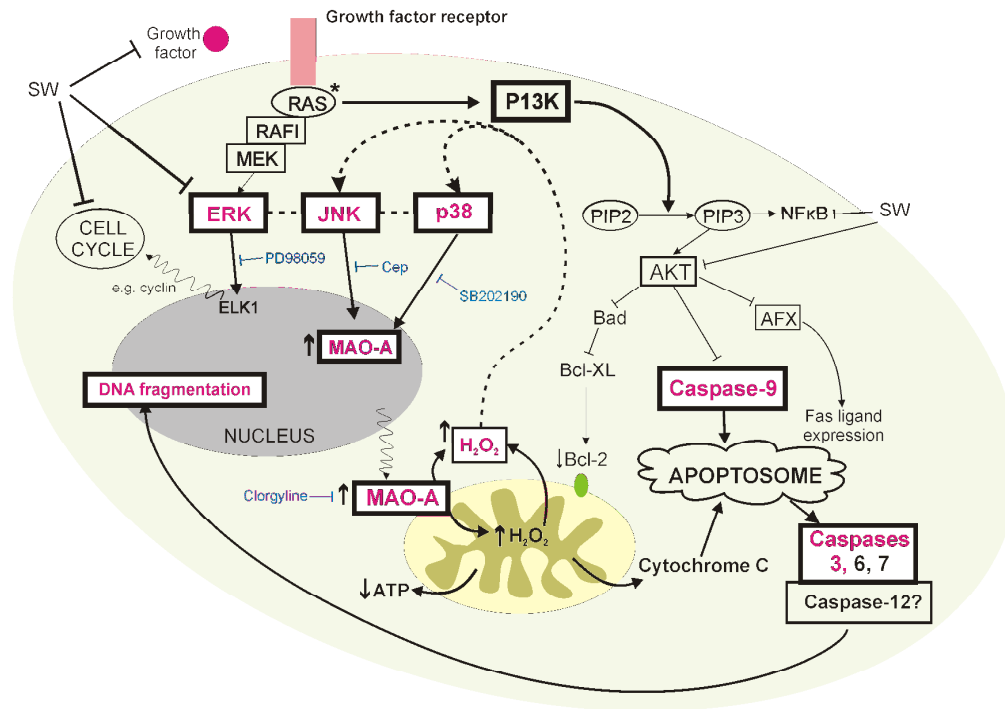


Figure 4. 29 The role of MAO in serum withdrawal-induced apoptosis

Constituents of the pathway elucidated in this study appear in *magenta*. Growth factor binding activates Ras and sends survival signals via the PI3K/Akt pathway and ERK MAPK pathway. Akt works by inhibiting Fas ligand expression, caspase-9 activation and Bad. ERK MAPK plays a major role in cell survival. ERK signals transcription factors such as ELK1 to up-regulate pro-survival and cell cycle genes. ERK is also known to inhibit apoptotic proteins such as caspase-9 by direct phosphorylation (Allan *et al.* 2003). Both PI3K/Akt and MAPK signalling pathways can tip in favour of death when survival factors are withdrawn or stress signals are elevated (Wang *et al.* 1998, Horbinski and Chu 2005). In the early phases, this may result in changes in Bcl-2 family proteins, cytochrome-c release and activation of caspase-9 followed by activation of caspases-3, 6, 7. At the same time JNK and p38 MAPK are activated following a cascade of phosphorylation triggered by Ras signalling events. JNK and p38 are known to target transcription factors such as c-jun and ATF-2 and promote up-regulation of pro-apoptotic genes (Yang *et al.* 2003), which following serum withdrawal includes up-regulation of MAO-A. Increased MAO-A expression results in increased H₂O₂ production at the OMM. MAO-generated ROS in the cytosol could re-activate stress-activated MAPK signalling cascades in a dose-dependent manner (Guyton *et al.* 1996, Yoon *et al.* 2002). MAO produced ROS can directly damage IMM proteins (Cohen *et al.* 1997), causing loss of function and release of cytochrome-c, ROS and ATP, resulting in activation of upstream caspases and eventually executioner caspases, cleavage of substrates, DNA fragmentation and cell dismantling. Hence, MAO-A enhances apoptosis following recruitment by JNK and p38.

CHAPTER 5

CONSEQUENCE OF MAO-A OVEREXPRESSION IN HUMAN NEUROBLASTOMA CELLS

OVEREXPRESSION OF MAO-A IN HUMAN NEUROBLASTOMA CELLS

5.1. INTRODUCTION

5.1.1 Increased MAO levels in humans - physiological relevance

Changes in MAO during the ageing process and in certain neurodegenerative disorders have been the focus of numerous publications. The majority of the work on humans has relied on *post mortem* brain samples or measurement of circulatory MAO-B in blood platelets, which has limited the collection of reliable data and resulted in some dispute over findings. Increased MAO-B activity has been linked to human ageing (Fowler *et al.* 1980b, Kornhuber *et al.* 1989, Sastre and Garcia-Sevilla 1993) and has been implicated in several neurodegenerative disorders, (reviewed by Strolin Benedetti and Dostert 1989). Indeed, increases in MAO-B expression have been observed in ageing mouse brain (Saura *et al.* 1994a) and human brain (Fowler *et al.* 1980b, Sparks *et al.* 1991). These increases in MAO-B expression are partly due to a general increase in enzymatic levels per cell, but may also be a result of increased glial cell numbers in ageing (Halliwell 1992, Ekblom *et al.* 1993). MAO-B activity (Adolfsson *et al.* 1980, Oreland and Gottfries 1986, Bonuccelli *et al.* 1988, Sparks *et al.* 1991, Saura *et al.* 1994b) and MAO-B mRNA levels are elevated in AD (Emilsson 2002). MAO-B activity has been reported to be elevated in PD (Gerlach and Riederer 1993, Bongioanni *et al.* 1996, Danielczyk 1998), although some studies have revealed no change in MAO expression from platelets and plasma of patients with PD compared with healthy controls (Finch *et al.* 1995, Ahlskog *et al.* 1996). Increased MAO-B expression has also been associated with Huntington's disease (Mann *et al.* 1980) and Pick's disease (Sparks *et al.* 1991).

Increased levels of MAO-A isoform expression have only been reported in the temporal pole and nucleus basalis of Meynert (nbM) in ageing humans (Sparks *et al.* 1991), in the hypothalamus and frontal pole of those suffering from AD (Sparks *et al.* 1991) and in the hypothalamus of those suffering from PD (Sparks *et al.* 1991).

Age-related increases in MAO levels result in increased oxidative stress that may act as a predisposing factor in the vulnerability of the brain to age-related neurodegenerative diseases such as PD (Westlund 1988, Cohen 1990, Kumar *et al.* 2003). Vulnerability of neurons to attack by free radicals is heightened by their low glutathione content, which in

the SNpc in PD is further reduced (Riederer *et al.* 1989). MAO-catalysed increased free radical production may contribute to age-related increase in the incidence of mitochondrial damage in the brain. Indeed MAO-generated oxidative stress has been linked with mitochondrial DNA mutation (Soong *et al.* 1992, Hauptmann *et al.* 1996), loss of mitochondrial respiratory capacity (Kumar *et al.* 2003) and disrupted mitochondrial electron flow (Cohen *et al.* 1997).

5.1.2 Changes in MAO expression in *in vitro* cell culture systems

MAO-B mRNA expression is increased following treatment of human hepatocytoma cells with phorbol 12-myristate 12-acetate (PMA), which was shown to be signalled via PKC, MAPK and regulated by the transcription factors *c-Jun* and *Egr-1* (Wong *et al.* 2002). The following year the same working group showed that MAO-B expression was up-regulated during Caco-2 cell differentiation and the transcription factors Sp1 and Sp3 have been implicated (Wong *et al.* 2003).

Increased MAO-A mRNA expression has also been observed in apoptosis induced by dexamethasone in human skeletal muscle cells (Manoli *et al.* 2005). MAO-A mRNA expression, protein levels and catalytic activity were increased during apoptosis induced by serum deprivation in rat pheochromocytoma cells (DeZutter and Davis 2001), which was shown to be regulated by the p38 MAPK pathway (DeZutter and Davis 2001). As noted in chapter 3, Ou and co-workers (2006) have recently shown that MAO-A mRNA expression and catalytic activity is increased in apoptotic human neuroblastoma cells deprived of serum and that the mechanism involved the p38 MAPK signalling pathway and the novel transcriptional repressor R1 (RAM2/CDCA7L/JPO2).

5.1.3 Increased MAO expression following genetic manipulation

Genetic manipulation of MAO expression *in vivo* has been limited to the creation of MAO knock out mice (Shih *et al.* 1999). Genetic elevation of MAO-B *in vitro* has been investigated previously by Kumar *et al.* (2003), who created an inducible rat pheochromocytoma (PC12) cell line where increased expression of MAO-B was similar to that observed during normal ageing. Kumar and colleagues showed that increased H₂O₂ production via subtle elevations of MAO-B levels causes inhibition of the metabolic enzyme α -ketoglutarate dehydrogenase, decreased flux through mitochondrial complex I, loss of spare respiratory capacity and inability of dopaminergic cells to cope with stress (Kumar *et al.* 2003).

Yi and colleagues recombinantly overexpressed MAO-B in SH-SY5Y cells, which markedly increased levels of MAO-B protein and activity. Increased MAO-B did not affect the sensitivity of the cells to apoptosis induced by N-methyl-(R)salsolinol, suggesting that the MAO-B isoform was not involved in N-methyl-(R)salsolinol-induced apoptosis (Yi *et al.* 2006a).

Methylation of the MAO-B promoter causes down-regulation/silencing of MAO-B gene expression (Wong *et al.* 2003). On the other hand, MAO-B mRNA expression and protein levels as well as catalytic activity were shown to be increased when SH-SY5Y, Si2 and HepG2 cells were co-transfected with a transforming growth factor- β -inducible early gene (TIEG)2 expression vector. The latter study concluded that the MAO-B core promoter region contained a response element to TIEG2 (Ou *et al.* 2004). This group have more recently investigated the MAO-A isoform, knocking down levels of the novel transcriptional repressor R1 in human medullablastoma cells indirectly resulting in an increase in MAO-A activity and reduced cell proliferation (Ou *et al.* 2006).

5.1.4 Rationale

To date, no attempt has been made to directly overexpress MAO-A either in animals or in *in vitro* cell models and MAO-B has been the focus of the majority of *in vivo* studies. Therefore this chapter further explores the role of MAO in apoptotic cell death by overexpressing the MAO-A gene in SH-SY5Y cells. This would allow an assessment of whether increased MAO-A levels can lead to increased oxidative stress and apoptosis and render the cells more sensitive to toxic insult. Since our knowledge of MAO-A in neurodegeneration is limited, this section of work is of high importance.

5.1.5 Aims of Chapter

- **To stably overexpress MAO-A in SH-SY5Y cells**

Human MAO-A was stably overexpressed in SH-SY5Y cells by cloning human MAO-A cDNA into the expression vector (pcDNA3.1(-), Invitrogen, Karlsruhe, Germany). The expressed plasmid DNA was transfected into SH-SY5Y cells by electroporation. Stable SH-SY5Y clones were then selected by their resistance to blasticidin.

- **To characterise the MAO-A status of stably transfected SH-SY5Y cell clones**

Characterisation of the MAO status of the cells included determination of MAO-A mRNA expression levels, catalytic activity, protein levels and protein distribution. Comparisons

were made between MAO-A overexpressing cells, mock transfected control cells (pcDNA3.1(-) without MAO-A insert) and wild type cells.

- **To assess viability and general characteristics of the stably transfected cells**

The effects of overexpression of MAO-A on cell morphology, growth rate, cell proliferation, ROS production, caspase-3 activity and ATP levels were assessed by comparing MAO-A overexpressing cells with mock transfected and wild type cells.

- **To assess the sensitivity of MAO-A over expressing cells to apoptotic inducers**

Finally, the effects of MAO-A overexpression on the response to three different apoptotic inducers (staurosporine, serum withdrawal and rotenone) was monitored. Markers included caspase-3, MAPK activation, ROS production, cell proliferation and ATP levels.

5.2. RESULTS

5.2.1 Characterisation of SH-SY5Y cells overexpressing MAO-A

5.2.1.1 Initial characterisation of MAO-A expression in stable overexpressing clones

Transient transfections were initially undertaken to determine the appropriate time course of transfection and amount of DNA required (see appendix), which was found to be 1 µg DNA for 48 h. SH-SY5Y cells were stably transfected with the pcDNA3.1(-) vector lacking the MAO-A sequence, referred to as mock and those transfected with pcDNA3.1(-) containing the MAO-A cDNA sequence, referred to as MAO-A+. Stable clones were selected by their resistance to the antibiotic geneticin. A titration of G418 was performed to determine the lowest concentration required to kill wild type cells (see appendix), which was found to be 700 µg/ml. RNA was extracted for characterisation of MAO-A mRNA expression levels. Approximately 24 MAO-A+ clones were picked from 96-well culture plates and expanded but only 4 clones grew sufficiently to passage and for MAO-A mRNA analysis. Figure 5. 1A shows that those MAO-A+ clones assayed exhibited increased MAO-A mRNA expression compared to wild type and mock transfected SH-SY5Y cells. Mock transfection resulted in approximately a two fold increase in MAO-A mRNA expression compared to wild type cell clones. Increased expression of MAO-A mRNA in MAO-A+ SH-SY5Y clones ranges from ~63-10,000 fold increase, compared to wild type expression. SH-SY5Y cell clones were then expanded further and extracts taken for evaluation of MAO-A catalytic activity. Clone 2H7 growth was strongly impaired (see

Figure 5. 2) and was omitted from MAO activity assays. MAO activity in MAO-A+ cell clones differed from changes seen in mRNA expression (Figure 5. 1). Mock transfected cell clones had similar MAO activities compared to wild type SH-SY5Y cells, whilst MAO-A+ clones had increased MAO catalytic activities ranging between ~4-11 fold of wild type (Figure 5. 1). MAO-A+ clone 1A9 which showed the highest expression of MAO-A mRNA did not show the highest increase in catalytic activity. Conversely, MAO-A+ clone 3I8, which had the lowest mRNA expression among all the over expressing MAO-A clones, showed the highest increase in catalytic activity (~11.4 fold of wild type).

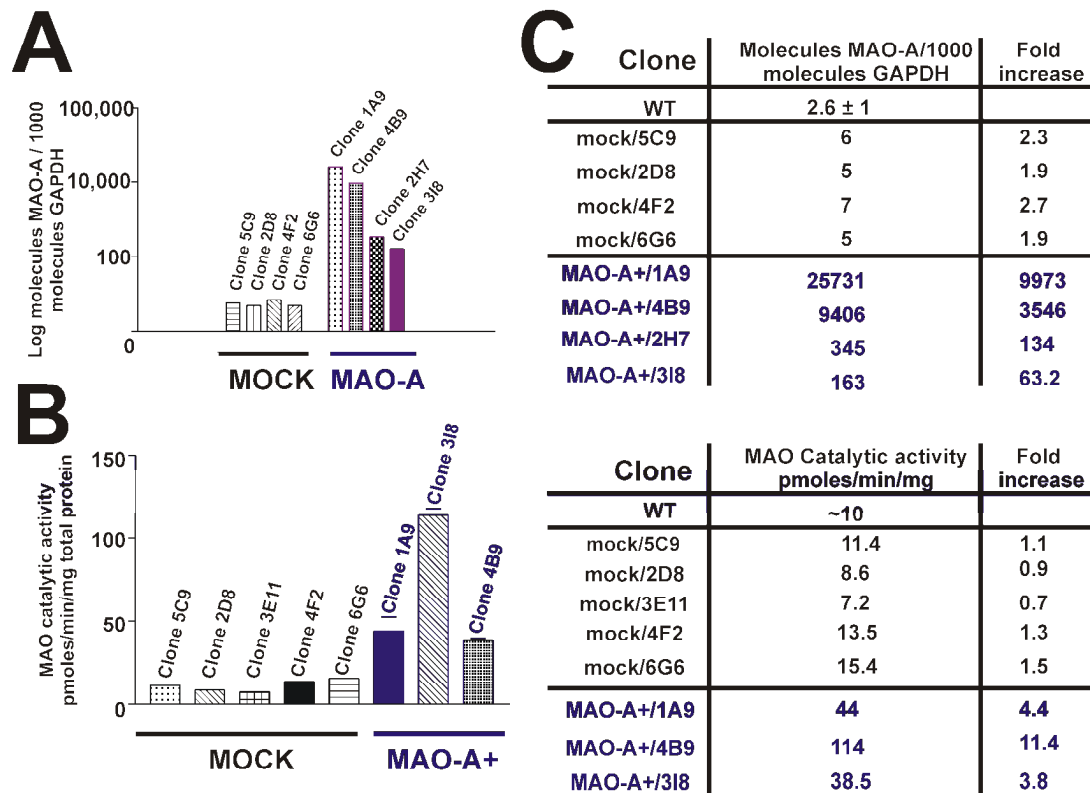


Figure 5. 1 MAO-A mRNA levels and catalytic activities are increased in MAO-A+ SH-SY5Y clones

(A) MAO-A mRNA expression was measured by qRT-PCR in stable SH-SY5Y cell clones (within 1 month following clonal expansion). Data represent duplicate values from one set of cell extracts. (B) MAO catalytic activities were measured in stable SH-SY5Y cell clones *in vitro* via a radiometric method using 14 C-Tyramine as a substrate and are expressed as pmoles/min/mg total protein \pm S.D. (C) MAO-A mRNA (*top panel*) and catalytic activity (*bottom panel*) data shown in figure 5.2A and 5.2B respectively, in a table format showing fold increase in mock and MAO-A+ stably transfected SH-SY5Y cell clones compared to wild type expression.

5.2.1.2 Morphology of stable clones

Mock transfected clones had wild type cell morphologies but some MAO-A+ clones (2H7 and 3I8, taken 3 weeks following clonal expansion) appeared to have difficulty growing (Figure 5. 2). MAO-A+/2H7 and MAO-A+/3I8 cells showed typical apoptotic

Figure 5. 2) and was omitted from MAO activity assays. MAO activity in MAO-A+ cell clones differed from changes seen in mRNA expression (Figure 5. 1). Mock transfected cell clones had similar MAO activities compared to wild type SH-SY5Y cells, whilst MAO-A+ clones had increased MAO catalytic activities ranging between ~4-11 fold of wild type (Figure 5. 1). MAO-A+ clone 1A9 which showed the highest expression of MAO-A mRNA did not show the highest increase in catalytic activity. Conversely, MAO-A+ clone 3I8, which had the lowest mRNA expression among all the over expressing MAO-A clones, showed the highest increase in catalytic activity (~11.4 fold of wild type).

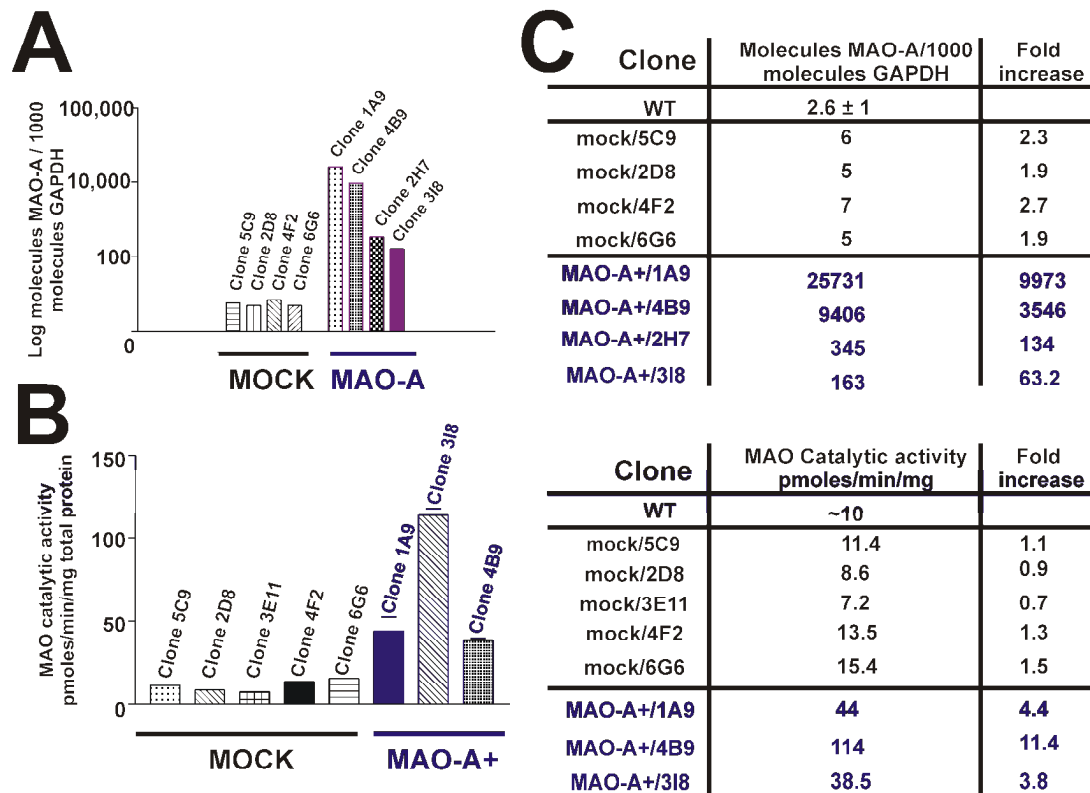


Figure 5. 1 MAO-A mRNA levels and catalytic activities are increased in MAO-A+ SH-SY5Y clones

(A) MAO-A mRNA expression was measured by qRT-PCR in stable SH-SY5Y cell clones (within 1 month following clonal expansion). Data represent duplicate values from one set of cell extracts. (B) MAO catalytic activities were measured in stable SH-SY5Y cell clones *in vitro* via a radiometric method using 14 C-Tyramine as a substrate and are expressed as pmoles/min/mg total protein \pm S.D. (C) MAO-A mRNA (*top panel*) and catalytic activity (*bottom panel*) data shown in figure 5.2A and 5.2B respectively, in a table format showing fold increase in mock and MAO-A+ stably transfected SH-SY5Y cell clones compared to wild type expression.

5.2.1.2 Morphology of stable clones

Mock transfected clones had wild type cell morphologies but some MAO-A+ clones (2H7 and 3I8, taken 3 weeks following clonal expansion) appeared to have difficulty growing (Figure 5. 2). MAO-A+/2H7 and MAO-A+/3I8 cells showed typical apoptotic

morphologies, few cell connections and were smaller than wild type clones, whereas MAO-A+ clones 1A9 and 4B9 grew more easily and had morphologies similar to wild type cells. Therefore, MAO-A+ clone 1A9 was chosen to work with since it exhibited sufficient growth rate and had a 4.4 fold increase in MAO-A catalytic activity. Mock transfected clone 2D8 was randomly chosen as a control.

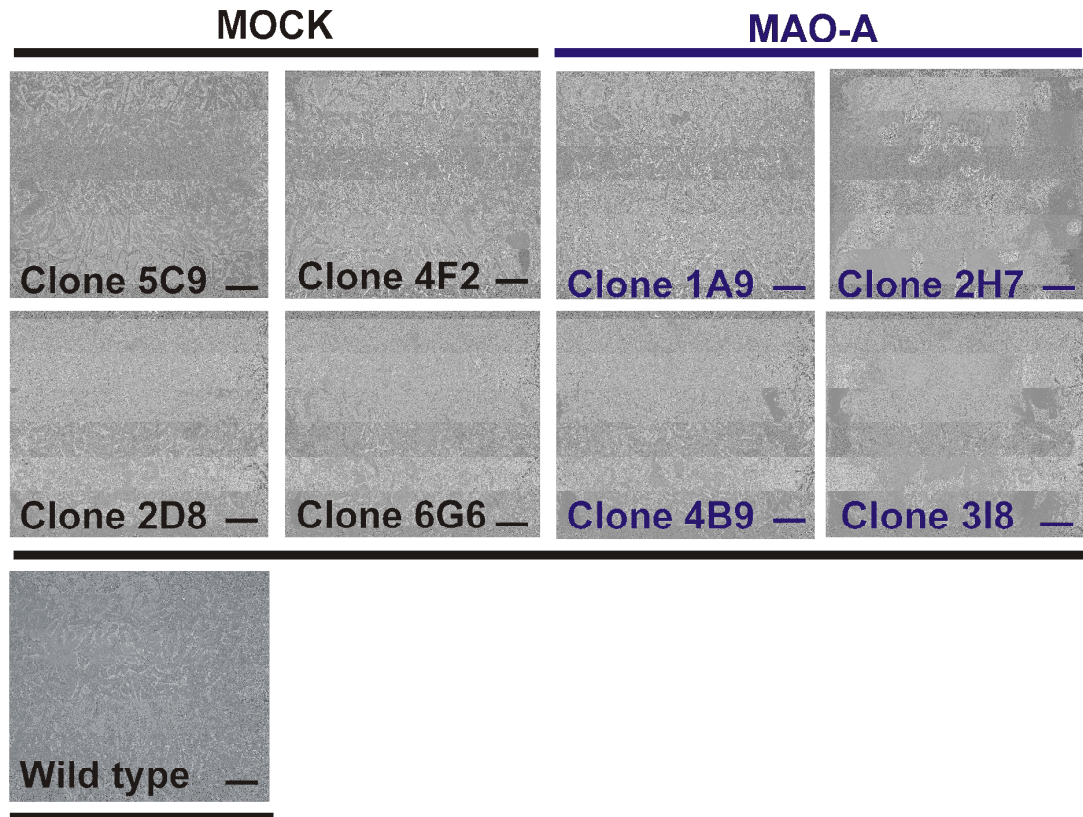


Figure 5. 2 Cell morphologies of mock transfected and MAO-A+ SH-SY5Y stable clones

Mock transfected and MAO-A+ stable SH-SY5Y clones observed by phase contrast microscopy (~3 weeks in culture following clonal expansion). Cells were visualised using a Nikon eclipse TS100 microscope. Photomicrographs ($\times 10$ objectives, taken on Nikon DN100 digital camera). Scale bar represents 20 μM .

5.2.2 Characterisation of newly cloned MAO-A+ (1A9, working clone)

5.2.2.1 MAO-A protein-levels and localisation

MAO-A protein in MAO-A+/1A9 cells compared to mock/2D8 cells, revealed by DAB staining (Figure 5. 3A) and confocal microscopy (Figure 5. 3B). Both methods reveal that MAO-A+/1A9 cells have significantly higher amounts of MAO-A protein compared to mock/2D8 cells.

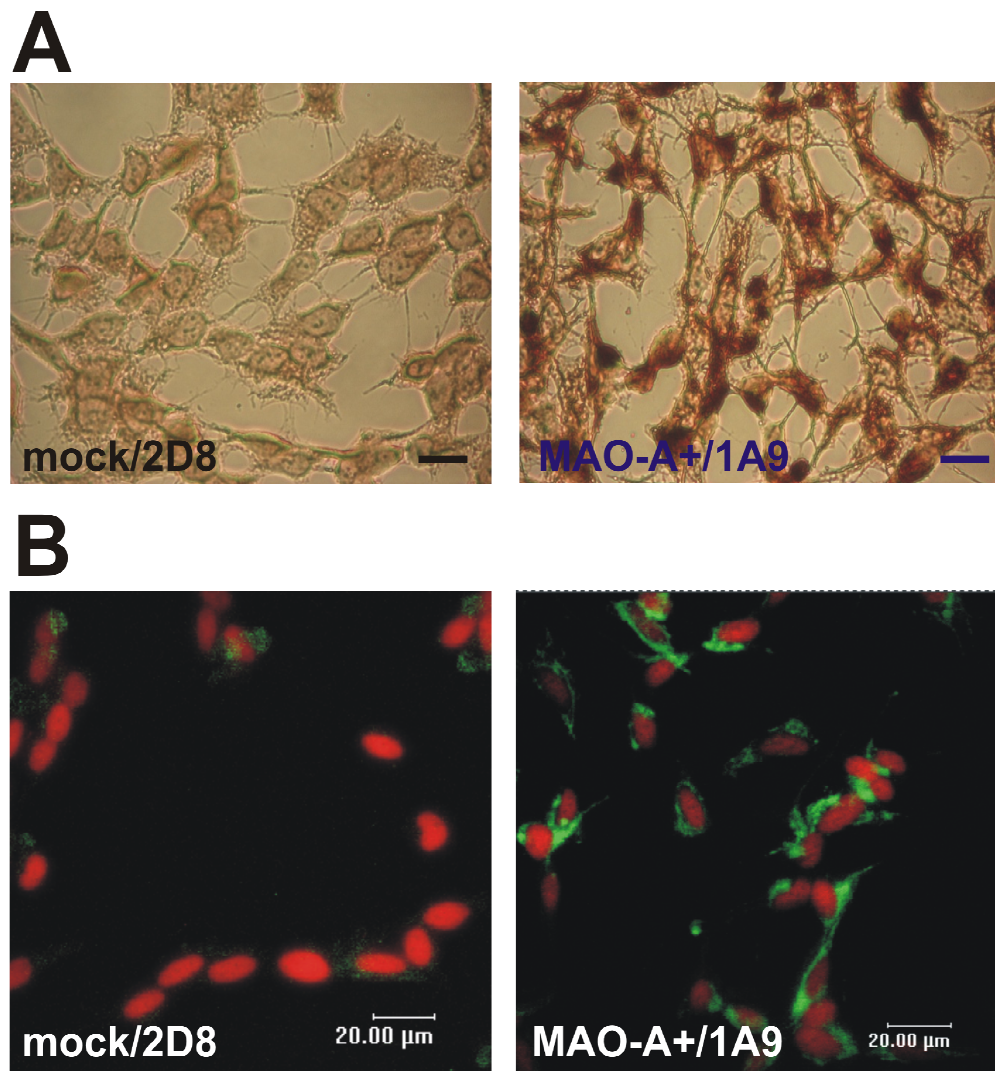


Figure 5.3 MAO-A protein levels in mock transfected and MAO-A+ SH-SY5Y cells

(A) Immunohistochemistry – Mock/2D8 and MAO-A/1A9 cells (~9 months in continuous cell culture) were stained with MAO-A (6G11-E1) specific antibody and revealed using HRP-conjugated secondary antibody with 3, 3'-Diaminobenzidine (DAB) as substrate. Control sections incubated in the absence of MAO-specific antibodies but revealed under the same conditions did not reveal staining and are not shown. MAO specific immunoreactivity is represented by dark brown/red staining. The images shown are from a representative experiment. Scale bar represents 20 µm. (B) Confocal microscopy – Mock/2D8 and MAO-A+ cells (~9 months in continuous cell culture) were exposed to MAO-A (6G11-E1) specific antibody and revealed using FITC-conjugated secondary antibody, which fluoresces green, visualised by a CLSM Leica microscope. Propidium iodide counterstained nuclei fluoresce red. Photomicrographs are representative of >6 independent experiments.

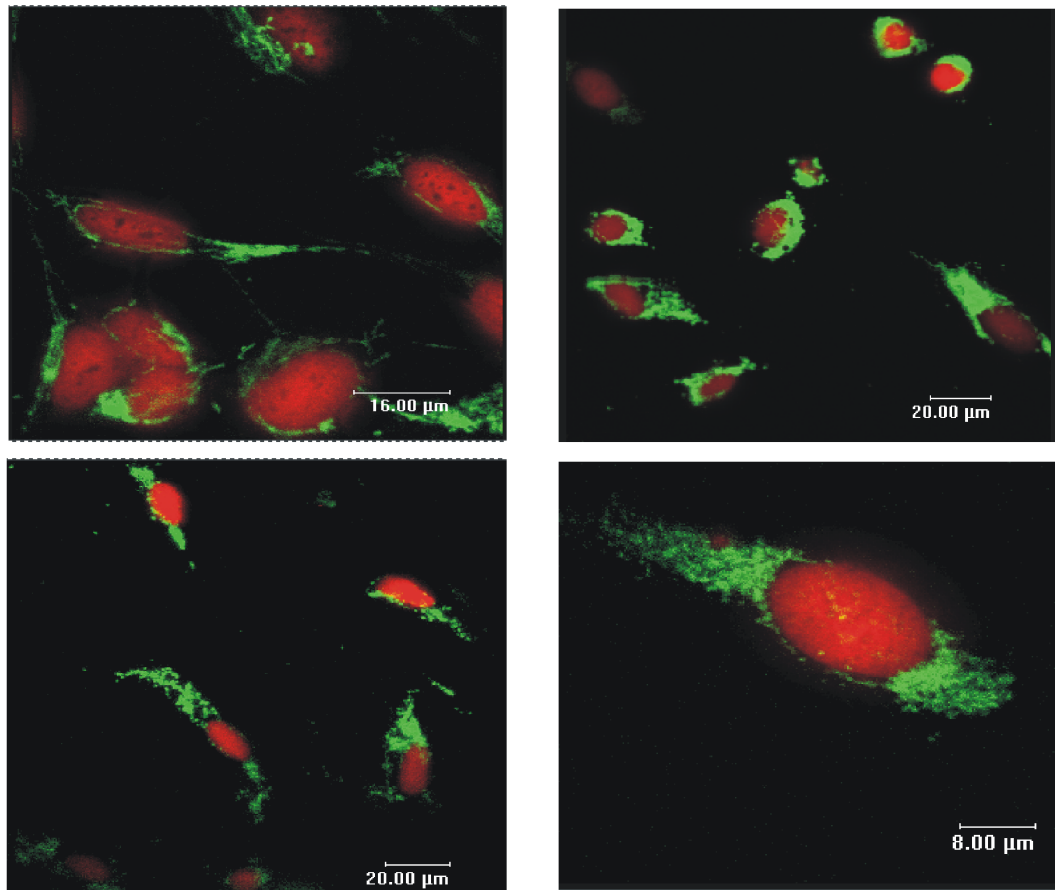


Figure 5. 4 MAO-A protein in MAO-A+/1A9 stable clones

MAO-A+/1A9 cells (~ 8 months in continuous culture) were exposed to MAO-A (6G11-E1) specific antibody and revealed using FITC-conjugated secondary antibody (green fluorescence), visualised using a CLSM Leica microscope. Nuclei were counterstained with propidium iodide (red fluorescence). Photomicrographs are representative of >6 independent experiments. Scale is stated on photomicrograph (taken at $\times 63$ objectives, with zoom function).

Figure 5. 5 shows co-localisation of MAO-A protein in MAO-A+/1A9 cells with the inner mitochondrial membrane enzyme cytochrome c oxidase, further signifying that overexpressed MAO-A in SH-SY5Y cells continues to localise to the mitochondria.

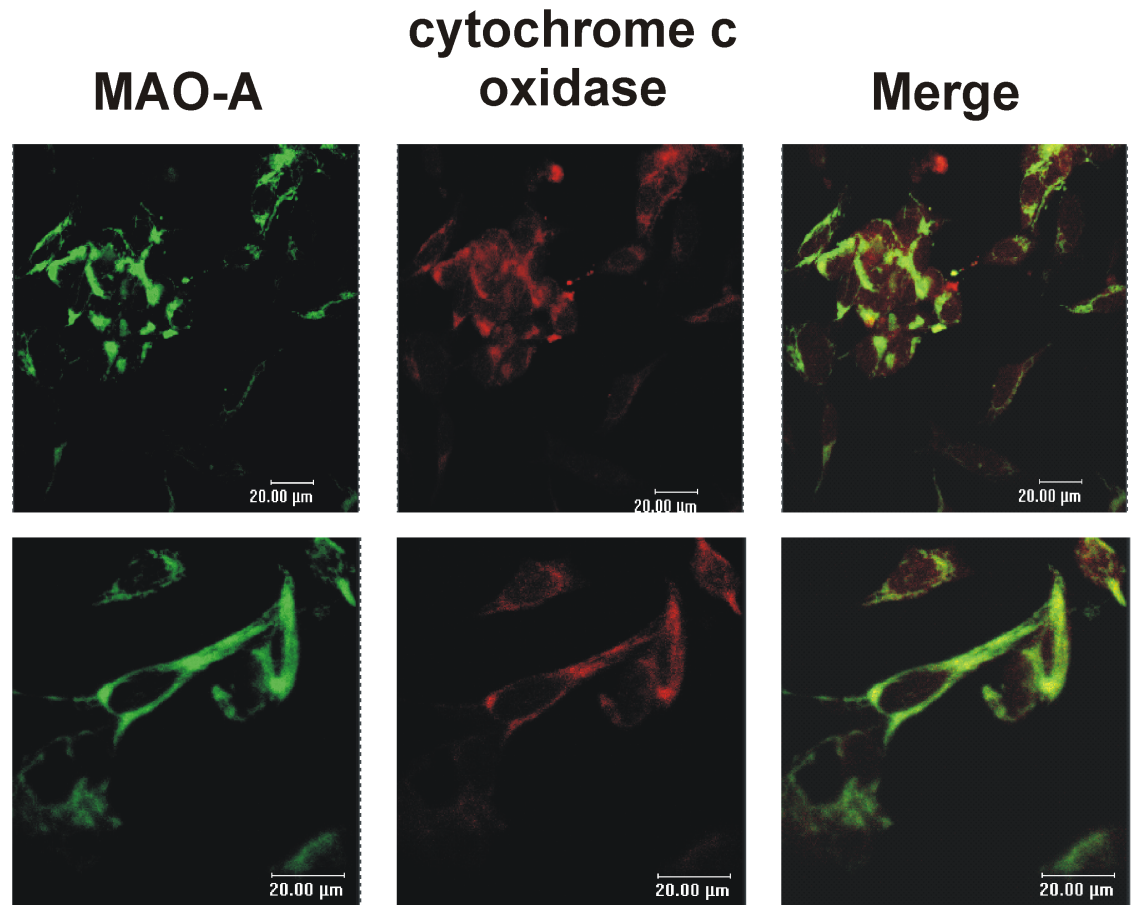


Figure 5.5 MAO-A in MAO-A+/1A9 cells is localised to mitochondria

MAO-A+/1A9 cells (~ 9 months in continuous culture) were exposed to MAO-A (6G11-E1) specific antibody and cytochrome c oxidase specific antibody at the same time and MAO-A revealed using a FITC-conjugated secondary antibody (green fluorescence) and cytochrome c oxidase revealed using a TRITC-conjugated secondary antibody (red fluorescence). In the same experiment co-localisation of MAO-A and Cytochrome c oxidase is shown by the yellow colour from merging the two images together. The *Top panels* show $\times 63$ magnification and the *bottom panels* show $\times 63$ magnification with zoom.

5.2.3 Characterisation of sub-cultured MAO-A+ stable SH-SY5Y cells (1A9 working clone)

5.2.3.1 Cell viability and growth

Following ~9 months in culture, growth rates of mock/2D8 and MAO-A+/1A9 clones were determined by viable cell count. Mock transfected cells and wild type cells have doubling times of 20 and 21 hours respectively (Figure 5. 6B). MAO-A+/1A9 clone has difficulty growing and have a doubling time of 54 hours (~2.7 times longer than mock transfected or wild type cells).

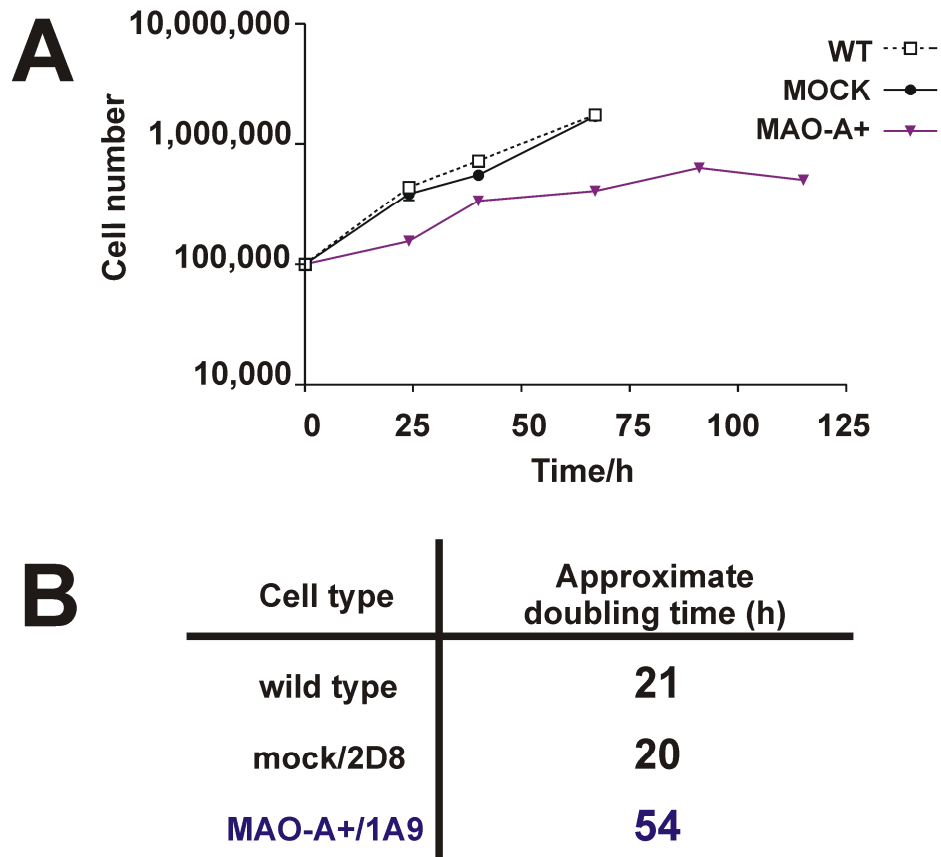


Figure 5. 6 Growth and doubling times of wild type, mock/2D8 and MAO-A+/1A9 cells

(A) Growth of wild type, mock/2D8 and MAO-A+/1A9 cells in culture, 9 months following initial expansion. Cell numbers were determined by viable cell counts from two independent cell populations and from four counts from the each sample. Data are expressed as mean cell number \pm SD. Data plotted on a log scale Y axis. (B) Doubling times were calculated and expressed as mean doubling time (h).

Figure 5. 7 illustrates the differences in cell proliferation/ metabolism between the three cell types. In wild type cells, MTT reduction increases over a 96 hour period. MTT reduction in Mock/2D8 is lower at 48 h, resulting in significantly lower MTT reduction over the time course. MTT reduction in MAO-A+/1A9 clones is significantly reduced compared to mock transfected controls (Figure 5. 7). Cell viability (MTT reduction) in MAO-A+/1A9 cells changes very little over 96 h, suggesting that cell viability is reduced in these cells already and/or these cells do not proliferate sufficiently to detect MTT reduction.

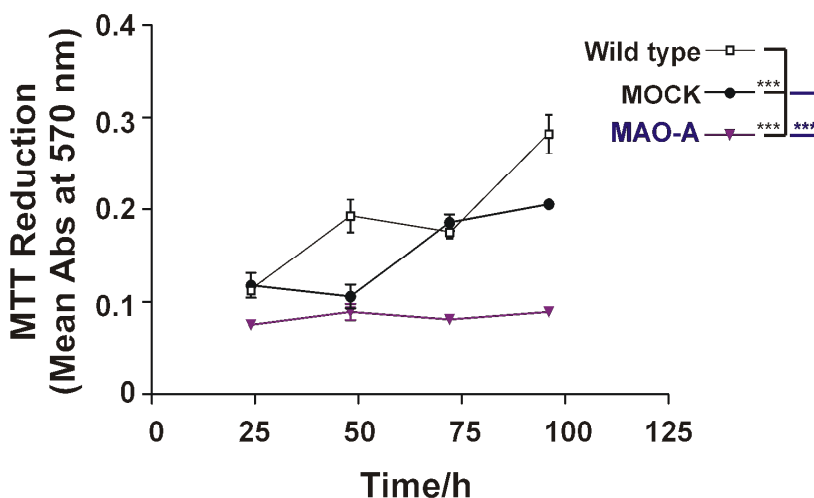


Figure 5.7 MTT reduction in wild type, mock/2D8 and MAO-A+/1A9 cells

MTT reduction was measured in wild type, mock/2D8 and MAO-A+/1A9 cells (8-9 months in continuous culture) over 96 hours and expressed as mean absorbance values at 570 nm \pm S. D. Replicates in assay=12 and $n=5$. MAO-A+ and mock/2D8 cell MTT reduction was statistically compared to wild type MTT reduction over time using two way ANNOVA test where *** $p<0.001$. Mock/2D8 MTT reduction over time was compared to MAO-A+/1A9 MTT reduction overtime using two way ANNOVA test, where *** $p<0.001$.

ATP levels in the stable cell lines were measured using a luciferase based assay (Figure 5. 8). ATP in mock/2D8 cells was significantly reduced (by approximately 50%, Figure 5. 8) compared to wild type levels. ATP in MAO-A+/1A9 clones was reduced further and compared to mock/2D8 levels, there was a significant reduction of approximately 66% (Figure 5. 8).

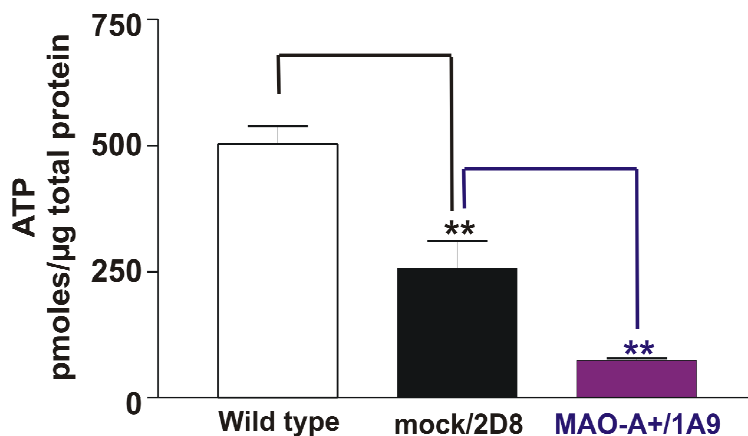


Figure 5.8 ATP levels in wild type, mock/2D8 and MAO-A+/1A9 cells

ATP levels were measured in untreated wild type, mock/2D8 and MAO-A+/1A9 cells (~ 10 months in continuous culture). ATP levels were determined using a luciferase based assay, amount of ATP was determined using ATP standards and expressed as mean pmoles/μg total protein \pm S. D. Replicates in assay=2 and $n=9$. MAO-A+/1A9 cell ATP levels were statistically compared to mock/2D8 cell ATP levels using the Student's t-test where ** $p<0.005$. Mock/2D8 cell ATP levels were statistically compared to wild type cell ATP levels using the Student's t-test where ** $p<0.005$.

5.2.3.2 Changes in morphology during long term culture

MAO-A+/1A9 cells that have been continuously sub-cultured have abnormal morphologies and make very few cell connections. These cells do not grow in close proximity and few show extended neuronal morphologies or axonal outgrowths (Figure 5. 9). They also show some curious morphological characteristics after long periods in culture (Figure 5. 9A and B). Cells of the mock/2D8 clone however continue to exhibit morphologies similar to wild type as shown in Figure 5. 9.

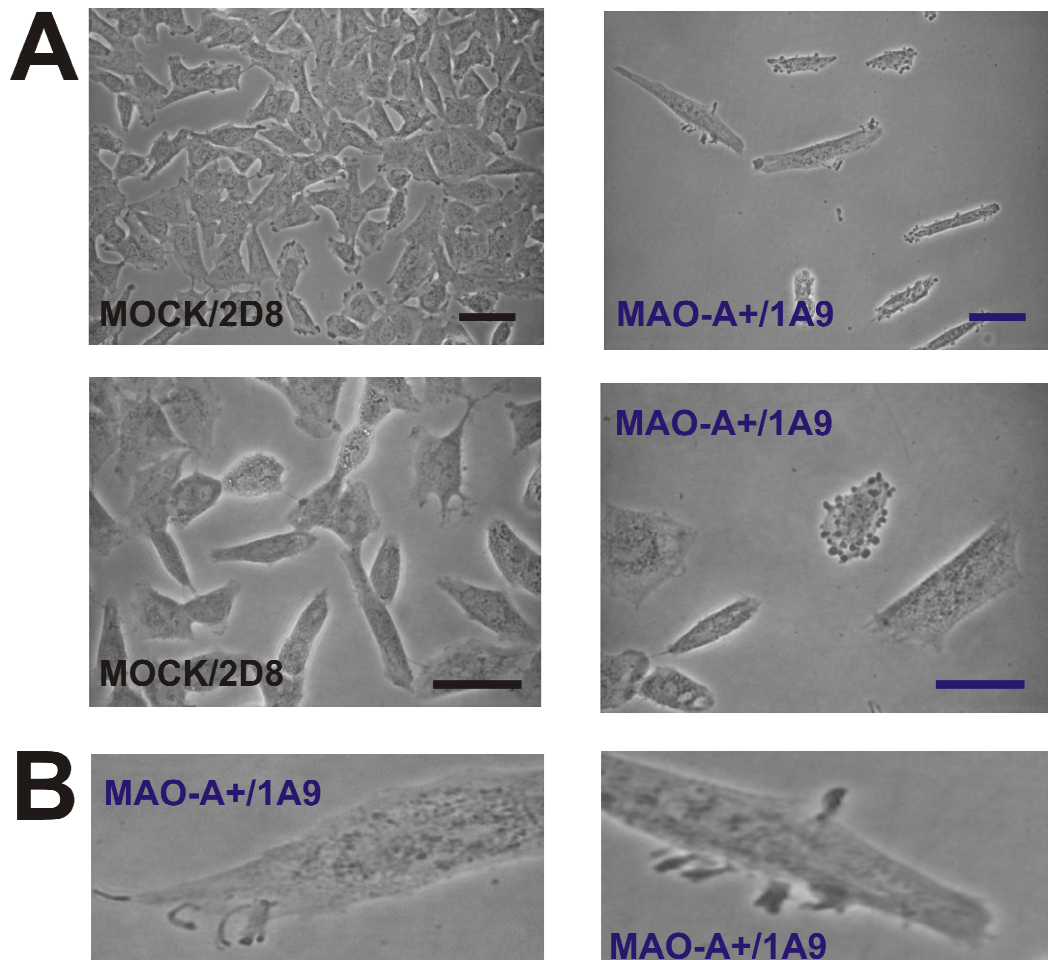


Figure 5. 9 Changing cell morphologies of MAO-A+/1A9 SH-SY5Y cells after long term culture.

(A) *Left column* shows Mock/2D8 SH-SY5Y cells and *Right column* shows MAO-A+/1A9 SH-SY5Y cells that have been in continuous subculture for ~ 10 months. Cells were visualised using a Nikon eclipse TS100 microscope. Photomicrographs ($\times 10$ and $\times 40$ objectives, taken on Nikon DN100 digital camera). Scale bar represents 20 μ M. (B) Enlarged photomicrographs of MAO-A+/1A9 cells, taken at $\times 40$ objectives, taken on Nikon DN100 digital camera, showing cell surface whiskers.

Figure 5. 10 shows morphologies of MAO-A+/1A9 cells that have been in continuous culture for 10 months (Figure 5. 10 *panels E and F*), or recovered from liquid nitrogen

stores and cultured for two weeks, termed 'new batch' (Figure 5. 10 *panels A and B*) and 'new batch' cells that have been cultured for two weeks in the presence clorgyline (Figure 5. 10 *panels C and D*). Cells cultured for >10 months appear sparse, apoptotic, do not have a flat neuronal phenotype, or make cell connections, and show extensive blebbing (Figure 5. 10 *panels E and F*). New batch MAO-A+/1A9 cultured for a total of 6 weeks (4 weeks prior to cryopreservation and 2 weeks following resuscitation) show a typical flat and elongated neuronal phenotype and lack blebbing seen in long term culture. They make cell-cell connections, divide and are less apoptotic (Figure 5. 10 *panels A and B*) The 'new batch' of MAO-A+/1A9 cultured in the presence of clorgyline had similar morphologies to the 'new batch cells' grown in growth medium except the population is denser (Figure 5. 10 *panels C and D*).

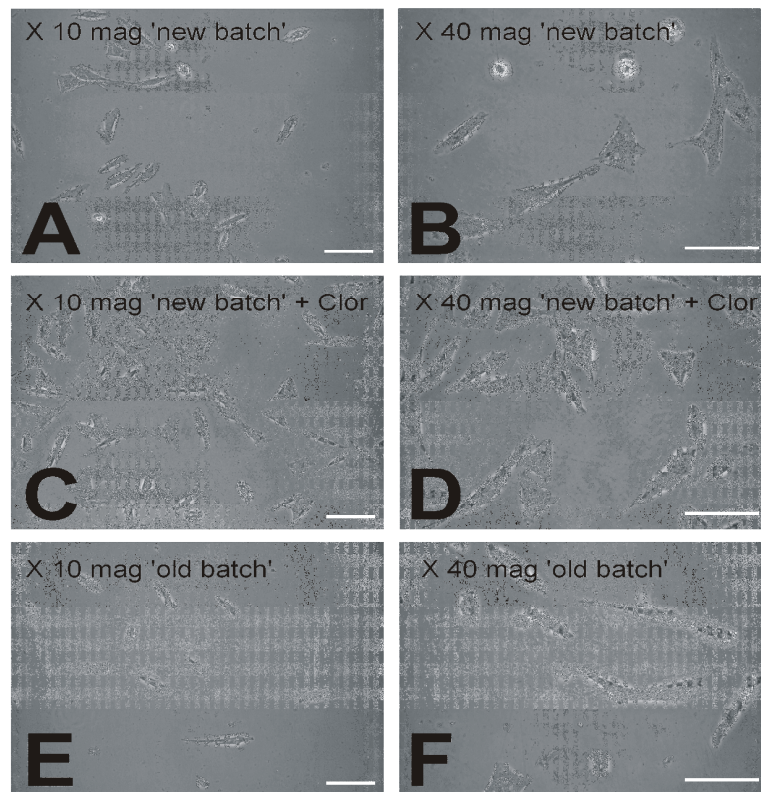


Figure 5. 10 Changes in morphology during long term culture following cloning of MAO-A+/1A9 cells MAO-A+/1A9 were picked and expanded (**I**) for cryopreservation and then resuscitated and expanded in a T25 cm² flask without clorgyline (*panels A and B*), or with clorgyline (*panels C and D*); **or** (**II**) continuously sub-cultured for 11 months (*panels E and F*), prior to taking photographs on a Nikon DN100 digital camera. Panels A, C and D are taken at × 10 and panels B, D and F at × 40 magnification.

Antibodies directed against cytoskeleton proteins, (α -tubulin and β -actin) were used to further investigate the structure of MAO-A+/1A9 clone cytoskeleton in new batch MAO-A+/1A9 cells (shown in Figure 5. 11) cultured for ~3 months. The distribution of α -tubulin

and β -actin is similar in wild type, mock/2D8 and MAO-A+/1A9 cells and there is no evidence of stress fibres that can be detected by β -actin staining. Some MAO-A+/1A9 cells appear apoptotic in their general shape and the cytoplasm appears shrunken and condensed compared to wild type and mock transfected controls, which is characteristic of apoptosis (Hengartner 2000).

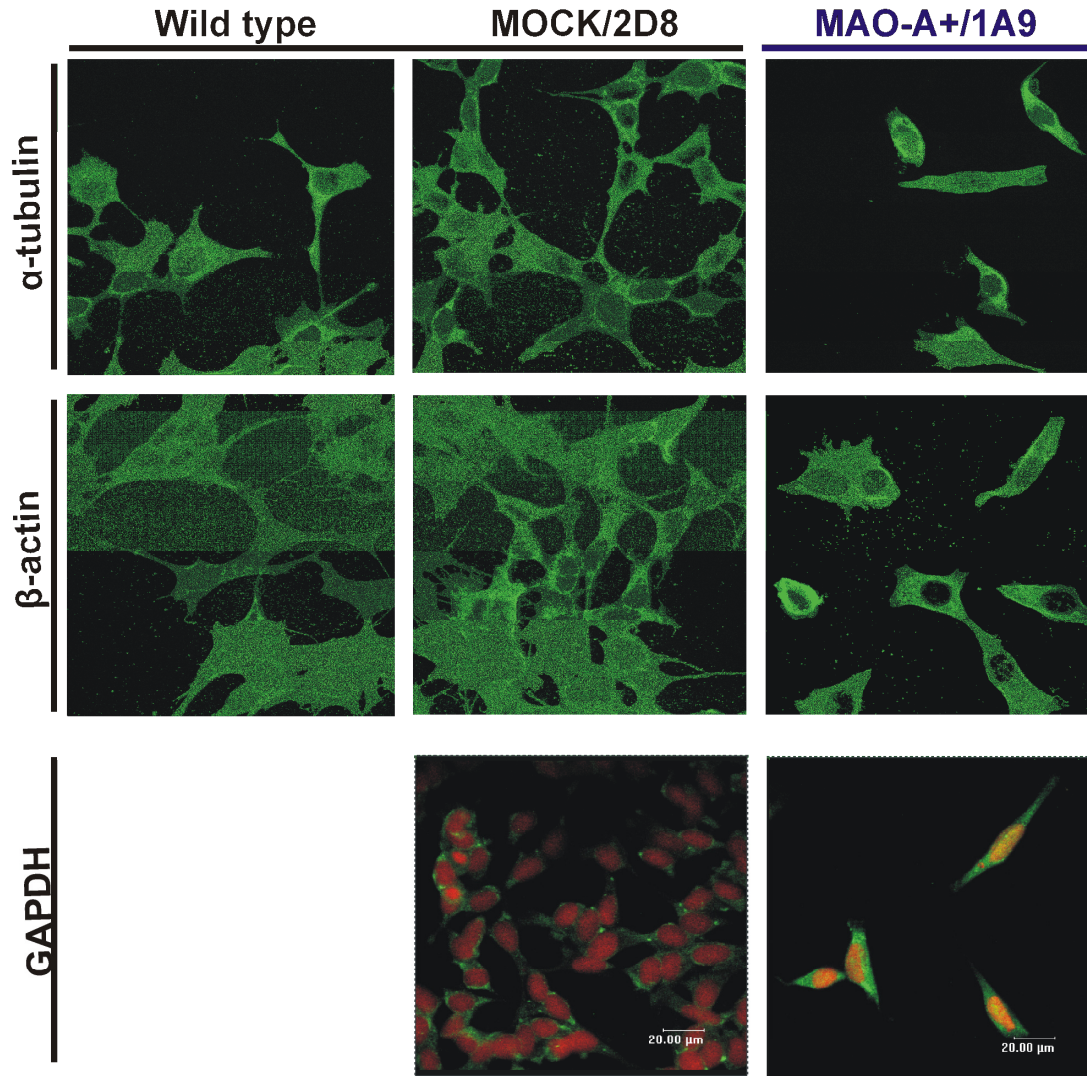


Figure 5. 11 Cytoskeletal proteins and GAPDH in wild type, mock/2D8 and MAO-A+/1A9 cells

Mock/2D8 and MAO-A+/1A9 cells that have been in continuous culture for ~3 months were exposed to α -tubulin, β -actin and GAPDH specific antibodies and revealed using a FITC-conjugated secondary antibody (which fluoresces green). Nuclei were counter-stained with propidium iodide (red). Images were taken at $\times 63$ magnification and scale bars are shown on each photomicrograph. Laser power was matched between different cell types for each protein of interest.

Data in Figure 5. 11 confirm that blebs on the surface of MAO-A+/1A9 cells contain cytoskeletal proteins, indicating that blebs are a protrusion of the cytoplasm and are not inclusions. Figure 5. 11 also shows staining for GAPDH in mock/2D8 and MAO-A+/1A9

cells. Some GAPDH in MAO-A+/1A9 cells is present in the nucleus, suggesting a certain amount of translocation from the cytosol, a hallmark of apoptosis (Berry and Boulton 2000).

5.2.3.3 Changing characteristics of MAO-A+/1A9 cells during long term culture

To assess basal levels of caspase-3 activity in MAO-A+/1A9 cells, caspase-3 activity of untreated cells was monitored over a culture period of 9 months (Figure 5. 12). At early time points, basal caspase-3 activity was higher than mock/2D8 and wild type cells (Figure 5. 12). Caspase-3 activity then dramatically decreased to below wild type levels in both mock/2D8 and MAO-A+/1A9 cells after continuous culture for 9 months (Figure 5. 12).

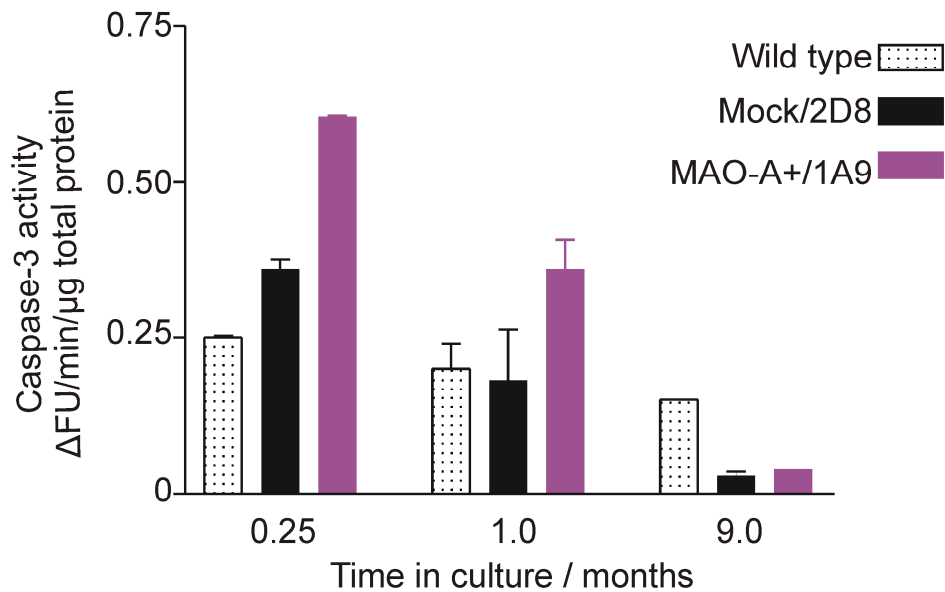


Figure 5. 12 Basal caspase-3 activities are reduced during long term culture of MAO-A+/1A9 cells

Basal caspase-3 activity measured using Acetyl-Asp-Glu-Val-Asp-7-Amidomethylcoumarin as substrate in wild type, mock/2D8 and MAO-A+/1A9 cells measured over a 9 month culture period and expressed as Δ FU/min/ μ g protein. Data represents values from single experiments over time where each extract was assayed in triplicate and intra-assay error shown.

MAO-A protein levels detected by dot blotting are elevated by ~4 fold in MAO-A+/1A9 cells compared to mock transfected and wild type controls (Figure 5. 13). Following continuous culture for ~25 weeks levels of MAO-A protein in MAO-A+/1A9 clones remains constant.

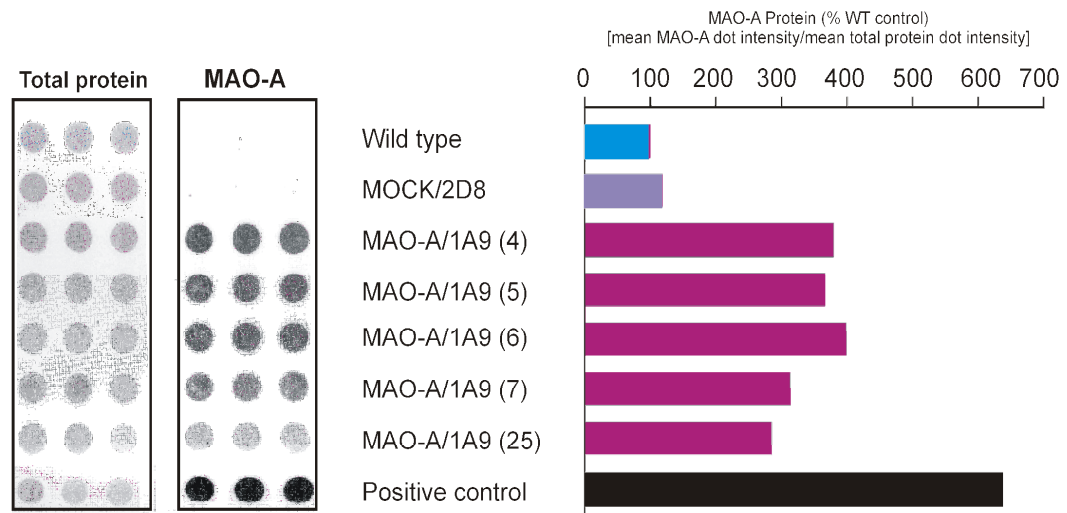


Figure 5. 13 MAO-A protein levels in MAO-A+/1A9 cells over a 6 month culture period

(left panel) Dot blot of MAO-A protein levels in SH-SY5Y stable clones. Equal protein homogenates (3 μ g) were loaded on to a nitrocellulose membrane (except positive control, 1 μ g) and probed with a MAO-A specific antibody. Mitochondrial membranes from human placenta are the positive control and no primary antibody was the negative control (not shown). (Right panel) Quantification of dots. The dots were digitised and densitometry was performed to quantify relative MAO-A protein levels normalised to total protein levels (copper stain) and expressed as % wild type control. Time in culture of MAO-A+/1A9 cells is shown in brackets (number of weeks).

5.2.3.4 Reactive oxygen species

Figure 5. 14 shows that ROS production is much larger in MAO-A+/1A9 cells compared to mock/2D8 cells, which produced negligible amounts of ROS.

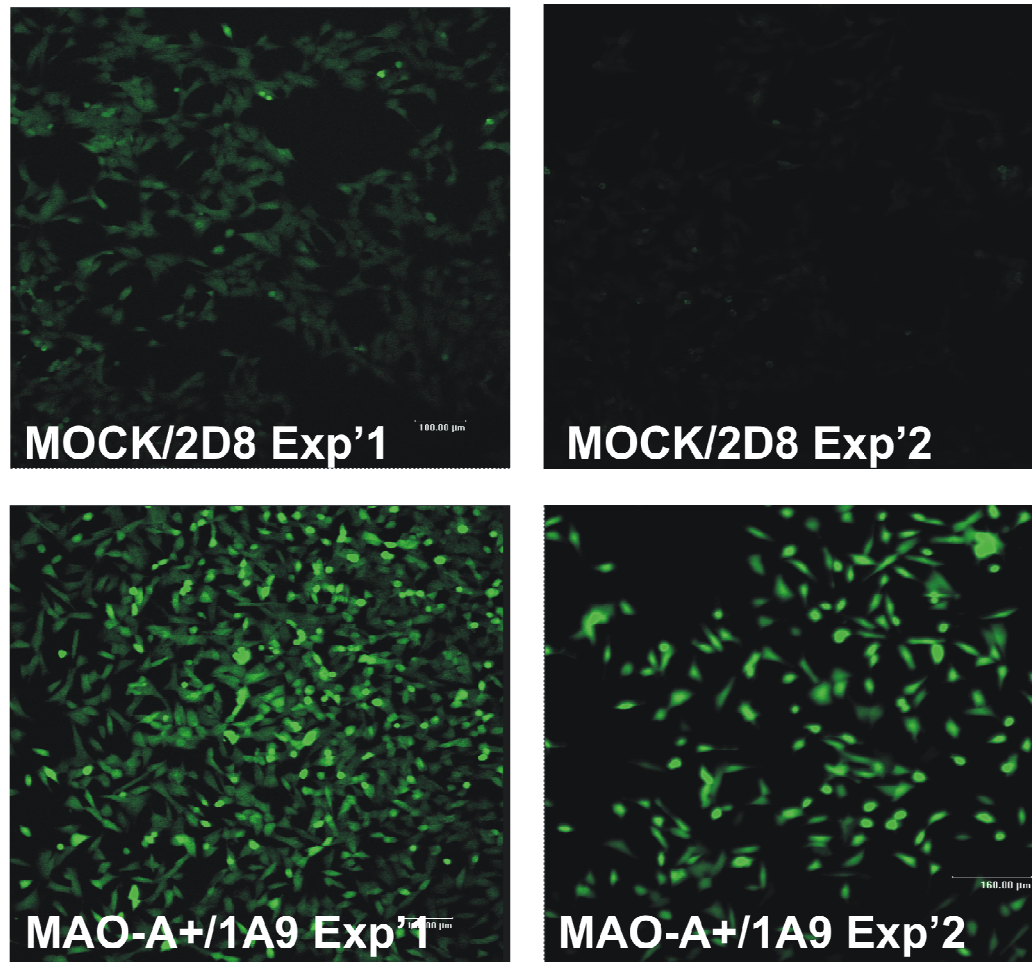


Figure 5. 14 Production of ROS is increased in MAO-A+/1A9 cells

DCDHF fluorescence was monitored in live mock/2D8 cells (*top panels*) and MAO-A+/1A9 cells (*bottom panels*, ~9 months of continuous culture) and visualised using a CLSM Leica microscope. Two photomicrographs are shown from two independent experiments, labelled experiment (Exp'1) and (Exp'2) and are representative of at least 4 independent experiments. Scale bar represents 100 μm in experiment 1 and 160 μm in experiment 2.

5.2.3.5 Survival and stress proteins

Levels of anti-apoptotic protein Bcl-2 were measured in untreated MAO-A+/1A9 cells (Figure 5. 15). Both western blotting analysis (Figure 5. 15A) and confocal microscopy (Figure 5. 15B) reveal loss of Bcl-2 in MAO-A+/1A9 cells compared to mock/2D8 controls. Confocal microscopy was particularly useful at this stage (~8 months in culture), since the MAO-A+/1A9 cells were struggling to grow in large volume plasticware. The small wells used for microscopy and the need for fewer cells allowed the detection of specific proteins in these cells.

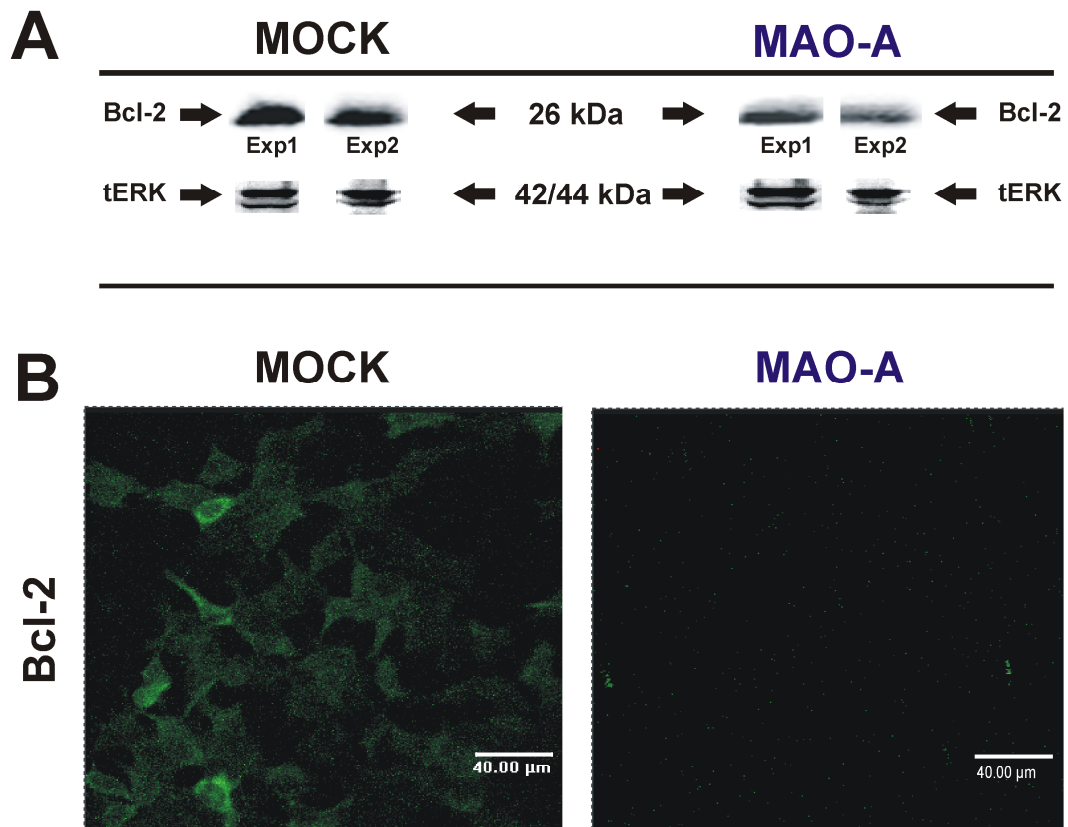


Figure 5. 15 Bcl-2 levels in mock/2D8 and MAO-A+/1A9 SH-SY5Y clones

(A) *Western blotting*: Equal protein aliquots (20 µg) of cells extracts from untreated mock/2D8 and MAO-A+/1A9 SH-SY5Y cells (~8 months in continuous culture) were separated on a 12 % (v/v) acrylamide SDS-PAGE gel prior to transfer to nitrocellulose membranes. Blots were probed with antibody directed to cleaved Bcl-2 (1:750 dilution). Blots shown are from two independent experiments and representative of >4 independent experiments (B) *Confocal microscopy*: Bcl-2 protein (shown by green fluorescence) levels were detected in fixed, untreated mock/2D8 and MAO-A+/1A9 SH-SY5Y cells. Cells were visualised using a CLSM Leica microscope.

Antibodies directed against activated stress-associated MAPK proteins were used to probe mock/2D8 and MAO-A+/1A9 cells and visualised using confocal microscopy (Figure 5. 16). The levels of both pJNK and the related transcription factor c-jun were increased in MAO-A+/1A9 cells. c-jun was detected predominantly in the nucleus of MAO-A+/1A9 cells and active JNK was seen in only few mock/2D8 cells. pP38 could not be detected using immunofluorescence.

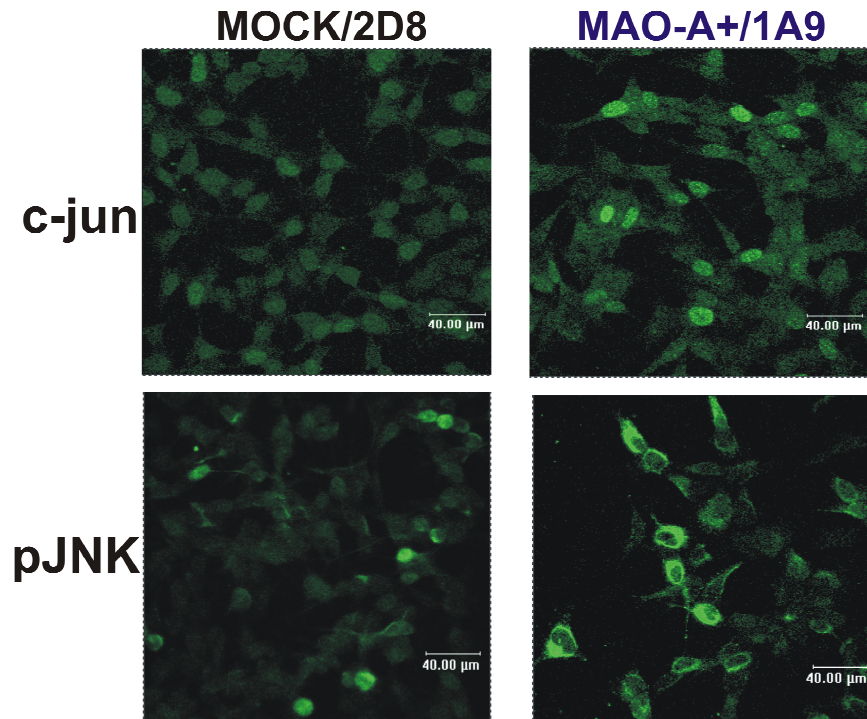


Figure 5. 16 Phosphorylated JNK and transcription factor c-jun in mock/2D8 and MAO-A+/1A9 cells
c-jun and phosphorylated JNK levels were detected (both shown by green fluorescence) in fixed, untreated mock/2D8 and MAO-A+/1A9 SH-SY5Y cells (~8 months in continuous culture). Cells were visualised using a CLSM Leica microscope. Photomicrographs are representative of 3 separate experiments.

5.2.4 Treatment of MAO-A+/1A9 SH-SY5Y stable clones with apoptotic inducers

5.2.4.1 Cell viability

Serum withdrawal significantly reduced MTT reduction by 72 h in both mock/2D8 and MAO-A+/1A9 clones (Figure 5. 17). In both cases the % reduction at 72 h was similar (54.8 % and 61.7 for the mock/2D8 and MAO-A+/1A9 cells respectively, Table 5. 1). A significant reduction in MTT reduction was also evident in both clones following 72 h rotenone treatment (Figure 5. 17) but the effect of rotenone was significantly less in the MAO-A+/1A9 clone (Table 5. 1).

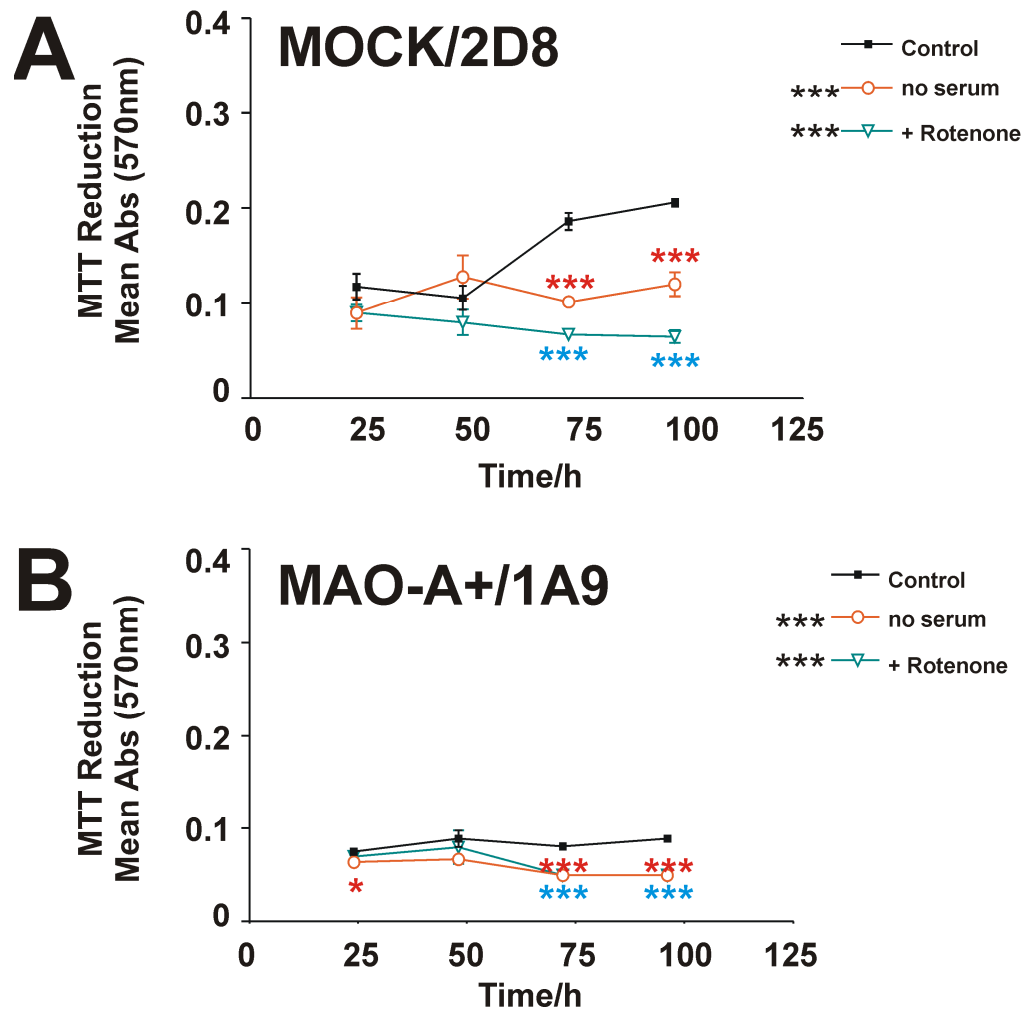


Figure 5. 17 Effect of apoptotic inducers on cell viability in wild type, mock transfected and over expressing MAO-A stable clones

Cell viability was measured in (A) mock/2D8 and (B) MAO-A+/1A9 SH-SY5Y cells (~8 months in continuous culture) over 96 hours in the presence of normal growth medium (control), serum free medium following washing (-serum) and 0.5 μ M rotenone (+ rotenone). MTT reduction was determined and expressed as mean absorbance values at 570 nm \pm S. D. Replicates in assay=12 and n=5. Treated cell MTT reduction were statistically compared to untreated cell MTT reduction in mock transfected and MAO-A+/1A9 cells using the Student's t-test where * = $p < 0.05$ and *** = $p < 0.001$ for serum withdrawal and rotenone treatments. Treated cell MTT reduction were statistically compared to untreated cell MTT reduction over the 96 h time course in mock/2D8 and MAO-A+/1A9 cells using two way ANNOVA, where *** = $p < 0.001$ (shown on key).

MTT Reduction (% untreated control)		
Cell type	Treatment	
	Serum deprivation	Rotenone
Wild type	64.2 ± 4.3	43.2 ± 7.2
MOCK/2D8	54.8 ± 8.3	36.0 ± 1.5
MAO-A+/1A9	61.7 ± 3.0	61.7 ± 0.0 ***

Table 5. 1 Effect of serum deprivation and rotenone treatment on MTT reduction

Data from Figure 5. 17 at a 72 hour end point only including wild type values, expressed as mean MTT reduction (% untreated control) ± S.D. Replicates in assay=12 and n=5. MTT reduction (% untreated control) in wild type cells were statistically compared to MTT reduction (% untreated control) in mock transfected cells and MTT reduction (% untreated control) in MAO-A+/1A9 cells were statistically compared to MTT reduction (% untreated control) in mock transfected cells using the Student's t-test where *** p<0.001.

Levels of reactive oxygen species in MAO-A+/1A9 cells were much higher than in mock/2D8 controls (Figure 5. 18A and B, *left panels*). Serum withdrawal resulted in detectable increases in ROS production in mock/2D8 control cells (Figure 5. 18A), but not in MAO-A+/1A9 cells (Figure 5. 18A). Following challenge with STS, on the other hand, ROS levels were increased further in both mock/2D8 and MAO-A+/1A9 cells (Figure 5. 18B). Clorgyline reduced ROS levels induced by serum withdrawal and STS in mock/2D8 and MAO-A+/1A9 cells (Figure 5. 18).

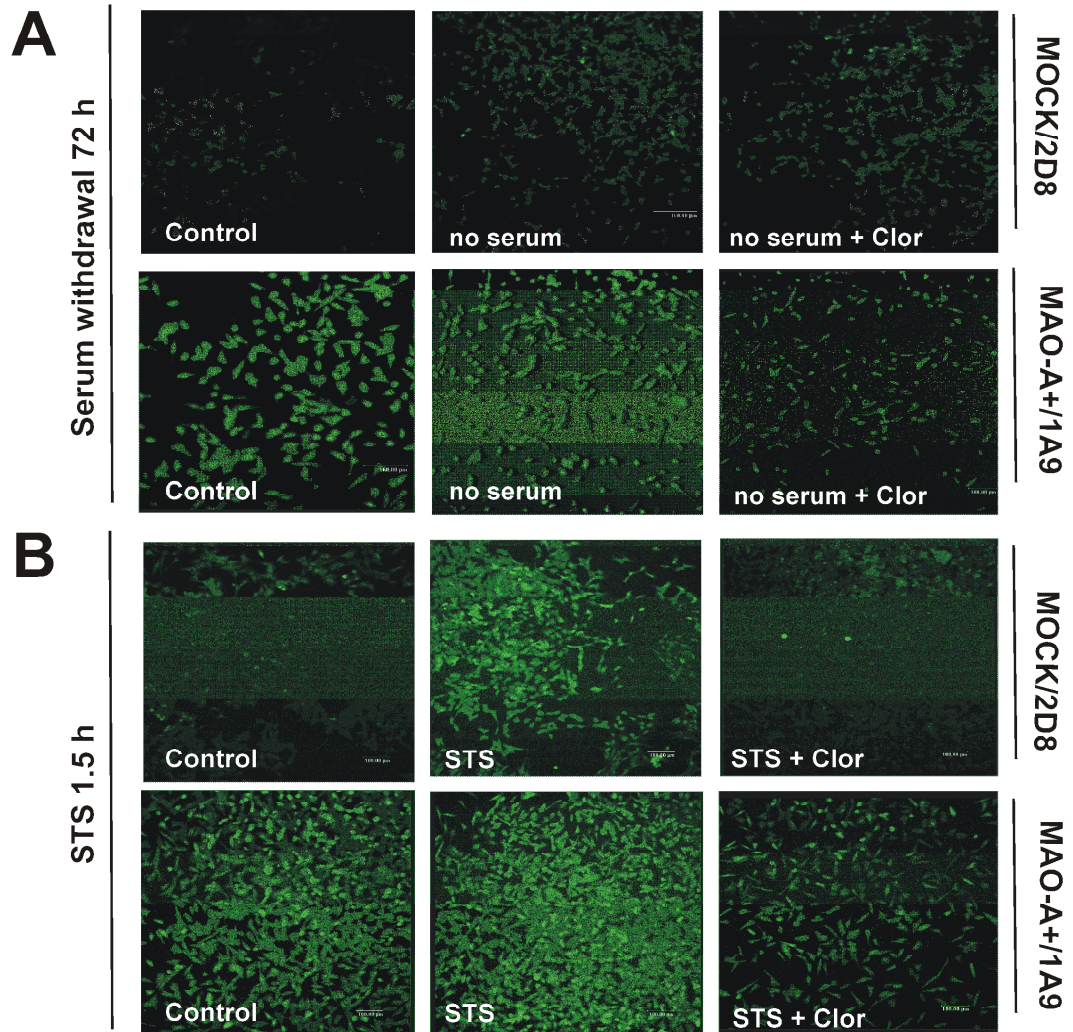


Figure 5.18 ROS production in mock/2D8 and MAO-A+/1A9 SH-SY5Y cells following STS and serum deprivation treatments

DCDHF fluorescence was monitored in live mock/2D8 and MAO-A+/1A9 cells (~9 months in continuous culture) in (A) Growth medium (control), in serum free medium (no serum) and serum free medium with 1 μ M clorgyline (no serum + clor) for 72 h. (B) In SFM (control), SFM containing 1 μ M STS (STS), SFM containing 1 μ M STS and 1 μ M clorgyline (STS + Clor) for 1.5 h. Cells were visualised using a CLSM Leica microscope, where laser power was matched. Scale bar represents 100 μ m.

5.3. DISCUSSION

5.3.1 Development of a stable SH-SY5Y cell line over expressing MAO-A

Human MAO-A cDNA was successfully cloned into the expression vector pcDNA3.1 (-), transformed into competent bacteria and transfected by electroporation into SH-SY5Y cells. Data were collected within the first month following the initial expansion of clones from single foci. Constitutive expression of MAO-A mRNA in wild type SH-SY5Y cells is ~3 molecules/1000 molecules GAPDH. Mock transfected clones showed similar MAO-A

mRNA expression to wild type cells, whilst clones overexpressing MAO-A had dramatically increased (up to 10,000 fold) MAO-A mRNA expression (Figure 5. 1). MAO catalytic activity in mock transfected clones was the same as in wild type cells. MAO catalytic activity in MAO-A+ clones ranged between ~4-11 fold of wild type levels and did not necessarily follow the pattern of MAO-A mRNA expression in each MAO-A+ clone.

Among overexpressing clones, the 3I8 MAO-A+ clone had relatively low MAO-A mRNA expression but high catalytic activity and grew slower than clones having lower catalytic activities (MAO-A+/1A9 and 4B9). This clone also showed apoptotic morphologies, including cell condensation and blebbing (Figure 5. 2). The initial assessment of SH-SY5Y clones overexpressing MAO-A suggested that increased MAO activity impairs viability, judged by cell morphology and observed growth rate. MAO-A+/1A9 was chosen as a working clone since in the initial weeks following expansion, it showed a ~4.4 fold increased MAO activity (also 4 fold increase in MAO-A protein level), appeared to proliferate and had a similar morphology to wild type and mock transfected control cells (Figure 5. 2). Mock transfected clone 2D8 was randomly chosen.

MAO-A+/1A9 cells contain more MAO-A protein than mock transfected control or wild type cells, shown non-quantitatively by confocal microscopy and immunohistochemistry (Figure 5. 3) and quantitatively by dot blotting (Figure 5. 13, around 4-fold compared to mock control). High magnification confocal microscopy of MAO-A protein in MAO-A+/1A9 cells revealed that MAO-A proteins are interspersed throughout the cell in distinct punctuated patches (Figure 5. 4), akin to mitochondrial staining in SH-SY5Y cells (for an example see Muqit *et al.* 2006). Indeed, MAO-A staining is almost completely co-localised with cytochrome c oxidase (Figure 5. 5), further indicating that overexpressed, intact MAO-A protein is inserted into the OMM.

Very high MAO-A mRNA levels in MAO-A+ clones driven by the expression vector could be a result of multiple insertion of the vector. High levels of expression in general, may be controlled by the cell at a number of post-transcriptional steps. Firstly, processed mRNA may not all be transported to the intended cytoplasmic location (Czaplinski and Singer 2006). Turnover of mRNA can control gene expression. Sites for mRNA decay known as P bodies are up-regulated when cells are overloaded with RNA (Sheth and Parker 2003). Another control point is translation of mRNA, which may be controlled by a complex range of processes (Richter 2007). Stability and function of the translated protein will be further regulated via protein degradation pathways and post-translational

modifications, which may control inactivation, maturation and compartmentalisation of the enzyme. The physical space on the outer mitochondrial surface should also be considered, since insertion of MAO into the OMM is critical for catalytic activity (Zhuang *et al.* 1992). MAO activity may ultimately be limited by the number of mitochondria per cell and the space available on the mitochondrial membrane regardless of the amount of mRNA produced. For example, reducing levels of the MAO-A repressor R1, causes a 6-fold increase in MAO-A mRNA expression but only 35-50% increase in MAO catalytic activity (Ou *et al.* 2006).

5.3.2 Consequences of MAO-A overexpression

5.3.2.1 Increased MAO-A causes oxidative stress

Measurement of reactive oxygen species in untreated mock/2D8 and MAO-A+/1A9 cells consistently revealed increased ROS in MAO-A+/1A9 cells (Figure 5. 14 and Figure 5. 18). Increased ROS (via MAO catalysed H₂O₂ production) in MAO-A+/1A9 cells may affect G protein signalling (Nishida 2000), activation of MAPK survival/mitogenesis pathways (Vindis *et al.* 2000), stress signalling MAPK pathways (Crossthwaite *et al.* 2002, Yoon *et al.* 2002, Ruffels *et al.* 2003, Halliwell and Gutteridge 2007), oxidant signalling (Finkel 1998), modification of proteins (Finkel 2003) and cell death processes (Tan *et al.* 1998). Indeed, overexpression of MAO-A resulted in increased levels of phosphorylated JNK and the transcription factor c-jun (Figure 5. 16) and decreased levels of anti-apoptotic Bcl-2 protein (Figure 5. 15).

The viability and growth of MAO-A/1A9 cells was assessed using MTT reduction assays and trypan blue viable cell counts. Both wild type and mock transfected SH-SY5Y cells proliferate in a similar manner (Figure 5. 6A) and have a doubling time of ~21 hours (Figure 5. 6B). Proliferation of MAO-A+/1A9 cells is greatly reduced (Figure 5. 7) and their doubling time is more than twice as long at ~54 hours (Figure 5. 6). MTT data showed the same general trends (Figure 5. 7), but MTT reduction in MAO-A+/1A9 cells was very low, indicating low metabolism. These data demonstrate that elevated MAO-A expression has a negative effect on cell survival, proliferation and metabolism. Reduced proliferation in MAO-A+/1A9 can be mainly attributed to increased MAO-A, since stable transfection of the vector and the presence of geneticin did not significantly affect proliferation of the mock transfected cells (Figure 5. 6). Increased MAO activity in MAO-A+/1A9 cells resulted in increased ROS production (Figure 5. 14) via increased H₂O₂,

which could potentially disrupt H_2O_2 homeostasis and signalling within the cells. Indeed, inhibition of MAO-A activity in MAO-A+/1A9 cells by clorgyline resulted in increased cell numbers compared to control (Figure 5. 10). In neuronal cells, oxidative metabolism of biogenic amines by MAO is a major contributor to the cytosolic and mitochondrial steady state levels of H_2O_2 (Cadenas and Davies 2000). Low levels of H_2O_2 are mitogenic in several cell types in culture (Halliwell and Gutteridge 2007) and also in cancer cells (Gius and Splitz 2006). However, *in vivo* small increases in H_2O_2 concentrations (above 500 nM) causes growth arrest and even higher (above 50 μM) can induce apoptosis (Giorgio *et al.* 2007, Figure 5. 19).

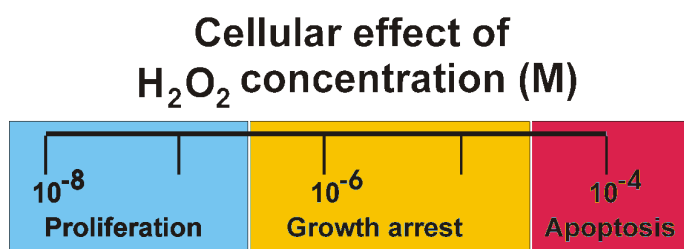


Figure 5. 19 Cellular effect of H_2O_2 concentration (modified from Giorgio *et al.* 2007)

Diagram showing the opposing effects of H_2O_2 concentration on the cell. The resting cell *in vivo* has a H_2O_2 concentration of ~100 nM alongside high concentrations of glutathione and ascorbate antioxidants (Halliwell and Gutteridge 2007), inducing proliferation. When the cellular concentration of H_2O_2 exceeds 500 nM, oxidative damage levels rise, transition metal ions that catalyse free radical reactions are released, free radicals damage DNA resulting in activation of transcription factors and adaptive response (increased levels of protective systems, e.g. chaperones, antioxidant enzymes). Growth is arrested to allow repair of DNA damage (Halliwell and Gutteridge 2007). H_2O_2 concentrations above 50 μM induce more severe mitochondrial and DNA damage, ensuing mitochondrially-mediated and p53-mediated apoptotic events and often execution of apoptosis (Giorgio *et al.* 2007, Halliwell and Gutteridge 2007).

5.3.2.2 Increased MAO-A reduces ATP levels and cell viability

The role of ATP in cell death is paradoxical, since ATP also provides the energy needed for cell death to occur and is often increased during the early phases of apoptosis. Lack of ATP ultimately kills cells because there is insufficient ATP for the sodium or calcium pumps (Brown 2005), which results in loss of membrane potential, swelling and rupture of the cell. ATP depletion is a classic marker of necrotic cell death, however apoptosis can lead to necrosis (Brown 2005). In a vicious cycle of events, stressful or apoptotic stimuli and mitochondrial dysfunction can also trigger ATP depletion. ATP levels and optimal ROS production are required for optimal mitochondrial activity and depletion of ATP has been shown to coincide with increased ROS production (Keating 2008). ATP levels in mock/2D8 cells are significantly lower than in wild type cells (by approximately 50%, Figure 5. 8). These data suggest that after 10 months in continuous culture, the long-term effects of geneticin and/or off target effects of stable transfection with the control vector

has caused reduced ATP. Nonetheless, ATP levels in MAO-A+/1A9 cells were significantly lower than mock/2D8 cells (around 66% less ATP, Figure 5. 8). This substantial loss of ATP in MAO-A+/1A9 cells (Figure 5. 8), implies that the electron transport chain/respiration is severely compromised by changes in H₂O₂ production. ATP depletion and increased ROS production has been shown to de-regulate exocytosis (Keating 2008). Impaired mitochondrial function and impaired regulation of exocytosis caused by or as a result of changes in ROS and ATP are implicated as underlying contributors to the initial stages of some human neurodegenerative disorders, including PD (Keating 2008). The present data support the hypothesis that MAO may be involved in these disorders.

5.3.2.3 Increased MAO-A activity causes changes in cell morphology and growth

Long term culture (~6 months) of MAO-A+/1A9 cells induced a state of growth arrest, associated with cell shrinkage and blebbing (Figure 5. 9). At this late stage, MAO-A+/1A9 cells became difficult to sub-culture, except when seeded in small culture areas such as chamber slides (for an example see Figure 5. 6).

Finally, resuscitated MAO-A+/1A9 cells grew normally, being neuronal-like and healthy compared to cells that had been in long term culture (Figure 5. 10). A population of early MAO-A+/1A9 cells (6 weeks in culture) were grown in media containing the MAO inhibitor clorgyline. These cells proliferated more quickly and showed healthier neuronal-like morphologies than the new batch cells without clorgyline or old MAO-A+/1A9 cells (Figure 5. 10). These data again indicate that chronic exposure to increased MAO activity is responsible for injury to the cell.

Extensive cell blebbing (as seen in Figure 5. 9), is typical of apoptotic cell death. However, other morphological characteristics of apoptosis such as cell shrinking, rounding and chromatin condensation were not always apparent in aged MAO-A+/1A9 cells (Figure 5. 9). Antibodies directed against two cytoskeletal proteins were used to investigate the general structure and cell surface structures of MAO-A+/1A9 cells. The organisation of α -tubulin is similar in mock/2D8 and wild type SH-SY5Y cells (Figure 5. 11). Actin filaments are normally highly concentrated in the cell cortex, just beneath the plasma membrane (Alberts *et al.* 1994). Mock/2D8 and wild type SH-SY5Y cells show similar staining of β -actin, and actin was present in the blebs at the cell surface, indicating that the blebs are apoptotic, since the structures are a protrusion of the cytoplasm.

5.3.2.4 Increased MAO-A levels result in apoptosis or necrosis

That MAO-A+/1A9 cells are apoptotic is further supported by GAPDH staining in their nuclei (Figure 5. 11). As previously discussed (see section 3.3), GAPDH translocates from the cytosol to the nucleus during apoptotic events, since GAPDH assists in regulating certain genes that will favour apoptosis (for a review see Berry and Boulton 2000).

During early phases of cell culture, caspase-3 activity was elevated in MAO-A+/1A9 cells, but at later stages negligible levels of caspase-3 were detected.

It is likely that during the early stages of culture following transfection, MAO-A+/1A9 cells are subjected to a moderate increase in oxidative stress which activates/up-regulates antioxidant defences, DNA repair mechanisms and possibly induces stress/apoptotic pathways including further regulation of MAO itself (although MAO-A protein remains stable over a 6 month period, Figure 5. 13). As indicated earlier, older cultures appear to be in a state of growth arrest or senescence. Response to oxidative stress may be reversible; for a variable period the cell is in an altered redox state which does not lead to cell death (Halliwell and Gutteridge 2007). Events triggered by this state can persist and become permanent (Halliwell and Gutteridge 2007). Senescence, a permanent state of non-division has been reported in a continuous culture of human fibroblast cells treated with 100-300 μM H_2O_2 (Chen 1998), however treatment with such high concentrations are not physiologically relevant or convincing. Senescence after long periods in cell culture can also in part be due to the oxidative stress of the culture process (Halliwell and Gutteridge 2007). Severe oxidative damage often initiates apoptosis; however, in a highly oxidised state caspases are oxidised via their active site $-\text{SH}$ groups and are inactive, leading to survival of badly damaged cells. Badly damaged cells that survive but are not able to recover are likely to die by necrosis.

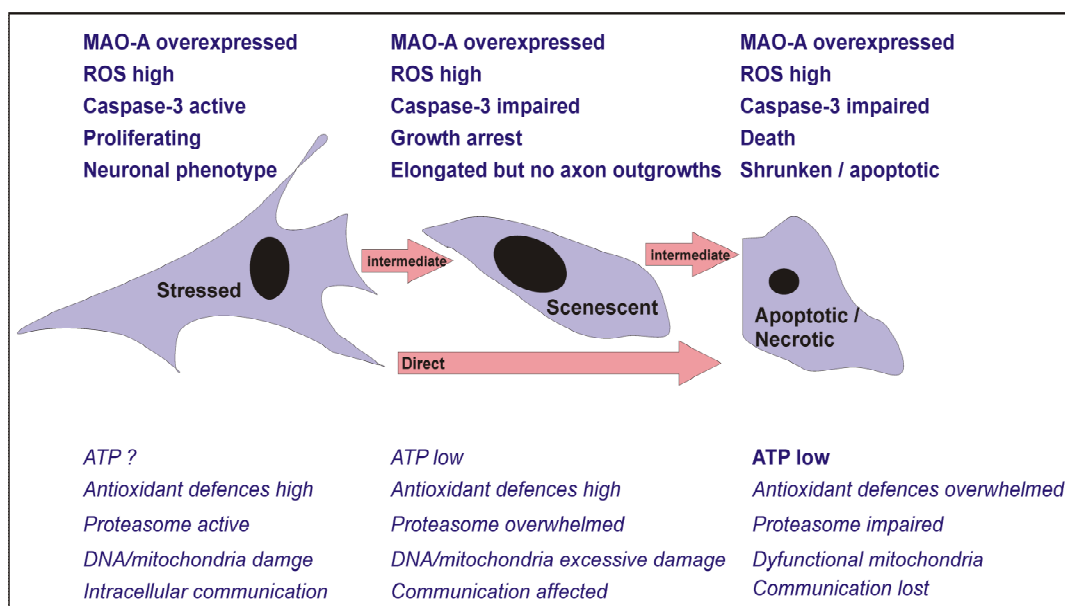


Figure 5. 20 Proposed effect of MAO-A overexpression on SH-SY5Y cells in long term culture

Diagram showing appearance of SH-SY5Y cells overexpressing MAO-A during long term culture. **Bold** text relates to known characteristics and *italic* text relates to unknown characteristics. Initially, MAO-A overexpression results in increased production of H_2O_2 , increased reactive species and hence stressed or injured cells. Basal caspase levels are high and cells may either execute apoptosis or, depending on the extent of the stress, continue to proliferate, adapt to the oxidative environment and maintain neuronal phenotype. If oxidative damage rises, DNA and mitochondria are damaged, ATP is low, caspases are shut-down, telomeres shortened, growth is arrested and repair mechanisms are working extensively to rescue the cell. The cell may be partly rescued enough for the cell to commit suicide through apoptosis, since it is badly damaged; this is preferred and protects integrity. However, the cell may eventually be damaged irreversibly, may not be able to undergo apoptosis, dies by necrosis, disintegrating into the surroundings.

5.3.3 Response of MAO-A+ SH-SY5Y cells to stress

Since MAO-A+/1A9 cells were severely damaged during cell culture in experiments involving further stressors were less useful than expected. Caspase levels were diminished in damaged cells and measurement of apoptosis was limited. MTT reduction assays were attempted following challenge with a subtle stressor (serum deprivation) and a mitochondrial toxin (rotenone). However, as discussed earlier MTT reduction assays are not very sensitive and are only a measure of cellular metabolism. Long term cultured MAO-A+/1A9 cells reduced MTT at extremely low levels (similar to rotenone treated cells). The fact that serum withdrawal affected MTT reduction to a similar extent in MAO-A+/1A9 and mock/2D8 cells does not suggest different sensitivity in the MAO-A+/1A9 cells. Indeed the reduced effect of rotenone on the MAO-A+/1A9 cells indicates that the electron transport chain is already impaired in these cells, supported by their very low ATP levels (Figure 5. 8). However, it is possible that if MAO-A+ cells in the early stages of culture had been tested, the cells may have been more sensitive to other stressors. STS

treatment appeared to result in a further increase in ROS in MAO-A+/1A9 cells, again suggesting that MAO-A may be up-regulated in response to oxidative stress.

5.3.4 Conclusion

Increased MAO-A expression in human neuroblastoma cells by genetic manipulation has confirmed a role for increased MAO in promoting cell death. A 4-fold increase in MAO-A activity caused oxidative stress and compromised mitochondrial function, which over time results in cell death by apoptosis or necrosis. An overview of the biochemical changes are shown in Figure 5. 21. MAO may fine tune or modulate the cells' response to different stressors. Mitochondria-generated ROS is thought to control lifespan/ageing (Giorgio *et al.* 2007) and may be involved in this process.

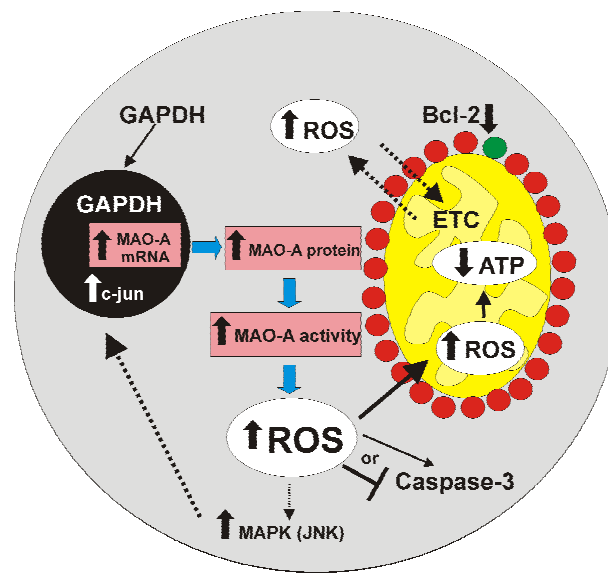


Figure 5. 21 Overview of biochemical changes in SH-SY5Y cells overexpressing MAO-A

Increased expression of MAO-A mRNA driven by expression vector results in ~4 times more MAO-A protein (shown as red circles) and more than 4-6 times catalytic activity. Increased MAO activity causes oxidative stress because of increased production of H_2O_2 during MAO catalysis and therefore increased levels of ROS. The increased oxidative environment favours GAPDH translocation to the nucleus, activation of stress-signalling pathways, decreased Bcl-2 levels, activation (low-moderate oxidative stress) or inhibition (high level oxidative stress) of caspase-3, and ATP depletion. MAO-generated oxidative stress damages mitochondria, mitochondrial dysfunction further compromises cell viability and eventually the cell dies by apoptosis or necrosis.

CHAPTER 6

THE EFFECT OF KNOCKDOWN OF MAO-A EXPRESSION IN NEUROBLASTOMA CELLS

THE EFFECT OF KNOCKDOWN OF MAO-A EXPRESSION IN NEUROBLASTOMA CELLS

6.1. INTRODUCTION

6.1.1 Reduced MAO in humans-physiological relevance

Reduced MAO expression has been reported in a wide range of human conditions, but as discussed in section 5.11, limited measurement of MAO levels in humans has led to some debate over the findings. However, the existence of rare mutations in MAO genes in humans and work on MAO knockout mice has confirmed that marked deficiency of MAO activity is compatible with life.

6.1.1.1 Norrie disease and Brunner syndrome

Norrie disease is rare X-chromosome linked recessive disorder of unknown pathogenesis (Norrie 1927, Sims *et al.* 1989b). The disorder is characterised by retinal dysplasia and consequent congenital blindness (Sims *et al.* 1989b). About half the patients also manifest CNS dysfunction, mental retardation and certain psychiatric symptoms (Sims *et al.* 1989b, Chen *et al.* 1995). Patients with an atypical form of the disease were discovered to have submicroscopic chromosomal deletions and MAO deficiency. This MAO deficiency state has been described in families, with features of altered amine levels, low intelligence and difficulty in impulse control (Chen *et al.* 1995), delayed sexual maturation, altered peripheral autonomic function, sleep disorders and seizures (Sims *et al.* 1989a). The Norrie disease gene (NDP) and MAO genes are tandemly arranged in the p11.4-p11.3 region of the human X chromosome in the order MAO-A-MAO-B-NDP (Chen *et al.* 1995). Two individuals with Norrie disease were found to lack the genes encoding MAO-A and -B. This was associated with a 90% reduction in urinary metabolites of the MAO-A substrate NA, a 100-fold increase in the MAO-B substrate PEA and no change in the metabolites of DA and 5-HT. Plasma amine oxidase activity however was found to be normal (Murphy *et al.* 2005).

Brunner syndrome is an X chromosome-linked form of mild mental retardation which was first identified in males from large Dutch family showing abnormal, aggressive and violent behaviour. Studies on five males with Brunner syndrome showed that they had complete and selective deficiency of MAO-A catalytic activity and a point mutation in the eighth

exon of the MAO-A structural gene, which changed a glutamine residue to a termination codon (Brunner *et al.* 1993).

Human condition	MAO Isoform	Measured in	Author	Year
Alcoholism	MAO-B	platelets	Sullivan <i>et al</i>	2000
Type A personality	MAO-B	platelets	Smith, A. F	1994
Pre-eclampsia	MAO-A	placenta	Sivasubramaniam <i>et al</i>	2002
Female bulimia nervosa	MAO-B	platelets	Carrasco <i>et al</i>	2000
Female anorexia nervosa	MAO-B	platelets	Diaz Marsa <i>et al</i>	2000
Pre-menstrual syndrome	MAO-B	platelets	Ashby <i>et al</i>	1988
Smoking	MAO-A and -B	platelets and peripheral organs	Fowler <i>et al</i>	1996 and 2003
Sensation seeking	MAO-B	platelets	Murphy <i>et al</i>	1977
Aggression/ violence	MAO-A	genetic assessment	Caspi <i>et al</i>	2002
Aggression/ violence	MAO-A	genetic assessment	Brunner <i>et al</i>	1993
Aggression/ violence	MAO-A and -B	genetic assessment	Sims <i>et al</i>	1989

Table 6. 1 Examples of some human conditions where MAO is reduced

The effect of decreased MAO activity on humans, showing condition, MAO isoform, method of study and reference to relevant publication.

6.1.1.2 Behaviour and addiction

Reduced MAO expression was reported in the blood platelets of schizophrenic patients (Murphy and Wyatt 1972). Although reduced MAO activity has been suggested to be a genetic marker for schizophrenia and many studies following Murphy and Wyatt's work have demonstrated reduced MAO expression (reviewed by Sandler *et al.* 1981), these studies have been complicated by effects of drug therapy and therefore remain controversial today. Decreased MAO activity has also been heavily associated with aggression and impulsive behaviour (review by Sandler *et al.* 1981, Oreland 1993, Shih *et al.* 1999).

Decreased MAO activity has been linked to alcoholism, and evidence suggests that decreased MAO in alcoholics is a trait rather than an artefact of ethanol consumption or withdrawal (Sandler *et al.* 1981, Sullivan *et al.* 1990). Interestingly, cigarette smoke inhibits MAO-A activity (Fowler *et al.* 1996) and low levels of MAO-B expression have been found in the peripheral organs of smokers (Fowler *et al.* 2003). Smokers have lower MAO activity in blood platelets and lowered incidence of Parkinson's disease (Oreland *et al.* 1981, Castagnoli and Murugesan 2003).

6.1.2 Reduced MAO in *in vitro* culture systems

6.1.2.1 Reduction of MAO with inhibitors

MAO inhibitors have been shown to protect against MPTP toxicity (Heikkila 1988). Propargylamine MAO inhibitors can prevent cell death in human neuroblastoma cells induced by various insults including MPP⁺ treatment, oxidative stressors and withdrawal of trophic factors (Naoi and Maruyama 2001, Akao *et al.* 2002, Maruyama *et al.* 2002). Inhibition of MAO-A by clorgyline can prevent apoptosis in human melanoma cells (Malorni *et al.* 1998), human neuroblastoma (Ou *et al.* 2006), mouse neuroblastoma (De Girolamo 2001) and rat pheochromocytoma cells (DeZutter and Davis 2001). MAO inhibitors prevent suppression of the mitochondrial electron transport chain caused by monoamine metabolism in rat brain mitochondria (Cohen *et al.* 1997). Hydroxyl radicals induced in rat mitochondria following ascorbate and Fe²⁺ treatment significantly and irreversibly inhibited both MAO-A and MAO-B activities (Soto-Otero *et al.* 2001), suggesting that overproduction of hydroxyl radicals can be regulated by MAO inhibition.

6.1.2.2 Reduction of MAO expression

A recent publication has shown that MAO expression is suppressed by the action of wild type Parkin (Jiang *et al.* 2006). Wild type Parkin has a protein-ubiquitin E3 ligase activity that targets protein substrates for proteolysis by the 26S proteasome. Mutations in Parkin are linked to early-onset PD and the absence of functional Parkin is thought to underlie the degeneration of DA neurons in PD (for review see McNaught *et al.* 2001, Dawson and Dawson 2003). Following work by Jiang and colleagues Parkin was shown to have the additional neuroprotective role by acting to suppress the expression of MAO mRNA, rather than controlling MAO protein degradation. Stable overexpression of Parkin in SH-SY5Y cells markedly reduced mRNA expression, protein and activities of both MAO-A and MAO-B (Jiang *et al.* 2006).

The Ca²⁺-binding protein (calbindin-D28K) is greatly reduced in AD brain (Cao *et al.* 2007). Whilst overexpression of calbindin-D28K in a mouse hippocampal cell line causes a significant reduction in MAO-A expression (Cao *et al.* 2007). These data suggest that increases in intracellular calcium availability could contribute to a MAO-A-mediated mechanism involving oxidative stress in AD.

6.1.3 MAO knockdown by genetic manipulation

6.1.3.1 MAO knockdown *in vitro*

To date, reduction of MAO expression directly using genetic techniques *in vitro* has only been achieved by Yi and co-workers in SH-SY5Y cells (Yi *et al.* 2006a). The endogenous dopaminergic neurotoxin, *N*-methyl(*R*)salsolinol induces apoptotic cell death in the SNpc of rats (Naoi *et al.* 1996) and SH-SY5Y cells (Maruyama *et al.* 1997). Yi's group used RNA interference (specifically siRNA) to knockdown MAO-A in SH-SY5Y cells and showed that MAO-A was a target of *N*-methyl(*R*) salsolinol. The MAO-A isoform was suggested to play a role in binding neurotoxins and MAO-A knockdown in this study resulted in significantly reduced binding of *N*-methyl(*R*) salsolinol. Interestingly, Salsolinol belongs to a group of compounds known as tetrahydroisoquinolines, potential neurotoxins that exist naturally in the body and may regulate pituitary function (for a review see Toth *et al.* 2002).

6.1.3.2 MAO-A and MAO-B deficient mice

An isolated line of transgenic mice in which a transgene integration caused a deletion in the gene encoding MAO-A provided the first animal model of MAO deficiency (Cases *et al.* 1995). Levels of 5-HT in MAO-A deficient pup brains were increased by nine fold and levels of norepinephrine were increased two fold in both pup and adult brains. MAO-A deficient mice are viable but have behavioural abnormalities as pups. These include trembling, fearfulness and difficulty in righting (autonomic reflexes), which were reversed by a 5-HT synthesis inhibitor, suggesting that behavioural changes are due to elevated 5-HT rather than a direct cause of MAO-A inhibition. Male adults developed enhanced aggression (Cases *et al.* 1995). Increased aggressive behaviour in MAO-A knockout mice is consistent with abnormal aggression reported in men from a Dutch family with complete MAO-A deficiency (Brunner *et al.* 1993), suggesting that elevated levels of 5-HT may be important in enhanced emotional learning that adult MAO-A knockout mice exhibit (Kim *et al.* 1997). MAO-B deficient mice were bred using homologous recombination by Grimsby and colleagues (Grimsby *et al.* 1997), where only the levels of PEA monoamines were increased. In 2004, a line of MAO-A/MAO-B knockout mice were isolated and bred from a litter of MAO-B knockout mice that spontaneously developed a point mutation in exon 8 of the MAO-A gene (Chen *et al.* 2004). Double knockout mice had reduced body weight, anxiety-like behaviour and greatly increased levels of monoamines. Brain levels of

5-HT, NA, DA and PEA were increased and 5-HT metabolites decreased compared to MAO-A or MAO-B single knockout mice (Chen *et al.* 2004). Differences between MAO double knockout mice and single knockout mice suggest that varying monoamine levels result in unique biochemical and behavioural phenotypes. More recently, Newman's group have shown that mother-reared male rhesus monkeys with a low MAO-A activity polymorphism were highly aggressive (Newman *et al.* 2005).

6.1.4 miRNA technology

RNAi interference (RNAi) is a naturally occurring cellular mechanism that induces post-transcriptional gene silencing (Gilmore *et al.* 2004). RNAi technology has had a revolutionary impact on molecular biology since its discovery in 1998 by Fire and colleagues who were working on gene silencing in *C. elegans* (Dykxhoorn *et al.* 2003).

In mammalian cells, RNAi is generally induced by one of two techniques. One approach relies on transfection of cells with a small interfering RNA (siRNA) which in brief, mimic the structure of microRNA (miRNA) duplex intermediates formed during the processing of endogenous miRNA transcripts. Although siRNA technology is simple and effective, synthetic siRNAs can be expensive and the effects are often transient (Cullen 2006). The alternative approach relies on the transcription by RNA polymerase III of short hairpin RNAs (shRNAs) which mimic the pre-miRNA hairpins that result from the processing of endogenous primary miRNA (Cullen 2006). For the down-regulation of MAO-A in this chapter of work, miRNAs targeted to MAO-A were expressed in SH-SY5Y cells, using the BLOCK-iT Pol II miR RNAi expression vector kit (Invitrogen, Karlsruhe, Germany). Unlike shRNAs, miRNAs are found embedded in long primary transcripts (pri-miRNAs), containing a hairpin structure and driven by RNA polymerase II (Lee *et al.* 2004).

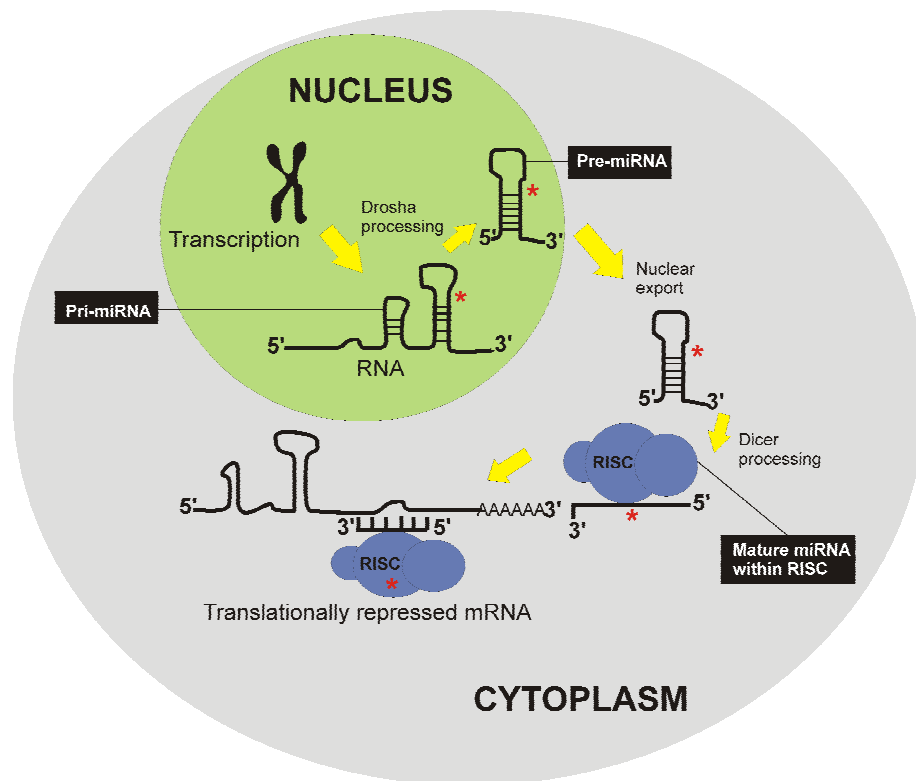


Figure 6. 1 An overview of miRNA gene silencing

Transcription-miRNAs are initially expressed as part of transcripts termed primary miRNAs (pri-miRNAs). They are transcribed by RNA polymerase II and include 5' caps and 3' poly(A) tails. The miRNA portion forms a hairpin loop with signals for dsRNA-specific nuclease cleavage. **Hairpin release**-The dsRNA-specific ribonuclease Drosha digests the pri-miRNA in the nucleus to release hairpin, precursor miRNA (pre-miRNA). Drosha also generates either the 5' or 3' end of the mature miRNA, depending on which strand is selected by the RNA induced silencing complex (RISC). **Export**-Pre-miRNAs are exported from the nucleus to the cytoplasm. **Dicer processing**-Dicer is a member of the RNase III superfamily of nucleases. Dicer cleaves pre-miRNA approximately 19 bp from the Drosha cut site. The resulting dsRNA has 1-4 nt 3' overhangs at either end. Only one of the two strands in the mature miRNA (some mature miRNAs derive from the leading strand and some derive from the lagging strand) is selected by RISC. **Strand selection by RISC**-Single stranded mature miRNA associates with the RISC complex to be able to control translation of target mRNAs. Most mRNAs contain multiple miRNA binding sites and many miRNAs usually act together to produce responsive miRNA-induced translational repression. The red asterisk * marks the journey of miRNA. Diagram and information from the Ambion Inc miRNA resource pages (www.ambion.com/techlib/resources/miRNA) accessed on 12th September, 2007 and the BLOCK-iT Pol II miR RNAi expression vector kit (Invitrogen, Karlsruhe, Germany) user manual (Catalogue number K4935-00 Version C, September 26, 2006).

6.1.5 Rationale

The main reasons for this chapter of work were: -

(1) to provide support to work in chapter 3 and chapter 4, where reduction of MAO activity was achieved using chemical inhibitors. However, down-regulation of MAO expression using miRNA technology has its disadvantages. These include off-target effects (reviewed by Pulverer *et al.* 2003, Cullen 2006) and increased stress induced by the transfection process. These effects can be monitored by using the correct basic, negative

miRNA, and quantitative controls and also by using multiple, well-designed miRNA sequences for the cloning.

(2) To compliment the work in chapter 5, where MAO-A was overexpressed, resulting in significant and detrimental changes to SH-SY5Y cells. This chapter will address whether reduced MAO activity has an effect on SH-SY5Y cell growth and sensitivity to apoptotic inducers.

6.1.6 Aims of Chapter

- **To reduce MAO-A expression in a stable SH-SY5Y cell line using miRNA**

SH-SY5Y cells were transfected with the Pol II miRNA (pcDNA6.2-GW/miR) containing an insert coding for pre-miRNA sequences that facilitate the targeting of MAO-A mRNA by RNAi (referred to as MAO-A knockdown or MAO-A-). SH-SY5Y cells were also stably transfected with the Pol II miRNAi (pcDNA6.2-GW/miR-neg) expression vector lacking MAO-A sequence but containing an insert that can form a hairpin structure and is processed into mature miRNA but does not target any known vertebrate gene (referred to as negative miRNA control or Neg) to monitor off-target effects.

- **To determine the MAO status in MAO-A stable knockdowns**

MAO-A-/miRNA stable SH-SY5Y clones and controls were assessed for MAO mRNA levels and catalytic activity and a suitable stable clone with reduced MAO-A levels and a control chosen for further work. MAO protein levels in working clones was determined by immunohistochemistry, confocal microscopy and dot blotting using a MAO-A specific monoclonal antibody, as before.

- **To characterise changes in MAO-A stable knockdown clones**

Once suitable clones had been chosen, SH-SY5Y cells with reduced MAO activity were characterised firstly for their growth, viability and morphology. ROS production using DCDHF/confocal microscopy was also detected in untreated cells.

- **To study the effect of MAO-A knockdown in SH-SY5Y cells in three different models of apoptosis**

Three different treatments comprising three different models previously used in this thesis, including STS, rotenone and serum withdrawal were used. Respectively, the three inducers represent three different types of stressor, one being a potent caspase-3 activator, one being a mitochondrial toxin and finally a subtle, slow activating stressor. Following treatments,

MAO-A- stable clones were assessed for changes in cell viability (MTT reduction), ATP levels and caspase-3 activity compared to both wild type SH-SY5Y cells and negative miRNA control clones.

6.2. RESULTS

6.2.1 Characterisation of MAO-A knockdown SH-SY5Y cells

Cells containing the miRNA vector are resistant to the antibiotic blasticidin. Stably transfected cells were grown in the presence of 6 µg/ml blasticidin (the predetermined concentration sufficient to kill wild type cells).

6.2.1.1 Initial characterisation of MAO-A expression in stable knockdown clones

Cell clones were expanded in the presence of the antibiotic blasticidin and RNA was extracted to determine the effects on MAO-A mRNA levels. Figure 6. 2A shows that MAO-A- SH-SY5Y clones exhibit decreased MAO-A mRNA expression compared to wild type and negative miRNA control SH-SY5Y cells. Transfection with the negative miRNA vector (Neg/2G11 clone) resulted in approximately a 60% increase in MAO-A mRNA expression compared to wild type expression. Knockdown of MAO-A mRNA expression in MAO-A- SH-SY5Y clones ranges from ~45-62 % knockdown, compared to wild type expression. These SH-SY5Y clones and other MAO-A- clones were then expanded further and extracts taken for evaluation of MAO-A catalytic activity. Negative miRNA transfected cell clones had MAO activity levels ranging between 8-20 pmoles/min/mg, with clone 2G11 having approximately 30% more MAO activity than wild type SH-SY5Y cells. All MAO-A- clones had significantly decreased MAO catalytic activities, (except clone 6F10) ranging between approximately 20-60 % knockdown of activity compared to the wild type (Figure 6. 2B). Four MAO-A- clones-10D8, 4F1, 5E2 and 5C8, showing MAO activity knockdown of 53%, 40%, 60% and 63% respectively-and four negative miRNA clones were chosen for further expansion.

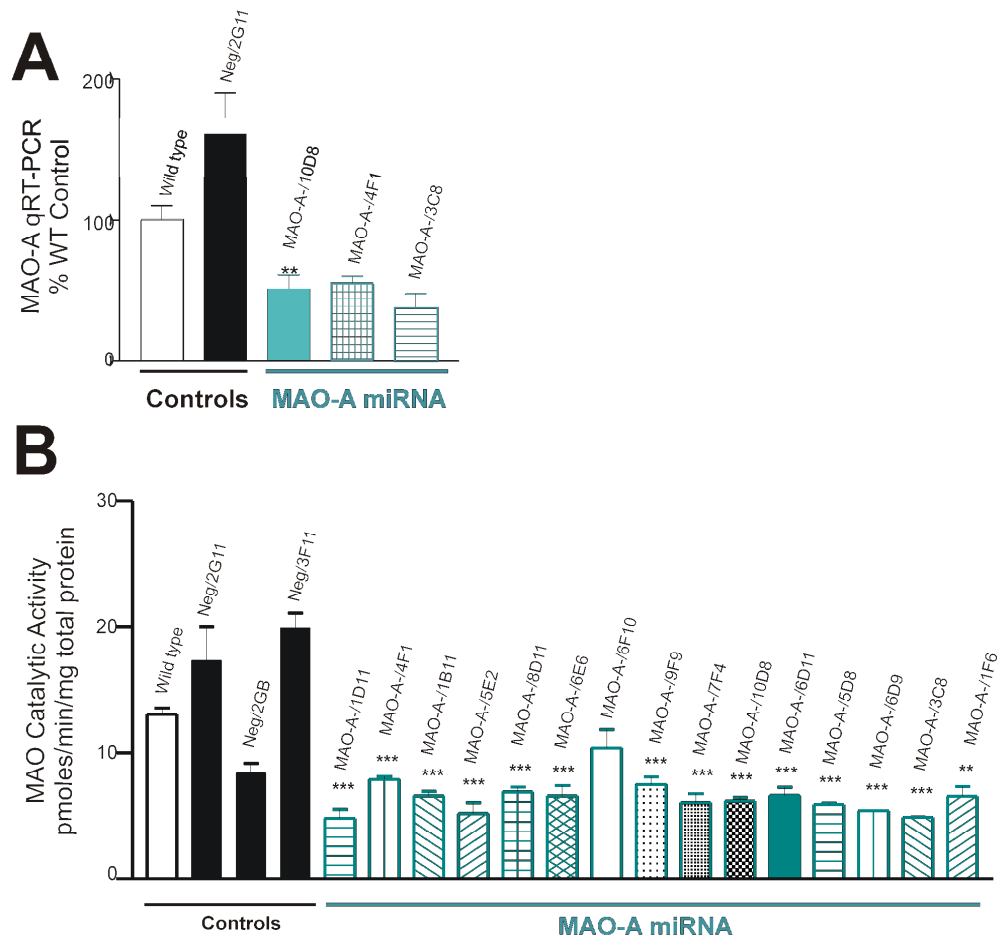


Figure 6. 2 MAO-A mRNA and catalytic levels are decreased in MAO-A- SH-SY5Y clones

(A) MAO-A mRNA expression was measured by qRT-PCR in stable SH-SY5Y cell clones and expressed as mean MAO-A qRT-PCR (% wild type) \pm S.D, where $n=3$ for wild type, neg/2G11 and MAO-A-/10D8 but $n=2$ for MAO-A-/4F1 and MAO-A-/3C8. MAO mRNA level in MAO-A-/10D8 was statistically compared to wild type mRNA levels using the Student's t-test where $**p<0.005$. (B) MAO catalytic activities were measured in stable SH-SY5Y cell clones in vitro via a radiometric method using ^{14}C -Tyramine as a substrate and are expressed as pmoles/min/mg total protein \pm S.D, where $n=4$. MAO catalytic activity in MAO-A- clones was statistically compared to wild type activity using the Student's t-test where $**p<0.005$ and $***p<0.001$.

6.2.1.2 Morphology of MAO-A knockdown SH-SY5Y stable clones

Figure 6. 3 shows negative miRNA and MAO-A- SH-SY5Y cell morphologies. Both negative control clones and MAO-A knockdown clones show similar morphologies to wild type cells following expansion from 96-well plates to 25 cm^2 flasks. MAO-A- clone 10D8 was chosen to work with since it exhibited sufficient growth rate and consistently had ~50% knockdown of both MAO-A mRNA and catalytic activity. SH-SY5Y clone neg/2G11 was randomly chosen as the negative miRNA control.

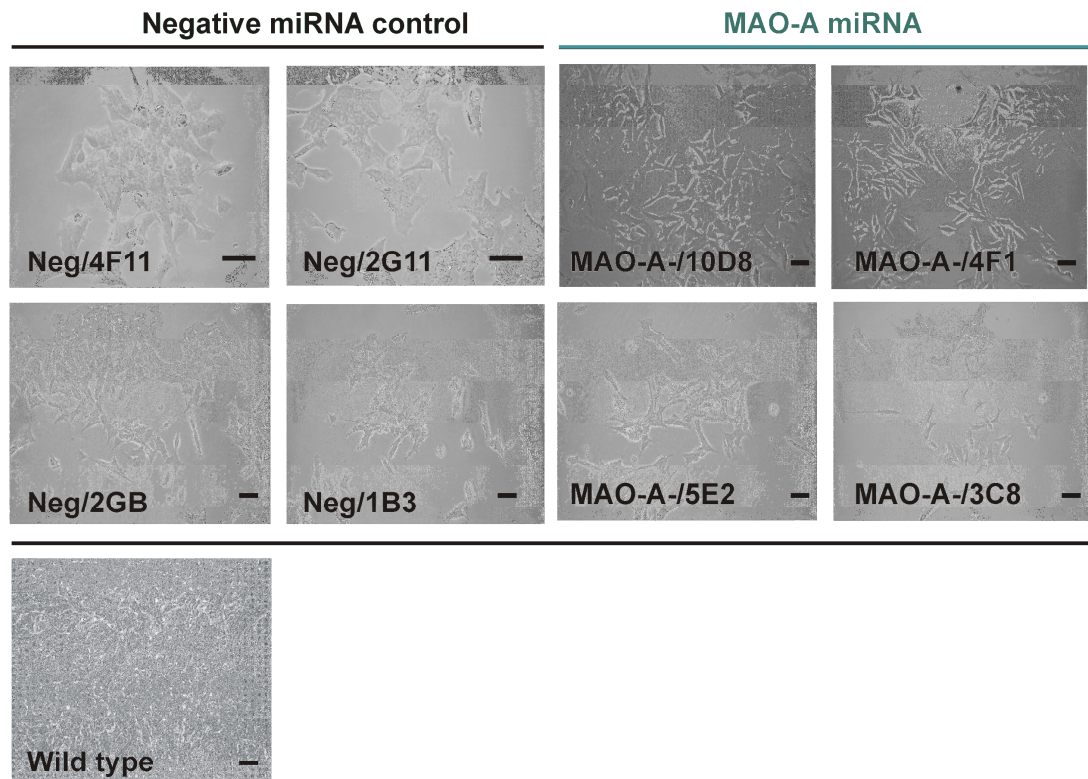


Figure 6. 3 Morphology of stable miRNA SH-SY5Y clones

Negative miRNA control transfected and MAO-A- miRNA stable SH-SY5Y clones observed by phase contrast microscopy. Cells were visualised using a Nikon eclipse TS100 microscope. Photomicrographs ($\times 20$ and $\times 40$ objectives, taken on Nikon DN100 digital camera). Scale bar represents $20 \mu\text{M}$.

6.2.2 Characterisation of working MAO-A knockdown clone 10D8

6.2.2.1 MAO-A protein levels

MAO-A protein levels in MAO-A-/10D8 cells were observed by immunohistochemistry (Figure 6. 4A), confocal microscopy (Figure 6. 4B) and dot blotting (Figure 6. 5) using the specific MAO-A monoclonal antibody 6G11-E1. MAO-A protein detected using DAB as a substrate (shown by red/brown staining) is visibly reduced in MAO-A-/10D8 cells compared to controls. MAO-A protein detected by confocal microscopy in control SH-SY5Y cells gives a weak signal (see Figure 6. 4B *top left panel*), however, when MAO-A is overexpressed (Figure 6. 4B *top right panel*), the signal and resolution is stronger. Whilst in MAO-A-/10D8 cells the signal is even weaker (Figure 6. 4B *bottom panels*).

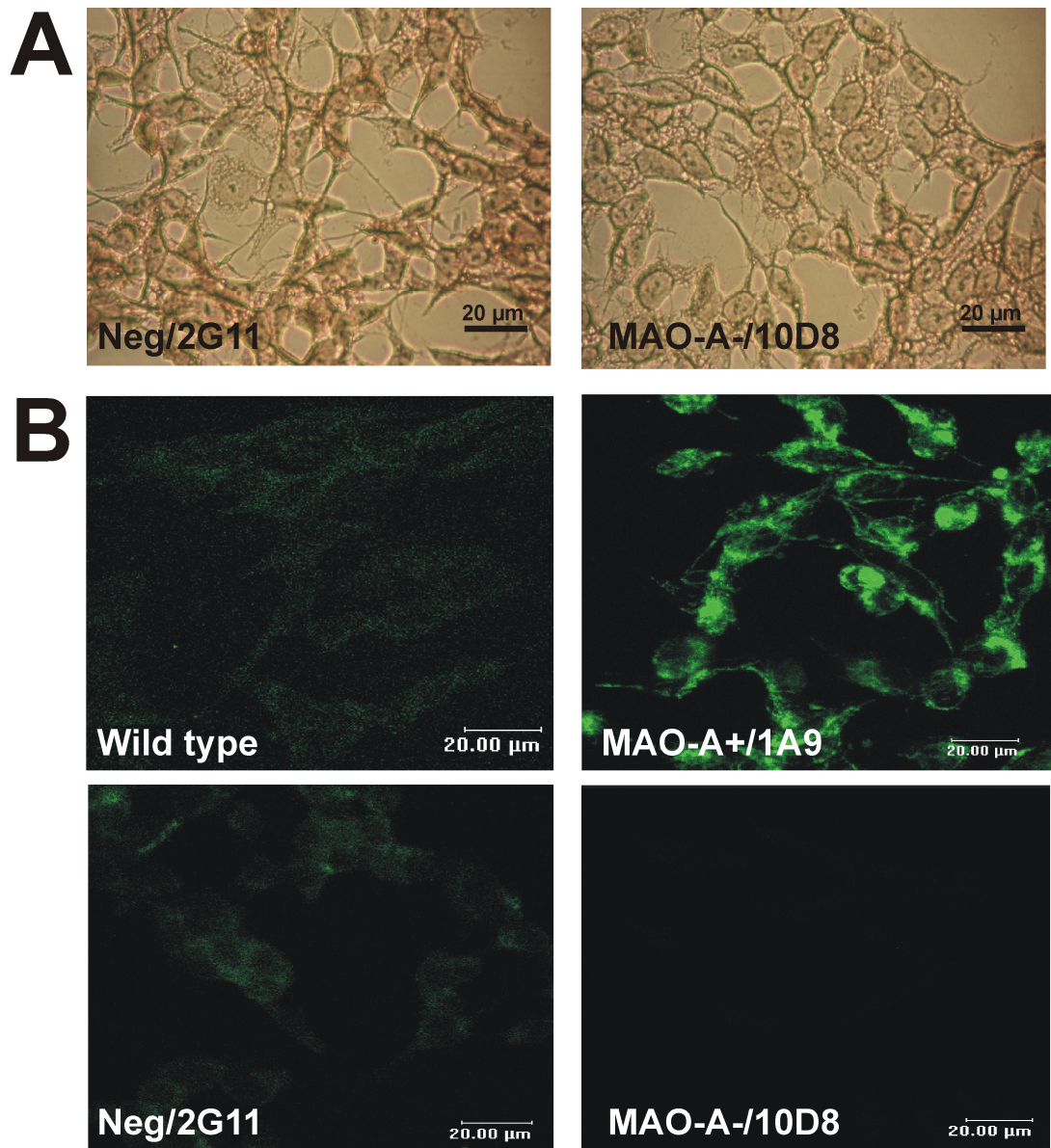


Figure 6. 4 MAO-A protein levels in MAO-A knockdown clone 10D8

(A) Immunohistochemistry – Negative miRNA control/2G11 and MAO-A-/10D8 clones were stained with MAO-A (6G11-E1) specific antibody and revealed using HRP-conjugated secondary antibody with 3, 3'-Diaminobenzidine (DAB) as substrate. Control sections incubated in the absence of MAO-specific antibodies but revealed under the same conditions did not reveal staining and are not shown. MAO specific immunoreactivity is represented by dark brown/red staining. The images shown are from a representative experiment. Scale bar represents 20 μm. (B) Confocal microscopy – Wild type, MAO-A+/1A9 (positive control), negative miRNA control/2G11 and MAO-A-/10D8 clones were exposed to MAO-A (6G11-E1) specific antibody and revealed using FITC-conjugated secondary antibody, which fluoresces green, visualised by a CLSM Leica microscope. Laser power is matched and all images are from the same experiment. Photomicrographs are representative of 2 independent experiments.

Figure 6. 5 shows a representative dot blot and quantification of MAO-A protein detected by MAO-A specific antibody in MAO-A-/10D8 clones. Dot blot (Figure 6. 5A) showing less MAO-A protein in MAO-A-/10D8 cells compared to negative miRNA control cells,

which is approximately half the amount of protein present in both the negative control clone 2G11 and wild type cells (Figure 6. 5B).

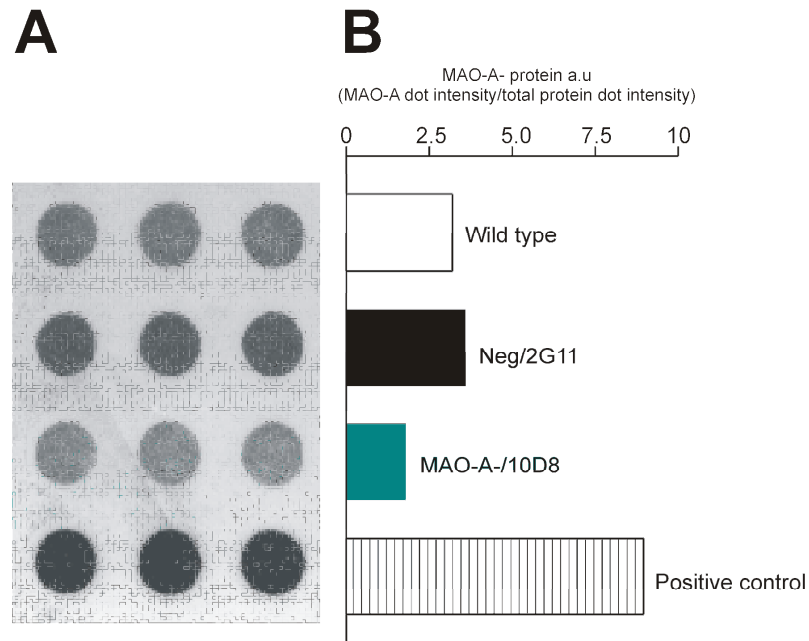


Figure 6. 5 MAO-A protein detected by dot blotting in MAO-A knockdown SH-SY5Y and controls (A) Dot blot of MAO-A protein levels in Neg/2G11 and MAO-A-/10D8 SH-SY5Y stable clones. Equal protein homogenates (3 μ g) were loaded on to a nitrocellulose membrane (except positive control, 1 μ g) and probed with a MAO-A specific antibody. Mitochondrial membranes from human placenta are the positive control and no primary antibody was the negative control (not shown). (B) Quantification of dots. The dots were digitised and densitometry was performed to quantify relative MAO-A protein levels normalised to total protein levels (copper stain) and expressed as normalised MAO-A protein in arbitrary units (a.u).

6.2.2.2 Cell growth and viability

Growth rates of Neg/2G11 and MAO-A-/10D8 clones were determined by viable cell counts and compared to the growth rate of wild type SH-SY5Y cells. Figure 6. 6A shows that Neg/2G11 cells grow slower than wild type cells and have a doubling time of ~31 hours, which is 10 hours longer than wild type doubling time (22 hours, Figure 6. 6B), supporting data in chapter 5. Two MAO-A- clones were assessed, MAO-A-/4F1 and MAO-A-/10D8. MAO-A-/4F1 grew at the same rate as wild type SH-SY5Y and had a similar doubling time. Compared to negative control, growth rates were faster in both MAO-A+ clones (Figure 6. 6B).

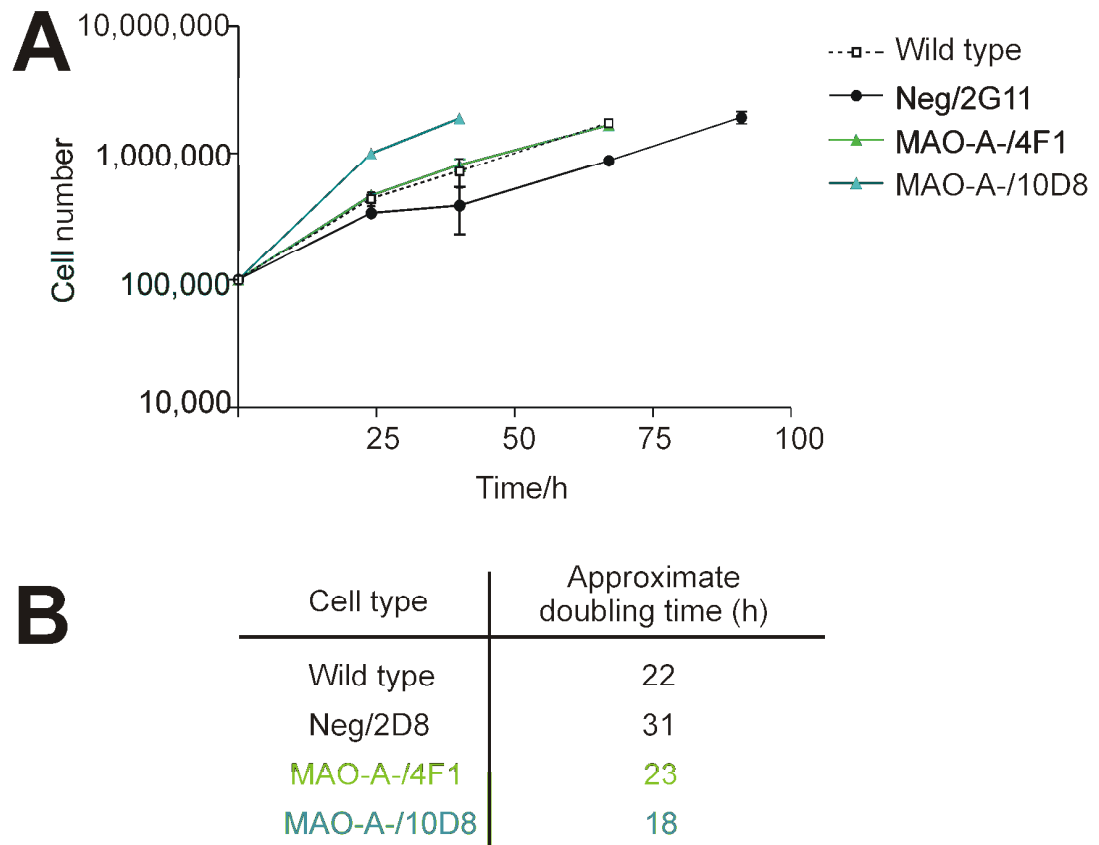


Figure 6. 6 Growth and doubling times of wild type, negative miRNA control and MAO-A- clones

(A) Growth of wild type, Neg/2G11 and MAO-A-/4f1 and 10D8 cells. Cell numbers were determined by viable cell counts from two independent cell populations and from four counts from the each sample. Data are expressed as mean cell number \pm SD. Data was plotted on a log scale Y axis. (B) Doubling times were calculated (see section 2.) and expressed as approximate doubling time (h).

Cell viability measured by MTT reduction (cell metabolism) in untreated MAO-A knockdown SH-SY5Y clones and controls revealed increased MTT reduction in both Neg/2G11 and MAO-A-/10D8 compared to wild type SH-SY5Y over a 72 h growth period (Figure 6. 7) and no difference between Neg/2G11 control and MAO-A knockdown clones.

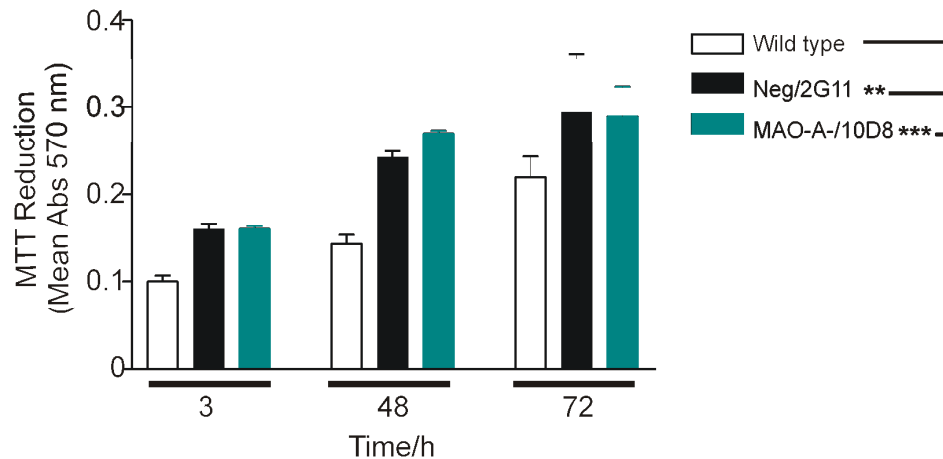


Figure 6. 7 MTT reduction in MAO-A knockdown SH-SY5Y cells and controls

MTT reduction was measured in wild type, Neg/2G11 and MAO-A-/10D8 cells over a 72 h culture period and expressed as mean absorbance values at 570 nm \pm S. D. Replicates in assay=12 and n=9. MAO-A- and Neg/2G11 cell MTT reduction was statistically compared to wild type MTT reduction over time using two way ANNOVA test where ** $p < 0.005$ and *** $p < 0.001$. Neg/2G11 MTT reduction over time was compared to MAO-A-/10D8 MTT reduction overtime using two way ANNOVA, which was not significantly different at confidence value $p = < 0.05$.

2 Cell structure and GAPDH localisation

To determine whether cell morphology and cytoskeleton is affected by MAO-A knockdown in SH-SY5Y cells, antibodies directed against the structural proteins α -tubulin and β -actin were revealed by confocal microscopy in MAO-A-/10D8 cells and neg/2G11 and wild type controls. MAO-A knockdown did not change structural proteins or cell morphology, compared to both negative miRNA and wild type controls (Figure 6. 8).

GAPDH translocates to the nucleus in SH-SY5Y cells overexpressing MAO-A in long term culture (Figure 5.12), whereas MAO-A-/10D8 SH-SY5Y clones have similar GAPDH distribution to Neg/2G11 control cells and no GAPDH in the nucleus (Figure 6. 8).

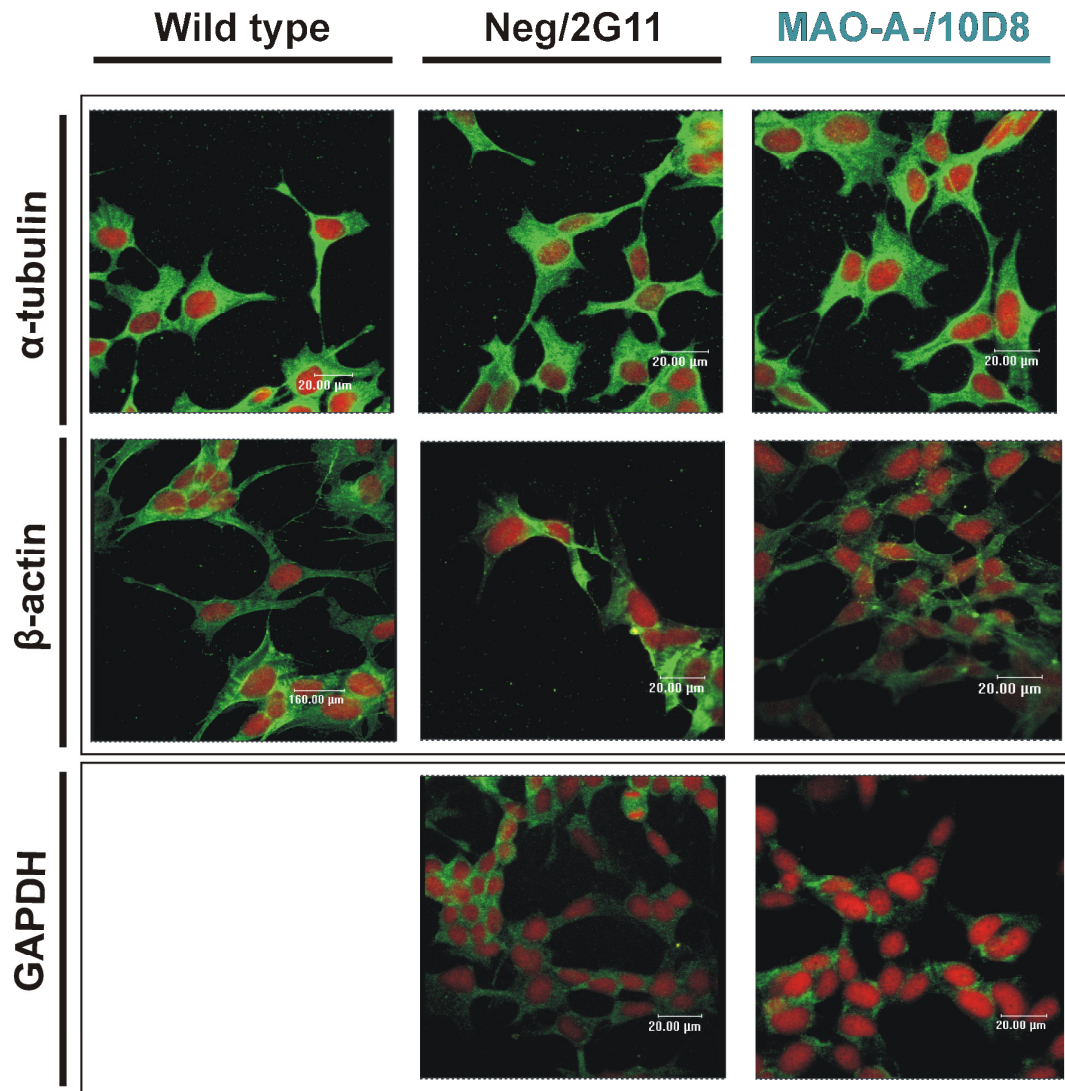


Figure 6. 8 Cytoskeletal and GAPDH proteins in MAO-A knockdown SH-SY5Y cells and controls

Wild type, negative miRNA and MAO-A-/10D8 clones were exposed to α -tubulin, β -actin and GAPDH specific antibodies and revealed using a FITC-conjugated secondary antibody (green). Nuclei were counter-stained with propidium iodide (red). Images were taken at $\times 63$ magnification and scale bars are shown on each photomicrograph. Laser power was matched between different cell types for each protein of interest.

2 ROS

ROS levels in untreated MAO-A-/10D8 cells are slightly reduced compared to negative control cells (Figure 6. 9).

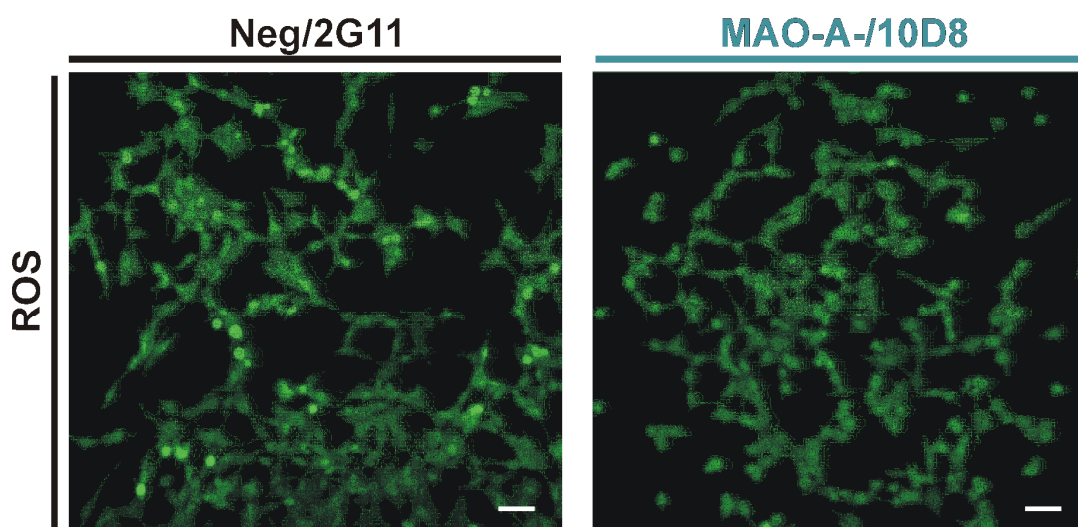


Figure 6.9 ROS levels in untreated MAO-A knockdown SH-SY5Y and negative miRNA control
DCDHF fluorescence was monitored in live Neg/2G11 cells (left panel) and MAO-A-/10D8 cells (right panel) and visualised using a CLSM Leica microscope. Photomicrographs shown are representative of three independent experiments. Laser power matched. Scale bar represents 40 μ m.

6.2.3 Effect of MAO-A knockdown on apoptotic induction

To determine the relevance of MAO-A in neuronal apoptosis, cell viability, ATP and caspase-3 assays were performed on MAO-A-/10D8 cells and their response to three different apoptotic inducers compared to control cells. Apoptotic cell death was induced by treatment with STS (previously characterised in chapter 3), rotenone (previously characterised in chapter 4) and serum withdrawal (previously characterised in chapter 4).

Cell metabolism was determined by MTT reduction. Following STS treatment for 3 h cell viability was not significantly reduced in wild type cells (see chapter 3). Negative miRNA cells had insignificant MTT reduction compared to wild type cells and MAO-A-/10D8 cells were unaffected by STS (Figure 6. 10A). Rotenone treatment for 48 h caused a ~40% reduction in cell viability in wild type cells, which was further and significantly reduced in negative miRNA control cells. Knockdown of MAO-A significantly reduced this loss in cell viability by approximately 25% (Figure 6. 10B). Serum withdrawal for a 72 h period resulted in approximately 30 % loss of cell viability in wild type cells, miRNA and MAO-A knockdown cells (Figure 6. 10C).

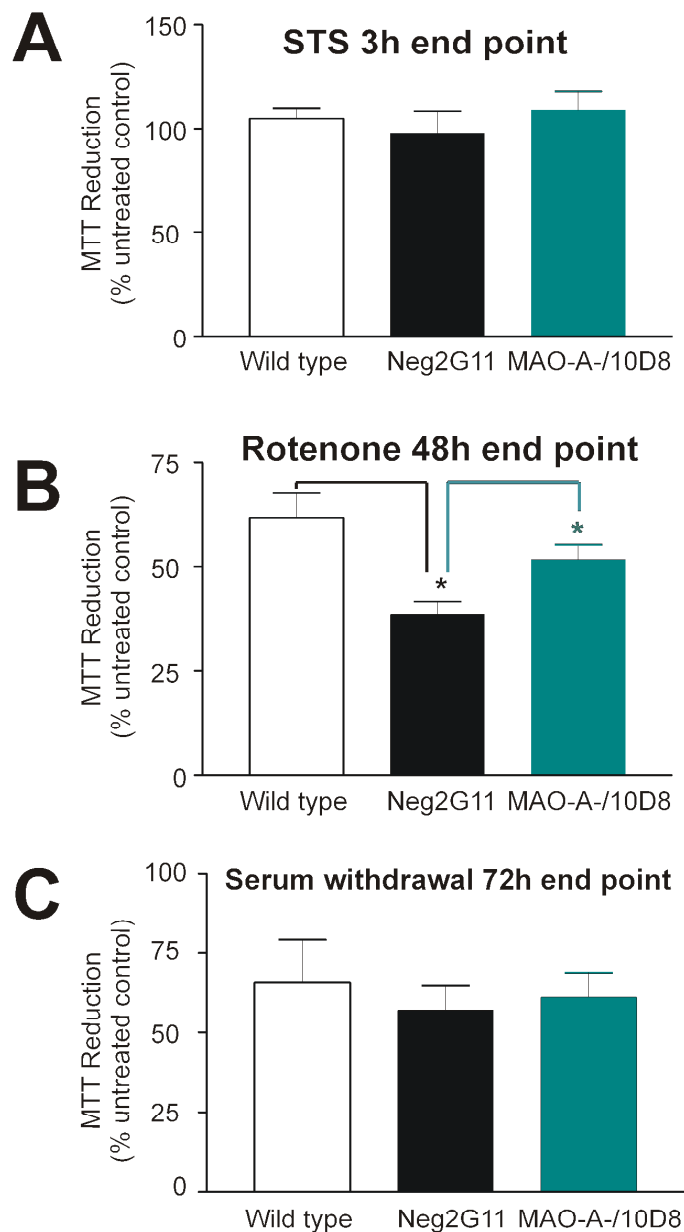


Figure 6.10 Effect of apoptotic inducers on cell viability of MAO-A knockdown SH-SY5Y and controls Cell viability was measured following (A) 1 μ M STS treatment for 3 h, (B) 0.5 μ M rotenone treatment for 48 h and (C) serum withdrawal treatment for 72 h. MTT reduction was determined and expressed as % untreated control \pm S. D. Replicates in assay=12 and n=4. % control untreated MTT reduction in wild type cells was statistically compared to MTT reduction in neg/2G11 and MAO-A-/10D8 cells using the Student's t-test, where *=p<0.05. % untreated control MTT reduction in neg/2G11 cells was statistically compared to % untreated control MTT reduction in MAO-A-/10D8 cells using the Student's t-test, where *=p<0.05.

ATP levels in untreated wild type, MAO-A+/10D8 and negative control cells were similar at around 500 pmoles/ μ g total protein following STS treatment for 3 h, albeit the levels in

the knockdown and negative control cells were not significantly higher than wild type cells (data not shown).

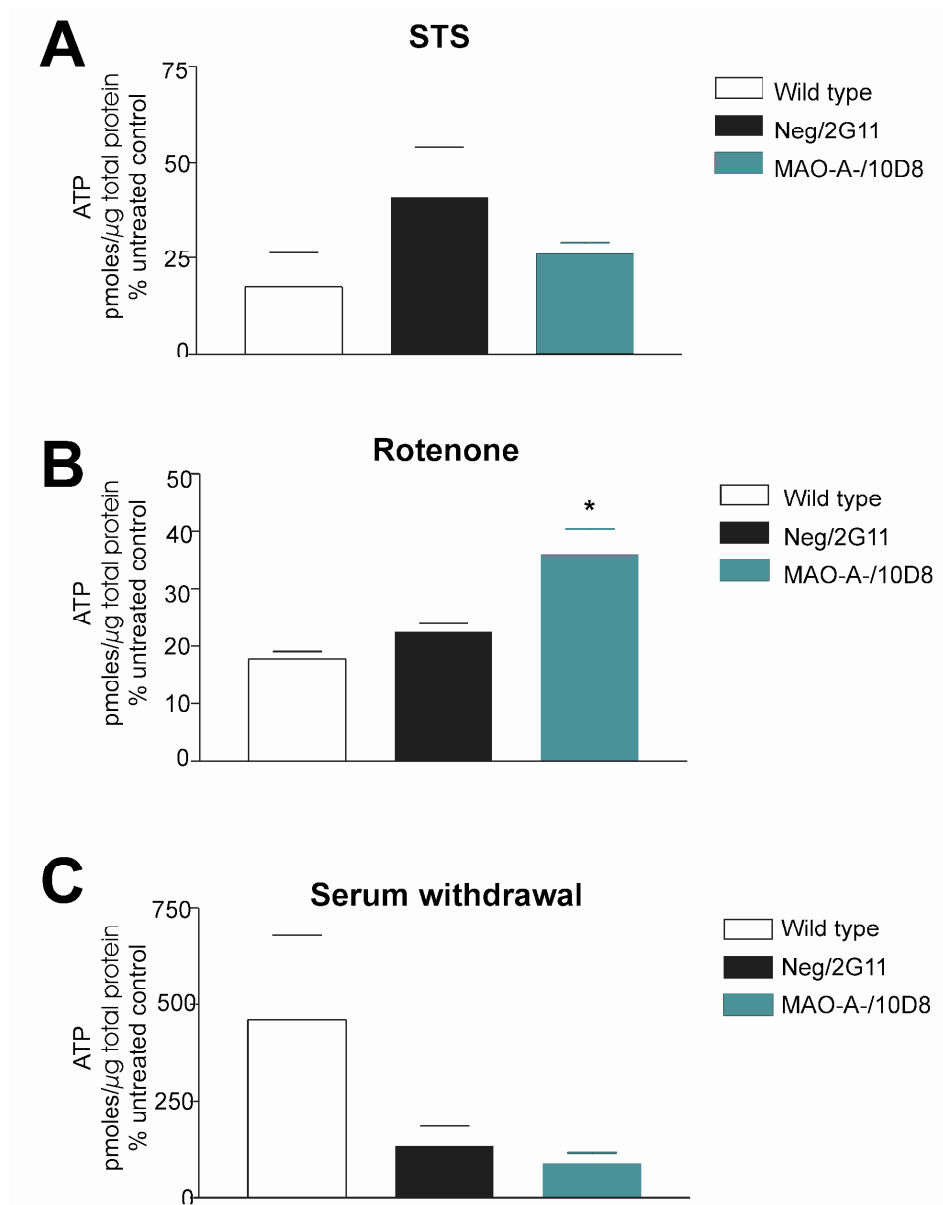


Figure 6. 11 Effect of apoptotic inducers on ATP levels in MAO-A knockdown SH-SY5Y and controls ATP was measured following (A) 1 μ M STS treatment for 3 h, (B) 0.5 μ M rotenone treatment for 48 h and (C) serum withdrawal treatment for 72 h. ATP levels were determined using a luciferase based assay, amount of ATP was determined using ATP standards and expressed as % untreated control \pm S. D. Replicates in assay=12 and n=3. ATP levels in wild type cells were statistically compared to ATP levels in negative miRNA controls and ATP levels in negative miRNA control cells were statistically compared to ATP levels in MAO-A-/10D8 cells using the Student's t-test, where *= p <0.05.

Rotenone reduced ATP levels in wild type cells and negative controls by around 80% (Figure 6. 11B). In MAO-A-/10D8 cells, ATP levels were reduced by ~70 % by rotenone ; this smaller loss of ATP was significantly less than in the negative control cells (Figure 6. 11B). Serum deprivation for 72 h caused increased ATP levels in wild type cells (more

than four fold untreated levels). Negative miRNA clones had reduced ATP levels following serum deprivation, but ATP levels in MAO-A knockdown were unchanged following serum deprivation (Figure 6. 11C).

Basal caspase-3 levels were similar in wild type, negative controls and MAO-A+/10D8 cells (Figure 6. 12). As previously described in chapter 3, 1 μ M STS induces apoptotic morphologies within 1 h of treatment in wild type cells. Negative control cells responded similarly to wild type cells following STS exposure (Figure 6. 12A, and chapter 3.2). MAO-A knockdown protected SH-SY5Y cells from apoptotic morphologies caused by STS in the early phases of apoptosis (1h, Figure 6. 12A). This is complimented by reduced caspase-3 activation (albeit this was not statistically significant) following 1 hr STS treatment (Figure 6. 12B). However, after 3 h STS treatment (peak caspase-3 activity in wild type cells), morphologies and caspase-3 activity in control cells and MAO-A-/10D8 cells are similar (Figure 6. 12C).

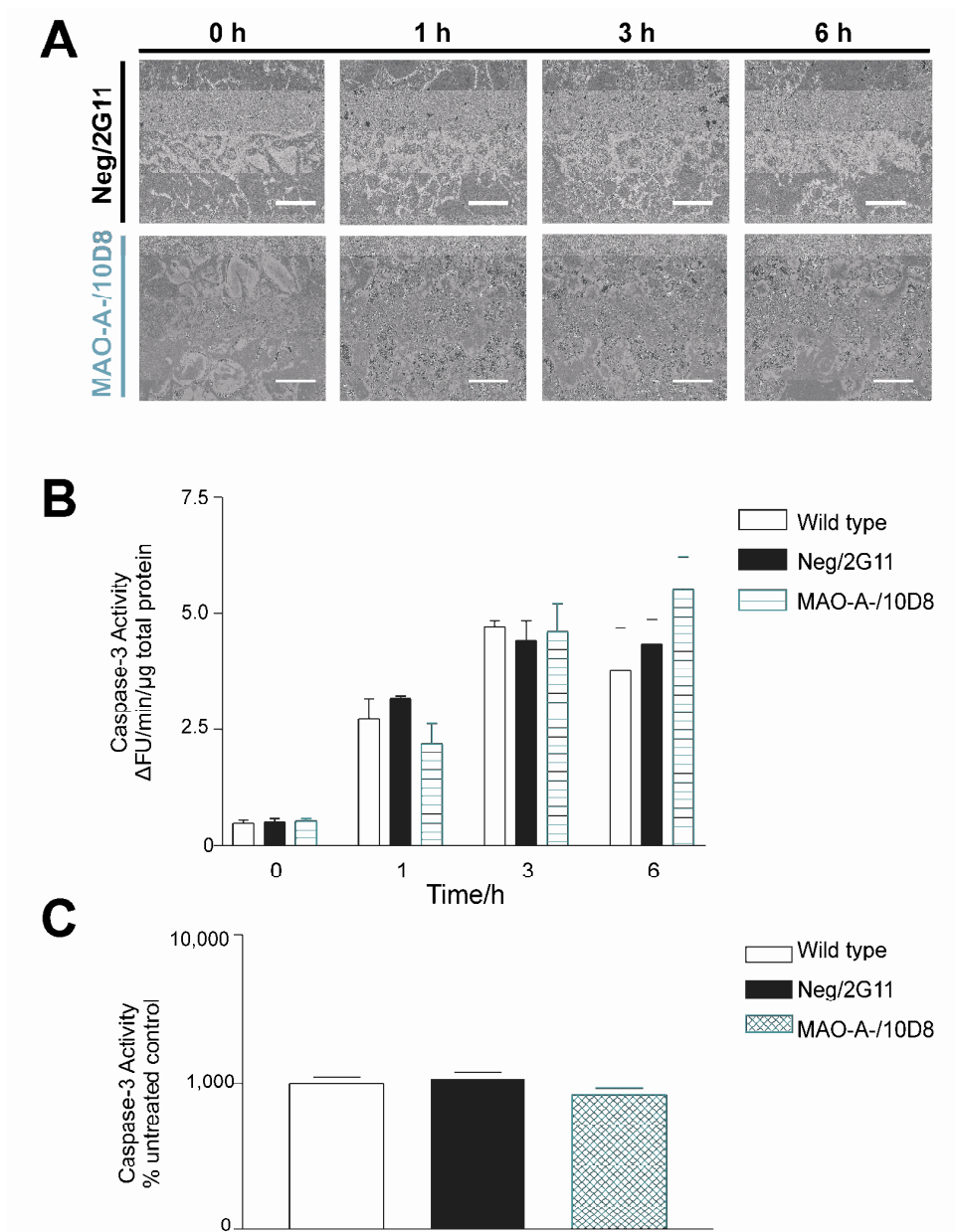


Figure 6. 12 Effect of STS treatment on caspase-3 activity and apoptotic morphology in MAO-A knockdowns

(A) Neg/2G11 and MAO-A-/10D8 SH-SY5Y clones observed by phase contrast microscopy following 1 μ M STS treatment over a 6h period. Cells were visualised using a Nikon eclipse TS100 microscope. Photomicrographs ($\times 40$ objectives, taken on Nikon DN100 digital camera). Scale bar represents 20 μ M. (B) Caspase-3 activity measured using Acetyl-Asp-Glu-Val-Asp-7-Amidomethylcoumarin as substrate in wild type, Neg/2G11 and MAO-A-/10D8 following 1 μ M STS treatment over a 6h period and expressed as Δ FU/min/ μ g protein S.D. Data represents values from four independent experiments over, where each extract was assayed in triplicate. (C) Data in B at 3h end point, expressed as % untreated control.

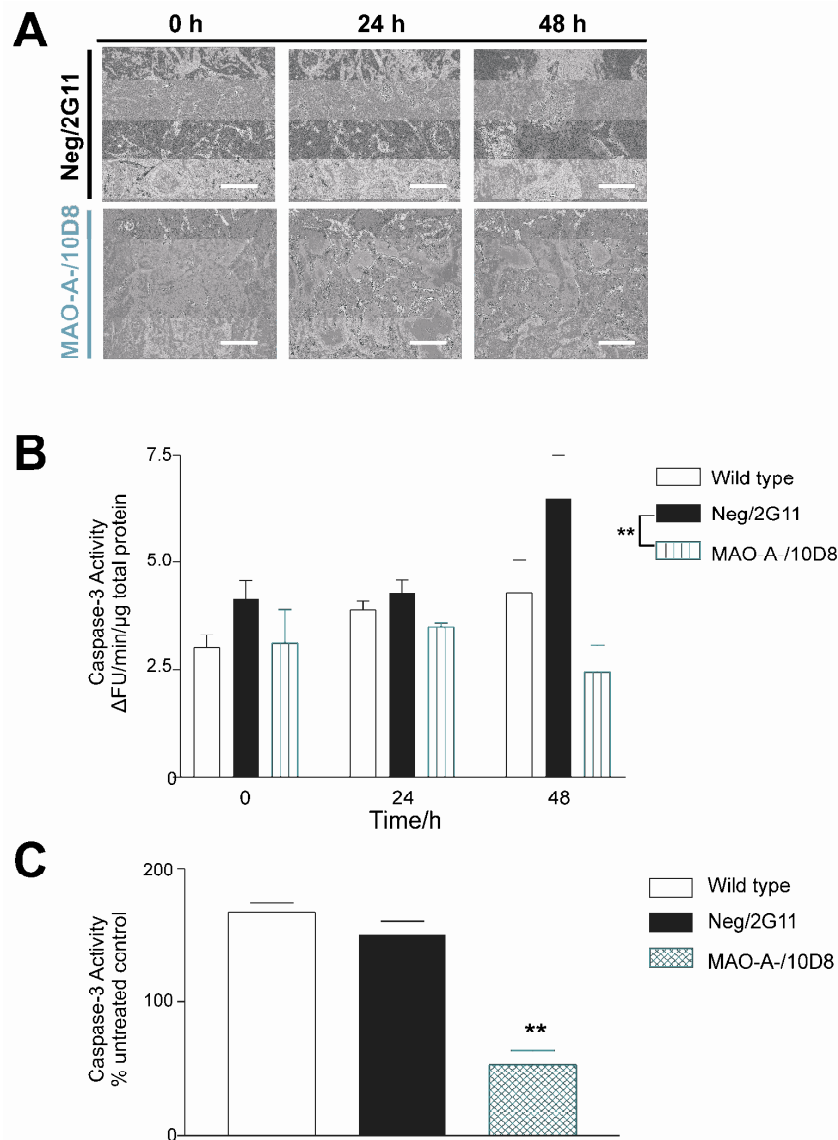


Figure 6. 13 Effect of rotenone treatment on caspase-3 activity and apoptotic morphology in MAO-A knockdowns

(A) Neg/2G11 and MAO-A-/10D8 SH-SY5Y clones observed by phase contrast microscopy following 0.5 μ M rotenone treatment over a 72h period. Cells were visualised using a Nikon eclipse TS100 microscope. Photomicrographs ($\times 40$ objectives, taken on Nikon DN100 digital camera). Scale bar represents 20 μ M. (B) Caspase-3 activity measured using Acetyl-Asp-Glu-Val-Asp-7-Amidomethylcoumarin as substrate in wild type, Neg/2G11 and MAO-A-/10D8 following 0.5 μ M rotenone treatment over a 48h period and expressed as Δ FU/min/ μ g protein \pm S.D. Data represents values from four independent experiments over, where each extract was assayed in triplicate. Statistical analysis was performed using the two way ANNOVA test for variance between Neg/2G11 controls and MAO-A-/10D8 cells following rotenone treatment over the time course, where $**=p<0.005$. (C) Data shown in B, at a 48 h end point and expressed at % untreated control. Caspase-3 levels in negative miRNA control cells were statistically compared to caspase-3 levels in MAO-A-/10D8 cells using the Student's t-test, where $*=p<0.05$.

Rotenone causes a dramatic loss of cell viability and apoptotic morphology after 48 h treatment in wild type and negative miRNA control cells (Figure 6. 13A), linked with a 50 % activation of caspase-3 (Figure 6. 13B). MAO-A knockdown reduces cell loss following

48 h rotenone treatment (Figure 6. 13A), but by 72 hrs cells are also floating and apoptotic (data not shown). Caspase-3 is not activated following 48 h rotenone treatment in MAO-A knockdown cells (Figure 6. 13C).

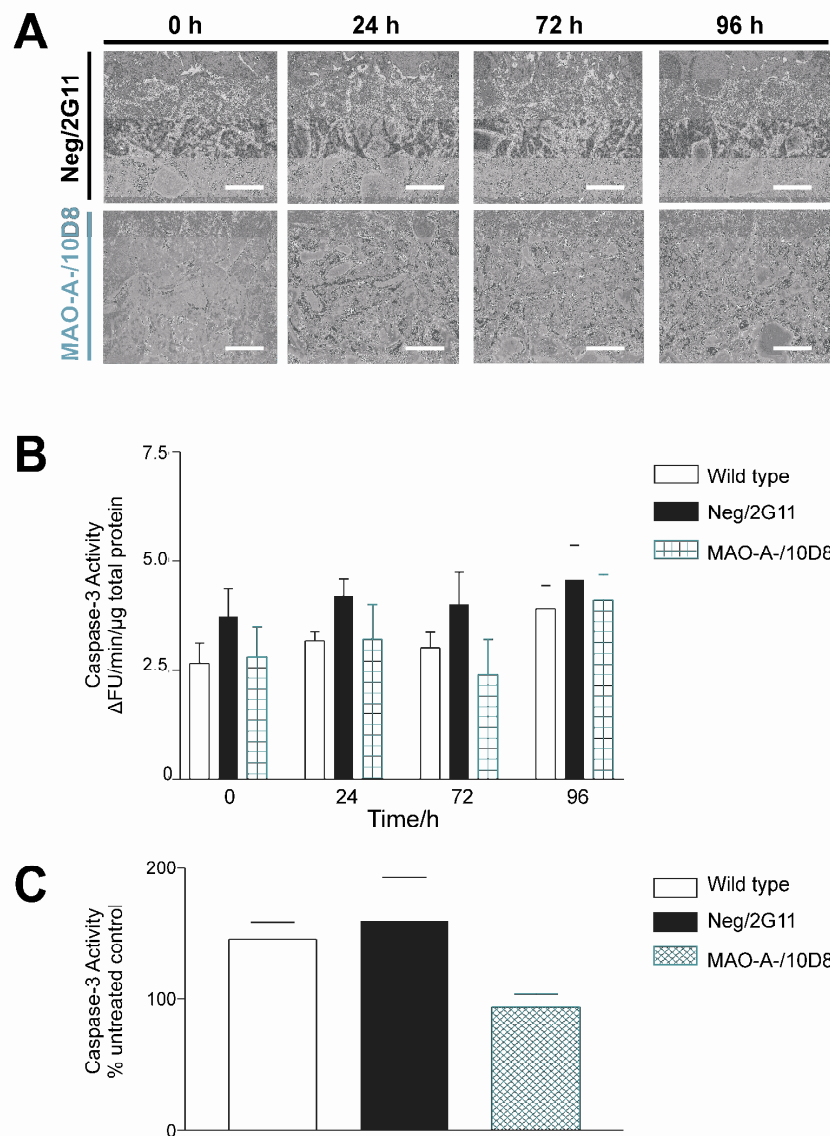


Figure 6. 14 Effect of serum withdrawal on caspase-3 activity and apoptotic morphology in MAO-A knockdowns

(A) Neg/2G11 and MAO-A-/10D8 SH-SY5Y clones observed by phase contrast microscopy following serum withdrawal over a 96h period. Cells were visualised using a Nikon eclipse TS100 microscope. Photomicrographs ($\times 40$ objectives, taken on Nikon DN100 digital camera). Scale bar represents 20 μ M. (B) Caspase-3 activity measured using Acetyl-Asp-Glu-Val-Asp-7-Amidomethylcoumarin as substrate in wild type, Neg/2G11 and MAO-A-/10D8 following serum withdrawal over a 96h period and expressed as Δ FU/min/ μ g protein \pm S.D. Data represents values from four independent experiments over, where each extract was assayed in triplicate. (C) Data shown in B, at a 48 h end point and expressed at % untreated control. Caspase-3 levels in negative miRNA control cells were statistically compared to caspase-3 levels in MAO-A-/10D8 cells using the Student's t-test, where $*=p<0.05$.

Serum withdrawal causes apoptotic morphologies in SH-SY5Y cells after 24 hrs of deprivation. However, MAO-A-/10D8 cells did not appear apoptotic until \sim 72-96 h

following serum deprivation (Figure 6. 14A). Caspase-3 activity in MAO-A+/10D8 cells remained unchanged at 72 h (Figure 6. 14C).

Treatment	Loss of cell viability (MTT)	Apoptotic morphologies	ATP level	Caspase-3 activation
<i>STS</i>	No effect	Protective	No effect	Protective only in early apoptotic phase
<i>Rotenone</i>	Significantly protective	Significantly protective	Significantly protective against depletion	Significantly protective
<i>Serum withdrawal</i>	No effect	Protective	Remains unchanged (no elevation during SW)	Remains Unchanged (no activation)

Table 6. 2 A summary of the effects of MAO-A knockdown in SH-SY5Y cells on their response to different apoptotic inducers

6.3. DISCUSSION

6.3.1 Stable MAO-A knockdown in SH-SY5Y cells

Stable knockdown of MAO-A was successful. Nearly all the SH-SY5Y clones expanded for MAO assays had significantly reduced MAO-A activity. Maximum knockdown of MAO-A activity achievable from the clones picked was around 50% (Figure 6. 2B). Similarly, MAO-A mRNA expression levels were also reduced by 50% in three MAO-A knockdown clones assayed by qRT-PCR (Figure 6. 2A). Semi-quantitative measurement of MAO-A protein levels in the MAO-A knockdown clone 10D8 revealed a 50% reduction compared to controls (Figure 6. 5). These data were supported by immuno-histochemical / -fluorescent analysis of protein levels (Figure 6. 4A and B).

Data from qRT-PCR and MAO activity assays indicated that transfection with the negative miRNA control vector caused small increases in MAO-A expression of around 20 % in the N2G11 clone (Figure 6. 2). This increase may result from the stress of the transfection procedure and/or the presence of the selection marker blasticidin. Nonetheless, the fact that sufficient knockdown of MAO-A was still achieved in the MAO-A/- clones indicates the efficiency of the method.

Although RNAi technology is the most specific and effective technique known to induce loss of function *in vitro* (Constans 2005), 100 % knockdown is rarely achieved. Part of the

aim of this chapter was to support data in this thesis using MAO inhibitors. *In situ*, both MAO inhibitors clorgyline and TCP were able to reduce MAO activity by approximately 90% in untreated cells (Figure 3.13), which is more effective than the 50% knockdown achieved here with miRNA technology. On the other hand, in the only known study where siRNA silencing of MAO-A has been reported, MAO activity was reduced by only 25% (Yi *et al.* 2006a).

6.3.2 Characteristics of stable MAO-A knockdown clone 10D8

MAO-A- stable clones had similar morphologies to wild type cells (Figure 6. 3) and grew at similar rates generally. However, Neg/2G11 cells grew at a slower rate than wild types cells (doubling times of 31 and 22 h respectively) and MAO-A-/10D8 cells had a faster growth rate than the negative control cells, having a doubling time of 18 h (Figure 6. 6). MTT reduction in both Neg/2G11 and MAO-A-/10D8 cells were significantly greater than in wild type cells over a 72 h period (Figure 6. 7), but there was no difference between the MAO-A-/10D8 and Neg/2G11 cells. Cytoskeletal staining remained unchanged for both α -tubulin and β -actin proteins in MAO-A-/10D8. These data imply that reduced MAO-A has no effect on cell division or cell structure.

In addition to its role in cell death mechanisms, MAO may also help to maintain steady state levels of ROS and therefore play a role in cell survival and proliferation. Further work is needed in this area to understand the mechanisms involved. Interestingly, ERK inhibition resulted in further increased MAO-A catalytic activity and MAO-A mRNA expression following serum withdrawal-induced MAO activation (Figure 4.27), implying that ERK MAPK may be involved in modulating MAO-A expression as part of cell survival mechanisms.

According to Cadenas and Davies (2000) calculations, if MAO-A activity is reduced by 50 % (as in the case of MAO-A-/10D8 cells), the steady state concentration of H₂O₂ formed from MAO will be approximately 4×10^{-7} M. In the resting cell, the effect of this reduction may not be apparent because of limitations of available detection methods. Indeed, ROS levels measured in MAO-A-/10D8 cells were only very slightly reduced compared to negative control cells (Figure 6. 9).

Untreated MAO-A-/10D8 cells showed no evidence of GAPDH in nuclei (Figure 6. 8) and levels of both ATP (Figure 6. 11) and active caspase-3 (Figure 6. 12) were similar to control levels. These data further confirm that resting MAO-A-/10D8 cells are not apoptotic and loss of MAO-A function is not detrimental. These findings are consistent with

our knowledge of decreased MAO-A expression *in vivo*, where even complete deletion of MAO-A expression is not fatal. The remaining MAO-A in MAO-A-/10D8 cells is able to maintain functionality as far as deamination of amines and possibly production of ROS as a second messenger in survival.

6.3.3 The effect of MAO-A knockdown in selected apoptotic models

Three different apoptotic inducers previously characterised in this thesis were used to challenge MAO-A-/10D8 cells. The three inducers STS, rotenone and serum withdrawal represent three distinct types of cell death.

6.3.3.1 STS

STS causes rapid and strong induction of caspase-3 activity in wild type cells (Figure 3.10 and Figure 6. 12) and depletes ATP levels in wild type cells, but has no significant effect on MTT reduction over 3 h (Chapter 3, Figure 3.15). MTT reduction in Neg/2G11 and MAO-A-/10D8 also remained unchanged following STS exposure for 3 h (Figure 6. 10). MTT is not a good measure of cell viability/proliferation in the STS model, since cells remain metabolically active throughout the short apoptotic time course. MAO-A knockdown had no significant effects on ATP levels at 3 h either. This might be explained by the nature of STS-induced cell death. At 3 h following STS treatment in wild type cells, caspase-3 levels are maximal and increased MAO activity occurs prior to caspase-3 activation. Since up-regulation of the MAO-A gene was not apparent in the wild type STS model (Chapter 3); post-transcriptional events were thought to be important. Hence, remaining MAO-A enzyme/ MAO-A mRNA levels in MAO-A-/10D8 cells may still be sufficient for post-transcriptional modification and therefore increased catalytic activity following STS insult. Events that follow MAO's early role here (such as ATP depletion) may be unaffected. Measurements of MAO activity in STS treated MAO-A-/10D8 cells should be undertaken to confirm this.

Interestingly, MAO-A knockdown slows caspase-3 activation, since at 1 h caspase-3 activity is reduced compared to control cells by around 30 % (Figure 6. 12B). This protection in the early phase is evident in cell morphologies following STS treatment (Figure 6. 12A). Reduction of MAO-A in MAO-A-/10D8 cells is relevant in the first hour since MAO acts upstream of apoptotic execution. However, a 50 % reduction of MAO may not be sufficient to override the apoptotic execution by this potent toxin.

6.3.3.2 Serum withdrawal

Serum withdrawal induced loss of cell proliferation (measured by MTT reduction) in control cells, by around 35%. MAO-A knockdown did not affect this loss of cell viability/proliferation (Figure 6. 10). MAO-A acts late in the death processes induced by serum withdrawal in wild type cells, enhancing already activated apoptotic signals. In wild type cells (chapter 4), MAO inhibitors had no effect on MTT reduction during serum withdrawal; therefore it was likely that MAO-A knockdown had no effect on MTT reduction levels.

Serum withdrawal causes a rise in ATP levels in wild type cells at 72 h (Figure 6. 11). Increased ATP reflects the cell's need for energy at this time. Since serum withdrawal is a slow, highly regulated process, increased ATP in serum withdrawal may be viewed as a necessary event for the progression of apoptosis and may arise from release of mitochondrial ATP. It is interesting that, in Neg/2G11 cells ATP levels are significantly reduced after 72 h. It is possible that Neg/2G11 cells (having more MAO expression and being consistently more sensitive), have more rapidly progressed into apoptosis and therefore have reduced ATP levels. ATP levels in MAO-A-/10D8 cells do not change in response to serum withdrawal, but the levels are significantly higher than in the miRNA control cells. The role of ATP is complicated and a time course of ATP events is needed.

Caspase-3 activity was not increased significantly in any cell type following serum withdrawal and therefore there was no difference in their response to serum deprivation. MAO inhibitors had no effect on caspase-3 activation during serum withdrawal; it is not surprising that MAO-A knockdown had no effect on caspase-3 activity during serum deprivation. Indeed, cell morphologies in Neg.2G11 and MAO-A-/10D8 cells were similar throughout the time course (Figure 6. 14A).

The lack of effect of MAO-A knockdown in serum withdrawal-induced apoptosis is a indication of the different roles of MAO in different types of cell death. It is feasible that following serum deprivation in MAO-A-/10D8 cells, apoptosis occurs upstream of MAO-A. For example other pro-apoptotic proteins may come into force. Another possibility is that MAO-A is up-regulated following serum withdrawal in MAO-A-/10D8 cells (as in wild type cells) and although MAO-A miRNA may continue to target existing MAO-A mRNA, the miRNA system may be counteracted by new MAO-A transcription or increased stabilisation of MAO-A mRNA. It is also worth mentioning that production of miRNA is quite slow and in transient transfection experiments, cells were left for at least 48 h post-transfection for the miRNA process to have an effect. Serum withdrawal-induced apoptosis is also a slow process, however overexpression of MAO-A begins within the first

24 h. miRNA may be efficient at inhibiting normal MAO-A expression, but following apoptotic induction miRNA processes driven by the expression vector may result in less than efficiency in apoptotic MAO-A- cells compared to non-apoptotic MAO-A- cells.

6.3.3.3 Rotenone

Rotenone produces significant differences in ATP levels, MTT reduction, caspase-3 activity and morphologies between MAO-A-/10D8 cells and their controls. Less reduction in cell viability and ATP levels in MAO-A-/10D8 cells indicate protection from rotenone-induced apoptosis. The effects of rotenone in the neg/2G11 cells was greater than in wild type cells, suggesting that their increased sensitivity is due to the genetic manipulation, the presence of the selection marker and increased MAO-A expression.

Rotenone treatment reduced ATP levels in control cells by around 80% after 48 h, revealing dysfunction of mitochondrial electron transport. MAO-A knockdown was able to significantly reduce this effect by around 40 % compared to negative miRNA control (Figure 6. 11). Caspase-3 activity was increased following rotenone exposure in wild type cells, however the activation was low (Figure 6. 13B). This supports the idea that caspase-3 independent pathways are responsible for the majority of rotenone induced apoptotic signals (as discussed in chapter 4). Caspase-3 activity is increased to a larger extent in Neg/2G11, further supporting the idea that these cells are more sensitive to toxic insult. Knockdown of MAO-significantly reduced caspase-3 activation during rotenone-induced apoptosis, compared to the miRNA control (Figure 6. 13B). Neg/2G11 cells showed extensive apoptotic morphologies and cell death (indicated by floating cells) at 48 h whereas MAO-A-/10D8 cells at this stage continue to show normal SH-SY5Y phenotype and there are very few floating cells (Figure 6. 13A).

One can conclude from these data that MAO is more relevant to cell death mechanisms that arise from mitochondrial dysfunction. Mitochondria can respond rapidly to cellular events by tuning their input and output of a wide range of important mediators involved in cell function (Pagliarini 2006).

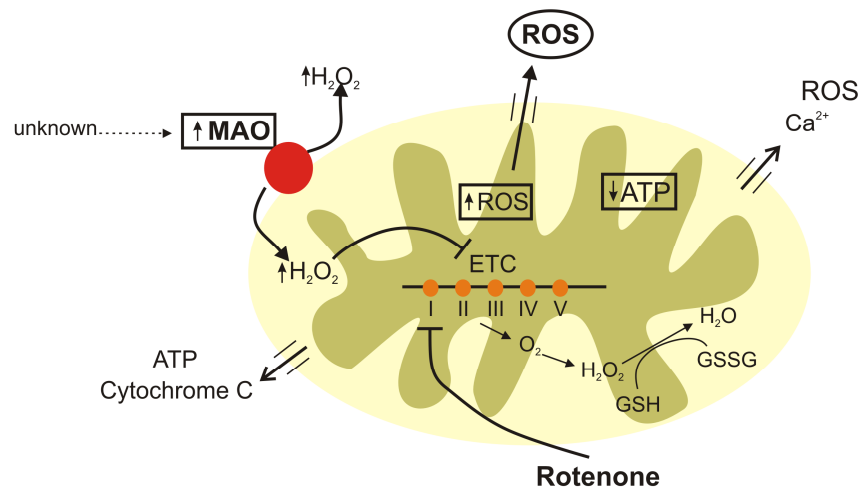


Figure 6. 15 Hypothetical schematic of MAO's ability to enhance rotenone-induced cell death

MAO activity is increased via an unknown mechanism. Increased production of ROS can affect mitochondrial respiration (Cohen and Kesler 1999) and this is thought to involve damage to electron transport chain proteins by H₂O₂ (Cohen et al. 1997).

6.3.4 Conclusion

Taken together these data reflect the role of MAO in each apoptotic model. MAO may enhance cell death mechanisms in the same way, regardless of the trigger (see general discussion). However, data shown in this chapter indicates that the apoptotic inducer rather affects how MAO is recruited. MAO-A knockdown only significantly reduced cell death induced by the mitochondrial toxin rotenone, but not by serum withdrawal or STS. These findings imply that MAO is involved in modulating mitochondrial function and therefore MAO plays a more important role in rotenone-induced cell death than in serum withdrawal or STS-induced death. This may have particular relevance in conditions such as PD where complex I dysfunction may be important.

CHAPTER 7

CONCLUSIONS AND FUTURE DIRECTIONS

CONCLUSIONS AND FUTURE DIRECTIONS

7.1. MAIN FINDINGS

In this study, the role of MAO in neuronal cell death was investigated in three diverse apoptotic models in human neuronal cells namely STS, serum withdrawal and rotenone. Elucidating the relevance of MAO in cell death was made possible by the use of MAO inhibitors and the creation of two stable neuronal cell lines where MAO levels were stably overexpressed or knocked down. The results suggested that MAO-A is involved in regulating cell death processes and that the mechanism and extent to which it is involved depends on the type of cell death and the nature of the inducer. These findings indicate that MAO-A may play a dynamic role in the cell. Indeed, MAO may have a dual role within the cell; to deaminate amines but at the same time to act as a sensor for mitochondrial function and stress and respond according. The MAO response appears to involve a combination of the promotion of oxidative stress at the mitochondria, redox imbalance and activation of apoptotic signalling pathways via its production of H₂O₂. However, the mechanism by which MAO is recruited and activated can change depending on the type of cell death. This was supported by the fact that in three very diverse models of apoptosis, MAO-A activation occurred by different mechanisms.

7.1.1 Role of MAO-A in STS and serum withdrawal models

In a classical model of apoptosis induced by staurosporine, my data shows for the first time that MAO-A was involved in this type of cell death. This occurs via MAPK signalling pathways upstream of apoptotic execution, which appears to be a result of MAO-A-dependent increase in ROS. However, the mechanism by which MAO-A activities are elevated is unknown, since up-regulation of the gene is not involved, although there is a transient increase in MAO-A protein levels. As discussed previously, post-transcriptional events account for a significant amount of expression regulation. Increased MAO-A in the STS model is likely to result from regulation of MAO-A RNA stability, catalytic environment or compartmentalisation of the enzyme. Increased MAO activity could also result from changes in the mitochondrial environment or a combination of these factors. Regulation of MAO catalytic activity may be influenced by the availability of substrates and co-factors and very recently Cao and colleagues (2007) showed that increased free calcium enhanced MAO-A catalytic activities via an unknown mechanism. Opening of the PTP following mitochondrial stress would certainly result in leakage of free calcium from

mitochondrial stores into the cytoplasm (Jacobson and Duchon 2002, Abou-Sleiman *et al.* 2006). Indeed H_2O_2 produced by MAO in rat brain mitochondria affects Ca^{2+} efflux and glutathione levels, two important factors in mitochondrial function (Sandri *et al.* 1990). An intense calcium flux in close vicinity to MAO enzyme could possibly increase activity (Cao *et al.* 2007).

In apoptosis induced by withdrawal of growth factors, the cell response was relatively slow but MAO-A gene expression, protein and activity levels were elevated after caspases were activated. These data suggest that the MAO-A gene is a target of stress-signalling pathways following serum withdrawal and that MAO generated oxidative stress impacts downstream of caspase-3 activities. It appears that the MAO-A gene is a target of the JNK and p38 MAPK signalling pathways in this model. This is the first time that JNK has been implicated in the expression regulation of MAO-A. The important role of the p38 signalling pathway was also confirmed, which was in agreement with previous reports (DeZutter and Davis 2001, Ou *et al.* 2006). As a consequence of elevated MAO-activity, it is likely that increased ROS cause PTP opening, release of Cyt-c and apoptosome formation since caspase 9 was activated. Inhibition of MAO consistently reduced caspase-9 activation. Inhibition of MAO may suppress PTP opening because of reduced ROS levels, which in turn reduces release of procaspase-9 stored within mitochondria (Krajewski *et al.* 1999).

Complete inhibition of MAO activity with clorgyline and TCP was significantly protective in each model of apoptosis.

7.1.2 Consequences of MAO-A overexpression

Overexpression of MAO caused cell death characterised by reduced cell growth rates, depleted ATP and loss of cell viability. Increased MAO activity resulted in massively increased oxidative stress (ROS levels) and eventually cell death. Chronic exposure to increased MAO-A activity induced a state of senescence/growth arrest and eventually death by necrosis. These data are in agreement with studies showing that H_2O_2 has a dose dependent effect on the cell and confirm that MAO has a central role in redox signalling, mitochondrial function and cell death. The fact that protective proteins such as Parkin suppress MAO-A expression (Jiang *et al.* 2006) support the finding that high MAO activity is pro-apoptotic.

7.1.3 Consequences of MAO-A knockdown

When levels of MAO activity were significantly reduced using inhibitory RNA technology, the cells were less sensitive to STS treatment in the early phases of apoptosis but not at peak caspase-3 activity. This supported the supposition that MAO is important in the initial phases of STS-induced apoptosis. MAO acts in the late phases of apoptosis in a serum withdrawal-apoptotic model and relies on up-regulation of pro-apoptotic genes, which may explain why MAO knockdown was not significantly protective. Increased gene expression in serum withdrawal may not be silenced by the miRNA efficiently for example.

Most significantly, reduced MAO-A levels protected against cell death induced by the complex 1 inhibitor rotenone, suggesting that MAO has an important role in regulating mitochondrial function. Rotenone-induced apoptosis was associated with reduced ATP levels, apoptotic morphologies and reduced cell metabolism, indicative of mitochondrial dysfunction, involving increased MAO activity and elevated ROS levels. ROS production is more relevant than ATP depletion to apoptosis induced by electron transport inhibitors (Watabe and Nakaki 2006), which may explain why MAO has a more significant role here. Rotenone also induced increased MAO activity levels in wild type cells.

7.1.4 Rotenone and mitochondrial regulation

Previously Cohen and others have described the mechanisms by which H_2O_2 produced by MAO can have a direct effect on inner mitochondrial invents by modifying IMM proteins such as those of the ETC. MAO-generated ROS is also known to damage mtDNA (Hauptmann *et al.* 1996) and reduce electron transport flux (Kumar *et al.* 2003). The OMM location of MAO is extremely important and MAO is often described in the literature as being a major source of mitochondrial ROS. As noted earlier increased H_2O_2 at the mitochondria is particularly toxic, since mitochondria harbour pools of copper and iron which can catalyse the Fenton reaction to produce the extremely damaging hydroxyl radical (Cadenas and Davies 2000). Even reversible damage to complex I can cause increased production of the equally damaging superoxide radical (Taylor *et al.* 2003). Decreases in respiratory chain complex activities and elevated iron concentrations have been implicated in neurodegenerative disorders such as PD (Davey *et al.* 1998, Anderson 2004). Mitochondrial damage mediated by MAO in rat brain caused deletions in mtDNA coding for ETC proteins, increased lipid peroxides and increased protein carbonyls which are suggestive of protein damage (Alves *et al.* 2007).

Since redox balance in the cell is tightly controlled it seems likely that MAO is also under the control of a set of signalling pathways. This is particularly true for other mitochondrial proteins that have recently been shown to be involved in protective signalling events that regulate mitochondrial function (Abou-Sleiman *et al.* 2006, Jiang *et al.* 2006). MAO expression has been shown to be under the control of a number of transcription factors and repressors that are inducible by diverse cellular signalling pathways, suggesting that MAO can be tightly controlled. Rotenone has been previously shown to mediate apoptosis via the activation of p38 and JNK MAPK in dopaminergic cells (Newhouse *et al.* 2004) and may be responsible for up-regulation of MAO-A activity following rotenone treatment in wild type cells.

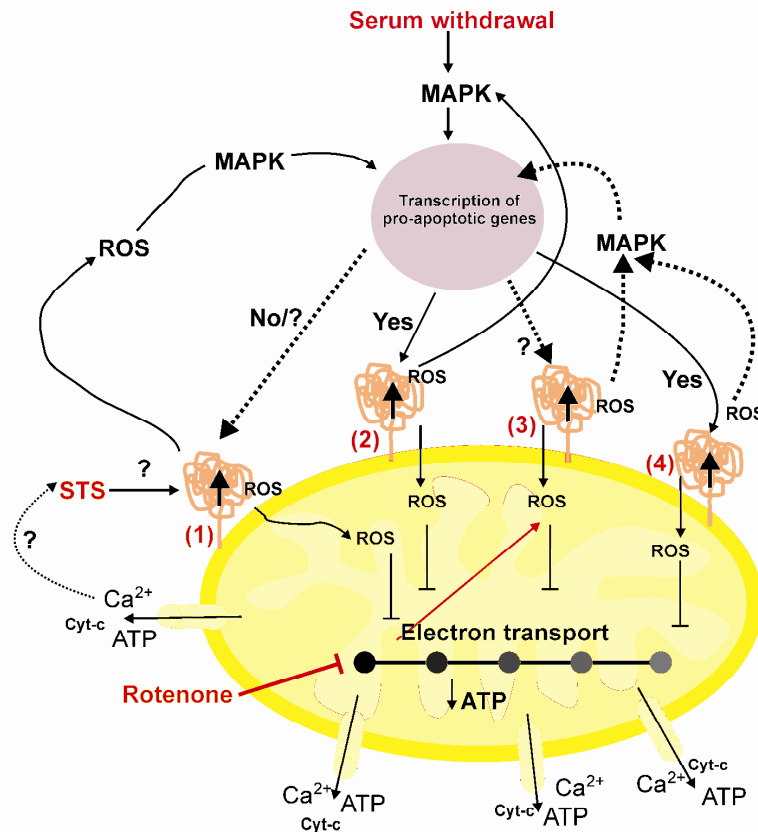


Figure 7. 1 Overview of role of MAO in mitochondrial dysfunction

During STS-induced apoptosis (1) MAO activity, protein and MAO-generated ROS are involved in enhancing apoptosis. The mechanism involves ROS activated MAPK signalling that is likely to target nuclear transcription of pro-apoptotic proteins. However, the activation of MAO is not a result of increased gene expression but may result from post-transcriptional events and/ or increased free calcium released from mitochondrial stores (loss of Bcl-2 levels indicated PTP opening). Serum withdrawal induced apoptosis (2) induces increased expression of MAO-A via MAPK signalling pathways which results in increased ROS and is contributes to the ensuing apoptotic events. Rotenone (3) inhibits complex 1 and therefore caused increased oxidative stress, ATP depletion, increased MAO activity and apoptosis. Increased MAO activity by genetic manipulation (4) causes massive elevation of mitochondrial ROS, ATP depletion and loss of cell death via apoptosis or as a result of caspase-3 inactivation and growth arrest and eventually necrosis. MAO-potentiated cell death is likely to involve reduced electron transport, PTP opening.

7.2. WIDER SIGNIFICANCE IN RELATION TO THE DEVELOPMENT AND TREATMENT OF PD

Increased MAO activity results in increased oxidative stress and both increased MAO activity and oxidative stress are linked to neurodegenerative diseases. In ageing and in PD, antioxidant defences are lowered (Riederer and Youdim 1986, Anderson 2004). PD therapies such as L-DOPA slow dopamine catabolism and therefore cause increased DA turnover in neuronal cells. The resulting increase in MAO activity may generate more ROS that have significant effects on an already overwhelmed system and may even contribute towards the rapid progression of the disease in the later stages. Preliminary studies in this work have shown that in GSH depleted cells, levodopa/carbidopa (Sinemet) induces apoptosis in a dose dependent manner (see appendix). Often L-DOPA is given in conjunction with MAO-B inhibitors such as deprenyl and carbidopa which inhibits COMT, but intervention with MAO inhibitors is often late stage. These data suggest that earlier intervention with MAO inhibitors may be useful. Indeed, the therapeutic effects of MAO inhibitors in AD have been mainly attributed to their antioxidant properties and may be useful in other dementias. Youdim et al (Maruyama *et al.* 2002, Youdim *et al.* 2003) have proposed that propargylamine inhibitors are neuroprotective because they signal up-regulation of Bcl-2 at the gene level involving the action of GAPDH translocation. Studies here were in disagreement with this proposal and suggest that the relationship of MAO with Bcl-2 maybe more complicated. Nevertheless, MAO inhibitors such as CGP3466 now in phase III trials for PD are thought to protect neurons by a mechanism that is not due to slowing of DA catabolism entirely. This has wider implications for the use of antioxidants as a preventative measure against ND but also as an alternative therapy. Indeed, in this work NAC prevented ROS production and protected against cell death to a similar extent to clorgyline and numerous publications have shown that antioxidants such as vitamin E and those found in green tea are neuroprotective (reviewed by Dunnett and Bjorklund 1999).

The JNK inhibitor Cep used in this study is now in phase II clinical trails for PD (Maroney *et al.* 2002). Data in this thesis has shown for the first time that JNK is important in regulating MAO-A expression during apoptosis and adds support for the use of JNK inhibitors for neuroprotection. Finally, the role of MAO as an enhancer of neuronal cell death raises questions about predisposition to ND with respect to both genetic and environmental factors. MAO activity levels in humans could potentially influence susceptibility to neurodegenerative diseases. Indeed, MAO levels are generally thought to

be elevated during ageing and smokers, who have reduced MAO activity are known to be less likely to develop PD (Castagnoli and Murugesan 2003). In addition, exposure to environmental pesticides that inhibit complex I have been linked with PD (Betarbet *et al.* 2000). Elevated MAO in these cases may give rise to additional problems.

Understanding of the mechanism by which neuronal cells die is also relevant in terms of our general understanding of ageing and disease. Changes in lifestyle and/ or preventative actions could reduce the need for late stage treatment and prolong quality of life.

7.3. FUTURE DIRECTIONS

A non-exhaustive list of possibilities for future directions is shown below.

7.3.1 Expanding insights into relevance of MAO-A overexpression and knockdown

Recombinant overexpression of MAO in SH-SY5Y cells caused cell death and culture of stable clones resulted in some experimental complications. In order to investigate the role of subtle elevation in MAO-A expression in a working model (I. e following challenge with apoptotic inducers), the creation of a stable cell line where elevation of MAO-A is inducible would be particularly valuable. A dox-inducible system may be considered for this purpose. The use of reversible MAO inhibitors such as TCP may also be useful for the culture of SH-SY5Y cells overexpressing MAO-A. An investigation into possible oxidative damage to ETC and other relevant proteins in MAO-A+ cells may also be of interest.

MAO-A- stable clones have proven extremely useful and expansion of this work is important. Mechanistic studies would be useful to elucidate signalling pathways involved in these cells following treatment. A study of changes in MAO-A mRNA, protein and activity levels following apoptotic induction in MAO-A- cells would indicate whether miRNA mechanism are able to cope with changing gene expression during different models of apoptosis and may explain some of differences between the apoptotic models in terms of protection in these cells.

7.3.2 The role of MAO-A in rotenone-induced cell death

The complete mechanistic studies to determine a wider knowledge of the role of MAO-A in rotenone-induced cell death in wild type SH-SY5Y cells is needed. Increased catalytic activity in this model may be a result of increased gene expression and /or protein levels or none of these. This knowledge would be invaluable considering the significant role of

MAO in mediating rotenone-induced mitochondrial dysfunction. Determining the levels of ROS in the presence and absence of MAO inhibitors could indicate how important MAO-produced ROS is in this model. Co-localisation studies involving ROS detection and mitochondrial markers would indicate sites of ROS production. On the same theme, mitochondrial function measures such as the selective mitochondrial stain JC-1, which changes colours depending on mitochondrial activity could give some interesting real time confocal footage in live cells in the presence and absence of signalling inhibitors.

7.3.3 The relationship between MAO and other mitochondrial proteins

To date the physical relationship between MAO and other mitochondrial proteins such as Bcl-2 at the mitochondrial surface have not been investigated. Overexpression of MAO-A resulted in decreased Bcl-2 levels. Whether or not this is due to apoptotic events or whether this is a result of OMM imbalance is not known but an interesting area for future research. It is possible that Bcl-2 family members or other OMM proteins interact with MAO to activate or suppress its activity and therefore regulate apoptosis. For example BH3-only proteins induce oligomerisation of certain Bcl-2 family protein via an unknown mechanism to regulate apoptosis (see chapter 1). It seems likely that as a membrane bound mitochondrial protein that MAO could also be involved here.

It is also possible that the activities of complex 1 and electron transport have a functional relationship with MAO (see Cohen *et al.* 1997), where MAO responds to ETC functionality and the ETC responds to MAO activity accordingly. A starting point for protein interaction work could involve co-immunoprecipitation; pull down assays and other functional studies aided by genetic manipulation. Co-immunoprecipitation work should be approached with care since avoiding artefacts from the isolation and solubilisation of mitochondrial membrane proteins is a particular challenge.

REFERENCES

- P. M. Abou-Sleiman, M. M. K. Muqit and N. W. Wood (2006). Expanding insights of mitochondrial dysfunction in Parkinson's disease. *Nature Neuroscience*. **7**,
- F. M. Achee and S. Gabay (1977). Some Aspects of Monoamine Oxidase Activity in Brain. *Progress in Neurobiology*. **8**, 325-348
- J. D. Adams, M. Chang and L. Klaidman (2001). Parkinson's Disease - Redox Mechanisms. *Current Medicinal Chemistry* **8**,809-814
- R. Adolfsson, G. C. Gottfries, L. Oreland, A. Wiberg and B. Winbald (1980). Increased activity of brain and platelet monoamine oxidase in dementia of Alzheimer type. *Life Sciences*. **27**, 1029-1034
- J. E. Ahlskog, R. J. Uitti, G. M. Tyce, J. F. O' Brian, R. C. Peterson and E. Cokmen (1996). Plasma catechols and monoamine oxidase metabolites in untreated Parkinson's and Alzheimer's disease. *Journal of Neurological Sciences*. **136**, 162-168
- Y. Akao, W. Maruyama, H. Yi, M. Shamoto-Nagai, M. Youdim, B. H and M. Naoi (2002). An anti-Parkinson's disease drug, N-propargyl-1(R)-aminoindan (Rasagiline), enhances expression of anti-apoptotic Bcl-2 in human dopaminergic SH-SY5Y cells. *Neuroscience Letters*. **326**, 105-108
- M. A. Akyuz, S. S. Erdem and D. E. Edmondson (2007). The aromatic cage in the active site of monoamine oxidase B: effect of the structural and electronic properties of bound benzylamine and *p*-nitrobenzylamine. *Journal of Neural Transmission*. **114**:(6), 693-698
- B. Alberts, D. Bray, J. Lewis, M. Raff, K. Roberts and J. D. Watson (1994). *Molecular Biology Of The Cell*, Third. *Garland Publishing*. New York
- L. A. Allan, N. Morrice, S. Brady, G. Magee, S. Pathak and P. R. Clarke (2003). Inhibition of caspase-9 through phosphorylation at Th 125 by ERK MAPK. *Nature Cell Biology*. **5**:(7), 647-654
- G. Alonso, C. Ambrosino, M. Jones and A. R. Nebreda (2000). Differential Activation of p38 Mitogen Activated Protein Kinase Isoforms Depending on Signal Strength. *The Journal of Biological Chemistry*. **275**:(51), 40641-40648
- E. Alves, T. Summavielle, C. J. Alves, J. Gomes-da-Silva, J. Custodio Barata, E. Fernandes, M. De Lourdes Bastos, M. A. Tavares and F. Carvalho (2007). Monoamine Oxidase-B Mediates Ecstasy-Induced Neurotoxic Effects to Adolescent Rat Brain Mitochondria. *The Journal of Neuroscience*. **27**:(38), 10203-10210
- J. K. Anderson (2004). Oxidative stress in neurodegeneration: cause or consequence? *Nature Reviews Neuroscience*. **5**, 18-25
- Antipodean Pharmaceuticals (2007) MitoQ. *10th* September, 2007.
- D. Arnoult (2006). Mitochondrial fragmentation in apoptosis. *TRENDS in Biochemical Sciences*. **17**:(1),
- M. Arrasate, S. Mitra, E. S. Schweitzer, M. R. Segal and S. Finkbeiner (2004). Inclusion body formation reduces levels of mutant huntingtin and the risk of neuronal death. *Nature*. **431**, 805-810
- C. R. Ashby, L. A. Carr, C. L. Cook, M. M. Steptoe and D. D. Franks (1988). Alteration of Platelet Serotonergic Mechanisms and Monoamine Oxidase Activity in Premenstrual Syndrome. *Biological Psychiatry*. **24**, 225-233
- P. C. Ashe and M. Berry, D (2003). Apoptotic signalling cascades. *Progress in Neuro-Psychopharmacology & Biological Psychiatry*. **27**, 199-214

- A. W. J. Bach, N. C. Lan, D. L. Johnson, C. W. Abell, M. E. Bembenek, S. Kwan, P. H. Seeburg and J. C. Shih (1988). cDNA cloning of human liver monoamine oxidase A and B: Molecular basis of differences in enzymic properties. *Proceedings of the National Academy of Sciences*. **85**, 4934-4938
- I. Bantounas, L. A. Phylactou and J. B. Uney (2004). RNA interference and the use of small interfering RNA to study gene function in mammalian systems. *Journal of Molecular Endocrinology*. **2004**, 545-557
- L. M. Barnes, C. M. Bentley and A. J. Dickson (2002). Stability of Protein Production From Recombinant Mammalian Cells. *Biotechnology and Bioengineering*. **81**:(6), 631-639
- K. J. Barnham, C. L. Masters and A. I. Bush (2004). Neurodegenerative diseases and oxidative stress. *Nature Reviews*. **3**, 205-214
- K. E. Beck (2004). Changes in cytoskeletal and signalling pathways in differentiated human neuroblastoma cells following MPP ion exposure. PhD. Nottingham Trent University
- M. Bennett, K. MacDonald, S. W. Chan, J. P. Luzio, R. Simari and P. Weissberg (1998). Cell surface trafficking of Fas: a rapid mechanism of p53-mediated apoptosis. *Science*. **282**, 290-293
- S. B. Berman and T. G. Hastings (1999). Dopamine Oxidation Alters Mitochondrial Respiration and Induces Permeability Transition in Brain Mitochondria: Implications for Parkinson's Disease. *Journal of Neurochemistry*. **73**, 1127-1137
- P. Bernardi, L. Scorrano, R. Colonna, V. Pertronilli and F. Di Lisa (1999). Mitochondria and cell death: Mechanistic aspects and methodological issues. *European Journal of Biochemistry*. **264**, 687-701
- M. Berry, D and A. A. Boulton (2000). Glyceraldehyde-3Phosphate Dehydrogenase and Apoptosis. *J Neuroscience Research*. **60**, 150-154
- M. D. Berry, A. V. Juorio and I. A. Paterson (1994). The Functional Role of Monoamine Oxidases A and B in the Mammalian Central Nervous System. *Progress in Neurobiology*. **42**, 375-391
- R. Bertrand, E. Solary, P. O'Connor, K. W. Kohn and Y. Pommier (2002). Induction of common pathways of apoptosis by staurosporine. *Experimental Cell Research*. **211**, 314-321
- R. Betarbet, T. B. Sherer, G. MacKenzie, M. Garcia-Osuna, A. V. Panov and J. T. Greenamyre (2000). Chronic systemic pesticide exposure reproduces features of Parkinson's disease. *Nature Neuroscience*. **3**:(12), 1301-1306
- N. Betz, (1999), Sensitivity of fluorometric and colorimetric caspase assays and purification of fragmented DNA from apoptotic cells, 10.10.02, www.promega.com/enotes/applications/htm
- N. Bhat and P. Zhang (1999). Hydrogen peroxide activation of multiple mitogen-activated protein kinases in an oligodendrocyte cell line: role of extracellular signal regulated kinase in hydrogen peroxide-induced cell death. *Journal of Neurochemistry*. **72**, 112-119
- P. Bianchi, M. Seguelas, A. Parini and C. Cambon (2003). Activation of Pro-Apoptotic Cascade by Dopamine in Renal Epithelial Cells is Fully Dependent on Hydrogen Peroxide Generation by Monoamine Oxidases. *Journal of the American Society of Nephrology*. **14**, 855-862

- J. L. Biedler, L. Helson and B. A. Spengler (1973). Morphology and Growth, Tumourgenicity, and Cytogenetics of Human Neuroblastoma Cells in Continuous Culture. *Cancer Research*. **33**, 2643-2652
- E. E. Billett (2004). Monoamine Oxidase (MAO) in Human Peripheral Tissues. *Neurotoxicology*. **25**, 139-148
- E. E. Billett and R. J. Mayer (1986). Monoclonal antibodies to monoamine oxidase B and another mitochondrial protein from human liver. *Biochemical Journal*. **235**, 2157-2163
- J. Bilsland, S. Roy, S. Xanthoudakis, D. W. Nicholson, Y. Han, E. Grimm, F. FHefti and S. J. Harper (2002). Caspase inhibitors attenuate MPP+ toxicity in primary cultures of mesencephalic dopaminergic neurons. *Journal of Neuroscience*. **22**, 2637-3649
- C. Binda, P. Newton-Vinson, F. Hubalek, D. E. Edmonson and A. Mattevi (2002). Structure of human monoamine oxidase B, a drug target for the treatment of neurological disorders. *Nature: structural biology*. **9**:(1), 22-26
- H. Blashko, D. Richter and H. Schlossmann (1937). The oxidation of adrenaline and other amines. *Biochemistry*. **31**, 2187-2196
- K. M. Boatright and G. S. Salvesen (2003). Mechanisms of caspase activation. *Current Opinion in Cell Biology*. **15**, 725-731
- J. Boix, N. Llecha, V. J. Yuste and J. X. Comella (1997). Characterisation of the cell death process induced by staurosporine in human neuroblastoma cell lines. *Neuropharmacology*. **36**, 811-821
- G. Bompert, N. Copin, F. Djoudi, C. Ordener and A. Parini (2001). Monoamine oxidase in developing rat renal cortex: effect of dexamethasone treatment. *European Journal of Pharmacology*. **415**, 19-26
- P. A. Bond and R. L. Cundall (1977). Properties of monoamine oxidase (MAO) in human blood platelets, lymphocytes, plasma and granulocytes. *Clin. Chim. Acta*. **80**, 317-326
- E. Bonfoco, D. Krainc, M. Ankarcona, P. Nicotera and S. A. Lipton (1995). Apoptosis and necrosis: two distinct events. *Proceedings of the National Academy of Sciences*. **92**, 7162-7166
- P. Bongioanni, C. Mondino, B. Boccardi, M. Borga and M. Castagna (1996). Monoamine oxidase molecular activity in platelets of Parkinsonian and demented patients. *Neurodegeneration*. **5**, 351-357
- U. Bonuccelli, P. Piccini, P. Bongioanni, A. Nuti, G. M. Pacifici and A. Muratorio (1988). Platelet monoamine oxidase in dementia of Alzheimer type. *Pharmacological Research Communications*. **20**:(S2), 52
- C. D. Bortner, N. B. E. Oldenburg and J. A. Cidlowski (1995). The role of DNA fragmentation in apoptosis. *Trends in Cell Biology*. **5**, 21-26
- V. Borutaite and G. C. Brown (2001). Caspases are reversibly inactivated by hydrogen peroxide. *FEBS letters*. **500**:(3), 114-118
- A. H. Boulares, A. G. Yakovlev, V. Ivanova, B. A. Stoica, G. Wang, S. Iyer and M. Smulson (1999). Role of Poly(ADP-ribose) Polymerase (PARP) Cleavage in Apoptosis. *Journal of Biological Chemistry*. **274**:(33), 22932-22940
- M. Bourin, M. Hascoet, M. Colombel, R. T. Coutts and G. B. Baker (2002). Clonidine potentiates the effects of tranlycypromine, phenelzine and two analogues in the forced swimming test in mice. *Rev. Psychiatr. Neurosci*. **27**:(3), 178-185

- S. B. Bratton and G. Cohen (2001). Apoptotic death sensor: an organelle's alter ego. *TRENDS in Biochemical Sciences*. **22**:(6), 306-315
- S. B. Bratton, M. MacFarlane, K. Cain and G. Cohen (2000). Protein Complexes Activate Distinct Caspase Cascades in Death Receptor and Stress-Induced Apoptosis. *Experimental Cell Research*. **256**, 27-33
- D. P. Brazil and B. A. Hemmings (2001). Ten years of protein kinase signalling: a hard Akt to follow. *TRENDS in Biochemical Sciences*. **26**:(11), 657-664
- D. P. Brazil, Z. Z. Yang and B. A. Hemmings (2004). Advances in protein kinase B signalling: AKTion on multiple fronts. *TRENDS in Biochemical Sciences*. **29**:(5), 233-242
- X. O. Breakefield, J. E. Pintar, R. M. Cawthon, M. S. Barbosa, M. Hawkins, C. Castiglione, F. P. Haseltine and U. Francke (1980). Biochemical and genetic studies of human monoamine oxidase. *American Journal of Human Genetics*. **32**, 36
- R. Brigelius-Flohe (1999). Tissue specific functions of individual glutathione peroxidases. *Free Radical Biology and Medicine*. **27**, 951-965
- B. B. Brodie, J. Axelrod, P. A. Shore and S. Udenfriend (1954). Ascorbic acid in aromatic hydroxylation. *The Journal of Biological Chemistry*.
- G. C. Brown (2005). Mitochondria and cell death: Apoptosis and necrosis. *The Biochemist*.
- G. K. Brown, J. F. Powell and I. W. Craig (1980). Molecular weight differences between human platelet and placental monoamine oxidase. *Biochemical Pharmacology*. **29**, 2595-2603
- H. G. Brunner, M. Nelen, X. O. Breakefield, H. H. Ropers and B. A. Van Oost (1993). Abnormal behavior associated with a point mutation in the structural gene for monoamine oxidase A. *Science*. **262**, 578-580
- T. D. Buckman, M. S. Sutphin and B. Mitrovic (1993). Oxidative stress in a clonal cell line of neuronal origin: effects of antioxidant enzyme modulation. *Journal of Neurochemistry*. **60**:(6), 2046-2058
- R. E. Burke (2008). Programmed cell death and new discoveries in the genetics of Parkinsonism. *Journal of Neurochemistry*. **in press**, DOI:10.1111/j.1471/4159.2007.05106.X
- W. Burke, S. W. Li, C. A. Schmitt, P. Xia, H. D. Chung and K. N. Gillespie (1999). Accumulation of 3,4-dihydroxyphenylglycoaldehyde, the neurotoxic monoamine oxidase A metabolite of norepinephrine, in locus ceruleus cell bodies in Alzheimer's disease: mechanism of neuron death. *Brain Research*. **816**, 633-637
- R. S. Burns, C. C. Chiueh, S. P. Markey, M. H. Ebert, D. M. Jacobowitz and I. J. Kopin (1983). A Primate Model of Parkinsonism - Selective Destruction of Dopaminergic-Neurons in the Pars Compacta of the Substantia Nigra by N-Methyl-4-Phenyl-1,2,3,6-Tetrahydropyridine. *Proceedings of the National Academy of Sciences of the United States of America-Biological Sciences*. **80**:(14), 4546-4550
- S. Bursztajn, J. J. Feng, S. A. Berman and A. Nanda (2000). Poly (ADP-ribose) polymerase induction is an early signal of apoptosis in human neuroblastoma. *Molecular Brain Research*. **76**:(2), 363-376
- E. Cadenas and K. J. A. Davies (2000). Mitochondrial Free Radical Generation, Oxidative Stress, and Aging. *Free Radical Biology and Medicine*. **29**:(3/4), 222-230

- C. Cande, F. Cecconi, P. Dessen and G. Kroemer (2002). Apoptosis-inducing factor (AIF): key to the conserved caspase-independent pathways of cell death? *Journal of Cell Science*. **115**:(24), 4727-4734
- B. Caneda-Ferron, L. A. De Girolamo, T. Costa, K. E. Beck, R. Layfield and E. E. Billett (2008). Assessment of the direct and indirect effects of MPP⁺ and dopamine on the human proteasome: implications for Parkinson's disease aetiology. *Journal of Neurochemistry*. **in press**, DOI:10.1111/J.1471/4159.2007.05130.X
- R. M. Canet-Aviles, M. A. Wilson, D. W. Miller, R. Ahmad and M. R. Cookson (2004). The Parkinson's disease protein DJ-1 is neuroprotective due to cysteine-sulfinic acid-driven mitochondrial localisation. *Proc. Natl. Acad. Sci. USA*. **101**, 9103-9108
- X. Cao, Z. Wei, G. G. Gabriel, X. Li and D. D. Mousseau (2007). Calcium-sensitive regulation of monoamine oxidase-A contributes to the production of peroxyradicals in hippocampal cultures: implications for Alzheimer disease-related pathology. *BMC Neurosci*. **8**:(1), 73
- M. R. Capecchi (2001). Generating mice with targeted mutations. *Nature Medicine*. **7**:(10), 1086-1090
- J. L. Carrasco, M. Diaz Marsa, E. Hollander, J. Cesar and J. Saiz Ruiz (2000). Decreased platelet monoamine oxidase activity in female bulimia nervosa. *European Neuropsychopharmacology*. **10**:(2), 113-117
- O. Cases, I. Seif, J. Grimsby, P. Gaspar, K. Chen, S. Pournin, U. Muller, M. Aguet, C. Babinet and J. C. Shih (1995). Aggressive behavior and altered amounts of brain serotonin and norepinephrine in mice lacking MAO-A. *Science*. **268**, 1763-1766
- A. Caspi, J. McClay, T. E. Moffitt, J. Mill, J. Martin, I. W. Craig, A. Taylor and R. Poulton (2002). Role of Genotype in the Cycle of Violence in Maltreated Children. *Science*. **297**, 851-854
- D. S. Cassarino, C. P. Fall, R. H. Swerdlow, T. S. Smith, E. M. Halvorsen, S. W. Miller, J. P. Parks, W. D. Parker and J. P. Bennett (1997). Elevated reactive oxygen species and antioxidant enzyme activities in animal and cellular models of Parkinson's disease. *Biochimica Et Biophysica Acta-Molecular Basis of Disease*. **1362**:(1), 77-86
- K. Castagnoli and T. Murugesan (2003). Tobacco leaf, smoke and smoking, MAO inhibitors, Parkinson's disease and Neuroprotection; Are There Links? *Neurotoxicology*. **XXX**, XXX-XXX
- R. M. Cawthon and X. O. Breakefield (1979). Differences in A and B forms of monoamine oxidase revealed by limited proteolysis and peptide mapping. *Nature*. **281**, 692-694
- R. M. Cawthon, J. E. Pintar, F. P. Haseltine and X. O. Breakefield (1981). Differences in the structure of A and B forms of human monoamine oxidase. *Journal of Neurochemistry*. **37**, 363-372
- P. Chaitidis, E. E. Billett, V. B. O'Donnell, A. Bermudez Fajardo, J. Fitzgerald, R. J. Kuban, U. Ungethuen and H. Kuhn (2004). Th2 Response of Human Peripheral Monocytes Involves Isoform-Specific Induction of Monoamine Oxidase-A. *The Journal of Immunology*. **173**, 4821-4827
- J. Chandra, A. Samali and S. Orrenius (2000). Triggering and modulation of apoptosis by oxidative stress. *Free Radical Biology and Medicine*. **29**, 323-333
- B. Chen and W. Chang (2000). Functional interaction between c-Jun and promoter factor Sp1 in epidermal growth factor-induced gene expression of human 12(S)-lipoxygenase. *Proceedings of the National Academy of Sciences*. **97**:(19), 10406-10411

- K. Chen, D. P. Holschneider, W. Wu, I. Rebrin and J. C. Shih (2004b). A spontaneous Point Mutation Produces Monoamine Oxidase A/B Knock-out Mice with Greatly Elevated Monoamines and Anxiety-like Behavior. *Journal of Biological Chemistry*. **279**:(38), 39645-39652
- K. Chen, X. Ou, G. Chen, S. H. Choi and J. C. Shih (2004a). R1, a Novel Repressor of the Human Monoamine Oxidase A. *The Journal of Biological Chemistry*. **280**:(12), 11552-11559
- Q. M. Chen (1998). Molecular analysis of H₂O₂-induced senescent like growth arrest in normal human fibroblasts. *Biochemical Journal*. **332**, 43
- S. Chen, J. C. Shih and Q. P. Xu (1985). 4-Fluoro-3-Nitrophenyl Azide, a Selective Photoaffinity Label for Type-B Monoamine-Oxidase. *Biochemical Pharmacology*. **34**:(6), 781-788
- Z. Y. Chen, R. M. Denney and X. O. Breakefield (1995). Norrie disease and MAO genes: nearest neighbors. *Human Molecular Genetics*. **4**, 1729-1737
- Z. Y. Chen, J. F. Powell, Y. P. P. Hsu, X. O. Breakefield and I. W. Craig (1992). Organisation of the human monoamine oxidase genes and long-range physical mapping around them. *Genomics*. **14**:(1), 75-82
- Y. Christen (2000). Oxidative stress and Alzheimer disease. *Am J Clin Nutr*. **621**, S1-9
- C. T. Chu, D. J. Levinthal, S. M. Kulich, E. M. Chalovich and D. B. DeFranco (2004). Oxidative neuronal injury. The dark side of ERK1/2. *European Journal of Biochemistry*. **271**, 2060-2066
- D. Chuang, C. Hough and V. V. Senatorov (2005). Glyceraldehyde-3-Phosphate Dehydrogenase, Apoptosis, and Neurodegenerative Diseases. *Annu. Rev. Pharmacol. Toxicol.* **45**, 269-290
- D. Chuang and R. Ishitani (1996). A role for GAPDH in apoptosis and neurodegeneration. *Nature Medicine*. **2**, 609-610
- R. G. Church, G. Robinson and E. E. Billett (1994). The localisation of monoamine oxidase in human placenta using a new specific monoclonal antibody to monoamine oxidase A. *Proc. R. Microsc. Soc.* **29**, 243
- V. Ciccarone, B. A. Spengler, M. B. Meyers, J. L. Biedler and R. A. Ross (1989). Phenotypic Diversification in Human Neuroblastoma Cells: Expression of Distinct Neural Crest Lineages. *Brain Research*. **49**, 219-225
- A. Ciechanover and P. Brundin (2003). The Ubiquitin Proteasome System In Neurodegenerative Diseases: Sometimes the Chicken, Sometimes the Egg. *Neuron* **40**, 427-446
- A. R. Clark, J. L. E. Dean and J. Saklavalala (2003). Post-transcriptional regulation of gene expression by mitogen-activated protein kinase p38. *FEBS letters*. **546**, 37-44
- G. Cohen (1983). The pathobiology of Parkinson's disease: biochemical aspects of dopamine neuron senescence. *J. Neural. Transmembr. Suppl.* **19**, 89-103
- G. Cohen (1983). The pathobiology of Parkinson's disease: biochemical aspects of dopamine neuron senescence. *Journal of Neural Transmission Suppl.* **19**, 89-103
- G. Cohen (1990). Monoamine oxidase and oxidative stress at dopaminergic synapses. *Journal of Neural Transmission Suppl.* **32**, 229-238
- G. Cohen (1997). Caspases: the executioners of apoptosis. *Biochem J*. **326**, 1-16

- G. Cohen (2000). Oxidative Stress, Mitochondrial Respiration and Parkinson's Disease. *Annals of the New York Academy of Sciences*. **899**, 112-120
- G. Cohen, R. Farooqui and N. Kesler (1997). Parkinson's disease: A new link between monoamine oxidase and mitochondrial electron flow. *Proceedings of the National Academy of Sciences*. **94**, 4890-4894
- G. Cohen and N. Kesler (1999). Monoamine Oxidase and Mitochondrial Respiration. *Journal of Neurochemistry*. **73**, 2310-2315
- Constans (2005). RNAi's Minor Setback. *The Scientist*.
- M. R. Cookson, C. Mead, S. M. Austwick and V. W. Pentreath (1995). Use of the MTT assay for estimating toxicity in primary astrocytes and C6 glioma cell cultures. *Toxicology In Vitro*. **9**, 39-48
- A. J. Crossthwaite, S. Hasan and R. J. Williams (2002). Hydrogen peroxide-mediated phosphorylation of ERK1/2, Akt/PKB and JNK in cortical neurones: dependence on Ca²⁺ and P13-kinase. *Journal of Neurochemistry*. **80**:(1), 24-35
- F. Cruz and D. E. Edmondson (2007). Kinetic properties of recombinant MAO-A on incorporation into phospholipid nanodisks. *Journal of Neural Transmission*. **114**:(6), 699-702
- B. R. Cullen (2006). Enhancing and confirming the specificity of RNAi experiments. *Nature Methods*. **3**:(9), 677-681
- K. Czaplinski and R. H. Singer (2006). Pathways for mRNA localization in the cytoplasm. *TRENDS in Biochemical Sciences*. **31**:(12), 687-693
- P. Damier, A. Kastner, Y. Agid and E. C. Hirsch (1996). Does monoamine oxidase type B play a role in dopaminergic nerve cell death in Parkinson's disease? *Neurology*. **46**:(5), 1262-1269
- M. L. Danielczyk (1998). Platelet MAO-B activity and the psychopathology of Parkinson's disease, senile dementia and multi-infarct dementia. *Acta Psychiatrica Scandinavia*. **78**, 730-736
- G. P. Davey, S. Peuchen and J. B. Clark (1998). Energy thresholds in brain mitochondria - Potential involvement in neurodegeneration. *Journal of Biological Chemistry*. **273**:(21), 12753-12757
- R. J. Davis (2000). Signal Transduction by the JNK Group of MAP Kinases. *Cell*. **103**, 239-252
- T. Dawson and V. L. Dawson (2003). Molecular Pathways of Neurodegeneration in Parkinson's Disease. *Science*. **302**, 819-822
- L. A. De Girolamo, Hargreaves, A. J. and Billett, E. E. (2001). Protection from MPTP-induced neurotoxicity in differentiating mouse N2a neuroblastoma cells. *Journal of Neurochemistry*. **76**, 650-660
- S. M. De La Monte, Y. K. Sohn, N. Ganju and J. R. Wands (1998). p53 and CD95 associated apoptosis in neurodegenerative diseases. *Laboratory Investigation*. **78**, 401-411
- O. Deas, C. Dumont, M. MacFarlane, M. Rouleau, C. Hebib, F. Harper, F. Hirsch, B. Charpentier, G. Cohen and A. Senik (1998). Caspase-Independent Cell Death Induced by Anti-CD2 or Staurosporine in Activated Human Peripheral T Lymphocytes. *Journal of Immunology*. **161**, 3375-3383

- L. D. DeColibus, M. Li, C. Binda, A. Lustig, D. E. Edmondson and A. Mattevi (2005). Three-dimensional structure of human monoamine oxidase A (MAO A): Relation to the structures of rat MAO A and human MAO B. *Proceedings of the National Academy of Sciences*. **102**, 12684-12689
- M. J. Del Rio and C. Velez-Pardo (2002). Monoamine neurotoxins-induced apoptosis in lymphocytes by a common oxidative stress mechanism: involvement of hydrogen peroxide (H₂O₂), caspase-3, and nuclear factor kappa-B (NF-kappa B), p53, c-Jun transcription factors. *Biochemical Pharmacology*. **63**:(4), 677-688
- R. M. Denney, N. T. Patel, R. R. Fritz and C. W. Abell (1982). A Monoclonal-Antibody Elicited to Human-Platelet Monoamine-Oxidase - Isolation and Specificity for Human Monoamine Oxidase-B but Not Oxidase-A. *Molecular Pharmacology*. **22**:(2), 500-508
- J. Desbarats, R. B. Birge, M. Mimouni-Rongy, D. E. Weinstein, J. Palerme and M. K. Newell (2003). Fas engagement induces neurite growth through ERK activation and p35 upregulation. *Nature Cell Biology*. **5**, 118-125
- G. S. DeZutter and R. J. Davis (2001). Pro-apoptotic gene expression mediated by the p38 mitogen-activated protein kinase signal transduction pathway. *Proceedings of the National Academy of Sciences*. **98**:(11), 6168-6173
- D. A. Di Monte (2001). The role of environmental agents in Parkinson's disease. *Clinical Neuroscience Research*. **1**, 419-426
- D. A. Di Monte (2003). The environment and Parkinson's disease: is the nigrostriatal system preferentially targeted by neurotoxins? *Lancet Neurology*. **2**, 531-538
- M. Diaz Marsa, J. L. Carrasco, E. Hollander, J. Cesar and J. Saiz Ruiz (2000). Decreased platelet monoamine oxidase activity in female anorexia nervosa. *Acta Psychiatr. scand.* **101**:(3), 226-230
- P. J. Dlugosz, L. P. Billen, M. G. Annis, W. Zhu, Z. Zhang, J. Lin, B. Leber and D. W. Andrews (2006). Bcl-2 changes conformation to inhibit Bax oligomerization. *The EMBO Journal*. **25**, 2287-2296
- C. Domenicotti, B. Marengo, M. Nitti, D. Verzola, G. BGaribotti, D. Cottalasso, G. Poli, E. Melloni, M. A. Pronzato and U. M. Marinari (2003). A novel role for protein kinase C. *Biochemical Pharmacology*. **66**:(8), 1521-1526
- M. Donepudi and M. G. Grutter (2002). Structure and zymogen activation of caspases. *Biophysical Chemistry*. **101-102**, 145-153
- C. H. Donnelly and D. L. Murphy (1977). Substrate-Related and Inhibitor-Related Characteristics of Human Platelet Monoamine-Oxidase. *Biochemical Pharmacology*. **26**:(9), 853-858
- G. Dotti, B. Savoldo, M. Pule, K. A. Straathof, E. Biagi, E. Yvon, S. Vigouroux, M. K. Brenner and C. M. Rooney (2005). Human cytotoxic T lymphocytes with reduced sensitivity to Fas-induced apoptosis. *Blood*. **105**:(12), 4677-4684
- T. A. Dowds and E. L. Sabban (2001). Endogenous and exogenous ARC in serum withdrawal mediated PC12 cell apoptosis: a new pro-apoptotic role for ARC. *Cell Death and Differentiation*. **8**, 640-648
- D. C. Duke, L. B. Moran, M. E. Kalaitzakis, M. Deprez, D. T. Dexter, R. K. B. Pearce and M. B. Graeber (2006). Transcriptome analysis reveals link between proteasomal and mitochondrial pathways in Parkinson's disease. *Neurogenetics*. **7**, 139-148

- C. Dunn, W. C. A. MacLaren and A. A. F. Gillespie (2002). Molecular mechanism and biological functions of c-Jun N-terminal kinase signalling via the c-Jun transcription factor. *Cellular Signalling*. **14**, 585-593
- S. B. Dunnett and A. Bjorklund (1999). Prospects for new restorative and neuroprotective treatments in Parkinson's disease. *Nature*. **399**:(6738), A32-A39
- D. M. Dykxhoorn, C. D. Novina and P. A. Sharp (2003). Killing the messenger: short RNAs that silence gene expression. *Nature Reviews Cell Biology*. **4**, 457-467
- O. Eberhardt, J. B. Schulz (2003). Apoptotic mechanisms and antiapoptotic therapy in the MPTP model of Parkinson's disease. *Toxicology Letters*. **139**, 1-17
- D. E. Edmondson, Binda, C. and Mattevi, A. (2004). The FAD Binding Sites of Human Monoamine Oxidases A and B. *Neurotoxicology*. **25**, 63-72
- D. E. Edmondson, L. DeColibus, C. Binda, M. Li and A. Mattevi (2007). New insights into the structures and functions of human monoamine oxidases A and B. *Journal of Neural Transmission*. **114**, 703-705
- A. Eggert, M. A. Grotzer, T. J. Zuzak, B. R. Wiewrodt, R. Ho, N. Ikegaki and G. M. Brodeur (2001). Resistance to Tumour Necrosis Factor-related Apoptosis-inducing Ligand-induced Apoptosis in Neuroblastoma Cells Correlates with a Loss of Caspase-8 Expression. *Cancer Research*. **61**, 1314-1319
- J. Ekblom, S. S. Jossan, M. Bergstruem, L. Oreland, E. Walum and S. M. Aquilonius (1993). Monoamine oxidase-B in astrocytes. *Glia*. **8**, 122-132
- J. Emerit, M. Edeas and F. Bricaire (2004). Neurodegenerative diseases and oxidative stress. *Pharmacother*. **58**, 39-46
- B. M. Emerling, Plataniias, L. C., Black, E., Nebreda, A. R., Davis, R. J., and Chandel, N. S. (2005). Mitochondrial Reactive Oxygen Species Activation of p38 Mitogen-Activated Protein Kinase Is Required for Hypoxia Signaling. *Molecular and Cellular Biology*. **25**:(12), 4853-4862
- L. Emilsson, Saetre, P., Balciuniene, J., Castensson, A., Cairns, N. and Jazin, E. E. (2002). Increased monoamine oxidase messenger RNA expression levels in frontal cortex of Alzheimer's disease patients. *Neuroscience Letters*. **326**, 56-60
- M. Enari, H. Sakahira, H. Yokoyama, K. Okawa, A. Iwamatsu and S. Nagata (1998). A caspase-activated DNase that degrades DNA during apoptosis and its inhibitor ICAD. *Nature*. **391**, 43-50
- M. Encinas, M. Iglesias, Y. Liu, H. Wang, A. Muhaison, V. Cena, C. Gallego and J. X. Comella (2000). Sequential treatment of SH-SY5Y cells with retanoic acid and brain-derived neurotrophic factor gives rise to fully differentiated, neurotrophic factor-dependent, human neuron-like cells. *Journal of Neurochemistry*. **75**, 991-1003
- A. Enemoto, N. Suzuki, A. Morita, M. Ito, C. Liu, Y. Matsumoto, K. Yoshioka, T. Shiba and Y. Hosoi (2003). Caspase-3 mediated cleavage of JNK during stress-induced apoptosis. *Biochemical and Biophysical Research Communications*. **306**, 837-842
- H. Enslin, Raingeaud, J. and Davis, R. J (1998). Selective Activation of p38 Mitogen-activated protein (MAP) Kinase Isoforms by the MAP Kinase Kinase MKK3 and MKK6. *The Journal of Biological Chemistry*. **273**, 1741-1748
- G. Ermak and K. J. A. Davies (2001). Calcium and oxidative stress: from cell signaling to cell death. *Molecular Immunology*. **38**, 713-721

- V. G. Erwin and L. Hellerman (1967). Mitochondrial membrane monoamine oxidase. Purification and characterisation of the bovine kidney enzyme. *Journal of Biological Chemistry*. **242**, 4230-4238
- C. P. Fall and J. P. Bennett (1999). Characterisation and time course of MPP⁺ induced apoptosis in human neuroblastoma cells. *Journal of Neuroscience Research*. **55**:(5), 620-628
- B. Ferger, C. Van Amsterdam, C. Seyfried and K. Kuschinsky (1998). Effects of alpha-phenyl-tert-butyl-nitron and selegiline on hydroxyl free radicals in rat striatum produced by local application of glutamate. *Journal of Neurochemistry*. **70**, 276-280
- K. Ferrell, Wilkinson, R. M., Dubiel, W. and Gordon, C. (2000). Regulatory subunit interactions of the 26s proteasome, a complex problem. *TIBS*. **25**, 83-88
- I. Ferrer, R. Blanco, M. Carmona, B. Puig, M. Barrachina, C. Gomez and S. Ambrosio (2001). Active, phosphorylation-dependent mitogen-activated protein kinase (MAPK/ERK), stress-activated protein kinase/c-Jun N-terminal kinase (SAPK/JNK), and p38 kinase expression in Parkinson's disease and Dementia with Lewy bodies. *J Neural Transmission*. **108**, 1383-1396
- J. P. M. Finberg and O. Sader-Mazbar (2007). Modification of L-DOPA pharmacological activity by MAO inhibitors. *Journal of Neural Transmission*. **114**:(6), 801-805
- C. Finch, C. S. L. Ho, A. C. Williams and E. E. Billett (1995). Platelet MAO activities and MAO-B protein concentrations in Parkinson's disease and controls. *Progress in Brain Research*. **106**, 85-90
- T. Finkel (1998). Oxygen radicals and signaling. *Current Opinion in Cell Biology*. **10**, 248-252
- T. Finkel (2003). Oxidant signals and oxidative stress. *Current Opinion in Cell Biology*. **15**, 247-254
- T. Finkel and N. J. Holbrook (2000). Oxidants, oxidative stress and the biology of ageing. *Nature*. **408**:(6809), 239-247
- J. C. Fitzgerald, C. Ufer and E. E. Billett (2007). A link between monoamine oxidase-A and apoptosis in serum deprived human SH-SY5Y neuroblastoma cells. *Journal of Neural Transmission*. **114**:(6), 807-810
- P. Foley, M. Gerlach, M. B. H. Youdim and P. Riederer (2000). MAO-B inhibitors: multiple roles in the therapy of neurodegenerative disorders? *Parkinsonism and Related Disorders*. **6**, 25-47
- C. J. Fowler, L. Orelund, J. Marcusson and B. Winbald (1980a). Titration of human brain monoamine oxidase-A and -B by clorgyline and deprenyl. *Archives of Pharmacology*. **311**, 263-272
- C. J. Fowler and K. F. Tipton (1984). On the substrate specificities of the two forms of monoamine oxidase. *J. Pharm Pharmacol*. **36**:(2), 111-115
- C. J. Fowler, A. Wiberg, L. Orelund, J. Marcusson and B. Winbald (1980b). The effect of age on the activity and molecular properties of human brain monoamine oxidase. *Journal of Neural Transmission*. **49**, 1-20

- J. S. Fowler, J. Logan, G. Wang, N. D. Volkow, F. Telang, W. Zhu, D. Franceschi, N. Pappas, R. Ferrieri, C. Shea, V. Garza, Y. Xu, D. Schlyer, S. J. Gatley, Y. Ding, D. Alexoff, D. Warner, N. Netusil, P. Carter, M. Jayne, P. King and P. Vaska (2003). Low monoamine oxidase B in peripheral organs in smokers. *Proc. Natl. Acad. Sci. USA*. **100**:(20), 11600-11605
- J. S. Fowler, N. D. Volkow, G. Wang, N. Pappas, J. Logan, C. Shea, D. Alexoff, R. R. MacGregor, D. Schlyer, I. Zezulcova and A. P. Wolf (1996). Brain monoamine oxidase A inhibition in cigarette smokers. *Proc. Natl. Acad. Sci. USA*. **93**, 14065-14069
- P. Freimuth (2006). Protein Overexpression in Mammalian Cell Lines. *Genetic Engineering*. **28**, 93-102
- R. M. Friedlander (2003). Apoptosis and Caspases in Neurodegenerative Diseases. *New England Journal of Medicine*. **348**, 1365-1375
- R. M. Friedlander and J. Yuan (1998). ICE, neuronal apoptosis and neurodegeneration. *Cell Death and Differentiation*. **5**, 823-831
- M. Gabbay, M. Tauber, S. Porat and R. Simantov (1996). Selective Role of Glutathione in Protecting Human Neuronal Cells from Dopamine-induced Apoptosis. *Neuropharmacology*. **35**:(5), 571-578
- J. E. Galvin, V. M. Y. Lee and J. Q. Trojanowski (1999). Pathology of the Lewy body. *Advances in Neurology*. **80**, 313-324
- N. L. Garneau, J. Wilusz and C. J. Wilusz (2007). The highways and byways of mRNA decay. *Nature Reviews*. **8**, 113-126
- C. Garrido, L. Galluzzi, M. Brunet, P. E. Puig, C. Didelot and G. Kroemer (2006). Mechanisms of cytochrome c release from mitochondria *Cell Death and Differentiation*. **13**, 1422-1433
- R. M. Geha, K. Chen and J. C. Shih (2000). Phe(208) and Ile(199) in human monoamine oxidase A and B do not determine substrate and inhibitor specificities as in rat. *Journal of Neurochemistry*. **75**:(3), 1304-1309
- R. M. Geha, K. Chen, J. Wouters, F. Ooms and J. C. Shih (2002). Analysis of conserved active site residues in monoamine oxidase A and B and their three-dimensional molecular modeling. *Journal of Biological Chemistry*. **277**:(19), 17209-17216
- R. M. Geha, I. Rebrin, K. Chen and J. C. Shih (2001). Substrate and inhibitor specificities for human monoamine oxidase A and B are influenced by a single amino acid. *Journal of Biological Chemistry*. **276**:(13), 9877-9882
- M. Gerlach and P. Riederer (1993). Human Brain MAO, *VSP Publishing*. Lorton, Virginia, 147-158
- S. Ghandi and N. W. Wood (2005). Molecular pathogenesis of Parkinson's disease. *Human Molecular Genetics*. **14**:(18), 2749-2755
- B. I. Giasson, H. Ischiropoulos, V. M. Y. Lee and J. Q. Trojanowski (2002). The relationship between oxidative/nitrative stress and pathological inclusions in Alzheimer's and Parkinson's diseases. *Free Radical Biology and Medicine*. **32**:(12), 1264-1275
- J. Gil, S. Ameida, C. K. Oliviera and A. C. Rego (2003). Cytosolic and mitochondrial ROS in staurosporine-induced retinal apoptosis. *Free Radical Biology and Medicine*. **35**:(11), 1500-1514

- I. R. Gilmore, S. P. Fox, A. J. Hollins, M. Sohail and S. Akhtar (2004). The design and exogenous delivery of siRNA for post-transcriptional gene silencing. *Journal of Drug Targeting*. **12**:(6), 315-340
- M. Giorgio, M. Trinei, E. Migliaccio and P. G. Pelicci (2007). Hydrogen peroxide: a metabolic by-product or a common mediator of ageing signals? *Nature Reviews* **8**,722-728
- C. Giulivi, Boveris, A. and Cadenas, E. (1995). Hydroxyl radical generation during mitochondrial electron transfer and the formation of 8-hydroxy-desoxyguanosine in mitochondrial DNA. *Archives of Biochemistry and Biophysics*. **316**:(909-916),
- D. Gius and D. R. Splitz (2006). Redox signalling in cancer biology. *Antioxidants & Redox Signaling*. **8**, 1249-1252
- V. Glover and M. Sandler (1986). Clinical-Chemistry of Monoamine-Oxidase. *Cell Biochemistry and Function*. **4**:(2), 89-97
- A. L. Goldberg (1995). Functions of the Proteasome: The Lysis at the End of the Tunnel. *Science*. **268**, 522-523
- P. Golstein and G. Kroemer (2006). Cell death by necrosis: towards a molecular definition. *TRENDS in Biochemical Sciences*. **32**:(1), 37-43
- J. Gong, F. Traganos and Z. Darzynkiewicz (1994). Staurosporine blocks cell cycle progression through G1, between cyclin D and cyclin E restriction points. *Cancer research*. **54**, 2993-2999
- V. Z. Gorkin (1966). Monoamine oxidases. *Pharmacological Reviews*. **18**, 115-120
- S. Grethe, M. P. S. Ares, T. Andersson and M. I. Porn-Ares (2004). p38 MAPK mediates TNF-induced apoptosis in endothelial cells via phosphorylation and downregulation of Bcl-x_L. *Experimental Cell Research*. **298**:(2), 632-642
- J. Grimsby, Chen, K., Wang, L., Lan, N. C. and Shih, J. C. (1991). Human monoamine oxidase A and B genes exhibit identical exon-intron organisation. *Proceedings of the National Academy of Sciences*. **88**, 3637-3641
- J. Grimsby, M. Toth, K. Chen, T. Kumazawa, L. Klaidman, J. D. Adams, F. Karoum, J. Gal and J. C. Shih (1997). Increased stress response and β-phenylethylamine in MAO-B deficient mice. *Nature Genetics*. **17**, 206-210
- M. Gu, J. M. Cooper, J. W. Taanman and A. H. V. Schapira (1998). Mitochondrial DNA Transmission of the Mitochondrial Defect in Parkinson's Disease. *Ann Neurol*. **44**, 177-186
- M. Gu, A. D. Owen, S. E. K. Toffa, J. M. Cooper, D. T. Dexter, P. Jenner, C. D. Marsden and A. H. V. Schapira (1998). Mitochondrial function, GSH and iron in neurodegeneration and Lewy body diseases. *Journal of Neurological Sciences*. **158**, 24-29
- Q. Guo, L. Sebastian, B. L. Sopher, M. W. Miller, G. W. Glazner, C. B. Ware, G. M. Martin and M. P. Mattson (1999). Neurotrophic factors (ADNF) and basic fibroblast growth factor interrupt excitotoxic neurodegenerative cascades promoted by PS1 mutation. *Proc. Natl. Acad. Sci. USA*. **96**, 4125-4130
- K. Z. Guyton, Y. Liu, M. Gorospe, Q. Xu and N. J. Holbrook (1996). Activation of Mitogen-activated Protein Kinase by H₂O₂. *The Journal of Biological Chemistry*. **271**:(8), 4138-4142
- A. Hald and J. Lotharius (2005). Oxidative stress and inflammation in Parkinson's disease: Is there a casual link? *Experimental Neurology*. **193**, 279-290
- B. Halliwell (1992). Reactive Oxygen Species and the Central Nervous System. *Journal of Neurochemistry*. **59**, 1609-1623

- B. Halliwell (1999). Vitamin C: poison, prophylactic or panacea? *TRENDS in Biochemical Sciences*. **24**:(7), 255-259
- B. Halliwell and J. M. C. Gutteridge (2007). Free Radicals in Biology and Medicine, Fourth. *Oxford University Press*. Oxford
- M. B. Hampton and S. Orrenius (1997). Dual regulation of caspase activity by hydrogen peroxide: implications for apoptosis. *FEBS Letters*. **414**, 552-556
- B. S. Han, H. S. Hong, W. S. Choi, G. J. Markelonis, T. H. Oh and Y. J. Oh (2003). Caspase-dependent and -independent cell death pathways in primary cultures of mesencephalic dopaminergic neurons after neurotoxin treatment. *Journal of Neuroscience*. **23**:(12), 5069-5078
- S. Han and G. Cohen (1996). Inhibition of catalase in mesencephalic cultures by L-DOPA and dopamine. *Neurochemistry International*. **29**:(6), 645-649
- K. Harada, S. Toyooka, N. Shivapurka, A. Maitra, J. L. Reddy, H. Matta, K. Miyajima, C. F. Timmons, G. E. Tomlinson, D. Mastrangelo, R. J. Hay, P. M. Chaudhary and A. F. Gazdar (2002). Deregulation of Caspase 8 and 10 Expression in Pediatric Tumors and Cell Lines. *Molecular Biology and Genetics*. **62**, 5897-5901
- J. Hardy (1997). Amyloid, the presenilins and Alzheimer's disease. *Trends in Neuroscience*. **20**:(4), 154-159
- M. L. C. Hare (1928). Tyramine oxidase. A new enzyme system in liver. *Biochemical Journal*. **22**, 968-979
- C. A. Harris, M. Deshmukh, B. Tsui-Pierchala, A. C. Maroney and E. M. Johnson (2002). Inhibition of the c-jun N-terminal Kinase Signaling Pathway by the Mixed Lineage Kinase Inhibitor CEP-1347 (KT7515) Preserves Metabolism and Growth of Trophic Factor-Deprived Neurons. *The Journal of Neuroscience*. **22**:(1), 103-113
- A. Hartmann, S. Hunot, P. P. Michel, M. Muriel, S. Vyas, B. A. Faucheux, A. Mouatt-Prigent, A. Turmel, A. Srinivasan, M. Ruberg, G. I. Evan, Y. Agid and E. C. Hirsch (2000). Caspase-3: A vulnerability factor and final effector in apoptotic death of dopaminergic neurons in Parkinson's disease. *Proceedings of the National Academy of Sciences*. **97**:(6), 2875-2880
- S. Hashimoto and A. Hagino (1989). Staurosporine-induced neurite outgrowth in PC12h cells. *Experimental Cell Research*. **184**:(2), 351-359
- Y. Hashimoto, Ito, Y., Arakawa, E., Kita, Y., Terashita, K., Niikura, T. and Nishimoto, I. (2002). Neurotoxic mechanisms triggered by Alzheimer's disease-linked mutant M146L presenilin 1: involvement of NO synthase via a novel pertussis toxin target. *Journal of Neurochemistry*. **80**, 426-437
- N. Hauptmann, J. Grimsby, J. C. Shih and E. Cadenas (1996). The metabolism of tyramine by monoamine oxidase A/B causes oxidative damage to mitochondrial DNA. *Archives of Biochemistry and Biophysics*. **335**, 295-304
- C. A. Hazzlan, E. Cano, A. Cuenda, M. J. Barratt, P. Cohen and L. C. Mahadevan (1996). p38/RK is essential for stress-induced nuclear responses: JNK/SAPKs and c-Jun/ATF-2 phosphorylation are insufficient. *Current Biology*. **6**:(8), 1028-1031
- R. E. Heikkila, W. J. Nicklas, I. Vyas and R. C. Duvoisin (1985). Dopaminergic toxicity of rotenone and the 1-methyl-4-phenyl pyridinium ion after their stereotaxic administration to rats: implications for the mechanism of 1-methyl-4-phenyl-1,2,3,6-tetrahydropyridine toxicity. *Neurosci Lett*. **62**(3), 389-94

- R. E. Heikkila (1988). 1-methyl-4-phenyl-1,2,3,6-tetrahydropyridine (MPTP)-A dopaminergic neurotoxin. *Journal of Neural Transmission*. **4**, 1-5
- M. O. Hengartner (2000). The biochemistry of apoptosis. *Nature*. **407**, 770-776
- Z. Herceg and Z. Q. Wang (1999). Failure of poly(ADP-ribose) polymerase cleavage by caspases leads to induction of necrosis and enhanced apoptosis. *Molecular and Cellular Biology*. **19**:(7), 5124-5133
- A. a. C. Hershko, A. (1992). The Ubiquitin System. *Annual Review Biochemistry*. **61**, 761-807
- M. Hetmen and A. Gozdz (2004). Role of extracellular regulated kinase 1 and 2 in neuronal survival. *European Journal of Biochemistry*. **271**, 2050-2055
- H. Hidaka and R. Kobayashi (1992). Pharmacology of protein kinase inhibitors. *Ann. Rev. Pharmacol. Toxicol.* **32**, 377-397
- R. Highfield, (2001), Daily Telegraph, When the brain goes to waste, 01.09.2001
- D. D. Hirsch and P. J. S. Stork (1997). Mitogen-activated protein kinase phosphatases inactivate stress-activated protein kinase pathways in vivo. *Journal of Biological Chemistry*. **272**:(7), 4568-4575
- G. U. Hoglinger, G. Carrard, P. P. Michel, F. Medja, A. Lombes, M. Ruberg, B. Friguet and E. C. Hirsch (2003). Dysfunction of mitochondrial complex I and the proteasome: interactions between two biochemical deficits in a cellular model of Parkinson's disease. *Journal of Neurochemistry*. **86**, 1297-1307
- D. P. Holschneider, T. Kumazawa, K. Chen and J. C. Shih (1998). Tissue-specific effects of estrogen on monoamine oxidase A and B in the rat. *Life Sciences*. **63**:(3), 155-160
- D. P. Holschneider and J. C. Shih (2000). Monoamine Oxidase: Basic and Clinical Perspectives, *American College of Neuropsychopharmacology*. Nashville,
- A. Holt, M. Berry, D and A. A. Boulton (2004). On the Binding of Monoamine Oxidase Inhibitors to Some Sites Distinct from the MAO Active Site, and Effects Thereby Elicited. *Neurotoxicology*. **25**, 251-266
- G. S. Homtamlisligil and X. O. Breakefield (1991). Human monoamine oxidase A gene determines levels of enzyme activity. *American Journal of Human Genetics*. **49**, 335-336
- S. Hopkins, P. Yan, K. Bourland, A. Muhlethaler, J. Bodmer and N. Gross (2002). Doxorubicin-induced death in neuroblastoma does not involve death receptors in S-type cells and is caspase-independent in N-type cells. *Oncogene*. **21**:(39), 6132-6137
- S. Hopkins-Donaldson, J. Bodmer, K. Bourland, C. B. Brognara, J. Tschopp and N. Gross (2000). Loss of Caspase-8 Expression in Highly Malignant Human Neuroblastoma Cells Correlates with Resistance to Tumour Necrosis Factor-related Apoptosis-inducing Ligand-induced Apoptosis. *Cancer research*. **60**, 4315-4319
- C. Horbinski and C. T. Chu (2005). Kinases signaling cascades in the mitochondrion: a matter of life or death. *Free Radical Biology and Medicine*. **38**, 2-11
- S. Horstmann, P. J. Kahle and G. D. Borasio (1998). Inhibitors of p38 Mitogen-Activated Protein Kinase Promote Neuronal Survival In Vitro. *Journal of Neuroscience Research*. **52**, 483-490
- C. Huang, Huang, N., Shyue, S. and Chern, Y. (2003). Hydrogen peroxide induces loss of dopamine transporter activity: a calcium-dependent oxidative metabolism. *Journal of Neurochemistry*. **86**, 1247-1259

- J. a. P. Huang, M. A. (1995). Distribution of glutathione and glutathione-related enzyme systems in mitochondria and cytosol of cultured cerebellar astrocytes and granule cells. *Brain Research*. **680**, 16-22
- G. Hughes, M. P. Murphy and E. C. Ledgerwood (2005). Mitochondrial ROS regulate the temporal activation of NF- κ B to modulate TNF-induced apoptosis: evidence from mitochondria-targeted antioxidants. *Biochemical Journal*. **389**, 83-89
- C. D. N. Humfrey, G. B. Steventon, S. G. Sturman, R. H. Waring, B. Griffiths and A. C. Williams (1990). Monoamine-Oxidase Substrates in Parkinsons-Disease. *Biochemical Pharmacology*. **40**:(11), 2562-2564
- S. Hunot, Vila, M., Teismann, P., Davies, R. J., Hirsch, E. T., Przedborski, P. R. and Flavell, R. A. (2003). JNK-mediated induction of cyclooxygenase 2 is required for neurodegeneration in a mouse model of Parkinson's disease. *Proceedings of the National Academy of Sciences*. **101**:(2), 665-670
- M. Iglesias, M. F. Segura, J. X. Comella and G. Olmos (2003). μ -opioid receptor activation prevents apoptosis following serum withdrawal in differentiated SH-SY5Y cells. *Neuropharmacology*. **44**, 482-492
- H. Imai and Y. Nakagawa (2003). Biological Significance of Phospholipid Hydroperoxide Glutathione Peroxidases in Mammalian Cells. *Free Radical Biology and Medicine*. **34**, 145-169
- C. Inglesias-DeLaCruz, P. Ruiz-Torres, J. Alcamí, L. Diez-Marques, R. Ortega-Velazquez, S. Chen, M. Rodriguez-Puyol, F. N. Ziyadeh and D. Rodriguez-Puyol (2001). Hydrogen peroxide increases extracellular matrix mRNA through TGF- β . *Kidney International*. **59**, 87-95
- Invitrogen (2006)
- I. Irwin and J. W. Langston (1985). Selective Accumulation of Mpp⁺ in the Substantia Nigra - a Key to Neurotoxicity. *Life Sciences*. **36**:(3), 207-212
- O. Isacson, B. B. Seo, L. Lin, D. Albec and A. Granholm (2002). Alzheimer's disease in Down's syndrome roles of APP in ACH. *Trends in Neuroscience*. **25**, 79-83
- T. Ishii, Sakurai, T., Usami, H. and Uchida, K. (2005). Oxidative Modification of Proteasome: Identification of an Oxidation-Sensitive Subunit in 26 S Proteasome. *Biochemistry*. **44**, 13893-13901
- Y. Ishikawa and M. Kitamura (1999). Dual potential of extracellular signal-regulated kinase for the control of cell survival. *Biochemical and Biophysical Research Communications*. **264**:(3), 696-701
- Y. a. N. Itano, Y. (1995). 1-Methyl-4-phenyl-pyridinium ion (MPP⁺) causes DNA fragmentation and increases Bcl-2 expression in human neuroblastoma, SH-SY5Y cells, through different mechanisms. *Brain Research*. **704**, 240-245
- Y. Ito, K. Oh-hashii, K. Kiuchi and Y. Hirata (2006). p44/42 MAP kinase and c-jun N-terminal kinase contribute to the up-regulation of caspase-3 in manganese-induced apoptosis in PC12 cells. *Brain Research*. **1099**, 1-7
- T. Jabs (1998). Reactive Oxygen Intermediates as Mediators of Programmed Cell Death in Plants and Animals. *Biochemical Pharmacology*. **57**, 231-245
- J. Jacobson and M. R. Duchon (2002). Mitochondrial oxidative stress and cell death in astrocytes - requirement for stored Ca²⁺ and sustained opening of the permeability transition pore. *Journal of Cell Science*. **115**, 1175-1188

- J. Jahngen, M. S. Obin, X. Gong, F. Shang, T. R. Nowell, J. Gong, H. Abasi, J. Blumberg and A. Taylor (1997). Regulation of Ubiquitin-conjugating Enzymes by Gluathione. *Journal of Biological Chemistry*. **272**:(45), 28218-28226
- R. J. Jakel and W. F. Maragos (2000). Neuronal cell death in Huntington's disease: a potential role for dopamine. *T.I.N.S.* **23**:(6), 239-245
- A. Jalava, J. Heikkila, M. Lintunen, K. Akerman and S. Pahlman (1992). Staurosporine induces a neuronal phenotype in SH-SY5Y human neuroblastoma cells that resembles that induced by the phorbol ester 12-O-tetradecanoyl phorbol-12 acetate (TPA). *FEBS letters*. **300**:(2), 114-118
- S. Jalkanen and M. Salmi (2001). Cell surface monoamine oxidases: enzymes in search of a function. *EMBO. J.* **20**, 3893-3901
- A. M. James, R. A. J. Smith and M. P. Murphy (2004). Antioxidant and prooxidant properties of mitochondrial Coenzyme Q. *Archives of Biochemistry and Biophysics*. **423**, 47-56
- B. Jang, T. Sanchez, H. Schaefer, O. Trifan, C. Liu, C. Creminon, C. Huang and T. Hla (2006). Serum withdrawal-induced Post-transcriptional stabilisation of cyclooxygenase-2 mRNA in MDA-MB-231 Mammary Carcinoma cells requires activity of the p38 stress-activated protein kinase. *The Journal of Biological Chemistry*. **275**:(50), 39507-39515
- R. U. Janicke, M. L. Sprengart, M. R. Wati and A. G. Porter (1998). Caspase-3 Is Required for DNA Fragmentation and Morphological Changes Associated with Apoptosis. *The Journal of Biological Chemistry*. **273**, 9357-9360
- P. Jenner (1994). Oxidative Damage in Neurodegenerative Disease. *Lancet*. **344**:(8925), 796-798
- P. Jenner and C. W. Olanow (1996). Oxidative stress and the pathogenesis of Parkinson's disease. *Neurology*. **47**:(6), 161S-170
- N. Jha, Kumar, M. J., Boonplueang, R. and Anderson, J. K. (2002). Glutathione decreases in dopaminergic PC12 cells interfere with the ubiquitin protein degradation pathway: relevance for Parkinson's disease? *Journal of Neurochemistry*. **80**, 555-561
- H. Jiang, Q. Jiang, W. Liu and J. Feng (2006). Parkin Suppresses the Expression of Monoamine Oxidases. *The Journal of Biological Chemistry*. **281**, 8591-8599
- J. P. Johnston (1968). Some observations upon a new inhibitor of monoamine oxidase in brain tissue. *Biochemical Pharmacology*. **17**:(7), 1285-1297
- A. Jones, R. Reed and J. Weyers (1998). Practical Skills in Biology, 2nd Ed *Longman*.
- T. Z. E. Jones, D. Balsa, M. Unzeta and R. R. Ramsay (2007). Variations in activity and inhibition with pH: the protonated amine is the substrate for monoamine oxidase, but uncharged inhibitors bind better. *Journal of Neural Transmission*. **114**:(6), 707-712
- S. S. Jossan, P. G. Gillberg, G. C. Gottfries, I. Karlsson and L. Oreland (1991). Monoamine oxidase B in brains from patients with Alzheimer's disease: A biochemical and autoradiographical study. *Neuroscience*. **45**, 1-12
- N. Joza, S. A. Susin, E. Daugas, W. L. Stanford, S. K. Cho, C. Y. J. Li, T. Sasaki, A. J. Elia, H. Y. M. Cheng, L. Ravagnan, K. F. Ferri, N. Zamzami, A. Wakeham, R. Hakem, H. Yoshida, Y. Y. Kong, T. W. Mak, J. C. Zuniga-Pflucker, G. Kroemer and J. M. Penninger (2001). Essential role of the mitochondrial apoptosis-inducing factor in programmed cell death. *Nature*. **410**:(6828), 549-554

- V. E. Kagan, A. V. Smirnov, V. M. Savov and V. Z. Gorkin (1984). Peroxidation of lipids in mitochondrial membranes, induced by enzymatic deamination of biogenic amines. *Vopr. Med. Khim.* **30**:(1), 112-118
- B. E. Kalisch, Demeris, S., Ishak, M. and Rylett, R. J. (2003). Modulation of nerve growth factor-induced activation of MAP kinase in PC12 cells by inhibitors of nitric oxide synthase. *Journal of Neurochemistry.* **87**, 1321-1332
- S. V. Kalivendi, Cunningham, S., Kotamraju, S., Joseph, J., Hillard, C. J. and Kalyanaraman, B. (2004). □Synuclein Up-regulation and Aggregation during MPP⁺ induced Apoptosis in Neuroblastoma Cells. *The Journal of Biological Chemistry.* **279**:(15), 15240-15247
- H. Kamata, S. Honda, S. Maeda, L. Chang, H. Hirata and M. Karin (2005). Reactive Oxygen Species Promote TNF α . *Cell.* **120**, 649-661
- S. H. Kaufmann, S. Desnoyers, Y. Ottaviano, N. E. Davidson and G. G. Poirer (1993). Specific proteolytic cleavage of poly(ADP-ribose) polymerase: An early marker of chemotherapy-induced apoptosis. *Cancer Research.* **53**, 3976-3985
- S. H. Kaufmann, S. Schlipf, J. Sanz, K. Neubert, R. Stein and C. Borner (2003). Characterization of the signal that directs Bcl-X_L, but not Bcl-2, to the mitochondrial outer membrane. *Journal of Cell Biology.* **160**, 53-64
- H. Kaufmann(S), M. Perez, W. Zhang, P. C. Bickford, D. B. Holmes and G. Tagliatela (2003). Free radical-dependent nuclear localization of Bcl-2 in the central nervous system of aged rats is not associated with Bcl-2 mediated protection from apoptosis. *Journal of Neurochemistry.* **87**, 981-994
- D. J. Keating (2008). Mitochondrial dysfunction, oxidative regulation of exocytosis and their relevance to neurodegenerative disorders. *Journal of Neurochemistry.* **104**, 298-305
- G. F. Kelso, C. M. Porteous, C. V. Coulter, G. Hughes, W. K. Porteous, E. C. Ledgerwood, R. A. J. Smith and M. P. Murphy (2000). Selective Targeting of a Redox-active Ubiquinone to Mitochondria within Cells. *The Journal of Biological Chemistry.* **276**, 4588-4596
- P. Kenchappa, A. Yadav, G. Singh, S. Nandana and K. Banerjee (2004). Rescue of TNF α -inhibited neuronal cells by IGF-1 involves Akt and c-Jun N-terminal kinases. *Journal of Neuroscience Research.* **76**:(4), 466-474
- A. Kim, Murphy, M. P. and Oberley, T. D. (2005). Mitochondrial redox state regulates transcription of the nuclear-encoded mitochondrial protein manganese superoxide dismutase: a proposed adaptive response to mitochondrial redox imbalance. *Free Radical Biology and Medicine.* **38**, 644-654
- J. J. Kim, J. C. Shih, K. Chen, L. Chen, S. Bao, S. Maren, S. G. Anagnostaras, M. S. Fanselow, E. De Maeyer, I. Seif and R. F. Thompson (1997). Selective enhancement of emotional, but not motor, learning in monoamine oxidase A-deficient mice. *Proc. Natl. Acad. Sci. USA.* **94**:(5929-5933),
- A. R. King, S. E. Francis, C. J. Bridgeman, H. Bird, M. K. B. Whyte and D. C. Crossman (2003). A Role for Caspase-1 in Serum Withdrawal-Induced Apoptosis of Endothelial Cells. *Laboratory Investigation.* **83**:(10), 1497-1508
- Y. Kitamura, M. Inden, A. Miyamura, J. Kakimura, T. Taniguchi and S. Shimohama (2002). Possible involvement of both mitochondria- and endoplasmic reticulum-dependent caspase pathways in rotenone-induced apoptosis in human neuroblastoma SH-SY5Y cells. *Neuroscience Letters.* **332**, 25-28

- J. Knoll and K. Magyar (1972). Some puzzling pharmacological effects of monoamine oxidase inhibitors. *Adv Biochem Psychopharmacol.* **5**, 393-408
- P. Knowles, C. Kurtis, J. Murray, C. Saysell, W. Tambryajah, C. Wilmot, M. McPherson, S. Phillips, D. Dooley, D. Brown, M. Rogers and M. Mure (2007). Hydrazine and amphetamine binding to amine oxidases: old drugs with new prospects. *Journal of Neural Transmission.* **114**:(6), 743-746
- L. M. Kochersperger, E. L. Parker, M. Siciliano, G. J. Darlington and R. M. Denney (1986). Assignment of Genes for Human Monoamine Oxidase-a and Oxidase-B to the X-Chromosome. *Journal of Neuroscience Research.* **16**:(4), 601-616
- L. M. Kochersperger, A. Waguespack, J. C. Patterson, C. C. W. Hsieh, W. Weyler, J. I. Salach and R. M. Denney (1985). Immunological Uniqueness of Human Monoamine Oxidase-a and Oxidase-B - New Evidence from Studies with Monoclonal-Antibodies to Human Monoamine Oxidase-A. *Journal of Neuroscience.* **5**:(11), 2874-2881
- J. Koh, M. B. Wie, B. J. Gwag, S. L. Sensi, M. T. Canzoniero, J. Demaro, C. Csernansky and D. W. Choi (1995). Staurosporine-Induced Apoptosis. *Experimental Neurology.* **135**:(2), 153-159
- G. Kohler and C. Milstein (1976). Derivation of Specific Antibody-Producing Tissue-Culture and Tumor Lines by Cell-Fusion. *European Journal of Immunology.* **6**:(7), 511-519
- J. Kornhuber, C. Konradi, F. Mack-Buckhardt, P. Riederer, H. Heinsen and H. Beckmann (1989). Ontogenesis of monoamine oxidase-A and -B in the human brain frontal cortex. *Brain Research.* **499**:(1), 81-86
- A. J. Kowaltowski, R. G. Fenton and G. Fiskum (2004). BCL-2 family proteins regulate mitochondrial reactive oxygen production and protect against stress. *Free Radical Biology and Medicine.* **37**:(11), 1845-1853
- E. Kragten, I. Lalande, K. Zimmermann, S. Roggo, P. Schindler, D. Muller, J. Van Oostrum and P. Furst (1998). Glyceraldehyde-3-phosphate Dehydrogenase, the Putative Target of the Antiapoptotic Compounds CGP 3466 and R-(-)-Deprenyl. *The Journal of Biological Chemistry.* **273**:(10), 5821-5828
- S. Krajewski, M. Krajewska, L. M. Ellerby, K. Welsh, Z. Xie, Q. L. Deveraux, G. S. Salvesen, D. E. Bredesen, R. E. Rosenthal, G. Fiskum and J. C. Reed (1999). Release of caspase-9 from mitochondria during neuronal apoptosis and cerebral ischemia. *Proceedings of the National Academy of Sciences.* **96**, 5752-5757
- B. C. Kramer, Yabut, J. A., Cheong, J., Jnobaptiste, R., Robakis, T., Olanow, C. W. and Mytilineou, C. (2004). Toxicity of glutathione depletion in mesencephalic cultures: a role for arachidonic acid and its lipoxygenase metabolites. *European Journal of Neuroscience.* **19**:(2), 280-286
- I. Kruman and Q. Guo (1998). Calcium and reactive oxygen species mediate staurosporine-induced mitochondrial dysfunction and apoptosis in PC12 cells. *Journal of Neuroscience Research.* **51**, 298-308
- H. Kuhn, Walther, M. and Kuban, R. J. (2002). Mammalian arachidonate 15-lipoxygenases Structure, function, and biological implications. *Prostaglandins and other lipid mediators.* **68-69**, 263-290
- H. Kuhn and A. Borchert (2002). Regulation of enzymatic lipid peroxidation: the interplay of peroxidising and peroxide reducing enzymes. *Free Radical Biology and Medicine.* **33**, 145-172

- M. J. Kumar, D. G. Nicholls and J. K. Anderson (2003). Oxidative α -Ketoglutarate Dehydrogenase Inhibition via Subtle Elevations in Monoamine Oxidase B Levels Results in Loss of Spare Respiratory Capacity. *The Journal of Biological Chemistry*. **278**:(47), 46432-46439
- J. L. Kummer, P. K. Rao and K. A. Heidenreich (1997). Apoptosis Induced by Withdrawal of Trophic Factors Is Mediated by p38 Mitogen-activated Protein Kinase. *The Journal of Biological Chemistry*. **272**:(39), 20490-20494
- O. R. Kunduzova, P. Bianchi, A. Parini and C. Cambon (2002). Hydrogen peroxide production by monoamine oxidase during ischemia/reperfusion. *European Journal of Pharmacology*. **448**, 225-230
- I. Kuwabara, Kuwarbara, Y., Yang, R., Schuler, M., Green, D. R., Zuraw, B. L., Hsu, D. K. and Liu, F. (2002). Galectin-7 (PIG1) Exhibits Pro-apoptotic Function through JNK Activation and Mitochondrial Cytochrome c Release. *The Journal of Biological Chemistry*. **277**:(5), 3487-3497
- T. Kuwana, J. J. Smith, M. Muzio, V. Dixit, D. D. Newmayer and S. Kornbluth (1998). Apoptosis induced by caspase-8 is amplified through the release of mitochondrial release of cytochrome c. *The Journal of Biological Chemistry*. **273**, 16589-16594
- S. Kweon, Z. Lee, S. Yi, Y. Kim, J. Han, S. Paik and K. Ha (2004). Protective Role of Tissue Transglutaminase in the Cell Death Induced by TNF α . *Journal of Biochemistry and Molecular Biology*. **37**:(2), 185-191
- C. Lai and P. H. Yu (1997). Dopamine and I- β -3,4-dihydroxyphenylalanine hydrochloride (L-DOPA)-induced cytotoxicity towards catecholaminergic neuroblastoma SH-SY5Y cells effects of oxidative stress and antioxidative factors. *Biochemical Pharmacology*. **53**, 363-372
- L. a. W. Lan, N. (1999). Phosphatidylinositol 3-kinase and protein kinase C are required for the inhibition of caspase activity by epidermal growth factor. *FEBS letters*. **444**, 90-96
- N. C. Lan, C. Heinzmann, A. Gal, I. Klisak, U. Orth, E. Lai, J. Grimsby, R. S. Sparkes, T. Mohandas and J. C. Shih (1989). Human monoamine oxidase A and B genes map to Xp11.23 and are deleted in patient with Norrie disease. *Genomics*. **4**, 552-559
- J. W. Langston, P. Ballard, J. W. Tetrud and I. Irwin (1983). Chronic Parkinsonism in Humans Due to a Product of Meperidine-Analog Synthesis. *Science*. **219**:(4587), 979-980
- P. Lassus, X. Opitz-Araya and Y. Lazebnik (2002). Requirement for caspase-2 in stress-induced apoptosis before mitochondrial permeabilization. *Science*. **297**:(5585), 1352-1354
- H. S. Lee, C. W. Park and Y. S. Kim (2000). MPP $^{+}$ increases the vulnerability to oxidative stress rather than directly mediating oxidative damage in human neuroblastoma cells. *Experimental Neurology*. **165**:(1), 164-171
- Y. Lee, M. Kim, J. Han, K. Yeom, S. Lee, S. H. Baek and V. N. Kim (2004). microRNA genes are transcribed by RNA polymerase II. *The EMBO Journal*. **23**, 4051-4060
- M. Leist and P. Nicotera (1997). The shape of cell death. *Biochemical and Biophysical Research Communications*. **236**:(1), 1-9
- E. Leroy, Boyer, R., Auburger, G., Leube, B., Ulm, G., Mezey, E., Harta, G., Brownstein, M. J., Jonnalagada, J., Chernova, T., Dehejia, A., Lavedan, C., Gasser, T., Steinbach, P. J., Wilkinson, K. D. and Polymeropoulos, M. H. (1998). The Ubiquitin pathway in Parkinson's disease. *Nature*. **395**, 451-452

- N. Lev, E. Melamed and D. Offen (2003). Apoptosis and Parkinson's disease. *Progress in Neuro-Psychopharmacology & Biological Psychiatry*. **27**, 245-250
- P. Levitt, Harvey, J. A., Friedman, E., Simansky, K. and Murphy, E. H. (1997). New evidence for neurotransmitter influences on brain development. *Trends in Neuroscience*. **20**, 269-274
- J. Li and N. J. Holbrook (2003). Common mechanisms for declines in oxidative stress tolerance and proliferation with aging. *Free Radical Biology and Medicine*. **35**:(3), 292-299
- S.-L. Liu, X. Lin, D.-Y. Shi, J. Cheng, C.-Q. Wu and Y.-D. Zhang (2002). Reactive oxygen species stimulated human hepatoma cell proliferation via cross-talk between PI3-K/PKB and JNK signaling pathways. *Archives of Biochemistry and Biophysics*. **406**, 173-182
- E. Lopez and I. Ferrer (2000). Staurosporine- and H-7-induced cell death in SH-SY5Y neuroblastoma cells is associated with caspase-2 and caspase-3 activation, but not with the activation of the FAS/FAS-L-caspase-8 signaling pathway. *Brain Res Mol Brain Res*. **85**:(1-2), 61-67
- O. H. Lowry, N. J. Rosebrough, A. L. Farr and R. J. Randall (1951). Protein measurement with the Folin phenol reagent. *The Journal of Biological Chemistry*. **193**, 265-275
- Y. Luo, H. Umegaki, X. Wang, R. Abe and G. S. Roth (1998). Dopamine Induces Apoptosis through an Oxidation-involved SAPK/JNK Activation Pathway. *The Journal of Biological Chemistry*. **273**:(6), 3756-3764
- J. Ma, M. Yoshimura, E. Yamashita, A. Nakagawa, A. Ito and T. Tsukihara (2004). Structure of Rat Monoamine Oxidase A and its Specific Recognitions for Substrates and Inhibitors *Journal of Molecular Biology*. **338**:(1), 103-114
- M. R. Macleod, T. E. Allsop, J. McLuckie and J. S. Kelly (2001). Serum withdrawal causes apoptosis in SH-SY5Y cells. *Brain Research*. **889**, 308-315
- W. Malorni, A. M. Giammarioli, P. Matarrese, P. Pietrangeli, E. Agostinelli, A. Ciaccio, E. Grassilli and B. Mondovi (1998). Protection against apoptosis by monoamine oxidase A inhibitors. *FEBS letters*. **46**, 155-159
- H. Manev (2000). 5-Lipoxygenase gene polymorphism and onset of Alzheimer's disease. *Medical Hypotheses*. **54**:(1), 75-76
- J. J. Mann, M. Stanley, S. Gerson and M. Rossor (1980). Mental symptoms in Huntington's disease and a possible primary aminergic neuron lesion. *Science*. **210**, 1369-1371
- I. Manoli, H. Le, S. Alesci, K. K. McFann, Y. A. Su, T. Kino, G. P. Chousos and M. R. Blackman (2005). Monoamine oxidase-A is a major target gene for glucocorticoids in human skeletal muscle cells. *The FASEB Journal*. **19**, 1359-1361
- W. F. Maragos, K. L. Young, C. S. Altman, C. B. Pocernich, J. Drake, D. A. Butterfield, I. Seif, D. P. Holschneider, K. Chen and J. C. Shih (2004). Striatal Damage and Oxidative Stress Induced by the Mitochondrial Toxin Malonate Are Reduced In Clorgyline-Treated Rats and MAO-A Deficient Mice. *Neurochemical Research*. **29**:(4), 741-746
- D. L. Marcus, C. Thomas, C. Rodriguez, K. Simberkoff, J. S. Tsai, J. A. Strafaci and M. L. Freedman (1998). Increased peroxidation and reduced antioxidant enzyme activity in Alzheimer's disease. *Experimental Neurology*. **150**:(1), 40-44

- G. Maret, N. Eltayar, P. A. Carrupt, B. Testa, P. Jenner and M. Baird (1990). Toxication of Mptp (1-Methyl-4-Phenyl-1,2,3,6-Tetrahydropyridine) and Analogs by Monoamine-Oxidase - a Structure-Reactivity Relationship Study. *Biochemical Pharmacology*. **40**:(4), 783-&
- A. C. Maroney, M. S. Saporito and R. L. Hudkins (2002). Mixed lineage kinase family, potential targets for preventing neurodegeneration *Current Medicinal Chemistry*. **2**:(2), 143-155
- V. S. Marsden, L. O'Connor, L. A. O'Reilly, J. Silke, D. Metcalf, P. G. Ekert, D. C. S. Huang, F. Cecconi, K. Kulda, K. J. Tomaselli, S. Roy, D. W. Nicholson, D. L. Vaux, P. Bouillet, J. M. Adams and A. Strasser (2002). Apoptosis initiated by Bcl-2-regulated caspase activation independently of the cytochrome c/Apaf-1/caspase-9 apoptosome. *Nature*. **419**, 634-637
- J. L. Martindale and N. J. Holbrook (2002). Cellular response to oxidative stress: signalling for suicide and survival. *Journal of Cellular Physiology*. **192**, 1-
- W. Maruyama, Y. Akao, M. C. Carrillo, K. Kitani, M. Youdim, B. H and M. Naoi (2002). Neuroprotection by propargylamines in Parkinson's disease. Suppression of apoptosis and induction of prosurvival genes. *Neurotoxicology and Tetratology*. **24**, 675-682
- W. Maruyama, M. Naoi, T. Kasamatsu, Y. Hashizume, T. Takahashi, K. Kohda and P. Dostert (1997). An endogenous dopaminergic neurotoxin, N-methyl-(R)-salsolinol, induces DNA damage in dopaminergic neuroblastoma SH-SY5Y cells. *Journal of Neurochemistry*. **69**, 322-329
- W. Maruyama, T. Yamamoto, K. Kitani, M. C. Carrillo, M. Youdim and M. Naoi (2000). Mechanism underlying anti-apoptotic activity of a (-)deprenyl-related propargylamine, rasagiline. *Mechanisms of Ageing and Development*. **116**:(2-3), 181-191
- J. C. Mathai and V. Sitaramam (1994). Stretch Sensitivity of Transmembrane Mobility of Hydrogen Peroxide Through Voids in the Bilayer. *The Journal of Biological Chemistry*. **269**:(27), 17784-17793
- J. R. Mathiasen, McKenna, B. A. W., Saporito, M. S., Ghadge, G. D., Roos, R. P., Holskin, B. P., Wu, Z., Trusko, S. P., Connors, T. C., Maroney, A. C., Thomas, B. A., Thomas, J. C. and Bozyczko-Coyne, D. (2004). Inhibition of mixed lineage kinase 3 attenuates MPP⁺-induced neurotoxicity in SH-SY5Y cells. *Brain Research*. **1003**, 86-97
- M. P. Mattson, Q. Guo, K. Furukawa and W. A. Pedersen (1998). Presenilins, the endoplasmic reticulum, and neuronal apoptosis in Alzheimer's disease. *Journal of Neurochemistry*. **70**:(1), 1-14
- M. Mayer and M. Noble (1994). N-Acetyl-L-Cysteine is a Pluripotent Protector Against Cell Death and Enhancer of Trophic Factor-Mediated Cell Survival in vitro. *Proceedings of the National Academy of Sciences*. **91**, 7496-7500
- K. M. McGinnis, Gnegy, M. E., Park, Y. H., Mukerjee, N. and Wang, K. K. W. (1999a). Procaspase-3 and Poly(ADP)ribose Polymerase (PARP) Are Calpain Substrates. *Biochemical and Biophysical Research Communications*. **263**, 94-99
- K. M. McGinnis, Gnegy, M. E. and Wang, K. K. W. (1999b). Endogenous Bax Translocation in SH-SY5Y Human Neuroblastoma Cells and Cerebellar Granule Neurons Undergoing Apoptosis. *Journal of Neurochemistry*. **72**, 1899-1906
- K. S. P. McNaught, C. W. Olanow, B. Halliwell, O. Isacson and P. Jenner (2001). Failure of the ubiquitin-proteasome system in Parkinson's disease. *Nature Reviews Neuroscience*. **2**, 589-594

- K. S. P. a. J. McNaught, P. (2001). Proteasomal function is impaired in substantia nigra in Parkinson's disease. *Neuroscience Letters*. **297**, 191-194
- C. McNeill-Blue, B. A. Wetmore, J. F. Sanchez, W. J. Freed and B. A. Merrick (2006). Apoptosis mediated by p53 in rat neural AF5 cells following treatment with hydrogen peroxide and staurosporine. *Brain Research*. **1112**, 1-15
- D. Meksuriyen and G. A. Cordell (1988). Biosynthesis of Staurosporine, 1. ¹H- and ¹³C-NMR Assignments. *J. Nat. Prod.* **51**, 884-892
- J. Mialet-Perez, P. Bianchi, O. R. Kunduzova and A. Parini (2007). New insights on receptor-dependent and monoamine oxidase-dependent effects of serotonin in the heart. *Journal of Neural Transmission*. **114**:(6), 823-827
- K. Mielke and T. Herdegen (2000). JNK and p38 stress kinases-degenerative effectors of signal-transduction-cascades in the nervous system. *Progress in Neurobiology*. **61**:(1), 45-60
- M. A. Miller, B. Karacay, X. Zhu, M. S. O'Dorisio and A. D. Sandler (2006). Caspase-8L, a novel inhibitory isoform of caspase-8, is associated with undifferentiated neuroblastoma. *Apoptosis*. **11**:(1), 15-24
- H. P. Misra and I. Fridovich (1972). The Role of Superoxide Anion in the Autoxidation of Epinephrine and a Simple Assay for Superoxide Dismutase. *The Journal of Biological Chemistry*. **247**:(10), 3170-3175
- A. Molnar, A. M. Theodoras, L. I. Zon and J. M. Kyriakis (1997). Cdc42Hs, but not Rac1, Inhibits Serum-stimulated Cell Cycle Progression at G₁/S through a Mechanism Requiring p38/RK. *The Journal of Biological Chemistry*. **272**:(20), 13229-13235
- N. Morishima, K. Nakanishi, H. Takenouchi, T. Shibata and Y. Yasuhiko (2002). An endoplasmic reticulum stress-specific caspase cascade in apoptosis - Cytochrome c-independent activation of caspase-9 by caspase-12. *Journal of Biological Chemistry*. **277**:(37), 34287-34294
- J. H. Morris (1995). Pick's disease, *Cambridge University Press*. Cambridge,
- M. Mouradian (2002). Recent advances in the genetics and pathogenesis of Parkinson's disease. *Neurology*. **58**, 179-185
- A. Mudher and S. Lovestone (2002). Alzheimer's disease-do tauists and baptists finally shake hands. *Trends in Neuroscience*. **25**, 22-25
- M. M. K. Muqit, P. M. Abou-Sleiman, A. T. Saurin, K. Harvey, S. Gandhi, E. Deas, S. Eaton, M. D. Payne Smith, K. Venner, A. Matilla, D. G. Healy, W. P. Gilks, A. J. Lees, J. Holton, T. Revesz, P. J. Parker, R. J. Harvey, N. W. Wood and D. S. Latchman (2006). Altered cleavage and localisation of PINK1 to aggresomes in the presence of proteasomal stress. *Journal of Neurochemistry*. **98**, 156-169
- D. L. Murphy, K. B. Sims, F. Faroum, N. A. Garrick, A. De la Chapelle, E. Sankila, R. Norio and X. O. Breakefield (2005). Plasma amine oxidase activities in Norrie disease patients with an X-chromosomal deletion affecting monoamine oxidase. *Journal of Neural Transmission*. **83**:(1-2), 1435-1463
- D. L. Murphy and R. J. Wyatt (1972). Reduced Monoamine Oxidase Activity In Blood Platelets from Schizophrenic Patients. *Nature*. **238**, 225-226

- M. P. Murphy, M. J. Krueger, S. O. Sablin, R. R. Ramsay and T. P. Singer (1995). Inhibition of complex I by hydrophobic analogues of N-methyl-4-phenylpyridinium (MPP⁺) and the use of an ion-selective electrode to measure their accumulation by mitochondria and electron transport particles. *Biochemical Journal*. **306**, 359-365
- C. Mytilineou, R. H. Walker, R. Jnobaptiste and W. Olanow (2003). Levodopa Is Toxic to Dopamine in Neurons in an in Vitro but Not an in Vivo Model of Oxidative Stress. *The Journal of Pharmacology and Experimental Therapeutics*. **304**:(2), 792-800
- S. Nagata (1997). Apoptosis by death factors. *Cell*. **88**, 355-365
- T. Nakagawa and J. Y. Yuan (2000). Caspase-12 mediates an ER-specific apoptosis pathway. *Faseb Journal*. **14**:(8), A1586-A1586
- T. Nakagawa and J. Y. Yuan (2000). Cross-talk between two cysteine protease families: Activation of caspase-12 by calpain in apoptosis. *Journal of Cell Biology*. **150**:(4), 887-894
- A. Nakagawara, M. Arimi-Nakagarawa, N. J. Scavarda, C. G. Azar, A. B. Cantor and G. M. Brodeur (1993). Association between high levels of expression of the TRK gene and favorable outcome in human neuroblastoma. *New England Journal of Medicine*. **328**, 847-854
- M. Naoi and W. Maruyama (2001). Future of neuroprotection in Parkinson's disease. *Parkinsonism and Related Disorders*. **8**, 98-103
- M. Naoi, W. Maruyama, P. Dostert, Y. Hashizume, D. Nakahara, T. Takahashi and M. Ota (1996). Dopamine-derived endogenous 1 (R), 2(N)-dimethyl-6,7-dihydroxy-1,2,3,4-tetrahydroisoquinoline, N-methyl-(R)-salsolinol, induced parkinsonism in rat: biochemical, pathological and behavioral studies. *Brain Research*. **709**, 285-295
- R. W. Neumar, Y. A. Xu, H. Gada, R. P. Guttmann and R. Siman (2003). Cross-talk between calpain and caspase proteolytic systems during neuronal apoptosis. *Journal of Biological Chemistry*. **278**:(16), 14162-14167
- K. Newhouse, S. Hsuan, S. H. Chang, B. Cai, Y. Wang and Z. Xia (2004). Rotenone-Induced Apoptosis is Mediated By p38 And JNK MAP Kinases in Human Dopaminergic SH-SY5Y Cells. *Toxicological Sciences*. **79**, 137-146
- T. K. Newman, Y. V. Syagailo, C. S. Barr, J. R. Wendland, M. Champoux, M. Graessle, S. J. Suomi, J. D. Higley and K. P. Lesch (2005). Monoamine oxidase A gene promoter variation and rearing experience influences aggressive behavior in rhesus monkey. *Biological Psychiatry*. **57**:(2), 167-172
- H. N. Nguyen, C. Wang and D. C. Perry (2002). Depletion of intracellular calcium stores is toxic to SH-SY5Y neuronal cells. *Brain Research*. **924**, 159-166
- D. W. Nicholson and N. A. Thornberry (1997). Caspases: Killer proteases. *TRENDS in Biochemical Sciences*. **22**, 299-306
- W. J. Nicklas, I. Vyas and R. E. Heikkila (1985). Inhibition of NADH-linked oxidation in brain mitochondria by 1-methy-4-phenylpyridine, a metabolite of the neurotoxin 1-methy-4-phenylpyridine. *Life Science*. **36**, 2503-2508
- V. G. Nicoletti and A. G. Stella (2004). Role of PARP Under Stress Conditions: Cell Death or Protection? *Neurochemical Research*. **28**:(2), 1573-6903
- A. Nicotra and S. H. Parvez (2000). Cell death induced by MPTP, a substrate for monoamine oxidase B. *Toxicology*. **153**:(1-3), 157-166
- A. Nicotra, F. Pierucci, H. Parvez and O. Senatori (2004). Monoamine Oxidase Expression During Development and Aging. *Neurotoxicology*. **25**, 155-165

- H. Niculescu, E. Bonfoco, Y. Kasuya, F. Claret, D. R. Green and M. Karin (1999). Withdrawal of survival factors results in activation of the JNK pathway in neuronal cells leading to Fas ligand induction and cell death. *Molecular and Cellular Biology*. **19**:(1), 751-763
- Y. Niikura, T. Nonaka and S. Imajoh-Oluni (2002). Monitoring of Caspase-8/FLICE Processing and Activation upon Fas Stimulation with Novel Antibodies Directed against Cleavage site for Caspase-8 and Its Substrate FLICE-Like Inhibitory Protein (FLIP). *The Journal of Biochemistry*. **132**:(1), 53-62
- M. Nishida, Y. Maruyama, R. Tanaka, K. Kontani, T. Nagao and H. Kurose (2000). G alpha i and G alpha o are target proteins of reactive oxygen species. *Nature*. **408**, 492-495
- S. Nishimoto and E. Nishida (2006). MAPK signalling: ERK5 versus ERK1/2. *EMBO reports*. **7**:(8), 782-786
- J. Nitobe, S. Yamaguchi, M. Okuyama, N. Nozaki, M. Sata, T. Miyamoto, Y. Takeishi, I. Kubota and H. Tomoike (2003). Reactive oxygen species regulate FLICE inhibitory protein (FLIP) and susceptibility to Fas-mediated apoptosis in cardiac myocytes. *Cardiovascular Research*. **57**, 119-128
- H. Nohl, L. Gille and K. Staniek (2004). The mystery of reactive oxygen species derived from cell respiration. *Acta Biochimica Polonica*. **51**:(1), 223-229
- G. Norrie (1927). Causes of blindness in children. *Acta Ophthalmology*. **5**, 357-386
- A. C. Nulton-Persoson, D. W. Starke, J. J. Mieval and L. I. Szweda (2003). Reversible inactivation of α -ketoglutarate dehydrogenase in response to alterations in the mitochondrial glutathione status. *Biochemistry*. **42**, 4235-4242
- M. O' Brian, R. Moravec and T. Riss (2003)
- C. W. Olanow and W. G. Tatton (1999). Etiology and Pathogenesis of Parkinson's disease. *Annual Review of Neuroscience*. **22**, 123-144
- P. Opal, J. J. Garcia, F. Propst, A. Matilla, H. T. Orr and H. Y. Zoghbi (2003). Mapmodulin/Leucine-rich Acidic Nuclear Protein Binds the Light Chain of Microtubule-associated Protein 1B and Modulates Neuritogenesis. *Journal of Biological Chemistry*. **278**, 34691-34699
- L. Oreland (1993). Monoamine oxidase in neuro-psychiatric disorders, *VSP Publishing*. Lorton, Virginia, 219-247
- L. Oreland (2004). Platelet monoamine oxidase, Personality and Alcoholism: The Rise, Fall and Resurrection. *Neurotoxicology*. **25**, 78-79
- L. Oreland, C. J. Fowler and D. Schalling (1981). Low platelet monoamine oxidase activity in cigarette smokers. *Life Science*. **29**, 2511-2518
- L. Oreland and G. C. Gottfries (1986). Brain and brain monoamine oxidase in aging and in dementia of Alzheimer's type. *Prog. Neuropharmacol. Biol. Psychiatr.* **10**, 533-540
- S. Orrenius, B. Zhivotovsky and P. Nicotera (2003). Regulation of cell death: the calcium-apoptosis link. *Nature Reviews*. **4**, 553-565
- X. Ou, K. Chen and J. C. Shih (2004). Dual Functions of Transcription Factors, Transforming Growth Factor- β -inducible gene (TIEG)2 and Sp3, Are mediated by CACCC Element and Sp1 Sites of Human Monoamine Oxidase (MAO) B Gene. *The Journal of Biological Chemistry*. **279**:(20), 21021-21928

- X. Ou, K. Chen and J. C. Shih (2006). Monoamine oxidase A and repressor R1 are involved in apoptotic signaling pathway. *Proceedings of the National Academy of Sciences*. **103**:(29), 10923-10928
- E. D. Owuor, Kong, A. T (2002). Antioxidants and oxidants regulated signal transduction pathways. *Biochemical Pharmacology*. **64**, 765-770
- D. J. Pagliarini, Dixon, J. E (2006). Mitochondrial modulation: reversible phosphorylation takes center stage? *TRENDS in Biochemical Sciences*. **31**:(1), 26-34
- S. Pahlman, J. C. Hoehner, E. Nanberg, F. Hedborg, S. Fagerstrom, C. Gestblom, I. Johansson, U. Larsson, E. Lavenius, E. Ortoft and H. Soderholm (1995). Differentiation and Survival Influences of Growth Factors In Human Neuroblastoma. *Eur. J. Cancer*. **31**:(4), 453-458
- S. Pahlman, L. Odelstad, E. Larsson, G. Grotte and K. Nilsson (1981). Phenotype changes of human neuroblastoma cells in culture induced by 12-O-tetradecanoyl-phorbol-13-acetate. *International Journal of Cancer*. **28**, 583-589
- S. Pahlman, A. I. Ruusala, L. Abrahamsson, M. E. K. Mattsson and T. Esscher (1984). Retanoic acid-induced differentiation of cultured human neuroblastoma cells: a comparison with phorbol ester-induced differentiation. *Cell Differentiation*. **14**:(135-144),
- B. Pardo, M. A. Mena and J. G. Yebenes (1995). L-Dopa inhibits complex IV of the electron transport chain in catecholamine rich human neuroblastoma NB69 cells. *Journal of Neurochemistry*. **64**, 576-582
- J. Parkinson (1817). An essay on shaking palsy. *Journal of Neuropsychiatry and Clinical Neuroscience*. **14**, 223-236
- R. K. B. Pearce, A. D. Owen, S. Daniel, P. Jenner and C. D. Marsden (1997). Alterations in the distribution of gluathione in the substantia nigra in Parkinson's disease. *Journal of Neural Transmission*. **104**, 661-677
- B. Pettmann and C. E. Henderson (2003). Killer wiles: growing interest in Fas. *Nature Cell Biology*. **5**, 91-92
- S. Philipsen and G. Suske (1999). A tale of three fingers: the family of mammalian Sp/XKLF transcription factors. *Nucleic Acids Research*. **27**:(15), 2991-3000
- J. W. Phillis, Horrocks, L. A and Farooqui, A. A (2006). Cyclooxygenases, lipoxygenases, and epoxygenases in CNS: Their role and involvement in neurological disorders. *Brain Research Reviews*. **in press**:(in press),
- H. Plun-Favreau, K. Klupsch, N. Moiso, S. Gandhi, S. Kjaer, D. Frith, K. Harvey, E. Deas, R. J. Harvey, N. McDonald, N. W. Wood, L. M. Martins and J. Downward (2007). The mitochondrial protease HtrA2 is regulated by Parkinson's disease-associated kinase PINK1. *Nature Cell Biology*. **9**, 1243-1252
- I. D. Podmore, H. Griffiths, K. E. Herbert, N. Mistry, P. Mistry and J. Lunec (1998). Vitamic C exhibits pro-oxidant properties. *Nature*. **392**, 559
- S. Poser, S. Impey, Z. Xia and D. R. Strom (2003). Brain-Derived Neurotrophic Factor Protection of Cortical Neurons from Serum Withdrawal-Induced Apoptosis Is Inhibited by cAMP. *The Journal of Neuroscience*. **23**:(11), 4420-4427
- J. A. Potashkin and G. E. Meredith (2006). The Role of Oxidative Stress in the Dysregulation of Gene Expression and Protein Metabolism in Neurodegenerative Disease. *Antioxidants & Redox Signaling*. **8**:(1&2), 144-151

- D. Pratico (2002). Alzheimer's disease and oxygen radicals: new insights. *Biochemical Pharmacology*. **63**, 563-567
- B. Pulverer, A. Schuldt, S. Swaminathan, N. Le Bot and S. Grisendi (2003). Whither RNAi? *Nature Cell Biology*. **5**:(6), 489-490
- M. M. Racke, M. Mosior, S. Kovacevic, C. Chang, H. S, A. L. Glasebrook, N. W. Roehm and S. Na (2002). Activation of caspase-3 alone is insufficient for apoptotic morphological changes in human neuroblastoma. *Journal of Neurochemistry*. **80**, 1039-1048
- M. Raff (1998). Cell suicide for beginners. *Nature*. **396**, 119-122
- M. Raffray and G. M. Cohen (1997). Apoptosis and necrosis in toxicology: A continuum or distinct modes of cell death? *Pharmacology & Therapeutics*. **75**:(3), 153-177
- R. R. Ramsay (1998). Substrate regulation of monoamine oxidases. *Journal of Neural Transmission Suppl.* **52**, 139
- R. Ramsey, Singer, T. P (1991). The kinetic mechanisms of monoamine oxidases A and B. *Amine Oxidases*. **19**, 219-223
- Pharmaceutical Business Review, (2007), Pipeline and commercial insight: Parkinson's disease-Market to grow as first round of life cycle management strategies succeed, Datamonitor, 29.10.2007, www.pharmaceutical-business-review.com/research.asp?guid=DMHC2326
- J. D. Richter (2007). CPEB: a life in translation. *TRENDS in Biochemical Sciences*. **32**:(6), 279-285
- P. Riederer, M. L. Danielczyk and E. Grunblatt (2004). Monoamine Oxidase-B Inhibition in Alzheimer's Disease. *Neurotoxicology*. **25**:(1-2), 271-277
- P. Riederer, E. Sofic, W. D. Rausch, B. Schmidt, G. P. Reynolds, K. Jellinger and M. B. Youdim (1989). Transition metals, ferritin, glutathione, and ascorbic acid in Parkinsonian brains. *Journal of Neurochemistry*. **52**:(2), 515-520
- P. Riederer and M. Youdim, B. H (1986). Monoamine Oxidase Activity and Monoamine Metabolism in Brains of Parkinsonian Patients Treated with L-Deprenyl. *Journal of Neurochemistry*. **46**:(5), 1359-1365
- A. R. Robbins, R. D. Ward and C. Oliver (1995). A mutation in glyceraldehyde-3-phosphate dehydrogenase alters endocytosis in CHO cells. *Journal of Cell Biology*. **130**, 1093-1104
- M. J. Robinson and M. H. Cobb (1997). Mitogen activated protein kinase signalling pathways *Curr. Opinion. Cell Biology*. **9**, 180-186
- S. Rocha, M. S. Soengas, S. W. Lowe, C. Glanzmann, D. Fabbro, K. Winterhalter, S. Bodis and M. Pruschy (2000). Protein kinase C inhibitor and irradiation-induced apoptosis: relevance of the cytochrome *c*-mediated caspase-9 death pathway. *Cell Growth and Differentiation*. **11**, 491-499
- M. J. Rodriguez, J. Saura, C. Finch, N. Mahy and E. E. Billett (2000). Localization of monoamine oxidase -A and -B in human pancreas, thyroid and adrenal glands. *J. Histochem. Cytochem.*, . **48** (1), 147-151
- T. T. Rohn, R. A. Rissman, M. C. Davis, Y. E. Kim, C. W. Cotman and E. Head (2002). Caspase-9 Activation and Caspase Cleavage of tau in the Alzheimer's Disease Brain. *Neurobiology of Disease*. **11**, 341-354

- D. S. Rosenthal, R. Ding, C. M. G. Simbulan-Rosenthal, J. P. Vaillancourt, D. W. Nicholson and M. Smulson (1997). Intact Cell Evidence for the Early Synthesis, and Subsequent Late Apoptain-Mediated Supression, of Poly(ADP-ribose) during Apoptosis. *Experimental Cell Research*. **232**, 313-321
- R. A. Ross, B. A. Spengler and J. L. Biedler (1983). Coordinate morphological and biochemical interconversion of human neuroblastoma cells. *Journal of the National Cancer Institute*. **71**:(4), 741-747
- J. Ruffels, M. Griffin and J. M. Dickenson (2003). Activation of ERL1/2, JNK and PKB by hydrogen peroxide in human SH-SY5Y neuroblastoma cells: role of ERK1/2 in H₂O₂-induced cell death. *European Journal of Pharmacology*. **483**:(2-3), 163-173
- S. M. Russell and R. J. Mayer (1983). Degredation of transplanted rat liver mitochondrial-outer-membrane proteins in hepatoma cells. *Biochem J*. **216**, 163-175
- V. C. Russo, K. Kobayashi, S. Najdovska, N. L. Baker and G. A. Werther (2004). Neuronal protection from glucose deprivation via modulation of glucose transport and inhibition of apoptosis: a role for the insulin-like growth factor system. *Brain Research*. **1009**, 40-53
- S. O. Sablin and R. R. Ramsay (1998). Monoamine Oxidase Contains a Reddox-active Disulfide *Journal of Biological Chemistry*. **273**:(23), 14074-14076
- J. D. Saffer, S. P. Jackson and M. B. Annarella (1991). Developmental expression of Sp1 in the mouse. *Molecular and Cellular Biology*. **11**:(4), 2189-2199
- J. Saklatvala, Dean, J. and Clark, A. (2003). Control of the expression of inflammatory response genes. *Biochemical Society Symposium*. **70**, 95-106
- G. S. Salvesen (2002). Caspases: opening the boxes and interpreting the arrows. *Cell Death and Differentiation*. **9**, 3-5
- M. Sandler, M. A. Reveley and V. Glover (1981). Human platelet monoamine oxidase activity in health and disease: a review. *Journal of Clinical Pathology*. **34**, 292-302
- G. Sandri, E. Panfili and L. Ernster (1990). Hydrogen peroxide produced by monoamine oxidase in isolated rat-brain mitochondria: its effect on glutathione levels and Ca²⁺ efflux. *Biochem Biophy Acta*, **1035**(3), 300-5
- M. Sano, M. Iwanaga, H. Fujisawa, M. Nagahama and Y. Yamazaki (1994). Staurosporine induces the outgrowth of neurites from the dorsal root ganglion of the chick embryo and PC12D cells. *Brain Research*. **639**:(1), 115-124
- M. Sastre and J. A. Garcia-Sevilla (1993). Opposite age-dependent changes of alpha 2A-adrenoceptors and nonadrenoceptor [3H]idazoxan binding sites (I2-imidazoline sites) in the human brain: strong correlation of I2 with monoamine oxidase-B sites. *Journal of Neurochemistry*. **61**:(3), 881-889
- J. Saura, Z. Bleuel, J. Ulrich, A. Mendelowitsch, K. Chen, J. C. Shih, P. Malherbe, M. DaPrada and J. G. Richards (1996). Molecular neuroanatomy of human monoamine oxidases A and B revealed by quantitative enzyme radioautography and in situ hybridization histochemistry. *Neuroscience*. **70**:(3), 755-774
- J. Saura, J. M. Luque, A. M. Cesura, M. Da Prada, V. Chan-Palay, G. Huber, J. Loffler and J. G. Richards (1994b). Increased monoamine oxidase b activity in plaque-associated astrocytes of Alzheimer's brains revealed by quantitative enzyme radioautography. *Neuroscience*. **62**:(1), 15-30

- J. Saura, G. Richards and N. Mahy (1994a). Differential age related changes of MAO-A and MAO-B in mouse brain and peripheral organs. *Neurobiology of Aging*. **15**, 399-408
- J. M. Savitt, S. S. Jang, W. Mu, V. L. Dawson and T. Dawson (2005). Bcl-XL Is Required for Proper Development of the Mouse Substantia Nigra. *Neurobiology of Disease*. **25**:(29), 6721-6728
- D. Schalling, Asberg, M., Edman, G. and Oreland, L. (1987). Markers for vulnerability to psychopathology: Temperament traits associated with platelet MAO activity. *Acta Psychiatrica Scandinavia*. **76**, 172-182
- A. H. V. Schapira (2006). Mitochondrial disease. *Lancet*. **368**, 70-82
- A. H. V. Schapira, J. M. Cooper and D. T. Dexter (1990). Mitochondrial complex I deficiency in Parkinson's disease. *Journal of Neurochemistry*. **54**, 823-827
- J. B. Schulz, J. Lindenau, J. Seyfried and Dichgans (2000). Glutathione, oxidative stress and neurodegeneration. *European Journal of Biochemistry*. **267**, 4904-4911
- M. Shamoto-Nagai, W. Maruyama, R. Kato, K. Isobe, M. Tanaka, M. Naoi and T. Osawa (2003). An Inhibitor of Mitochondrial Complex I, Rotenone, Inactivates Proteasome by Oxidative Modification and Induces Aggregation of Oxidised Proteins in SH-SY5Y Cells. *Journal of Neuroscience Research*. **74**, 589-597
- S. K. Sharma, E. C. Carlson and M. Ebaldi (2003). Neuroprotective actions of Selegiline in inhibiting 1-methyl, 4-phenyl pyridinium ion (MPP+)-induced apoptosis in SK-N-SH neurons. *Journal of Neurocytology*. **32**, 329-343
- T. B. Sherer, R. Betarbet, C. M. Testa, B. B. Seo, J. R. Richardson, J. H. Kim, G. W. Miller, T. Yagi, A. Matsuno-Yagi and J. T. Greenamyre (2003b). Mechanism of Toxicity in Rotenone Models of Parkinson's Disease. *The Journal of Neuroscience*. **23**:(34), 10756-10764
- T. B. Sherer, J. H. Kim, R. Betarbet and J. T. Greenamyre (2003a). Subcutaneous Rotenone Exposure Causes Highly Selective Dopaminergic Degeneration and α -Synuclein Aggregation. *Experimental Neurology*. **179**, 9-16
- U. Sheth and R. Parker (2003). Decapping and decay of messenger RNA occur in cytoplasmic processing bodies. *Science*. **300**, 805-808
- M. Shibata, H. Hattori, T. Sasaki, J. Gotoh, J. Hamada and Y. Fukuuchi (2003). Activation of caspase-12 by endoplasmic reticulum stress induced by transient middle cerebral artery occlusion in mice. *Neuroscience*. **118**:(2), 491-499
- J. C. Shih (1979). Monoamine oxidase in aging human brain. In Singer T. P., Von Korff, R. W., Murphy, D. L, editors. Monoamine oxidase: structure, function and altered functions. *New York: Academic Press*. 413-421
- J. C. Shih (1991). Molecular-Basis of Human Mao-a and Mao-B. *Neuropsychopharmacology*. **4**:(1), 1-7
- J. C. Shih (2003). Cloning, After Cloning, Knock-out Mice, and Physiological Functions of MAO A and B. *Neurotoxicology*. **in press**, in press
- J. C. Shih, K. Chen and M. J. Ridd (1999). MONOAMINE OXIDASE: From Genes to Behaviour. *Annual Review Neuroscience*. **22**, 197-217
- H. Shinohara, H. Yagita, Y. Ikawa and N. Oyaizu (2000). Fas drives cell cycle progression in glioma cells via extracellular signal-regulated kinase. *Cancer Research*. **60**, 1766-1772

- Z. A. Sibenaller, Etame, A. B., Ali, M. M., Barua, M., Braun, T. A., Cassavant, T. L. and Ryken, T. C. (2005). Genetic characterisation of commonly used glioma cell lines in the rat animal model system. *Neurosurgery Focus*. **19**:(4), 1-8
- S. Sigaud (2005). H₂O₂-induced proliferation of primary alveolar epithelial cells is mediated by MAP kinases. *Antioxidants & Redox Signaling*. **7**, 6
- S. Simizu, M. Takada, K. Umezawa and M. Imoto (1998). Requirement of Caspase-3(-like) Protease-mediated Hydrogen Peroxide Production for Apoptosis Induced by Various Anticancer Drugs. *The Journal of Biological Chemistry*. **273**:(41), 26900-26907
- S. G. Simonson, J. Zhang, A. T. Canada, Y. F. Su, H. Benveniste and C. A. Piantadosi (1993). Hydrogen-Peroxide Production by Monoamine-Oxidase During Ischemia Reperfusion in the Rat-Brain. *Journal of Cerebral Blood Flow and Metabolism*. **13**:(1), 125-134
- G. M. Simpson, J. C. Shih, K. Chen, C. Flowers, T. Kumazawa and B. Spring (1999). Schizophrenia, Monoamine Oxidase Activity, and Cigarette Smoking. *Neuropsychopharmacology*. **20**, 392-394
- K. B. Sims, A. De la Chapelle, R. Norio, E. Sankila, Y. P. P. Hsu, W. B. Rinehart, T. Corey and X. O. Breakefield (1989). Monoamine oxidase deficiency in males with an X chromosome deletion. *Neuron*. **2**, 1069-1076
- K. B. Sims, L. Ozelius, T. Corey, W. B. Rinehart, R. Liberfarb, J. Haines, W. Chen, J. R. Norio, E. Sankila, A. De la Chapelle, D. L. Murphy, J. Gusella and X. O. Breakefield (1989). Norrie Disease Gene Is Distinct from the Monoamine Oxidase Genes. *American Journal of Human Genetics*. **45**, 424-434
- T. P. Singer and R. R. Ramsay (1993). New Aspects of the Substrate Specificities, Kinetic Mechanisms and Inhibition of Monoamine Oxidases. *Monoamine Oxidase*. 23-43
- M. A. Sirover (2005). New Nuclear Functions of the Glycolytic Protein, Glyceraldehyde-3Phosphate Dehydrogenase, in mammalian Cells. *J Cellular Biochemistry*. **95**, 45-52
- S. D. Sivasubramaniam, C. C. Finch, M. A. Billett, P. H. Baker and E. E. Billett (2002). Monoamine oxidase expression and activity in human placentae from pre-eclamptic and normotensive pregnancies. *Placenta*. **23**:(2-3), 163-171
- A. F. Smith (1994). Type A personalities tend to have low platelet monoamine oxidase activity. *Acta Psychiatr. scand*. **89**:(2), 88-91
- P. K. Smith, R. I. Krohn, G. T. Hermanson, A. K. Mallia, F. H. Gartner, M. D. Provenzano, E. K. Fujimoto, N. M. Goetze, B. J. Olson and D. C. Klenk (1985). Measurement of protein using bicinchoninic acid. *Analytical Biochemistry*. **150**:(1), 76-85
- R. S. Sohal and R. Weindruch (1996). Oxidative stress, caloric restriction and ageing. *Science*. **273**, 59-63
- C. Soldani, M. C. Lazze, M. G. Bottone, G. Tognon, M. Biggiogera, C. E. Pellicciari and A. I. Scovassi (2001). Poly(ADP-ribose) Polymerase Cleavage during Apop. *Experimental Cell Research*. **269**, 193-201
- X. Song and M. Ehrich (1998). Uptake and Metabolism of MPTP and MPP⁺ in SH-SY5Y Human Neuroblastoma Cells. *In Vitro and Molecular Toxicology*. **11**:(1), 3-12
- X. Song, M. Ehrich, D. Flaharty, Y. Wang, X and N. Castagnoli (1996). Biotransformation of the MPTP Analog trans-1-Methyl-4-[4-dimethylaminophenylethenyl]-1,2,3,6-tetrahydropyridine to a Fluorescent Pyridinium Metabolite by Intact Neuroblastoma Cells *Toxicology and Applied Pharmacology*. **137**:(2), 163-172

- N. M. Soong, D. R. Hinton, G. Cortopassi and N. Arnheim (1992). Mosaicism for a specific somatic mitochondrial DNA mutation in adult human brain. *Nature Genetics*. **2**, 318-323
- H. Sorimachi, S. Ishiura and K. Suzuki (1997). Structure and physiological function of calpains. *Biochemical Journal*. **328**, 721-732
- R. Soto-Otero, E. Mendez-Alvarez, A. Hermida-Ameijeiras, I. Sanchez-Sellero, A. Cruz-Landeira and M. Lopez-Rivadulla Lamas (2001). Inhibition of brain monoamine oxidase activity by generation of hydroxyl radicals Potential implications in relation to oxidative stress. *Life Sciences*. **69**, 879-889
- D. L. Sparks, V. M. Woeltz and W. R. Markesbery (1991). Alterations in brain monoamine oxidase activity in aging, Alzheimer's disease and Pick's disease. *Archives of Neurology*. **48**, 718-728
- M. B. Spina and G. Cohen (1989). Dopamine turnover and glutathione oxidation: Implications for Parkinson's disease. *Proceedings of the National Academy of Sciences*. **86**, 1398-1400
- M. B. Spina, S. P. Squinto, J. Miller, R. M. Lindsay and C. Hyman (1992). Brain-Derived Neurotrophic Factor Protects Dopamine Neurons Against 6-Hydroxydopamine and N-Methyl-4-Phenylpyridinium Ion Toxicity: Involvement of the Glutathione System. *Journal of Neurochemistry*. **59**:(1), 99-106
- B. Stein, M. X. Yang, D. B. Young, R. Janknecht, T. Hunter, B. W. Murray and M. S. Barbosa (1997). p38-2, a novel mitogen-activated protein kinase with distinct properties. *Journal of Biological Chemistry*. **272**:(31), 19509-19517
- A. H. Stokes, Hastings, T. G. and Vrana, K. E. (1999). Cytotoxic and genotoxic potential of dopamine. *Journal of Neuroscience Research*. **55**, 659-665
- J. Stone and S. Yang (2006). Hydrogen peroxide: A Signaling Messenger. *Antioxidants & Redox Signaling*. **8**, 243-270
- J. St-Pierre, S. Drori, M. Uldry, J. M. Silvaggi, J. Rhee, S. Jager, C. Handschin, K. Zheng, J. Lin, W. Yang, D. K. Simon and R. Bachoo (2006). Suppression of reactive oxygen species and neurodegeneration by the PGC-1 transcriptional coactivators. *Cell*. **127**, 397-408
- M. Strolin Benedetti and P. Dostert (1989). Monoamine oxidase, brain ageing and degenerative diseases. *Biochemical Pharmacology*. **38**:(4), 555-561
- L. Stryer (1996). Biochemistry, 4. W. H. Freeman and Company, New York. New York
- J. L. Sullivan, J. C. Baenziger, D. L. Wagner, F. P. Rauscher, J. I. Nurnberger and J. S. Holmes (1990). Platelet MAO in subtypes of alcoholism. *Biological Psychiatry*. **27**:(8), 911-922
- X. Sun, M. Butterworth, M. MacFarlane, W. Dubiel, A. Ciechanover and G. Cohen (2004). Caspase Activation Inhibits Proteasome Function During Apoptosis. *Molecular Cell*. **14**, 81-93
- H. Tajima, K. Tsuchiya, M. Yamada, K. Kondo, N. Katsube and R. Ishitani (1999). Over-expression of GAPDH induces apoptosis in COS-7 cells transfected with cloned GAPDH cDNAs. *NeuroReport*. **10**, 2029-2033
- S. Tan, Y. Sagara, Y. Liu, P. Maher and D. Schubert (1998). The Regulation of Reactive Oxygen Species Production during Programmed Cell Death. *Journal of Cell Biology*. **141**:(6), 1423-1432

- D. Tang, J. M. Lahti and V. J. Kidd (2000). Caspase-8 Activation and Bid Cleavage Contribute to MCF7 Cellular Execution in a Caspase-3-dependent Manner during Staurosporine mediated Apoptosis. *Journal of Biological Chemistry*. **275**, 9303-9307
- Y. a. K. Tanimoto, H. (2002). Proteasome inhibitors block Ras/ERK signaling pathway resulting in downregulation of Fas ligand expression during activation-induced cell death in T cells. *Journal of Biochemistry*. **131**:(3), 319-326
- N. A. Tatton (2000). Increased caspase 3 and Bax immunoreactivity accompany nuclear GAPDH translocation and neuronal apoptosis in Parkinson's disease. *Experimental Neurology*. **166**:(1), 29-43
- W. G. Tatton, R. Chalmers-Redman and N. Tatton (2003). Neuroprotection by deprenyl and other propargylamines: glyceraldehyde-3-phosphate dehydrogenase rather than monoamine oxidase-B. *Journal of Neural Transmission*. **110**, 509-515
- W. G. Tatton and C. E. Greenwood (1991). Rescue of dying neurons: a new action for deprenyl in MPTP Parkinsonism. *Journal of Neuroscience Research*. **30**, 666-672
- W. G. Tatton, W. Y. L. Ju, D. P. Holland, C. Tai and M. Kwan (1994). (-)-Deprenyl reduces PC12 cell apoptosis by inducing new protein synthesis. *Journal of Neurochemistry*. **63**:(4), 1572-1575
- W. G. Tatton and W. Olanow (1999). Apoptosis in neurodegenerative diseases: the role of mitochondria. *Biochimica et Biophysica Acta*. **1410**, 195-213
- E. R. Taylor, F. Hurrell, R. Shannon, T. Lin, J. Hirst and M. P. Murphy (2003). Reversible Glutathionylation of Complex I Increases Mitochondrial Superoxide Formation. *The Journal of Biological Chemistry*. **278**:(22), 19603-19610
- E. R. Taylor, F. Hurrell, R. Shannon, T. K. Lin, J. Hirst and M. P. Murphy (2003). Reversible Glutathionylation of Complex I increases Mitochondrial Superoxide Formation. *The Journal of Biological Chemistry*. **278**:(22), 19603-19610
- P. Teismann, Tieu, K., Choi, D., Wu, D., Naini, A., Hunot, S., Vila, M., Jackson-Lewis, V. and Przedborski, S. (2003). Cyclooxygenase-2 is instrumental in Parkinson's disease neurodegeneration. *Proceedings of the National Academy of Sciences*. **100**:(9), 5473-5478
- L. R. Thomas, D. J. Stillman and A. Thorburn (2002). Regulation of Fas-associated Death Domain Interactions by the Death Effector Domain Identified by a Modified Reverse Two-hybrid Screen. *The Journal of Biological Chemistry*. **277**:(37), 34343-34348
- T. Thomas (2000). Monoamine oxidase-B inhibitors in the treatment of Alzheimer's disease. *Neurobiology of Aging*. **21**, 343-348
- T. Thomas (2000). Monoamine oxidase-B inhibitors in the treatment of Alzheimer's disease. *Neurobiology of Aging*. **21**, 343-348
- M. J. Thomenius and C. W. Distelhorst (2003). Bcl-2 on the surface of endoplasmic reticulum: protecting the mitochondria from a distance. *Journal of Cell Science*. **116**, 4493-4499
- K. Tieu, D. M. Zuo and P. H. Yu (1999). Differential effects of staurosporine and retanoic acid on the vulnerability of SH-SY5Y neuroblastoma cells: Involvement of Bcl-2 and p53 proteins. *Journal of Neuroscience Research*. **58**, 426-435
- K. F. Tipton (1973). Biochemical Aspects of Monoamine Oxidase. *British Medical Bulletin*. **29**, 116-119
- K. F. Tipton, S. Boyce, J. O'Sullivan, G. P. Davey and J. Healy (2004). Monoamine Oxidases: Certainties and Uncertainties. *Current Medicinal Chemistry*. **11**, 1965-1982

- K. F. Tipton and T. P. Singer (1993). Advances in Our Understanding of the Mechanisms of the Neurotoxicity of MPTP and Related Compounds. *Journal of Neurochemistry*. **61**:(4), 1191-1206
- R. B. Tjalkens, Ewing, M. M. and Philbert, M. A. (2000). Differential cellular regulation of the mitochondrial permeability transition in an in vitro model of 1,3-dinitrobenzene-induced encephalopathy. *Brain Research*. **874**, 165-177
- M. B. Toledano, A. Delaunay, L. Monceau and F. Tacnet (2004). Microbial H₂O₂ sensors as archetypical redox signaling molecules. *TRENDS in Biochemical Sciences*. **29**:(7), 351-357
- A. Toninello, P. Pietrangeli, U. De Marchi, M. Salvi and B. Mondoci (2006). Amine oxidases in apoptosis and cancer. *Biochimica et Biophysica Acta*. **1765**, 1-13
- B. E. Toth, I. Bodnar, K. G. Homicsko, F. Fulop, M. I. K. Fekete and G. M. Nagy (2002). Physiological role of Salsolinol: Its hypophysiotrophic function in the regulation of pituitary prolactin secretion. *Neurotox and Teratol*, **24**, 655-66.
- C. Tournier, P. Hess, D. D. Yang, J. Xu, T. K. Turner, A. Nimnual, D. Bar-Sagi, S. N. Jones, R. A. Flavell and R. J. Davis (2000). Requirement of JNK for stress-induced activation of the cytochrome c-mediated death pathway. *Science*. **288**:(5467), 870-874
- C. M. Troy, S. A. Rabacchi, W. J. Friedman, T. F. Frappier, K. Brown and M. L. Shelanski (2000). Caspase-3 mediates neuronal cell death induced by β -amyloid. *Journal of Neuroscience*. **20**, 1386-1392
- Y. Tsugeno and A. Ito (1997). A key amino acid responsible for substrate selectivity of monoamine oxidase A and B. *Journal of Biological Chemistry*. **272**:(22), 14033-14036
- H. Vaghefi, A. L. Hughes and K. E. Neet (2004). Nerve Growth Factor Withdrawal-mediated Apoptosis in Naive and Differentiated PC12 Cells through p53/Caspase-3-dependent and -independent Pathways. *The Journal of Biological Chemistry*. **279**:(15), 15604-15614
- A. V. Veselovsky, Ivanov, A. S. and Medvedev, A. E. (2003). Computer Modelling and Visualisation of Active Site of Monoamine Oxidases. *Neurotoxicology*. **25**, 37-46
- C. Vindis, M. Seguelas, P. Bianchi, A. Parini and C. Cambon (2000). Monoamine Oxidase B Induces ERK-Dependent Cell Mitogenesis by Hydrogen Peroxide Generation *Biochemical and Biophysical Research Communications*. **271**:(1), 181-185
- C. Vindis, M. H. Seguelas, S. Lanier, A. Parini and C. Cambon (2001). Dopamine induces ERK activation in renal epithelial cells through H₂O₂ produced by monoamine oxidase. *Kidney International*. **59**, 76-86
- L. Vonknorring and L. Oreland (1985). Personality-Traits and Platelet Monoamine-Oxidase in Tobacco Smokers. *Psychological Medicine*. **15**:(2), 327-334
- B. Wahlund, Saaf, J. and Wetterberg, L. (1995). Clinical symptoms and platelet monoamine oxidase in subgroups and different states of affective disorders. *Journal of Affective Disorders*. **35**, 75-87
- P. C. Waldmeier (1987). Amine oxidases and their endogenous substrates (with special reference to monoamine oxidase and the brain). *J Neural Transm Suppl*. **23**, 55-72
- D. C. Wallace (1992). Diseases of the mitochondrial DNA. *Annu. Rev. Biochem*. **61**, 1175-1212

- J. Wang and D. E. Edmondson (2007). Do monomeric vs dimeric forms of MAO-A make a difference? A direct comparison of the catalytic properties of rat and human MAO-A's. *Journal of Neural Transmission*. **114**:(6), 721-724
- X. Wang, S. Li, A. P. Chou and J. M. Bronstein (2006). Inhibitory effects of pesticides on proteasome activity: Implications in Parkinson's disease. *Neurobiology of Disease*. **23**, 198-205
- X. Wang, J. L. Martindale, Y. Liu and N. J. Holbrook (1998). The cellular response to oxidative stress: influences of mitogen-activated protein kinase signalling pathways on cell survival. *Biochemistry Journal*. **333**, 291-300
- X. S. Wang, Diener, K., Manthey, C. L., Wang, S., Rosenzweig, B., Bray, J., Delaney, J., Coles, C. N., Chan-Hui, P., Mantlo, N., Lichenstein, H. S., Zukowski, M. and Yao, Z. (1997). Molecular Cloning and Characterization of a Novel p38 Mitogen-activated Protein Kinase. *The Journal of Biological Chemistry*. **272**:(38), 23668-23674
- A. J. Waskiewicz and J. A. Cooper (1995). Mitogen and Stress-Response Pathways - Map Kinase Cascades and Phosphatase Regulation in Mammals and Yeast. *Current Opinion in Cell Biology*. **7**:(6), 798-805
- M. Watabe and T. Nakaki (2006). ATP depletion does not account for apoptosis induced by inhibition of mitochondrial electron transport chain in human dopaminergic neurons. *Neuropharmacology*. **in press**, 1-6
- Q. Wei (1996). Genetic elevation of monoamine oxidase levels in dopaminergic PC12 cells results in increased free radical damage and sensitivity to MPTP. *Journal of Neuroscience Research*. **46**, 666-673
- W. Wei, D. D. Norton, X. Wang and J. W. Kusiak (2002). A β 17-42 in Alzheimer's disease activates JNK and caspase-8 leading to neuronal apoptosis. *Brain* **125**:(9), 2036-2043
- P. Weingarten and Q. Zhou (2001). Protection of intracellular dopamine cytotoxicity by dopamine disposition and metabolism factors. *Journal of Neurochemistry*. **77**, 776-785
- M. Weller, Frei, K., Groscurth, P., Krammer, P. H., Yonekawa, Y. and Fontana, A. (1994). Anti-Fas/APO-1 Antibody-mediated Apoptosis of Cultured Human Glioma Cells. *Journal of Clinical Investigation*. **94**, 954-964
- P. a. C. Werner, G. (1991). Intramitochondrial formation of oxidised glutathione during the oxidation of benzylamine by monoamine oxidase. *FEBS letters*. **280**:(1), 44-46
- K. N. Westlund, Denney, R. M., Rose, R. M. and Abell, C. W. (1988). Localization of distinct monoamine oxidase A and monoamine oxidase B cell populations in human brainstem. *Neuroscience*. **25**:(2), 439-456
- W. Weyler (1989). Monoamine Oxidase-a from Human-Placenta and Monoamine Oxidase-B from Bovine Liver Both Have One Fad Per Subunit. *Biochemical Journal*. **260**:(3), 725-729
- R. Wiesner, Kasuschke, A., Kuhn, H., Anton, M. and Schewe, T. (1989). Oxygenation of mitochondrial membranes by the reticulocyte Lipoygenase - Action on Monoamine oxidase activities A and B. *Biochimica et Biophysica Acta*. **986**:(1), 11-17
- R. Wiesner, Kuhn, H., Anton, M. and Schewe, T. (1990). Oxygenation of mitochondrial membranes by the erythroid lipoygenase. Consequences for membrane properties. *Biomed Biochim Acta*. **49**:(2-3), 35-38

- S. S. Wigdal, R. A. Kirkland, J. L. Franklin and M. Haak-Frendscho (2002). Cytochrome *c* release precedes mitochondrial membrane potential loss in cerebellar granule neuron apoptosis: lack of mitochondrial swelling. *Journal of Neurochemistry*. **82**, 1029-1038
- P. Wipf, J. Xiao, J. Jiang, N. A. Belikova, V. A. Tyurin, M. P. Fink and V. E. Kagan (2005). Mitochondrial Targeting of Selective Electron Scavengers: Synthesis and Biological Analysis of Hemigramicidin-TEMPO Conjugates. *Journal of the American Chemical Society*. **127**, 12460-12461
- M. G. Wise, D. M. Hilty and G. Cerda (1995). Pick's disease, 387-413
- W. K. Wong, K. Chen and J. C. Shih (2001). Regulation of human monoamine oxidase B gene by Sp1 and Sp3. *Molecular Pharmacology*. **59**(4), 852-859
- W. K. Wong, K. Chen and J. C. Shih (2003). Decreased Methylation and Transcription Repressor Sp3 Up-regulated Human Monoamine Oxidase (MAO) B Expression during Caco-2 Differentiation. *The Journal of Biological Chemistry*. **278**(38), 36227-26235
- W. K. Wong, X. Ou, K. Chen and J. C. Shih (2002). Activation of Human Monoamine Oxidase B Gene Expression by a Protein Kinase C MAPK Signal Transduction Pathway Involves c-Jun and Egr-1. *The Journal of Biological Chemistry*. **277**(25), 22222-22230
- J. Woodgett (2000). Protein Kinase Functions, *Oxford University Press*. Oxford
- R. Wu, R. Chen and C. C. Chiueh (2000). Effect of MAO-B Inhibitors on MPP⁺ Toxicity *in Vivo*. *Annals of the New York Academy of Sciences*. **899**, 255-261
- X. G. Xia, T. Harding, M. Weller, A. Bieneman, J. B. Uney and J. B. Schulz (2001). Gene transfer of the JNK interacting protein-1 protects dopaminergic neurons in the MPTP model of Parkinson's disease. *Proceedings of the National Academy of Sciences*. **98**(18), 10433-10438
- Z. Xia, M. Dickens, J. Raingeaud, R. J. Davis and M. E. Greenberg (1995). Opposing effects of ERK and JNK-p38 MAP kinases on apoptosis. *Science*. **270**, 1326-1331
- M. Yamada, Yasahura, H. (2003). Clinical Pharmacology of MAO Inhibitors: Safety and Future. *Neurotoxicology*. **25**, 139-149.
- S. Yamamoto, H. Jiang, K. Nishikawa, M. Ishihara, J. C. Wang and R. Kato (1992). Protein kinase-C-dependent and -independent actions of a potent protein kinase inhibitor, staurosporine. *European Journal of Pharmacology*. **277**, 113-122
- S. Yang, A. D. Sharrocks and A. J. Whitmarsh (2003). Transcriptional regulation by the MAP kinase signaling cascades. *Gene* **320**, 3-21
- R. Yao and G. M. Cooper (1995). Requirement for phosphatidylinositol 3-kinase in the prevention of apoptosis by nerve growth factor. *Science*. **267**, 2003-2006
- H. Yi, Y. Akao, W. Maruyama, K. Chen, J. C. Shih and M. Naoi (2006a). Type A monoamine oxidase is the target of an endogenous dopaminergic neurotoxin, N-methyl(R)salsolinol, leading to apoptosis in SH-SY5Y cells. *Journal of Neurochemistry*. **96**, 541-549
- H. Yi, W. Maruyama, Y. Akao, T. Takahashi, K. Iwasa, M. Youdim, B. H and M. Naoi (2006b). N-Propargylamine protects SH-SY5Y cells from apoptosis induced by an endogenous neurotoxin, N-methyl(R)salsolinol, through stabilisation of mitochondrial membrane and induction of anti-apoptotic Bcl-2. *Journal of Neural Transmission*. **113**, 21-32

- M. S. Yoo, H. S. Chun, J. J. Son, L. A. DeGiorgio, D. J. Kim, C. Peng and J. H. Son (2003). Oxidative stress regulated genes in nigral dopaminergic neuronal cells: correlation with the known pathology in Parkinson's disease. *Molecular Brain Research*. **110**, 76-84
- S. Yoon, C. Yun and A. Chung (2002). Dose effect of oxidative stress on signal transduction in aging. *Mechanisms of ageing and development*. **123**, 1597-1604
- M. Youdim, B. H, T. Amit, O. B. Falach-Yogev and W. Maruyama (2003). The essentiality of Bcl-2, PKC and proteasome-ubiquitin complex activations in the neuroprotective-antiapoptotic action of the anti-Parkinson dug, rasagiline. *Biochemical Pharmacology*. **66**:(8), 1635-1641
- M. Youdim, B. H and J. P. M. Finberg (1987). Monoamine oxidase B inhibition and the "cheese effect". *Journal of Neural Transmission Suppl*. **25**, 27-33
- M. Youdim, B. H and T. L. Sourkes (1966). Properties of purified, soluble monoamine oxidase. *Canadian Journal of Biochemistry*. **44**, 1397-1400
- M. B. H. Youdim and Y. S. Bakhle (2006). Monoamine oxidase: isoforms and inhibitors in Parkinson's disease and depressive illness. *Br J Pharmacol*. **147**:(Suppl. 1), S287-296
- M. B. H. Youdim, D. E. Edmondson and K. F. Tipton (2006). The therateutic potential of monoamine oxidase inhibitors. *Nature Reviews Neuroscience*. **7**, 295-309
- R. J. Youle and M. Karbowski (2005). Mitochondrial fission in apoptosis. *Nature Reviews*. **6**, 657-662
- J. Yuan and B. A. Yankner (2000). Apoptosis in the nervous system. *Nature*. **407**, 802-809
- Y. Yung, Z. Yao, T. Hanoch and R. Seger (2000). ERK1b, a 46-kDa ERK Isoform That is Differentially Regulated by MEK. *The Journal of Biological Chemistry*. **275**:(21), 15799-15808
- V. J. Yuste, I. Sanchez-Lopez, C. Sole, M. Encinas, J. R. Bayascas, J. Boix and J. X. Comella (2002). The prevention of staurosporine-induced apoptosis by Bcl-XL but not Bcl-2 or caspase inhibitors, allows the extensive differentiation of human neuroblastoma cells. *Journal of Neurochemistry*. **80**, 126-139
- N. Zandwijk (1995). N-Acetylcysteine (NAC) and glutathione (GSH): Antioxidant and chemopreventative properties, with special reference to lung cancer. *Journal of Cellular Biochemistry*. **59**:(S22), 24-32
- L. Y. Zang and H. P. Misra (1993). Generation of Reactive Oxygen Species During the Monoamine Oxidase-Catalyzed Oxidation of the Neurotoxicant, 1-Methyl-4-Phenyl-1,2,3,6-Tetrahydropyridine. *Journal of Biological Chemistry*. **268**:(22), 16504-16512
- X. D. Zhang, S. K. Gillespie and P. Hersey (2004). Staurosporine induces apoptosis of melanoma by both caspase-dependent and -independent apoptotic pathways. *Molecular Cancer Therapeutics*. **3**:(2), 187-197
- Y. Zhang, V. L. Dawson and T. Dawson (2000). Oxidative Stress and Genetics in the Pathogenesis of Parkinson's Disease. *Neurobiology of Disease*. **7**, 240-250
- Z. P. Zhaung, B. Marks and R. B. McCauley (1992). The insertion of monoamine oxidase A into the outer mitochondrial membrane of rat liver mitochondria. *The Journal of Biological Chemistry*. **267**:(1), 591-596
- Z. P. Zhaung and R. McCauley (1989). Ubiquitin Is Involved in the Invitro Insertion of Monoamine Oxidase-B into Mitochondrial Outer Membranes. *Journal of Biological Chemistry*. **264**:(25), 14594-14596

- M. Zhiping, Z. K. Mirdics and N. F. Schor (2006). Bcl-2 overexpression disrupts the morphology of PC12 cells through reduced ERK activation. *Brain Research*. **1112**, 46-55
- B. P. Zhou, Wu, B., Kwan, S. and Abell, C. W. (1998). Characterization of a Highly Conserved FAD-binding site in Human Monoamine Oxidase B. *The Journal of Biological Chemistry*. **273**, 14862-14868
- Q. S. Zhu, K. Chen and J. C. Shih (1994). Bidirectional Promoter of Human Monoamine-Oxidase-a (Mao-a) Controlled by Transcription Factor Sp1. *Journal of Neuroscience*. **14**:(12), 7393-7403
- Q. S. Zhu, J. Grimsby, K. Chen and J. C. Shih (1992). Promotor organisation and activity of human monoamine oxidase (MAO) A and B genes. *The Journal of Neuroscience*. **12**, 4437-4446
- X. Zhu, O. Ogawa, G. Perry and M. A. Smith (2003). JKK1, an upstream activator of JNK/SAPK, is activated in Alzheimer disease. *Journal of Neuropathology and Experimental Neurology*. **62**:(5), 551-551

APPENDIX

APPENDIX 1

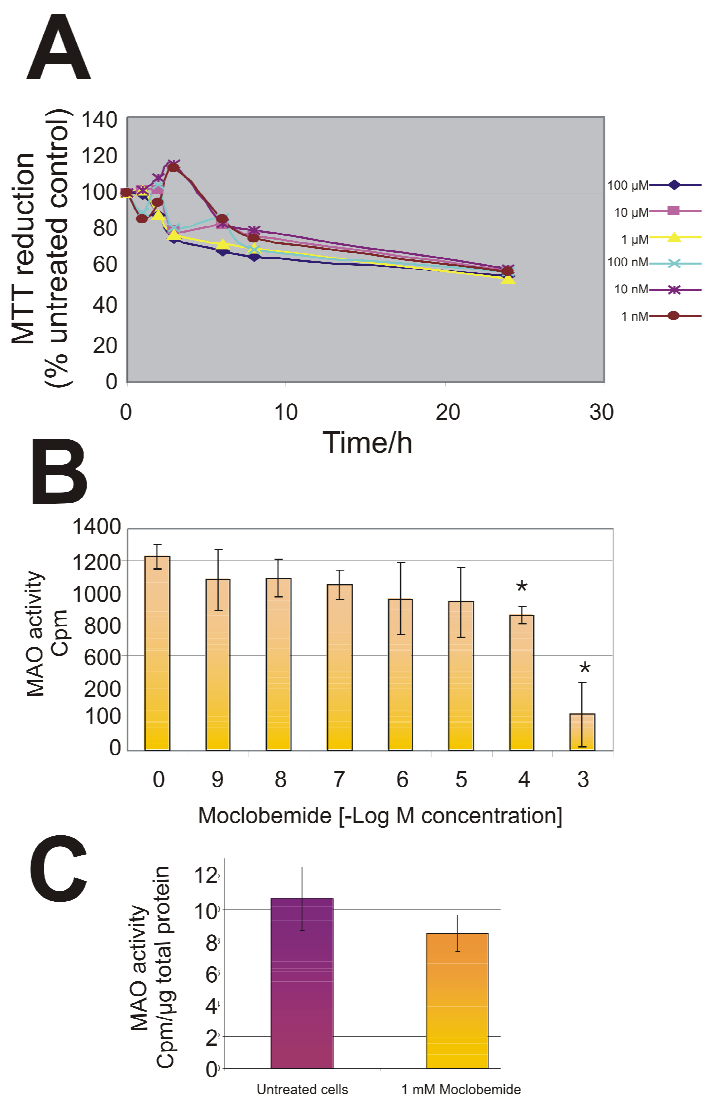


Figure A1. 1 The concentration of moclobemide required to inhibit MAO *in situ* is toxic to SH-SY5Y cells

(A) MTT reduction was measured in SH-SY5Y cells over 24 hours, following the addition of 1 nM, 10 nM, 100 nM, 1 μ M, 10 μ M and 100 μ M moclobemide. MTT reduction was determined and expressed as mean MTT reduction % untreated control. (B) MAO activity was measured in SH-SY5Y extracts *in vitro* following the addition of 1 nM, 10 nM, 100 nM, 1 μ M, 10 μ M and 100 μ M moclobemide via a radiometric method, using 14 C-Tyramine as a substrate. MAO catalytic activity was expressed as mean counts per minute (Cpm) \pm S.D. Data represent triplicate values from three independent experiments ($n=3$). Untreated controls were statistically compared to treated cells at each concentration using the Student's t-test where * = $p<0.05$. (C) MAO activity was measured in SH-SY5Y cells *in situ* following the addition of 1 mM moclobemide after 3 h, via a radiometric method, using 14 C-Tyramine as a substrate. MAO catalytic activity was expressed as mean counts per minute (Cpm) \pm S.D.

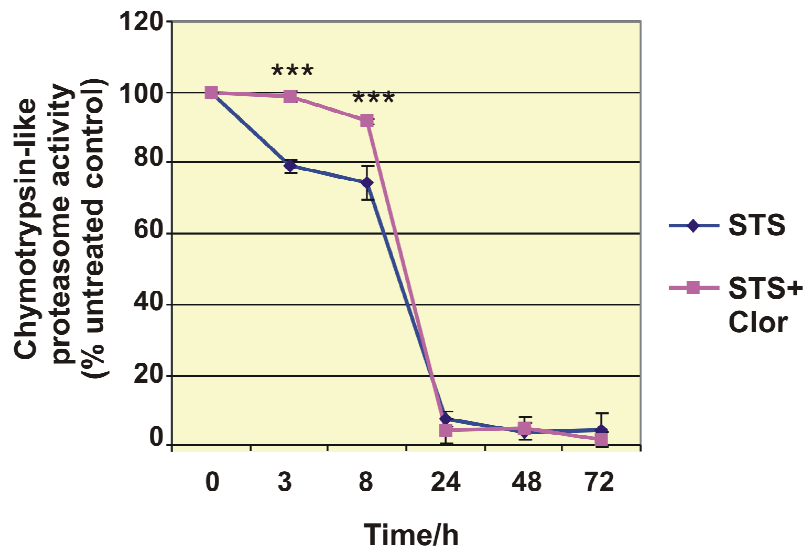


Figure A1.2 Effect of clorgyline on proteasome activity during STS-induced apoptosis

Proteasome activity (CLA) was measured in SH-SY5Y cells over 72 h, following the addition of 1 μ M STS or 1 μ M STS + 1 μ M clorgyline. Proteasome activity was determined and expressed as mean proteasome activity (% untreated control) \pm S.D. Data represent triplicate values from three independent experiments ($n=3$). Untreated controls were statistically compared to treated cells at each concentration using the Student's t-test where *** = $p < 0.001$.

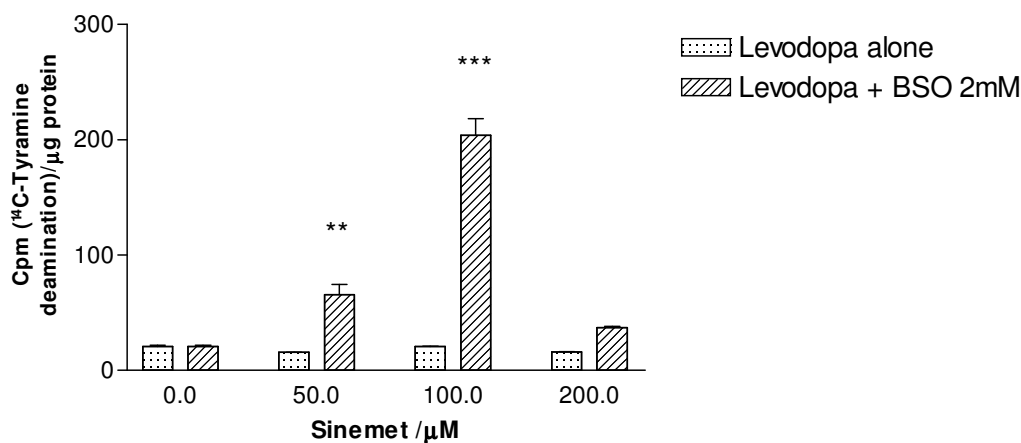


Figure A1.3 Effect of Sinemet and BSO on MAO catalytic activity

MAO activity was measured in SH-SY5Y cells following the addition of 50 μ M, 100 μ M, 200 μ M Sinemet preparation either in the presence or absence of 2 mM BSO and measured via a radiometric method, using ¹⁴C-Tyramine as a substrate. MAO catalytic activity was expressed as mean counts per minute (Cpm) \pm S.D. Data represent triplicate values from three independent experiments ($n=3$). Untreated controls were statistically compared to treated cells at each concentration using the Student's t-test where ** = $p < 0.01$ and *** = $p < 0.001$.

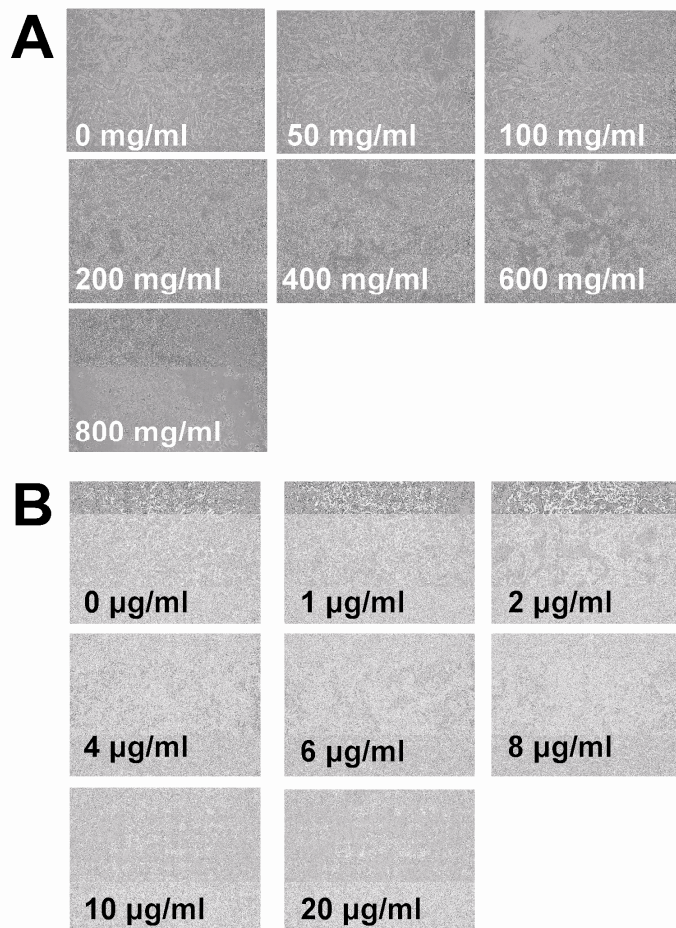


Figure A1. 4 Determination of a working concentration of G418 sulphate (geneticin) and blasticidin for use in SH-SY5Y cells

(A) The effect of 50, 100, 200, 400, 600 and 800 µg/ml G418 sulphate (geneticin) on SH-SY5Y cell morphology after 4 days treatment. (B) The effect of 1, 2, 4, 6, 8, 10 and 20 mg/ml blasticidin on SH-SY5Y cell morphology after 4 days treatment Cells were visualised using a Nikon eclipse TS100 microscope.